Universidade do Minho
Escola de Engenharia

José Filipe Gonçalves Maciel

Microalgae production strategies to increase carotenoid and polyunsaturated fatty acid composition for food and feed

Microalgae production strategies to increase carotenoid and polyunsaturated fatty acid composition for food and feed
José Filipe Gonçalves Maciel
UMinho | 2022

October 2022

Universidade do Minho
Escola de Engenharia

José Filipe Gonçalves Maciel

Microalgae production strategies to increase carotenoid and polyunsaturated fatty acid composition for food and feed

PhD Thesis
Chemical and Biological Engineering

Supervisors:
António Augusto Martins de Oliveira Soares Vicente, PhD
Joana Gabriela Laranjeira da Silva, PhD

October 2022

DIREITOS DE AUTOR E CONDIÇÕES DE UTILIZAÇÃO DO TRABALHO POR TERCEIROS

AGRADECIMENTOS

Com o fechar deste importante e marcante ciclo da minha vida académica e pessoal não posso deixar de mencionar as instituições e pessoas que dele fizeram parte e contribuíram significativamente para a sua conclusão. A todos eles quero deixar o meu profundo agradecimento.

À Fundação para a Ciência e a Tecnologia pelo financiamento deste projeto através das bolsas SFRH/BD/133005/2017 e COVID/BD/152455/2022. Ao professor António Vicente, orientador desta tese de Doutoramento, pelos seus sábios e valiosos conselhos, pelo seu contributo científico, disponibilidade, mas sobretudo pela confiança constante nas minhas capacidades e pelas palavras amigas e encorajadoras nos momentos mais difíceis. À Doutora Joana Silva pela sua colaboração e disponibilidade como co-orientadora e pelo seus importantes conselhos e visão sobre o plano de trabalhos a seguir. Obrigado por me ter recebido na Allmicroalgae - Natural Products, S.A, permitindo-me contactar de perto com a realidade industrial/empresarial e integrar a equipa de I&D, à qual agradeço a valiosa colaboração, em especial ao Hugo Pereira, Joana T. Silva, Imma Gifuni, Bernardo Carvalho, Pedro Quelhas e Margarida Costa. À professora Rosário Domingues por me ter acolhido no Departamento de Química da Universidade de Aveiro e orientado durante a análise lipidómica, assim como à Daniela Couto pelos seus ensinamentos e ajuda laboratorial. A todos os membros do Laboratório de Indústria e Processos do Centro de Engenharia Biológica (CEB). Desde há muito que tem sido a minha segunda casa, pelo que deixo aqui o meu obrigado pela camaradagem, ajuda e pelos bons momentos e convívios proporcionados. Em especial ao Pedro Geada pela constante partilha de ideias e ajuda preciosa na elaboração desta tese; e ao Ricardo Pereira pela sua disponibilidade e partilha de conhecimento. Aos alunos de mestrado Leandro Madureira, Mariana Barreiros e Joana Araújo - obrigado pela vossa inesgotável colaboração e pelos momentos de aprendizagem que me proporcionaram. Ao Paulo Berni pela ajuda na análise de pigmentos. Ao pessoal técnico do CEB: Vitória, Engª Madalena, Maura, Aline e Raquel o meu obrigado por serem sempre prestáveis, mas sobretudo ao Sr. Santos pela ajuda na construção dos sistemas de cultivo.

O meu profundo agradecimento aos meus Pais. Nada disto seria possível sem o vosso suporte, dedicação, amor e crença nos meus sonhos nesta caminhada de 32 anos. À minha irmã Sónia, ao Pedro e aos meus sobrinhos Gonçalo e Maria Inês pelo afeto e alegria. À família Meira pelos convívios animados e por serem a minha segunda família.

Por fim, o meu agradecimento especial à Ana, pelo amor, paciência, compreensão, incentivo e companhia nos bons e maus momentos. Obrigado por teres estado sempre presente.

STATEMENT OF INTEGRITY

I hereby declare having conducted this academic work with integrity. I confirm that I have not used plagiarism or any form of undue use of information or falsification of results along the process leading to its elaboration.

I further declare that I have fully acknowledged the Code of Ethical Conduct of the University of Minho

Resumo: Estratégias de produção de microalgas para a obtenção de carotenóides e de ácidos gordos polinsaturados para nutrição humana e animal, num contexto de descarbonização da economia

As microalgas têm sido destacadas como uma fonte promissora e sustentável de importantes compostos bioactivos para as indústrias farmacêutica e alimentar, como por exemplo: carotenóides, ácido eicosapentaenóico (EPA) e ácido docosahexaenóico (DHA). Este trabalho teve como objetivo otimizar e caracterizar a produção de biomassa da *Pavlova gyrans* através de uma abordagem multivariada. Inicialmente foram avaliados os efeitos de 17 fatores abióticos na produtividade da biomassa de *P. gyrans*. As variáveis que apresentaram um impacto significativo ($p < 0,10$) no crescimento da *P. gyrans* foram a intensidade de luz, $NaNO_3$, e $CuSO_4,5H_2O$, sendo a última a única a afetar negativamente o crescimento da *P. gyrans*. Numa segunda etapa estas variáveis, juntamente com o $NaH_2PO_4.H_2O$, foram estudadas de forma a otimizar a produção de biomassa da *P. gyrans*, resultando as seguintes condições ótimas de crescimento: 700 µmol.photons.m^{-2}.s^{-1} de intensidade luminosa, 1500 mg.L^{-1} NaNO3, 6 µg.L^{-1} $CuSO_4.5H_2O$ e 40 mg.L^{-1} $NaH_2PO_4.H_2O$. Em comparação com as condições controlo a formulação ótima permitiu um aumento de 3,8 vezes no valor máximo de biomassa produzida (2,26 g AFDW.L-1) assim como uma melhoria generalizada no perfil bioquímico (teor de proteínas, PUFA, ácidos gordos n-3, DHA e EPA).

Além disso, foi também avaliado o efeito dos 17 fatores abióticos na produção de xantofilas e carotenos d*e P. gyrans* ($p < 0,10$), com especial ênfase na fucoxantina (Fx), β-caroteno (βCar), e a soma de todos os carotenóides analisados individualmente (TCar). Na gama de valores testada verificou-se que a produção de Fx foi aumentada usando maiores concentrações de azoto e menor intensidade luminosa. Além disso, o azoto e o ferro foram positivamente correlacionados com a acumulação de βCar. O conteúdo de TCar aumentou em concentrações mais elevadas de azoto, ferro e cobalto, bem como em níveis mais baixos de salinidade e iluminação. As condições de crescimento formuladas para maior acumulação de Fx e TCar melhoraram a respetiva produção ($p < 0,05$). Entre as experiências de validação, os valores mais elevados de Fx e TCar alcançados por *P. gyrans* foram 6,153 e 11,794 mg.g-1 DW, o que representou um aumento de 3 e 2 vezes, respectivamente, em comparação com o meio de controlo (Walne). Os resultados deste trabalho permitiram compreender a importância dos diferentes fatores abióticos no crescimento e composição bioquímica da *P. gyrans*, assim como entender a importância nutricional que esta microalga apresenta. Os dados aqui apresentados poderão facultar informação relevante para a possível produção à escala industrial desta microalga.

Palavras-chave: DHA, EPA, fucoxantina, condições de cultivo, otimização, *Pavlova gyrans*

Abstract: Microalgae production strategies to increase carotenoid and polyunsaturated fatty acid composition for food and feed applications

Microalgae have been presented as a source of important bioactive compounds for nutraceutical and pharmaceutical industries, such as carotenoids, eicosapentaenoic acid (EPA) and docosahexaenoic acid (DHA). The aim of this work was to optimize and characterize the biomass production of *Pavlova gyrans* through a multivariate approach. Firstly, the effects of seventeen abiotic factors on the biomass productivity of *P. gyrans* were evaluated. Light intensity, $NaNO_3$, and $CuSO_4.5H_2O$, were identified as the most significative abiotic factor ($p < 0.10$), with the latter negatively affecting the growth of *P. gyrans*. Together with $NaH_2PO_4.H_2O$, these variables were further studied to maximize the biomass production of *P. gyrans*, being the optimum growth conditions reached when applying 700 μmol.photons.m^{-2}.s^{-1} of light intensity, 1500 mg.L^{-1} $NaNO_3$, 6 μg.L^{-1} $CuSO_4.5H_2O$ and 40 mg.L^{-1} $NaH_2PO_4.H_2O$. The optimized conditions were validated against the control (Walne's medium) and allowed a 3.8-fold increase in biomass production of *P. gyrans* (2.26 g AFDW.L^{-1}). The biochemical profile of *P. gyrans* was also improved ($p < 0.05$), namely with increased protein content (10.59-30.76 % DW), PUFA content (37.13-47.11 %TFA), n-3 fatty acids (26.49-38.27 %TFA), DHA (5.73-10.33 %TFA) and EPA (17.09-20.69 %TFA – $p > 0.05$).

In addition it was assessed the effect of the seventeen abiotic factors in xanthophylls and carotenes production of *P. gyrans* ($p < 0.10$), with especial emphasis in fucoxanthin (Fx), β-carotene (βCar), and the sum of all carotenoids individually analyzed (TCar). In the experimental range tested, Fx production was increased under higher levels of nitrogen and lower light intensity. Additionally, nitrogen and iron were positively correlated with βCar accumulation. TCar content was enhanced at higher concentrations of nitrogen, iron, and cobalt, as well as lower levels of salinity and illumination. The modified growth conditions formulated for Fx and TCar improved the respective production ($p < 0.05$). Among the validation experiments, the highest Fx and TCar values achieved by *P. gyrans* were, respectively, 6.153 and 11.794 mg.g^{-1} DW, which represented an increase of 3- and 2- fold compared to the control (Walne's medium). The results of this work provided an understanding of the importance of different abiotic factors on the growth of *P. gyrans*, which are relevant data for further large-scale production of this microalgae with beneficial nutritional indices for human consumption.

Keywords: DHA, EPA, fucoxanthin, growth conditions, optimization, *Pavlova gyrans*

TABLE OF CONTENTS

INDEX OF FIGURES

INDEX OF TABLES

LIST OF GENERAL NOMENCLATURE

Abbreviations

19-HFx. 19'-hexanoyloxifucoxanthin

AA. Amino acid

ACCase. Acetyl-CoA Carboxylase

ACP. Acyl carrier protein

AFDW. Ash-Free Dry Weight

AI. Atherogenic index

ANOVA. Analysis of variance

ATP. Adenosine triphosphate

BL. Betaine lipid

BtaA. Betaine lipid synthase A

BtaB. Betaine lipid synthase B

CCM. CO2-concentrating mechanism

CDP-DAG. Cytidine diphosphate diacylglycerol cytidine diphosphate diacylglycerol

CDP-ME. Diphosphocytidylyl methylerythritol

CDP-MEP. Diphosphocytidylyl methylerythritol 2-phosphate

CDS. Cytidine diphosphate diacylglycerol synthase

Chl. Chlorophyll

CLS. Cardiolipin synthase

CMK. CDP-ME kinase

CMS. CDP-ME synthase

cPAV. Divinyl form of chlorophyll c

CVD. Cardiovascular diseases

DAG. Diacylglycerols

DDE. Diadinoxanthin de-epoxidase

Ddx. Diadinoxanthin, Diadinoxanthin

DEP. Diatoxanthin epoxidase

DGCC. Diacylglycerylcarboxyhydroxymethylcholine

DGDG. Digalactosyldiacylglycerol

DGTA. Diacylglycerylhydroxymethyl-trimethylalanine

DGTS. Diacylglyceryl trimethylhomoserine

DH. β-hydroxylacyl-ACP dehydrase, Dehydrogenase

DHA. Docosahexaenoic acid

DMAPPp. Dimethylallyl pyrophosphate

DOXP. 1-deoxy-D-xylulose 5-phosphate

Dtx. Diatoxanthin, Diatoxanthin

DV. Divinyl form

DXR. DOXP-reductoisomerase

DXS. 1-deoxy-D-xylulose-5-phosphate synthase

EA. Eyespot apparatus

EFSA. European Food Safety Authority

EPA. Eicosapentaenoic acid

EPS. Exopolysaccharides

ER. Endoplasmic reticulum

FA. Fatty acid

FAS. Fatty Acid Synthase

FPP. Farnesyl pyrophosphate

Fx. Fucoxanthin

G3P. Glycerol-3-phosphate

GC-MS. Gas chromatography-mass spectrometry

GGPP. Geranylgeranyl pyrophosphate

GL. Glycolipid

GPAT. Glycerol-phosphate acyltransferase

GPP. Geranyl pyrophosphate

HDR. HMBPP reductase

HDS. HMBPP synthase

HI. Hypocholesterolemic index

HMBPP. Hydroxymethylbutenyl pyrophosphate

IEM. Inner envelope membrane

IPI. Isopentenyl pyrophosphate isomerase

IPP. Isopentenyl pyrophosphate

KR. β-ketoacyl-ACP reductase, Ketoacyl-reductase

KS. β-ketoacyl-ACP synthase, Ketoacyl-synthase

KS III. β-ketoacyl-ACP synthase III

LACS. Long chain acyl-CoA synthetase

LC-PUFA. Long chain polyunsaturated fatty acid

LED. Light Emitting Diodes

LHC. Light harvesting complex proteins

LPAAT. Lyso-phosphatidic acid acyltransferase

MAG. Monoacylglycerols

MCS. MEcDP synthase

MEcPP. Methylerythritol 2,4-cyclodiphosphate

MEP. 2-C-methyl-D-erythriol 4-phosphate

MGDG. Monogalactosyldiacylglycerol

MgDVP. Mg-[3,8-divinyl]-phytoporphyrin-132-methylcarboxy

MUFA. Monounsaturated fatty acid

MV. Monovinyl form

NADPH. Nicotinamide adenine dinucleotide phosphate

NMR. Nuclear Molecular Ressonance

OA. Oleic acid

P. Phosphorus

PAP. Phosphatidic acid phosphatase

PAR. Photosynthetically Active Radiation

PB. Placket-Burman

PC. Phosphatidylcholine, Volumetric productivity of the carotenoids

PDS. Phytoene desaturase

PG. Phosphatidylglycerol

PGPS. Phosphatidylglycerolphosphate synthase

Phosphatidylethanolamine

PKS. Polyketide synthase pathway

PL. Phospholipid

PSI. Photosystems I

PSII. Photosystem II

PSY. Phytoene synthase

PTPMT1. Protein tyrosine phosphatase mitochondrial 1

PUFA. Polyunsaturated fatty acids

RCCD. Rotatable Central Composite Design

RE. Relative error

ROS. Reactive oxygen species

Rubisco.Ribulose-1,5-bisphosphate carboxylase/oxygenase

SA. Stearic acid

SFA. Saturated fatty acid

SG. Acylated steryl glycosides

SQDG. Sulfoquinovosyldiacylglycerol

TAG. Triacylglycerol

TCar. Sum of all carotenoids analyzed

TFA. Total fatty acids

TI. Thrombogenic index

Vx. Violaxanthin

αCar. α- carotene

β-car. β-carotene

βER. β-enoyl-ACP reductase, Enoyl-reductase

Symbols

A_{FA}. Integrated area of a single fatty acid

A_{TFA}. Total area of all the fatty acids identified

P_x. Biomass productivity

X_{max}. Maximum biomass produced

CHAPTER 1 GENERAL INTRODUCTION

1.1 RESEARCH BACKGROUND AND THESIS MOTIVATION

In recent years, we have seen a growing lifestyle trend that consumers demand goods with clean label, healthy properties and achieved through sustainable resources and ethical manufacturing. For instance, the vegan lifestyle - which determines not to eat or use any type of animal-derived product – became increasingly popular and widespread during the 2000s [1,2], representing a growing food market with a compound annual growth rate of 10.41% that predicts a market size worth of US$ 65.4 billion by 2030 [3]. To cope with this, both policymakers and Industry have been looking for sustainable sources and appropriate technologies that can meet the demanding standards [1].

Microalgae have been suggested as one of the most highlighted and promising sources that comprises the features previously stated. These microorganisms are predominantly photoautotrophic eukaryotes and are widely distributed in nature [4]. Their commercially application as an alternative resource for the production of different commodities is mainly linked to their particular characteristics, such as high CO_2 fixation, metabolic plasticity, fast and controlled growth and their bioactive-rich biomass [5]. However, only a few species of microalgae are industrially produced, and fewer are those commercialized for human consumption [6]. Thus, among the challenges that microalgae industry has facing in the recent years stands out the identification of viable species for large-scale production and the respective optimization of the growth conditions in order to improve the cost-effectiveness of their production.

Pavlovophyceae species have been pointed out as an interesting source of highly demanded metabolites for feed, nutraceutical and pharmaceutical industries. The importance of these species for aquaculture has been well documented [7,8], thanks to their ability to accumulate high levels of important polyunsaturated fatty acids – eicosapentaenoic acid and docosahexaenoic acid -, sterols and carotenoids [9–11]. Recently, several studies have described the numerous benefits for human health related to the intake of these metabolites [12–15], motivating the urge for a thorough understanding of the abiotic factors involved in maximizing the biomass of Pavlovophyceae biomass, as well as identifying the main parameters responsible for modulating the biochemical composition.

Thus, the workplan of the current thesis aimed to assess and to fully understand the impact of seventeen culture variables in *Pavlova gyrans* growth performance and metabolites production, namely fatty acids and carotenoids. With the outcomes from this work we pretend to develop knowledge that may support the development of growth medium formulations that enable the implementation of *P. gyrans* on large scale production, as well as develop of different growth strategies that take advantage of its rich metabolite composition.

1.2 RESEARCH AIMS

This thesis had as the main objective to identify and to optimize, through a multivariate approach, the impact of seventeen abiotic factors in the growth performance and biochemical composition – fatty acids and carotenoids - of *P. gyrans*. To accomplish that goals the workplan was divided in two main tasks:

Task 1: Identify the main growth variables involved in biomass production of *P. gyrans*, and their statistical optimization for enhanced biomass production as well as its biochemical characterization on fatty acid profile and lipid and protein content.

Task 2: Discover the key abiotic factors involved in the production and accumulation of carotenoids of *P. gyrans*. The growth conditions identified as the most important were used for further development of medium formulations and microalgae growth strategies able to increase the carotenoids content in *P. gyrans* without to compromise its growth performance.

The Task 1 aimed to identify among the seventeen abiotic factors, using a Placket-Burman design, those with statistical significance for the growth performance of *Pavlova gyrans*, namely the volumetric biomass productivity. Then, the significant culture variables were set to a new range of values and studied, using a Rotatable Central Composite design (RCCD), in order to achieve the optimum conditions for the maximum biomass produced by *P. gyrans*. The assays produced in the optimization phase were further characterized for their protein and lipid content and analyzed through gas chromatography-mass spectrometry to determine the fatty acid profile, and especially the composition of EPA and DHA. The results allowed the construction of contour curves for each response variable (biomass, protein, EPA and DHA), unravelling the synergistic effects between the significant abiotic factors in *P. gyrans*.

Regarding the Task 2, it was designed to explore the impact of the abiotic factors established in Placket-Burman experiment on the pigment composition of *P. gyrans*. The whole pigment profile was assessed using the High-Pressure Liquid Chromatography technique, in order to discriminate the main variations promoted by the different growth conditions among the identified carotenoids: diadinoxanthin, diatoxanthin, fucoxanthin, α-carotene and β-carotene. These data would allow to find the key variables involved in the production of each carotenoid, which would be used later to formulate new culture conditions and growth strategies to maximize the overall carotenoid composition of *P. gyrans*, as well the fucoxanthin and β-carotene content – two highly sought-after carotenoids on the market.

1.3 THESIS OUTLINE

According to the objectives previously mentioned, the present thesis, in addition to the present chapter, is composed for Chapter 2, 3, 4 and 5. Chapter 2 gives an extensive overview of microalgae as producer of fatty acids and carotenoids. In Chapter 3 and 4 are exposed the main results produced during this thesis, highlighting the relevance of growth variables on growth performance and biochemical composition of *P. gyrans*.

Chapter 2: several themes related with the production of carotenoid and fatty acid by microalgae were reviewed. Among them, the metabolic pathways responsible for the carotenoid and fatty acids synthesis were described, their biological and commercial interest for human consumption, the main structural and biochemical features of Pavlovophyceae species, the potential applications of this class of microalgae, the relevance of the nutritional conditions on the growth of microalgae and the impact on their carotenoid and fatty acid composition, especially in Pavlovophyceae, were described.

Chapter 2: several topics related to the production of carotenoids and fatty acids by microalgae were reviewed. Among them, the metabolic pathways responsible for the synthesis of carotenoids and fatty acids, their biological and commercial interest for human consumption, the main structural and biochemical characteristics of Pavlovophyceae species, the potential applications of this class of microalgae, the relevance of nutritional conditions on the growth of microalgae and the impact on their carotenoid and fatty acid composition, especially in Pavlovophyceae, were described.

Chapter 3: using a Plackett-Burman design, followed by a Central Composite Rotatable Design, seventeen growth variables were assessed and optimized to improve biomass production of *P. gyrans*. In the second optimization step as well as the validation experiments the biomass was characterized forits protein and lipid content and fatty acid profile.

Chapter 4: the impact of the same seventeen abiotic factors tested in Plackett-Burman design were also assessed on the carotenoid profile of *P. gyrans*. The key growth variables responsible for the highest accumulation of fucoxanthin, diadinoxanthin, diatoxanthin and β-carotene were identified, which were used to design the optimum growth conditions for each carotenoid, as well as to develop growth strategies capable of improving the carotenoid content of *P. gyrans*.

Chapter 5: the general conclusions of this work was presented, as well as suggestions for future works.

1.4 REFERENCES

1. Morocho-Jácome AL, dos Santos BB, de Carvalho JCM, de Almeida TS, Rijo P, Velasco MVR, et al. Microalgae as a Sustainable, Natural-Oriented and Vegan Dermocosmetic Bioactive Ingredient: The Case of Neochloris oleoabundans. Cosmetics. MDPI; 2022;9.

2. Marangon F, Tempesta T, Troiano S, Vecchiato D. Toward a Better Understanding of Market Potentials for Vegan Food. A Choice Experiment for the Analysis of Breadsticks Preferences. Agriculture and Agricultural Science Procedia. Elsevier BV; 2016;8:158–66.

3. Vegan Food Market Size, Share, Trends | Report 2022 to 2030 [Internet]. [cited 2022 Sep 15]. Available from: https://www.precedenceresearch.com/vegan-food-market

4. Geada P, Vasconcelos V, Vicente A, Fernandes B. Microalgal Biomass Cultivation. Algal Green Chemistry: Recent Progress in Biotechnology. 2017. p. 257–84.

5. Guedes AC, Amaro HM, Malcata FX. Microalgae as sources of carotenoids. Mar Drugs. MDPI AG; 2011. p. 625–44.

6. Geada P, Moreira C, Silva M, Nunes R, Madureira L, Rocha CMR, et al. Algal proteins: Production strategies and nutritional and functional properties. Bioresour Technol. Elsevier Ltd; 2021.

7. Tibbetts SM, Patelakis SJJ, Whitney-Lalonde CG, Garrison LL, Wall CL, MacQuarrie SP. Nutrient composition and protein quality of microalgae meals produced from the marine prymnesiophyte Pavlova sp. 459 mass-cultivated in enclosed photobioreactors for potential use in salmonid aquafeeds. J Appl Phycol. 2020;32:299–318.

8. Milke LM, Bricelj VM, Parrish CC. Biochemical characterization and nutritional value of three Pavlova spp. in unialgal and mixed diets with Chaetoceros muelleri for postlarval sea scallops, Placopecten magellanicus. Aquaculture. 2008;276:130–42.

9. Ahmed F, Zhou W, Schenk PM. Pavlova lutheri is a high-level producer of phytosterols. Algal Res [Internet]. Elsevier B.V.; 2015;10:210–7. Available from: http://dx.doi.org/10.1016/j.algal.2015.05.013

10. Fernandes T, Martel A, Cordeiro N. Exploring Pavlova pinguis chemical diversity: a potentially novel source of high value compounds. Sci Rep. 2020;10:1–11.

11. Guihéneuf F, Stengel DB. Interactive effects of light and temperature on pigments and n-3 LC-PUFA-enriched oil accumulation in batch-cultivated Pavlova lutheri using high-bicarbonate supply. Algal Res [Internet]. Elsevier B.V.; 2017;23:113–25. Available from: http://dx.doi.org/10.1016/j.algal.2017.02.002

12. Zhu Y, Cheng J, Min Z, Yin T, Zhang R, Zhang W, et al. Effects of fucoxanthin on autophagy and apoptosis in SGC-7901cells and the mechanism. J Cell Biochem. Wiley-Liss Inc.; 2018;119:7274–84.

13. Zhang Y, Xu W, Huang X, Zhao Y, Ren Q, Hong Z, et al. Fucoxanthin ameliorates hyperglycemia, hyperlipidemia and insulin resistance in diabetic mice partially through IRS-1/PI3K/Akt and AMPK pathways. J Funct Foods. Elsevier Ltd; 2018;48:515–24.

14. Peet M, Stokes C. Omega-3 Fatty Acids in the Treatment of Psychiatric Disorders. Drugs. 2005;65.

15. Fotuhi M, Mohassel P, Yaffe K. Fish consumption, long-chain omega-3 fatty acids and risk of cognitive decline or Alzheimer disease: A complex association. Nat Clin Pract Neurol. 2009;5:140–52.

CHAPTER 2 THE POTENTIAL OF PAVLOVOPHYCEAE SPECIES AS A SOURCE OF VALUABLE PIGMENTS AND LIPIDS

2.1 INTRODUCTION

Microalgae represent a large group of uni- and multicellular microorganisms – it is estimated the existence of up to 1,000,000 species – divided into prokaryotes (cyanobacteria) and eukaryotes. Most of these organisms are photoautotrophic, using solar energy and CO_2 to thrive; however, some species are also capable of growing either heterotrophically (using organic compounds as source of carbon) or mixotrophically (combining both autotrophic and heterotrophic mechanisms) [1]. Recently, microalgae have been receiving increasing attention by researchers and the Industry itself as consequence of the multitude of metabolites displayed (proteins, carbohydrates, lipids, pigments, vitamins, etc.) and, consequently, diversity of potential applications in distinct biotechnology sectors (e.g., pharmaceutical, cosmetics, food & feed). Nevertheless, despite all the recognized potential of microalgae, the number of species utilized at industrial scale is limited to nearly 200 [2].

Pavlovophyceae is a class of eukaryotic, unicellular and motile marine microalgae belonging that inhabit littoral, brackish water and, occasionally, freshwater environments [1,3]. These spherical microalgae characterized by the presence of two golden-brown or yellow-green chloroplasts, organic body scales, and a unique filamentous appendage, called haptonema, have arisen as promising microalgae to explore commercially, mainly due to their high content in polyunsaturated fatty acids (PUFAs), such as eicosapentaenoic acid (EPA) and docosahexaenoic acid (DHA) [1] These n-3 fatty acids, usually ingested through the consumption of fish (or derivates) are associated with interesting bioactivities, human development, and diseases treatment or prevention [4–8]. The potential of Pavlovophyceae is though not limited to the production of PUFAs, since these microalgae are also capable of synthesising pigments (e.g., carotenoids), sterols, and other lipids with interesting market value [9,10]. Despite the interesting features reported, the number of studies focusing on strategies to take advantage of Pavlovophyceae species potential is still scarce, being aquaculture feeding its main application.

Similarly to what happens for most of the microalgal species, the widespread commercialization of Pavlovales (and/or their biocompounds) faces some common challenges related to high production and downstream processing costs, as well as low productivity rates in terms of biomass or metabolites of interest. This fact highlights the necessity to optimize cultivation conditions and production systems, but also to employ holistic approaches involving process integration and circular economy, zero waste or biorefinery concepts in order to substantially improve the cost/benefit ratio of microalgal biomass and high-added value compounds production. In addition, more sustainable processes and economies would

be ensured using these strategies, meeting therefore the worldwide guidelines that have been established over the last years, such as the United Nations Sustainable Development Goals.

This review intends to unveil the full potential of microalgae as an interesting source of PUFAs and carotenoids, with special attention to the Pavlovophyceae members, providing a thorough overview of the benefits and applications of their biomass and produced bioactive compounds. Particular focus will be given to growth conditions optimization and to strategies envisaging not only the maximization of high-value compounds' production.

2.2 MICROALGAE AS A PROMISING CELL FACTORY FOR PUFAS PRODUCTION

Fatty acids usually contain 14 to 24 carbon atoms and can be classified as saturated (SFAs), monounsaturated (MUFAs), or polyunsaturated fatty acids (PUFAs). Most of them are provided to the body through diet but can also be synthesized in the human body by other fatty acids or non-lipid precursors such as glucose. Although, there are exceptions – essential fatty acids – that comes exclusively from food [11–13]. PUFAs, especially n-3 PUFAs such as EPA (C20:5n-3) and DHA (C22:6n-3), are essential fatty acids strongly recommended for human diet [14] (see Section 4 – commercial interest). EPA and DHA are mostly produced by microalgae and transferred to the upper levels of the food chain [15]. Kingdom Chromista includes promising candidate species for commercial production of n-3 PUFAs (Table 2-1) [2]. Some of them are already approved by the European Food Safety Authority (EFSA) for human consumption in EU, such as *Odontella aurita*, *Schizochytrium* sp. and *Ulkenia* sp. [16–19]. The total FA composition is highly variable from species to species; however, species belonging to the Kingdom Chromista usually present high levels of one n-3 PUFA, EPA (C20:5n-3) or DHA (C22:6n-3) (Table 2-1), relying on the effect of abiotic factors (see Chapter 2.5).

2.2.1 Distribution of microalgae lipids classes

Microalgal lipids comprise two main groups: i) polar lipids (phospholipids, glycolipids and betaine lipids) and ii) non-polar or neutral lipids (acylglycerols, sterols, free fatty acids, hydrocarbons, wax and steryl esters). According to its chemical structure different types of phospholipids (PLs) are found in microalgae, namely phosphatidylcholine (PC), phosphatidylethanolamine (PE), and phosphatidylglycerol (PG) [20,21]. Considering the glycolipids (GLs) they are subdivided in three groups: monogalactosyldiacylglycerol (MGDG), digalactosyldiacylglycerol (DGDG), and sulfoquinovosyldiacylglycerol (SQDG) [22–24]. PLs and GLs are essential structural components of biological membranes - membrane systems in microalgae can be divided into the photosynthetic active thylakoid membrane and the structural membranes

surrounding compartments (e.g., inner and outer membranes of the chloroplast, mitochondria and endoplasmic reticulum) (Figure 2-1) [25]. These lipids maintain specific membrane functions and provide the permeability barrier surrounding cells, organelles within cells, as well as providing a matrix for various metabolic processes. Some polar lipids may act as key intermediates in cell signalling pathways (e.g., oxidative products of PUFAs). The classes of betaine lipids (BLs) described in microalgae are diacylglyceryl trimethylhomoserine (DGTS), diacylglycerylhydroxymethyl-trimethylalanine (DGTA) and diacylglycerylcarboxyhydroxymethylcholine (DGCC). BLs are present in both the photosynthetic and the non-photosynthetic membranes, and it has been suggested that BLs may have similar functions or even surpass the function of PLs [26]. The non-polar lipids, mainly triacylglycerols (TAGs), are abundant storage products synthesized in the chloroplast or at the endoplasmic reticulum (ER) membrane [21,27], which can be easily catabolised to provide metabolic energy. Sterols are also present in biological membranes as structural components [28].

2.2.2 Synthesis of n-3 Polyunsaturated Fatty Acids in Microalgae

The conventional fatty acids (FA) biosynthesis is similar among plants and microalgae species and comprise three distinct pathways: (i) first, the biosynthesis of palmitic acid (C16:0) and other saturated fatty acids is achieved through Fatty Acid Synthase (type II FAS) pathway using acetyl-CoA as substrate, (ii) then further chain elongations, and (iii) desaturations occur as part of the n-3 and n-6 pathways to produce more complex polyunsaturated fatty acids. FA biosynthesis involves cooperation of two subcellular organelles, the chloroplast stroma (*de novo* FA synthesis) and the ER (LC-PUFA synthesis) [36]. The metabolic pathways involved in lipid synthesis are initiated by acetyl-CoA, which could be provided by the conversion of a) pyruvate, in chloroplast and mitochondria (Figure 2-2, A and B), b) citrate or c) acetate, both in cytosol (Figure 2-2, C and D); and require energy (ATP) and reducing power (NADPH) (Figure 2-2, E) [21,37].

2.2.2.1 Synthesis of Saturated Fatty Acids

The microalgal *de novo* FA synthesis requires the participation of two multienzyme complexes, acetyl-CoA carboxylase (ACCase) and fatty acid synthase (type II FAS). The first step is the conversion of acetyl-CoA to malonyl-CoA through plastidial ACCase (Figure 2-2, stage 1). Then, the transfer of the malonyl moiety to holo-acyl carrier protein, promotes the malonyl-acyl carrier protein (malonyl-ACP) intermediates to type II FAS cyclic condensation reactions, in which occurs the extension of the acyl group to middle chain length fatty acids (<C18) [38,39]. Type II FAS is composed by six enzymes that ensure the following cyclic

four enzymatic reactions: condensation (C-C bond formation), reduction (C-OH), dehydration (C=C) and hydrogenation (C-C) (Figure 2-2, stage 2) [40].

These reactions are catalysed by β-ketoacyl-ACP synthase (KS), β-ketoacyl-ACP reductase (KR), β-hydroxylacyl-ACP dehydrase (DH) and β-enoyl-ACP reductase (βER), respectively, to produce C4 to C18 fatty acids. The first cycle (n=1) of FAS is initiated by β-ketoacyl-ACP synthase III (KS III), which uses a fatty acyl-ACP (C_{2n}) and malonyl-ACP as substrates to form 3-ketoacyl-ACP, that in turn is used by successive enzymes, KR, DH and βER to produce a C4 fatty acyl-ACP (C_{2n+2}), butyryl-ACP (C4:0-ACP) (C2 to C4). The next six cycles (n=2 to n=7) are initiated by KS I to produce a C16 fatty acid (C_{2n+2}), palmitoyl-ACP (C16:0-ACP) (C4 to C16). At last cycle (n=8), the reaction between palmitoyl-ACP and malonyl-ACP is allowed by KS II and results in C18 fatty acid (C_{2n+2}) synthesis, stearoyl-ACP (C18:0-ACP) (C16 to C18). FAs can be exported to the FA cytosolic pool (Figure 2-2, G) or they are released from the acyl-ACP as CoA esters by acyl-ACP thioesterases (FAT) and further incorporated into the FA plastid pool (Figure 2-2, F) which can be used to form chloroplast lipids (Figure 2-2, stage 4) [41]. The localization of the pools is maintained due to acyl-CoA form not being able to cross the intracellular membranes. Only FAs esterified to acyl-ACP can cross membranes [40–42].

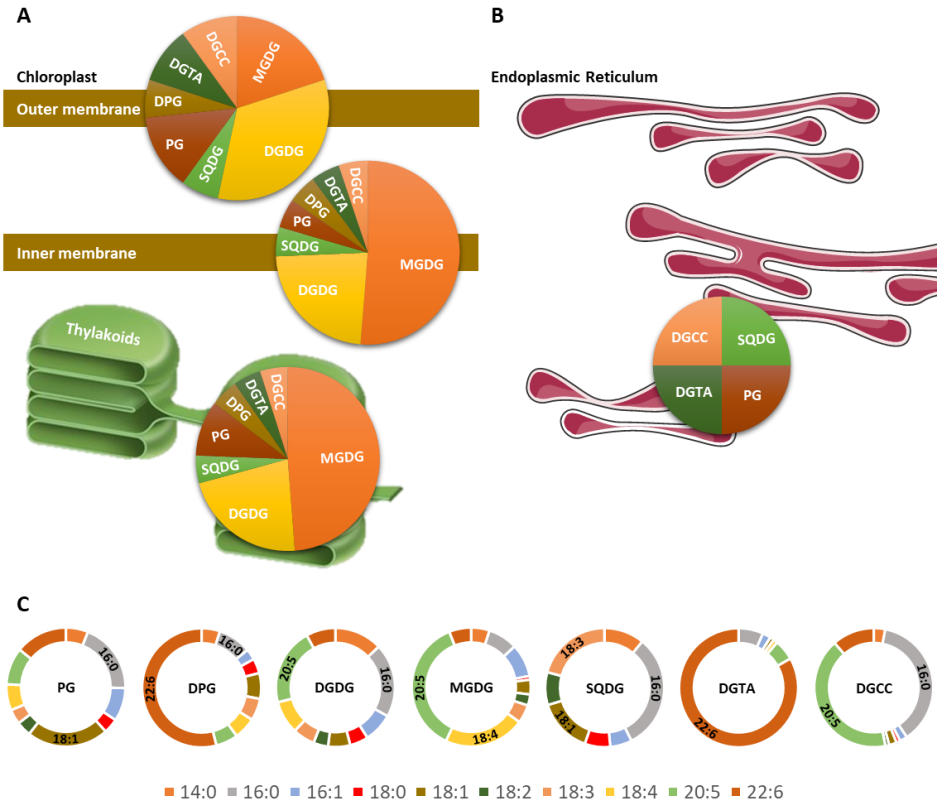

Figure 2-1: Distribution and composition of chloroplast- and endoplasmic reticulum-specific lipids from microalgae. A) The relative composition of lipid classes in the chloroplast OEM, IEM, thylakoid and B) ER membranes [20,22,24,29–33]. C) Typical fatty acid abundance of the major lipid classes from Diacronema lutheri [24,34,35]. PG, phosphatidylglycerol; DPG, diphosphatidylglycerol or cardiolipin; DGDG, digalactosyl-diacylglycerol; MGDG, monogalactosyldiacylglycerol; SQDG, sulfoquinovosyl-diacylglycerol; DGTA, diacylglycerylhydroxymethyl-trimethylalanine; DGCC, diacylglyceryl-carboxyhydroxymethylcholine.

2.2.2.2 Synthesis of Polyunsaturated Fatty Acids

Elongation and desaturation processes, characterized in microalgae, seem to comprise i) the hexadecatrienoic acid (C16:3-ACP) synthesis, in chloroplasts (Figure 2-2, stage 3), ii) the polyketide synthase pathway (PKS pathway), also in chloroplasts (Figure 2-2, H) and iii) the n-3 and n-6 pathways, in ER (Figure 2-2, stage 12) [43]. PKS pathway and n-3 and n-6 pathways favor long-chain polyunsaturated fatty acids (LC-PUFA) synthesis. Microalgal acyltransferases – glycerol-phosphate acyltransferase (GPAT), lyso-phosphatidic acid acyltransferase (LPAAT) and phosphatidic acid phosphatase (PAP) – are required for the esterification of FAs to the desired *sn*-position of the glycerol-backbone and appear to be located either in the chloroplast- or ER-membranes (Figure 2-2, stage 4 and 10) [29]. Chloroplast- and ER-bound Δ6, Δ9 and Δ12 desaturases are also described for microalgal cells (Figure 2-2, stage 3 and 12). The remaining desaturases and elongases engaged for n-3 and n-6 pathways only occurs in ER membrane and facing the cytosol [44].

The plastidial acyl-ACP pool provides C16:0-ACP for the C16:3-ACP synthesis. Desaturation of C16:0-ACP to C16:3-ACP can take place through high substrate specific plastidial-located Δ9, Δ12 and Δ6 desaturases, in this sequence (Figure 2-2, stage 3). The final step of this pathway is to synthesize microalgal membrane lipids through the C16:3-ACP esterification to a glycerol lipid backbone (Figure 2-2, stage 4) [44]. The origin of the lipid backbones can be distinguished by the fatty acid length at the *sn*-2 position on the glycerol-3-phosphate (G3P). The chloroplast-lipid derived pathway, called prokaryotic pathway, esterifies C16 fatty acids at the *sn*-2 position of G3P, whereas the ER-lipid derived pathway, called eukaryotic pathway, have C18 fatty acids esterified at the *sn*-2 position [28,45].

Inside the chloroplast, GPAT esterifies a FA onto the *sn*-1 position of G3P with either C16 (C16:0- CoA or C16:3- CoA) or C18 (C18:0-CoA or C18:1-CoA) FAs. Then LPAAT esterifies a C16 (C16:0-CoA or C16:3-CoA) fatty acid onto the lyso-phosphatidic acid (lyso-PA) at the *sn*-2 position [46]. The resulting PA is dephosphorylated by PAP to generate DAG (Figure 2-2, stage 4). PA and DAG as well as other phospholipids can act as precursors to produce PLs (Figure 2-2, stage 5), GLs (Figure 2-2, stage 6) and TAGs (Figure 2-2, stage 7) [27,47]. For example, DAG can be assembled into MGDG or SQDG – with the characteristic 16 carbon fatty acid at the *sn*-2 position – through MGD and SQD synthases, both placed at the chloroplast inner envelope membrane. DGD synthases also mediate the production of DGDG, however they are localized at the chloroplast outer envelope membrane (Figure 2-2, stage 8) [48,49].

Most FAs released from the *de novo* FA synthesis are exported using the membrane transport protein, fatty acid export 1 (FAX1), and the long chain acyl-CoA synthetase (LACS) (Figure 2-2, stage 9) to reach

the cytoplasm as acyl-CoAs where they are incorporated into the FA cytosolic pool (Figure 2-2, G) for further processed at the ER [50–52]. The fatty acid C18:0 reaches cytosol either in form of C18:0-CoA (stearoyl-CoA) or C18:1-CoA (oleoyl-CoA). Desaturation of stearic acid (SA, C18:0) to oleic acid (OA, C18:1) can take place through a *Δ*9 desaturase in the chloroplast (Figure 2-2, stage 3) or the ER (Figure 2-2, stage 12). Except for *Δ*9 desaturase, ER-located desaturases and elongases use acyl-lipids (FAs linked to the glycerol-backbone) as substrates [22,53]. The ER lipid synthesis – eukaryotic pathway – commonly occurs through the Kennedy pathway (Figure 2-2, stage 10) or the acyl-editing pathway [47,54].

The absence of PC and PE production by *Diacronema lutheri* raises the question if the acyl-editing pathway actually takes place in these microalgae [24,34,35]. Regarding *Diacronema lutheri*, DAG is then incorporated into TAGs and other lipids, instead of PC and PE. Thus, it remains unknown if this pathway can occur with other lipid classes, such as lyso-DGCC (a lyso-type form previously discovered in *Diacronema lutheri*), if not, it is likely that this pathway is absent from Pavlovales [55,56].

Although the Kennedy pathway (Figure 2-2, stage 10) be similar to fatty acid incorporation in the chloroplast (Figure 2-2, stage 4), the ER membrane LPAAT exhibit a strong preference for >C18 as its substrate esterifies a FA into the *sn*-2 position instead of C16 FA, such as the chloroplast LPAAT [57]. The resulting phosphatidic acid (PA) is converted to DAG or cytidine diphosphate diacylglycerol (CDP-DAG) via the PAP or cytidine diphosphate diacylglycerol synthase (CDS), respectively. DAG is then incorporated into >C18 lipids (PLs, BLs and TAGs). In contrast to PLs and TAGs, information regarding the biosynthesis of BLs is relatively scarce [26,35]. DGTS biosynthesis has been characterized for prokaryotes and eukaryotes. In prokaryotes, two enzyme systems, betaine lipid synthase A and B (BtaA and BtaB), role the DGTS production [26]. This mechanism appears to suffer some modifications in eukaryotes. In the microalgae *Chlamydomonas reinhardtii*, a single bifunctional enzyme, Bta1, which contains both BtaA- and BtaB-like domains, can carry out the complete synthesis [58]. In further research, Murakami *et al.* identified putative Bta1 homologs (Bta1L and Bta1S) in *N. oceanica* (Figure 2-2, stage 11) [59]. According to Vogel and Eichenberger, the *sn*-2 position of DGTS was predominantly attached to C18 FAs, suggesting that DGTS was synthesized mainly through the eukaryotic pathway in the ER. It has been also established that DGTS is the precursor of DGTA by de-carboxylation and re-carboxylation reactions [33]. Very few information appears to be known about the DGCC biosynthesis.

In the other branch CDP-DAG gives rise to PG and DPG [21,47,60]. As the higher plants, microalgal PG may be synthesized in at least three subcellular compartments, namely, the plastids, the ER, and the

mitochondria. The biosynthetic pathway in each organelle is essentially the same, i.e., PA is converted to CDP-DAG, which is then converted to PG trough phosphatidylglycerolphosphate synthase (PGPS) and protein tyrosine phosphatase mitochondrial 1 (PTPMT1) (Figure 2-2, stage 5). The ER-derived PG is desaturated, to yield more unsaturated molecular species (>C18), by desaturases (Δ) that are located in the ER (Figure 2-2, stage 12) [20]. Opposite to the PG that is synthesized in plastids and in the ER, the PG that is synthesized in mitochondria is used for the DPG biosynthesis, through PG and CDP-DAG arrangement by cardiolipin synthase (CLS) (Figure 2-2, stage 14) [31]. The origins of the fatty acids used for the biosynthesis of PG and DPG in mitochondria remain to be clarified. It seems likely that FAs, synthesized in plastids, or more unsaturated lipid species PA and CDP-DAG, synthesized in ER, are transported to mitochondria and then converted to PG and DPG [20].

ER-derived lipids could be transported to the inner envelope membrane (IEM) of chloroplasts to generate plastid lipids with >C18 FAs on the *sn*-2 position of glycerol backbones. There are multiple hypotheses that describe the mechanisms by which lipid transport occurs between the ER and the chloroplast inner envelope membrane; however, none of the hypotheses were described neither investigated in haptophytes [29]. Currently, evidence suggests that PA, PG, DGCC and CDP-DAG are transported from the ER to the IEM (Figure 2-2, from 13 stage to 15). Eichenberger and Gribi suggested that DGCC could be a candidate lipid species to shuttle FAs from the ER to the chloroplast IEM of *Diacronema lutheri*, since the relative content of betaine lipids (such as DGCC) is directly proportional to PUFAs content [35]. Membrane contact sites, vesicular transport, membrane hemifusion and proteins identified as chloroplast lipid transporters are the four mechanisms proposed for lipid transport [29]. When lipid backbones reached the chloroplast, PG and DPG are incorporated directly into membranes and PA is converted to DAG by plastidial PAP. Ultimately, DAG – esterified to a PUFA (>C18), such as EPA – is used by MGD (Figure 2-2, stage 6) and DGD synthases (Figure 2-2, stage 8) to form EPA-rich galactosylglycerides MGDG and DGDG [61].

An alternative non-oxygen dependent pathway for PUFA biosynthesis is known as PKS pathway (Figure 2-2, H). The polyketide synthases are subdivided into three types, I, II and III. Type I PKS and type II PKS have been identified in Haptophytes species *Emiliania huxleyi*, *Chrysochromulina polylepis* and *Prymnesium parvum*, and rely on the same four enzymes as the FAS pathway and can be completed with two isomerases (2.3i or 2.2i) [62–64]. The precursors of the PKS pathway are the same to those of the FAS pathway i.e., acetyl-CoA and malonyl-CoA. The ketoacyl-synthase (KS) and ketoacyl-reductase (KR) rule the addition of 2C while the dehydrogenase (DH) (alone or associated with the isomerases) and enoyl-

reductase (βER) are responsible for the C-C bond formation. EPA and DHA production through the FAS (in chloroplast) and n-3 and n-6 pathways (in ER), requires 21 and 26 NADPH units, respectively, whereas the PKS derived EPA and DHA (in chloroplast) consume 13 and 14 NADPH units, respectively. PKS pathway for PUFAs synthesis involves fewer intermediates and consumes less NADPH compared to n-3 and n-6 pathways; however it remains unknown which pathway is more active in Haptophytes species [65].

2.2.2.3 Lipid remodelling

In most microalgal species, LC-PUFAs are mainly accumulated in polar lipids, especially in phospholipids and glycolipids. These lipids maintain specific membrane functions and provide the permeability barrier surrounding the cells and between organelles. Both the nature of the polar headgroup and the length and saturation level of their FA chains influence the membrane's physical properties, such as fluidity, permeability, bilayer thickness, charge and intrinsic curvature [66,67]. Thus, LC-PUFAs, mainly EPA and DHA are essential to maintain the stability and function of membranes upon stress conditions as nutrient, temperature, salinity and light intensity shifts. Additionally, polar lipids act as a matrix for various metabolic processes as well as an intervenient in cellular signaling pathways (e.g., under stress conditions, DHA synthesis protect microalgal cells from oxidative damage) [68].

Several authors indicate that EPA and DHA partitioning into TAGs results from an expedite adjustment of the composition of the cell membranes in response to a stress condition. Specific parameters discussed below seem to initiate cell remodelling processes, where thylakoid membrane lipids are broken down and their constitutive n-3 PUFAs rebuilt into TAGs, avoiding a slower cycle of synthesis, assembly, and distribution (Figure 2-2, stage 16) [34,35,69–71]. Usually, EPA and DHA synthesis are elevated under favouring growth conditions – exponential growth phase – such as nitrogen and phosphorus repletion, most probably due to elevated synthesis of membranes in actively growing cells [35,71]. During exponential growth phase, *Diacronema lutheri* presented PLs, namely PG and DPG, and BLs as DHA-enriched lipids and GLs, mainly MGDG, as EPA-enriched lipids [24]. Hence, by changing cultivation parameters it might be possible to optimize the overall production and/or the fatty acid profile of membrane lipids.

PG and DPG are the major PLs in thylakoid membranes of *Diacronema lutheri*. PG can be used as a precursor of DPG located on the inner mitochondrial membrane that are required for proper functioning of the oxidative phosphorylation enzymes [72]. Variations in the DGDG/MGDG ratio could modify the stability of chloroplast membranes. When the expression level of MGDG was reduced, the electrical

conductivity of the thylakoid membrane increased, and consequently decrease the photoprotective effect of the thylakoid membrane. DGDG confers thermotolerance to microalgae due to its bilayer-stabilizing properties and along with PG, are involved in the binding of extrinsic proteins, stabilizing the manganese cluster in Photosystem II (PSII). MGDG and DGDG are non-ionic lipids while SQDG is a negatively charged glycolipid, composed of more saturated fatty acids and it is probably required to maintain the balance of negative charges in the thylakoid membranes [73].

Nitrogen (N) starvation has been considered as the most critical condition triggering neutral lipids (mainly TAG) accumulation. In general, under N-starvation, chlorophyll content decreases and photosynthetic capacity of PSII reaction centres was partially inhibited, thus inhibiting the light energy capture and inorganic carbon fixation. The activity of the four major enzymes of Kennedy pathway, GPAT, LPAAT, PAP and DAG acyltransferase (DGAT) are also constrained.

Therefore, without activation of *de novo* FA synthesis, TAGs are mainly assembled from membrane plastid-lipids hydrolysis [74–76]. On the contrary, under Phosphorus (P) starvation, neither light harvesting complexes nor PSII reaction centres appeared to be hindered, enhancing carbon fluxes to TAG assemble. This carbon accumulation occurs without massive degradation of essential membranes and maintaining a relatively high photosynthetic capacity. Both nutrient limitations contributed to TAG accumulation and LC-PUFAs partitioning to TAG in *Diacronema lutheri* [77]. Particularly P-starvation is also characterized by a replacement of phospholipids by glycolipids and/or betaine lipids since the predicted genes encoding SQDG synthase 1 (SQD1), MGDG synthase (MGD1), phosphatidate cytidylyltransferases (CDS) and betaine lipid synthesis enzymes (BTA1) were upregulated at the transcriptional level under P-limited conditions [75].

BLs functions sill lack a comprehensive understanding, in part, due to the variability of BLs fatty acid profiles among microalgae and in response to different stress conditions [78]. It has been proposed that, under phosphorous starvation conditions, microalgae increase their content in BLs, such as DGTS, associated to a reduction in PLs. Therefore, P used to membrane lipid synthesis are now pointed forward to other essential metabolic pathways – PLs are degraded to release cellular P and to provide DAG backbones for a part of DGTS synthesis. It is commonly accepted that DGTS replaces PLs to act in the adaption to a fluctuating environment in microalgae [79,80]. During N starvation, Yang *et al.*, demonstrated an increasing trend of DGTS was accompanied by TAG accumulation, in microalgae *Chlamydomonas reinhardtii* – thus acyl groups of BLs (i.e., DAGs backbones) may be employed for TAG synthesis [81].

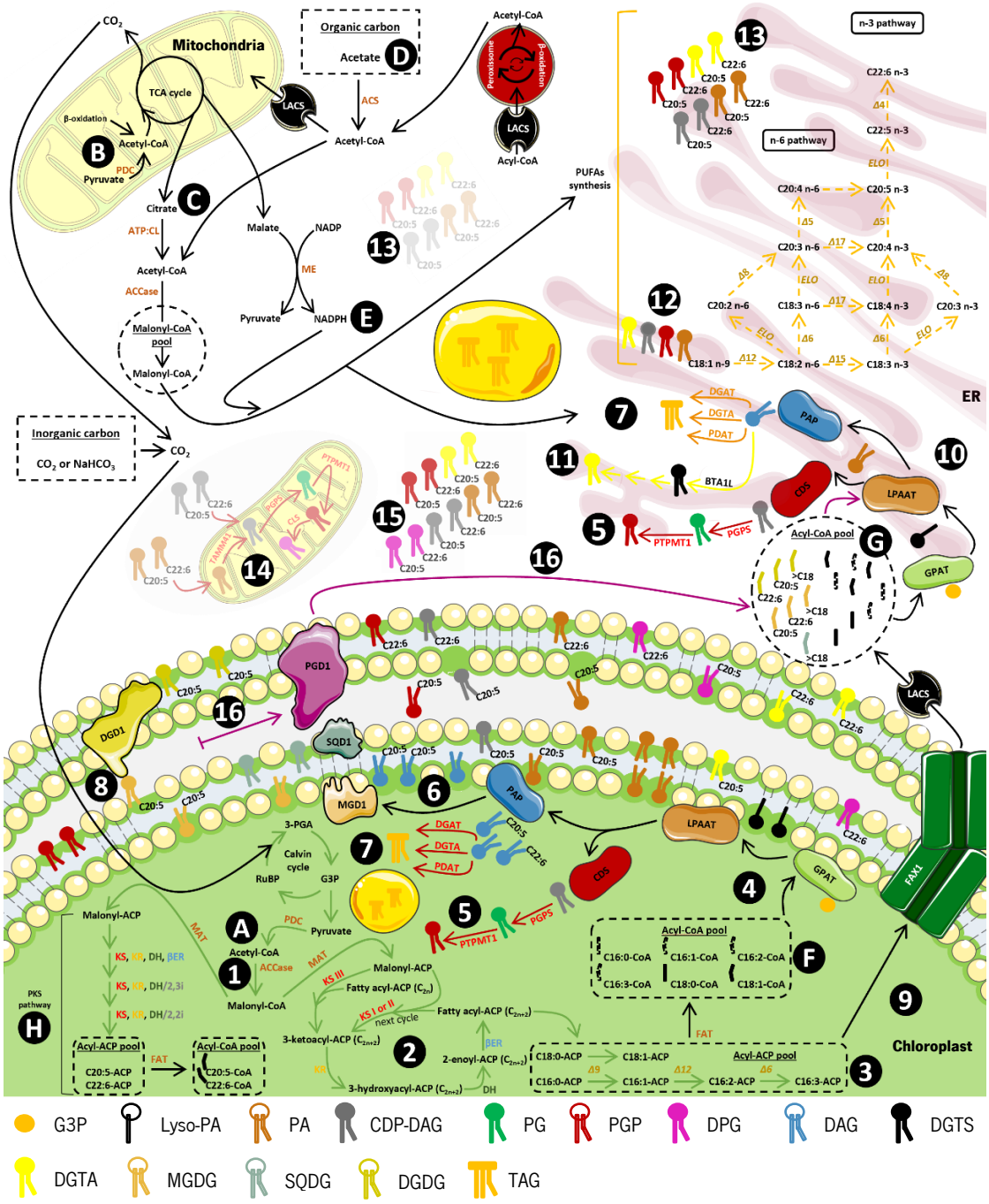

Figure 2-2: Overview of FA and LC-PUFAs synthesis in Haptophytes. Δ, desaturases; 2,2i, dehydrase 2-trans, 2-cis isomerase; 2,3i, dehydrase 2-trans, 3-cis isomerase; 3-PGA, 3-phosphoglyceric acid; ACCase, acetyl-CoA carboxylase; ACS, acyl-CoA synthetase; ATP:CL, ATP-citrate lyase; BTA1L, betaine lipid synthase 1; CDP-DAG, cytidine diphosphate diacylglycerol; CDS, cytidine diphosphate diacylglycerol synthase; CLS, cardiolipin synthase; DAG, diacylglycerol; DGAT, DAG acyltransferase; DGD1, digalactosyldiacylglycerol synthase 1; DGDG, digalactosyldiacylglycerol; DGTA, diacylglycerol: diacylglycerol transacylase; DGTA, diacylglycerylhydroxymethyl-trimethylalanine; DGTS, diacylglyceryl trimethylhomoserine; DH, β-hydroxylacyl-ACP dehydrase; DPG, diphosphatidylglycerol or cardiolipin; ELO, elongases; FAT, fatty acyl-ACP thiosterase; FAX1, fatty acid export 1; G3P, glyceraldehyde-3-phosphate; Glycerol-3-P, glycerol-3-phosphate; GPAT, glycerol-phosphate acyltransferase; KR, β-ketoacyl-ACP reductase; KS, β-ketoacyl-ACP synthase; LACS, long chain acyl-CoA synthetase; LPAAT, lyso-phosphatidic acid acyltransferase; MAT, malonyl-CoA:ACP transacylase; ME, malic enzyme; MGD1, monogalactosyldiacylglycerol synthase 1; MGDG, monogalactosyldiacylglycerol; PA, phosphatidic acid; PAP, phosphatidic acid phosphatase; PDAT, phospholipid:diacylglycerol acyltransferase; PDC, pyruvate dehydrogenase complex; PG, phosphatidylglycerol; PGD1, plastid galactolipid degradation 1 protein; PGP, phosphatidylglycerol phosphate; PGPS, phosphatidylglycerolphosphate synthase; PTPMT1, protein tyrosine phosphatase mitochondrial 1; RuBP, ribulose-1,5-biphosphate; SQD1, sulfoquinovosyldiacylglycerol synthase 1; SQDG, sulfoquinovosyldiacylglycerol; TAG, triacylglycerol; TAMM41, enzyme with CDS activity; βER, β-enoyl-ACP reductase.

On the other hand, some authors have suggested that BLs may be involved in the transfer of FAs from the ER to the chloroplast, as well as they may be the primary acceptor of *de novo* fatty acids before their processing and redistribution to other lipids [59,82]. It remains unclear if BLs can act as a source of DAGs to other lipids, given the ether bond in DGTS be much stronger than the phosphoryl ester bond in PC – ether bond is resistance to phospholipases C and D and no enzyme that cleaves this linkage has yet been identified [26].

2.3 STRUCTURAL CHARACTERISTICS OF CAROTENOIDS

Carotenoids are natural pigments with colour ranging from yellow to red. These pigments are isoprenoid compounds with C40 backbones [83]. Their isoprenoid carbon chain is terminated at both ends by cyclic ring structures, which contain a double bond and could be attached to oxygen functional groups (e.g., hydroxy groups). The strict hydrocarbon carotenoids without any substituent (or even oxygen) in their structures are known as carotenes, namely β-carotene (β-car) and lycopene. The oxygen-containing carotenoids are identified as xanthophylls – lutein and zeaxanthin are two xanthophylls with –OH groups in their structures, whereas astaxanthin has both –OH and =O groups in its structure [84]. Moreover, some carotenoids such as violaxanthin (Vx) and diadinoxanthin (Ddx) contain epoxy groups, and others such as fucoxanthin (Fx) has acetyl groups in its structure [85]. The hydrocarbon chain highly contributes to hydrophobic character of carotenoids; however, the presence of polar functional groups may modify the polarity of carotenoids and in turn influence their localization within biological membranes and their interactions with various molecules. The roles of carotenoids are predominantly determined by their size, geometry and presence of functional groups [86].

2.3.1 Carotenoids localization and function

Carotenoid distribution among microalgal cells is related to its function[5]. In plants and microalgae both thylakoids and chloroplast envelope are the two major places for localization of primary carotenoids [84]. Although mainly located in the photosynthetic apparatus, carotenoids are not restricted to photosynthetic membranes [87]. Regarding the non-photosynthetic secondary carotenoids, which its production is triggered under stress conditions, they are accumulated in plastidial lipid droplets, mainly composed by TAGs. It is important to note that microalgae may contain three distinct pools of lipid droplets in cell: 1) the cytoplasmatic lipid droplets, 2) the plastidial lipid droplets or plastoglobules and 3) the eyespot apparatus (EA) [88–92]. Currently, the distribution and composition of carotenoids on these components only be assessed for higher plants [84,87,93].

In the thylakoid membrane, carotenoids are commonly bound to pigment-protein complexes and are required as functional and structural components of the photosynthetic apparatus [93]. Photosystems I (PSI) and PSII are large pigment-protein complexes consisting of a reaction centre surrounded by antennae complexes (or light harvesting complex proteins, LHCI and LHCII) that harvest and transfer light energy to the reaction centres [84]. As occurs at higher plants, microalgae reaction centres (PSI and PSII core complexes) may be Chl *a* binding complex with significant amount of β-carotene while light harvesting complex proteins (LHCI and LHCII) seems contain, besides Chl *a*, c_1+ c_2 and β-carotene, Fx and low amounts of Ddx and diatoxanthin (Dtx) [87]. Opposite to the other carotenoids, diadinoxanthin and diatoxanthin are not strictly bound to protein complexes, they are also present as free pigments within thylakoid and chloroplast envelope membranes [84]. This is required for their enzymatic activity in the xanthophyll cycle (see Chapter 2.3.3).

Chloroplast envelope consists of the outer and inner chloroplast membranes. It is where part of carotenoid biosynthesis and the biosynthesis of GLs (MGDG, DGDG, SQDG), PLs (PG) and TAGs take place (see Chapter 2.3.2). The major carotenoids in these membranes may be the xanthophyll diadinoxanthin. Fucoxanthin and β-carotene could also be present [84].

Most flagellate microalgae displaying phototaxis hold a specialized light sensitive organelle, the EA. It enables an oriented movement response based on the direction and intensity of light. EA is a single orange-red structure formed by one or several layers of carotenoid-rich lipid globules (plastoglobules) within the chloroplast [91,94]. In fact, Kato *et al .,* shown that carotenoids in the eyespot apparatus are required for triggering phototaxis in phytoflagellate microalgae *Euglena gracilis* [91]. The major carotenoids of the EA also are species-specific. β-carotene is predominant in cells where the EA is located in a large and strongly pigmented chloroplast, , whereas cells with a less pigmented chloroplast have other predominant carotenoids (*e.g.* γ-carotene and lycopene) [94].

2.3.2 Synthesis of carotenoids

In cyanobacteria (*Synechocystis* sp.) and several microalgae genera (*e.g. Chlorella, Dunaliella* and *Phaeodactylum)* the biosynthesis of carotenoids follows the plastidial 2-C-methyl-D-erythriol 4-phosphate (MEP) pathway [95]. In chloroplast envelope, several nucleus-encoded membrane proteins are involved in the synthesis of carotenoids (Figure 2-3, stage 1 and 2) [96,97]. It was shown that most of the enzymes required for carotenoid biosynthesis are exclusively localized at envelope membranes [98,99]. However, the localization of carotenogenesis within envelope membranes is not yet clearly established. Some

evidence suggest that inner envelope membrane may be a site of carotenoid synthesis [100]. The produced carotenoids may be freely in the membrane lipids or in part, bound to outer-envelope proteins. Only xanthophyll cycle enzymes (Figure 2-3, stage 4) and phytoene desaturase (PDS) are found in thylakoids. The pigments transport mechanism towards the thylakoid remains unknown (Figure 2-3, stage 3) [100].

MEP pathway starts by adding pyruvate to G3P yielding 1-deoxy-D-xylulose 5-phosphate (DOXP) (Figure 2-3, stage 1). This reaction is catalysed by 1-deoxy-D-xylulose-5-phosphate synthase (DXS). In the second enzymatic step, DOXP-reductoisomerase (DXR) converts DOXP to MEP. The conversion of MEP into diphosphocytidylyl methylerythritol (CDP-ME), followed by its conversion to diphosphocytidylyl methylerythritol 2-phosphate (CDP-MEP), is regulated by CDP-ME synthase (CMS) and CDP-ME kinase (CMK), respectively. The following step requires the enzyme MEcDP synthase (MCS) to produce the cyclo-diphosphate-containing intermediate of the MEP pathway, methylerythritol 2,4-cyclodiphosphate (MEcPP). In the last two steps, MEcPP is converted into hydroxymethylbutenyl pyrophosphate (HMBPP) catalysed by HMBPP synthase (HDS) and then HMDPP is reduced to isopentenyl pyrophosphate (IPP) and dimethylallyl pyrophosphate (DMAPPp) by HMBPP reductase (HDR) [95,101].

The IPP or DMAPP (C_5 building block) initiate biosynthesis of carotenoids (C_{40} isoprenoids) due to chain elongation steps, which results into successive condensation of DMAPP to the growing polyprenyl pyrophosphate chain. IPP and DMAPP are isomerized by isopentenyl pyrophosphate isomerase (IPI). Chain elongation is catalysed by prenyl transferases that synthesize geranyl pyrophosphate (GPP, C_{10}), farnesyl pyrophosphate (FPP, C_{15}) or geranylgeranyl pyrophosphate (GGPP, C_{20}), which are the precursors of mono-, di-, and tri-terpenes and carotenoids. FPP (C_{15}) and GGPP (C_{20}) are the immediate precursors of C_{30} and C_{40} carotenoids [95,101].

The first step of carotenoid biosynthesis is the condensation of two molecules of GGPP to raise the first uncoloured carotenoid, phytoene, catalysed by phytoene synthase (PSY). There are many publications that review the carotenoid biosynthetic pathway in microalgae [84,95,97,101–107]. Therefore, aligning the reviewed data with carotenoids composition of *Diacronema lutheri*, *Pavlova gyrans* and *Pavlova pinguis* [10,108–111], it be feasible to theorize the carotenoid biosynthesis pathway in Haptophytes. Figure 2-3 represent an overview of carotenoids synthesis in Haptophytes.

2.3.3 Xanthophyll cycles

Xanthophyll cycles involve the de-epoxidation or epoxidation of xantophylls when microalgae are exposed to signficant changes in their culture parameters, such as light intensity and temperature. The main xanthophyll cycles known in microalgae are the Vx and the Ddx cycles. Microalgae containing the Ddx cycle include diatoms, haptophytes and dinophytes (Figure 2-3, stage 4) [112].

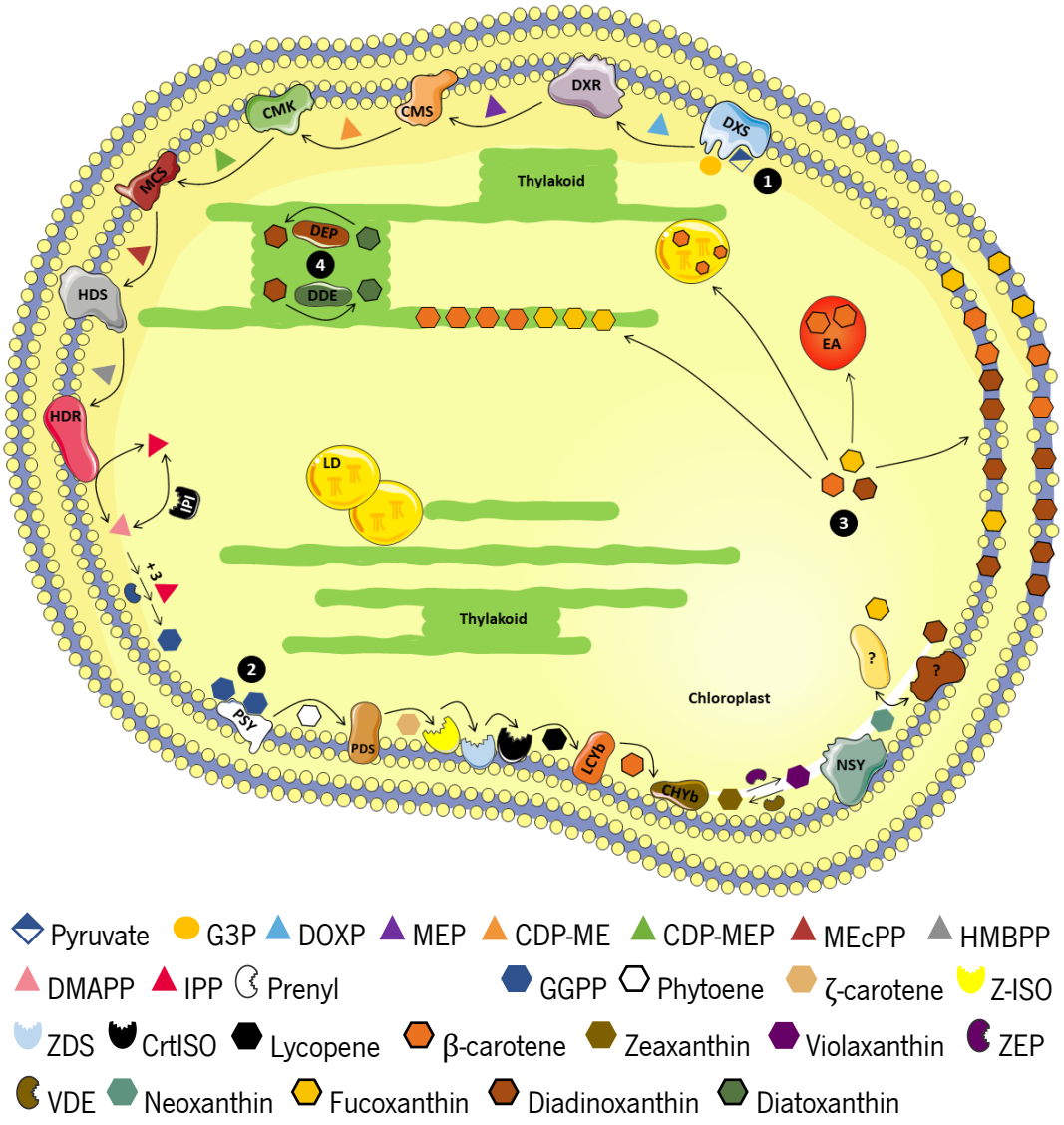

Figure 2-3: Overview of carotenoids synthesis in Haptophytes. ? - not described; CDP-ME, diphosphocytidylyl methylerythritol; CDP-MEP, diphosphocytidylyl methylerythritol 2-phosphate; CHYb, carotene β-hydroxylase; CMK, CDP-ME kinase; CMS, CDP-ME synthase; CrtISO, carotene isomerase; DDE, diadinoxanthin de-epoxidase; DEP, diatoxanthin epoxidase; DMAPP, dimethylallyl pyrophosphate; DOXP, 1-deoxy-D-xylulose 5-phosphate; DXR, DOXP-reductoisomerase; DXS, 1-deoxy-D-xylulose-5-phosphate synthase; EA, eyespot apparatus; G3P, glyceraldehyde-3-phosphate; GGPP, geranylgeranyl pyrophosphate; HDR, HMBPP reductase; HDS, HMBPP synthase; HMBPP, hydroxymethylbutenyl pyrophosphate; IPI, isopentenyl pyrophosphate isomerase; IPP, isopentenyl pyrophosphate; LCYb, lycopene β-cyclase; LD, lipid droplet; MCS, MEcDP synthase; MEcPP, methylerythritol 2,4-cyclodiphosphate; MEP, 2-C-methyl-D-erythriol 4-phosphate; NSY, neoxanthin synthase; PDS, phytoene desaturase; PSY, phytoene synthase; VDE, violaxanthin de-epoxidase; ZDS, ζ-carotene desaturase; ZEP, zeaxanthin epoxidase; Z-ISO, ζ-carotene isomerase.

During stress conditions (*e.g.* high illumination or temperature), the di-epoxy xanthophyll Ddx is de-epoxidized to Dtx (epoxy-free xantophyll) in the Ddx cycle, which requires the enzyme diadinoxanthin de-

epoxidase (DDE) and the cofactors: ascorbate and MGDG. This reaction is reversible when microalgae are again exposed to favourable conditions – the back reaction is catalysed by diatoxanthin epoxidase (DEP) and demands high concentrations of NADPH and O_2 in order to re-introduces one epoxy-group into Dtx, which results in Ddx regeneration [112].

High light intensity and temperature enhance the production of reactive oxygen species (ROS) and its diffusion in the thylakoid membrane. Therefore, the reduction in the rate of oxygen and ROS diffusion in the membrane has been identified as the major protect mechanism against damage of the photosynthetic apparatus [113]. It was established that under mentioned stress conditions the thylakoid membrane fluidity decreases, and consequently the membrane diffusion rate, due to increased xanthophyll cycles activity. The membrane rigidity was directly related to the conversion of Ddx to Dtx [114,115]. Additionally, the interaction of the LHCs, mainly LHCII and MGDG also plays a crucial role in establishing and maintaining the lipid bilayer structure. MGDG is the main lipid of thylakoid membranes and is required to solubilize the hydrophobic Ddx cycle pigments [115]. When present at high concentration in thylakoid membranes, MGDG forms non-bilayer inverted hexagonal phases, which may be located outside of the membrane bilayer, within the thylakoid lumen, or within the plane of the thylakoid membrane. These lipid phases surrounding the LHCs are where the de-epoxidases bind after their activation due to the thylakoid lumen acidification, and where the Ddx cycle occurs [116].

2.4 COMMERCIAL INTEREST OF PIGMENTS AND LIPIDS FROM MICROALGAE

Microalgae have been seen as a promising sustainable source of high added value bioactives such as pigments and lipids (Table 2-1). In fact, most of these valuable compounds are not produced by human organism, and their traditional sources present several drawbacks like the environmental impact, the presence of contaminants harmful for human health or are synthetically produced which hinders their use in human diet [117–119]. According to some market research reports, consumer awareness of a healthy lifestyle has led to a growing interest in using algae as a nutraceutical or food supplement, accounting for about 70 % of the value of the global algae-based products market in 2018 [120]. Continued research and development in the algae industry promises to maintain the growth trend seen in recent decades, with an estimated 6 % annual increase in the global algae products market value between 2018 and 2027, reaching around US$ 56.5 billion [120].

Regarding the importance of microalgae pigments, especially the carotenoids, their natural source and the powerful antioxidant activity described in protective mechanisms on microalgae, made these

carotenoids a target for up-scale production and extraction for further implementation in food, nutraceutical and pharmaceutical products. Unlike synthetic pigments, natural carotenoids are a mixture of the *trans* and the *cis* isomer forms. The *cis* form improves the solubility of these carotenoids, increasing the bioaccessibility from 2 to 6.7 times when compared to *trans* form [121]. In addition, natural carotenoids showed 14-55 times greater antioxidant power than the same synthetic form [119].

With the global market for carotenoids estimated to be worth US$ 2.0 billion in 2022 [122] and mainly produced via chemical synthesis, some of the most demanded and commercialized natural carotenoids are the β-carotene (US$ 300–1500 kg^{-1}- *Dunaliella*), fucoxanthin (US$ 180–42000 kg^{-1} - *Phaeodactylum*), astaxanthin (US$ 200–7000 kg^{-1} – *Haematococcus*) and lutein (US$ 910–15000 kg^{-1} – *Scenedesmus, Muriellopsis, Chlorella*) [123,124]. As reported in Figure 2-4, several health benefits of these pigments have been described in literature. For instance, fucoxanthin, a carotenoid widely distributed in Pavlovophyceae species [10], is known to prevent and treat chronic diseases such as cancer, diabetes and obesity [125,126].

Regarding the lipid compounds, special interest in the PUFAs fraction from microalgae has been highlighted, especially the essential fatty acids EPA and DHA. They are incorporated in various body parts, namely cell membranes where they play important roles related to flexibility and anti-inflammatory processes of cells, Figure 2-4. They are essential to the appropriate fetal development and healthy growth and act as precursors of several metabolites (*e.g.* resolvins and protectins), which are considered potent beneficial lipid mediators in prevention or treatment of mental health disorders dementia, Alzheimer's disease [144,145]. In European countries the mean intake of these fatty acids varies according to sex, age group, and dietary habits.

Based on cardiovascular risk diseases, EFSA recommends a daily intake between 250 and 500 mg of EPA and DHA, a value much higher than the current intake verified in several European populations (25-100 mg n-3 PUFAs.day^{-1}) [146]. The DHA is also a key component of all cell membranes and it's abundantly present in the brain and retina, promoting efficient visual and neural development of the fetus, as well as prevents perinatal maternal depression [147,148].

In contrast to n-6 FAs, the presence of n-3 FAs in the human diet has become scarce due to the massification of the food industry during the 20th century. In Western diets there is an estimated >15-fold increase in the consumption of n-6 FAs compared to the ancestral diet [14,149,150].

Table 2-1: Biochemical composition of microalgae and common food sources for the human diet

Microalgae	Lipid content (% DW)	n-3 PUFAs (% DW)	Carotenoids (%DW)	Chlorophyll (%DW)	Ref.
Pavlova sp. (Haptophyta)	21.87 - 25.11	***DHA***: 0.267 - 1.32 16.4 [c] / ***EPA:*** 0.473 - 1.8 34.2 [c] / ***ALA:*** 0.118 - 0.180	***Fucox.:*** 0.181 - 0.735[d] / ***Diatox.:*** 0.027 - 0.104[d] / ***Diadin.:*** 0.098 - 0.594[d] / ***β-car:*** 0.025 - 0.092[d]	***Chl a:*** 61.0 - 97.7[e] / ***Chl c:*** 0.084 - 0.232[d]	[5,6,17–20]
Diacronema sp. (Haptophyta)	35.5 12 - 50.14[b]	***DHA:*** 0.85 - 10 5.6 - 11.2 [c] / ***EPA:*** 1.93 - 25 11.0 - 27.6 [c] / ***ALA:*** 0.6 - 2.3[c]	***Fucox.:*** 6.0 - 16.8[a] / ***Diatox.:*** 0 - 8.5[a] / ***Diadin.:*** 13.9 - 37.4[a] / ***β-car.:*** 8.1 - 46.9[a]	***Chl a:*** 17.9 - 36.8[a]; 0.117 - 0.840[b] / ***Chl c:*** 6.1 - 12.2[a]	[21–24]
Tisochrysis sp (Haptophyta)	8.473 - 15.739	***DHA:*** 0.858 - 2.586	***Fucox.:*** 0.394 - 1.309	***Chl a:*** 0.487 - 1.894	[25,26]
Isochrysis sp (Haptophyta)	22.4 - 27.4	***DHA:*** 1.58 / ***EPA:*** 0.08 / ***ALA:*** 0.38	***Fucox.:*** 0.223 - 1.643 / ***Diatox.:*** 0.040 / ***Diadin.:*** 0.025 / ***β-car.:*** 0.053	***Chl a:*** 0.106 / ***Chl c:*** 0.196	[17,22,27,28]
Nannochloropsis sp. (Chlorophyta)	24.4 - 35.7	***EPA:*** 2.34 / ***ALA:*** 0.05	***Violax.:*** 0.337 / ***Zeax.:*** 0.010 / ***β-car.:*** 0.100	***Chl a:*** 0.08 - 2.1	[17,21,22,29,30]
Phaeodactylum sp. (Bacillariophyta)	18.7	***DHA:*** 1.32 / ***EPA:*** 2.84 / ***ALA:*** 0.03	***Fucox.:*** 0.220 - 1.270 / ***Diatox.:*** 0.044 ***Diadin.:*** 0.032 - 0.377 / ***β-car.:*** 0.006 - 0.055	***Chl a:*** 0.237 - 1.211 / ***Chl c$_2$:*** 0.033 - 0.199	[17,22,27,31]
Dunaliella sp. (Chlorophyta)	9.2 - 24.3	***ALA:*** 0.03 - 3.0	***β-car.:*** 0.485 - 10	***Chl a:*** 0.6 – 2 / ***Chl b:*** 0.3 - 1.3	[32,33]
Fish	0.2 - 12	***DHA:*** 0.040 - 1.610/ ***EPA:*** 0.003 - 0.448/ ***ALA:*** 0 - 0.230	n.d.	n.d.	[34]
Carrot	n.d.	n.d.	***β-car.:*** 0.101 - 0.128	n.d.	[35]
Spinach	n.d.	n.d.	***Lutein:*** 0.167 - 0.219 / ***β-car.:*** 0.148 - 0.185	***Chl a:*** 1.19 / ***Chl b:*** 0.32	[35]

[a] % molar; [b] %AFDW; [c] % w/w lipids; [d] Pigments to chl *a* ratios (mol: mol); [e] $\mu g.L^{-1}$; n.d.: not described. Pavlovophyceae species – underlined in yellow

Among the main changes responsible for such a low intake of n-3 FAs are the widespread use of vegetable oils rich in n-6 FAs (*e.g.* oilseed oil, soybean oil) as cooking oils, the high consumption of cereals (mainly rice, corn and wheat), the substitution of natural dietary supplements rich in n-3 FAs (cod liver oil) for synthetic ones (vitamin A and D), the intensive production of livestock fed mainly on cereals instead of grass, and the lower n-3 FAs content of foods produced by the agri-food industry compared to their wild counterparts [149–151]. This imbalance in dietary intake has been linked to various health problems such as inflammatory diseases, cancer, and cardiovascular disease, highlighting the importance of a balanced diet with proper EPA and DHA supplementation [151].

The global n-3 fatty acids market was valued at US$ 3.3 billion in 2017 and with an annual growth rate of 14.7%, it is estimated to reach US$ 9.8 billion by 2025 [152]. The food industry to meet the increased demand for n-3 PUFAs has been developing products enriched with n-3 PUFAs, such as milk, cheese, yogurts, bakery products, infant formulas, eggs and meat [153]. However, most solutions deal with some drawbacks regarding consumer acceptance and health safety. The main source of n-3 PUFAs is strongly associated with fish and fish oil, which have as problems the potential prevalence of contaminants (methylmercury and dioxins in fish) as well as the inability to be used in vegan and vegetarian diets [153].

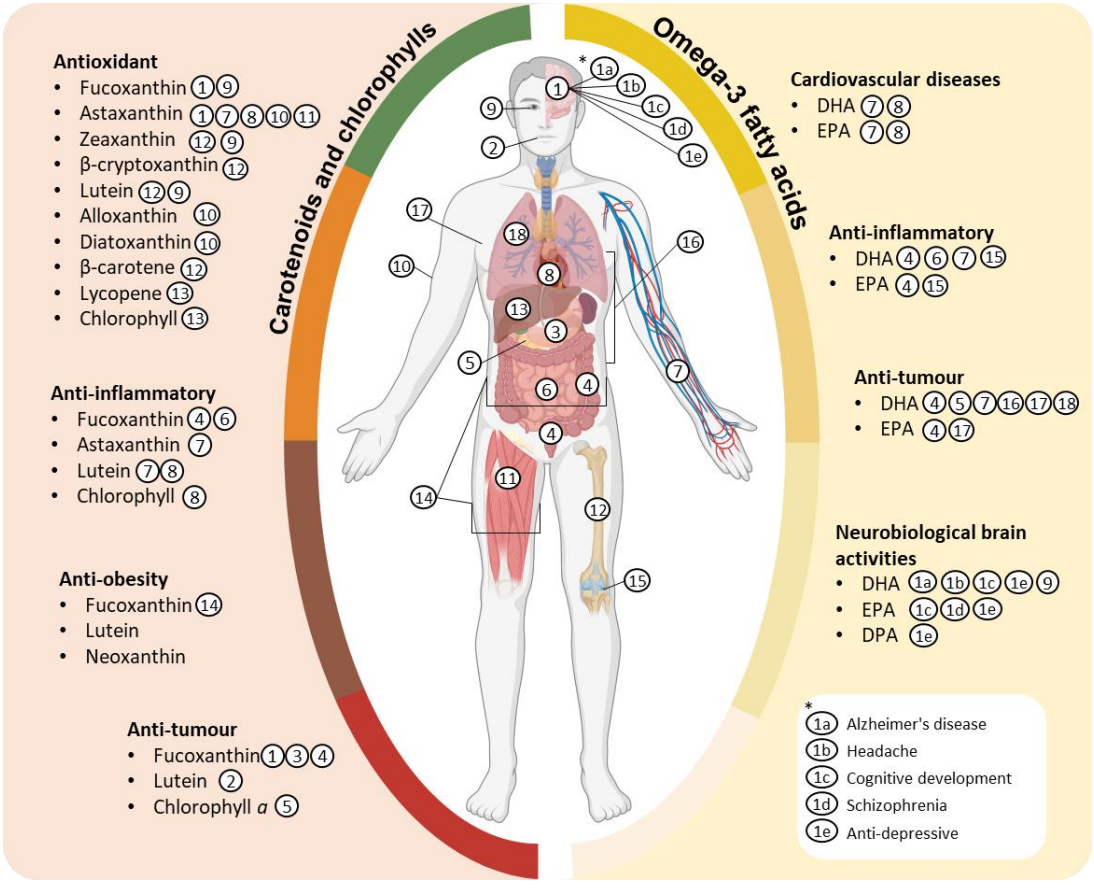

Figure 2-4:Effects of omega-3 fatty acid and carotenoid supplementation on human health [15,49–75].

In order to overcome these drawbacks, several species of microalgae, as presented in the Table 2-1, have been presented as an alternative, productive and sustainable source of these biocompounds [4,154].

2.5 EFFECT OF ABIOTIC FACTORS ON MICROALGAE BIOMASS PRODUCTION AND ITS BIOCHEMICAL PROFILE

In the last decades, microalgae have been recognized as a promising resource to address some of the most challenging problems of the world population since i) they are a key player against the climate changes due to high carbon dioxide fixation, ii) a bioremediation agent of pollutant wastewaters, and iii) a bioactive rich source for pharmaceutical and nutritional applications. However, the worldwide production and market implementation of microalgae products remains strongly affected by the cost associated to its manufacture. An effort has been done to identify microalgae species with promising features for industry application and, at the same time, identify the main up- and downstream parameters that influence the biomass production, the biocompounds profile and the economic feasibility at large-scale production. Considering the upstream parameters, the impact assessment of the abiotic factors such as nutrient availability (macro- and micronutrients concentration), temperature, pH value, CO_2 concentration, and the light quality and intensity has been the research subject in several species, to maximize the biomass production and understand the mechanisms underlying the production and accumulation of bioactive compounds, namely, lipids and pigments.

2.5.1 Temperature

Temperature has an important role in the biomass productivity and modulation of bioactives composition of microalgae. Although in some cases changing the temperature did not affect the final cell density, increase from 15 to 25 °C improved the biomass productivity, shortening by five days the time needed to reach the stationary phase of *D. lutheri* [34]. In addition to illumination, temperature is one of the factors which greatly impacts the performance of microalgal growth in outdoor cultivations, as demonstrated by the decreased biomass productivity with *P. viridis* when cultured under low irradiance and low temperature [182]. However, the response to changes in growth temperature is species-dependent, as exhibited by *D. vlkanium*, in which higher temperatures (18 vs 26 °C) limited the maximum specific growth rate and promoted a marked decrease in the cell density (5- fold) (18 vs 26 °C) [183]. On the other hand, *Pavlova* OPMS 30543 showed higher growth performance with increasing temperatures, over the range of 15-35 °C, reaching 3.32 g $DW.L^{-1}$ after 6 days at 35 °C [184]. Regardless the high- or low-light intensity applied, *D. lutheri* produced the highest nitrate consumption, the maximum

cell densities and maximum average growth rates when grown with intermediate temperature (12 and 18 °C) in contrast with 8 and 28 °C. Cultivation under high temperature and high light promoted fully inhibition of this species [185]. In fact, temperature was shown to have a more pronounced effect on final X_{max} than light intensity, and the opposite was verified for μ_{max} [186]. The understanding of the heat stress on microalgae has been highlighted as a crucial stage to successful implementation of at industrial scale, being necessary to assess their thermal tolerance within a wide range of temperature to simulate the outdoor conditions. The decreasing of photosynthetic activity or even the cell death with increasing temperatures has been associated to membrane denaturation or enzymatic degradation, which greatly impacts the cell viability and the economic feasibility of algal production. For instance, the viability and photosynthetic activity of *Dunaliella salina* were strongly affected when exposed to temperatures above 43 °C, promoting productivity losses of 35-40 % when grown outdoors without efficient temperature control [187]. According to the intensity of thermal stress, the decrease of photosynthetic activity can be attributed to i) the inactivation of thermosensitive PS II which, among others, is promoted by the dissociation of protein/cofactor complexes, production of ROS and fluidity changes on thylakoid membranes as well as the ii) reduced affinity of Rubisco for CO_2, reducing the biomass production [188].The identification of species that are thermotolerant to diurnal temperature variations is a sustainable option compared to the development of reactors and cooling systems to reduce the cost and losses of biomass production. Barten et al. 2021 [189], estimated a 26.2 % reduction in industrial operating costs by using the thermotolerant microalgae *Picochlorum* sp. which is able to grow optimally at a daytime temperature of 40 °C. As a response to different temperatures, microalgae alter the lipid and fatty acid composition as an adaptation response. At lower temperatures, *D. lutheri* increased the content of BLs (4-fold), PG and SQDG, while reduced the MGDG and, specially, the TAG content. Lowering the growth temperature of *D. lutheri* and *D. vlkanium*, the SFAs and MUFAs fraction decreased, whereas the LC-PUFAs (EPA and DHA) fraction increased [34,183]. The increase of EPA at a lower temperature was noticeable in all lipid fractions (TAG, MGDG, SQDG and BL), in contrast with DHA which increases solely in TAG and BL [34]. Similar response was attained regarding the TAG and LC-PUFA content of *P. viridis* when was cultured in the outdoor 60 L photobioreactor with different temperature and illumination profiles [182]. Likewise, the decrease of temperature growth had a positive effect on microalgae accumulation of other lipid soluble compounds, such as α-tocopherol in *D. vlkanium* with a >3-fold gain in late exponential phase between 18 and 26 °C [183], as well as the increasing content of 4-desmethyl sterols in *P. salina* [190]. *D. lutheri* grown under sub-optimal temperatures resulted in total or partial growth inhibition, implying a reduced content of TFA thanks to the low assimilation of nitrate from the

extracellular medium. The highest fraction of PUFAs - 39.7 % - was achieved in the mid-exponential phase at 12 °C and 40 μmol photons·m^{-2}·s^{-1}, whereas the highest content of EPA (19.3 mg·g^{-1} AFDW) and DHA (8.5 mg·g^{-1} AFDW) was observed after nitrate depletion at 18 °C. Such growth temperature and nitrate depletion promoted the highest membrane lipid turnover, TAG accumulation, and superior partition of EPA and DHA from PL to TAG in *D. lutheri* [70]. The decrease in both lipid fraction and unsaturation of fatty acids with increasing temperatures has been described as the adaptive mechanism of microalgae cells to stabilize the cell membrane by reducing its fluidity [189]. Similarly, when exposed to lower temperatures (10 °C) *C. reinhardtii* increased the biosynthesis and accumulation of LC-PUFA (66 %TFA), especially alpha-linolenic acid (44 %TFA), to increase membrane fluidity under these culture conditions, which showed an adverse effect on the biomass and lipid productivity [191]. Despite the lack of variation in the fatty acid profile, one day under high temperature stimulation (40 °C) promoted a 40 % increase in the lipid content of *Scenedesmus quadricauda* [192].

Temperature had also been shown as an abiotic factor able to modulate the pigment composition in microalgae. *D. vlkanium* was strongly affected by the increase of 8 °C on temperature culture, with the carotenoid and chlorophyll *a* concentration decreasing from 6.5 to 2.1 mg g^{-1} DW and from 3.0 to 1.5 mg g^{-1} DW, respectively. This factor also impacted then carotenoids profile, which comprised a 10 % gain in astaxanthin and depletion of lutein when cultured at higher temperature [183]. The increase of growth temperature also reduced the total pigments, carotenoids and chlorophylls of *D. lutheri* but solely when grown in high light conditions (200 μmol photons·m^{-2}·s^{-1}) [70]. However, opposite results were presented by Carvalho et al. [193] where temperature was suggested as an inducer of carotenogenesis, leading to higher contents of carotenoids and chlorophyll *a* in the whole set of light intensities tested [193]. The increment of total chlorophyll in *Dunaliella viridis* when the temperature raised from 25 to 35 °C was linked with the up-regulation of PSI and PSII subunit related genes and increased transcript levels of LHC proteins after the heat stress [194]. Nitrogen starved *Chlorococcum* sp. nearly doubled the astaxanthin (6.8-11.6%) and secondary carotenoid content (4.4-8.4 mg g^{-1} DW) when the growth temperature increased from 20 to 35 °C, suggesting better performance at higher temperatures of enzymes involved in keto-carotenoids biosynthesis [195]. Despite the known importance of carotenoids as an antioxidant agent under stress conditions for microalgae cells, increasing growth temperature did not always produce an increase in these pigments. The lutein and violaxanthin content of *Picochlorum* sp. remained constant with increasing diurnal temperatures, while the content of important ROS scavengers, antheraxanthin and zeaxanthin, decreased [189].

2.5.2 Salinity

Salinity variation in growth medium impact the photosynthetic activity and biochemical profile of microalgae. The importance of this abiotic factor is normally linked to the effect of micronutrients, such as sodium, which are a threat to microalgae when its composition reaches toxic levels [196]. For instance, saline variations affect the cell membrane stability and fluidity [197], cell motility and morphology, as well as reduces or even ceases photosynthetic activity [198]. Salt can damage PSII and PSI due to the production of ROS and alter the protein profile in PSII reaction centres that will reduce electron transport to the plastoquinone pool [198].

Changes in salinity media can greatly modify the biomass production and biochemical composition of microalgae. The absence of seawater fully inhibited the growth of *Pavlova* OPMS 30543, probably due to the low levels of Ca^{2+} and Mg^{2+} in culture media, whereas the remaining concentrations tested (25-100 % seawater) presented comparable biomass productivities, with the highest content of 6.16 g $DW.L^{-1}$ achieved with 50 % seawater [184]. Similarly, *D. lutheri* grown at higher NaCl concentrations (35 and 40 ppt) promoted higher lipid content and biomass formation (X_{max}: 0.026-0.025 $g.L^{-1} d^{-1}$, respectively) compared with 15, 20, 25 ppt NaCl (X_{max}:0.007-0.014 $g.L^{-1} d^{-1}$) [199]. *D. lutheri* cultures grown at 35‰ salinity did not vary their final composition and sterol content when submitted to osmotic shock by changing the salt medium concentration to 15, 25, 35 or 45‰ [200]. However, the main variations in sterol profile were triggered immediately after the changes in salt concentration and only occurred until the full adaptation of the cell membrane to the new salinity levels [200]. On the other hand, the sterol content of *D. vlkanium* was reduced by 70 % when salinity increased from 5 to 50, regardless of growth stage [201].

The hypersaline media also promoted a strong decrease of the antioxidant capacity, chlorophyll *a* and lipid content of *Diacronema vlkanium* [201]. Between the tested salinities (5, 20, 35 and 50 ppt) the intermediate concentrations produced the higher cell densities, while increasing salinity promoted growth retardation or even cessation (50 ppt) during the lag phase. Concerning the lipid classes, cultures with salinity of 50 ppt produced higher percentage of TAGs, MGDG, DGDG, PG, and sterol esters, in opposite to the lowest content of SL and DGTA lipids. The hypersaline condition proved to negatively impact the nutritional value of the microalgae mostly due to lower content of EPA and DHA [201]. Likewise, the saline stress of 400 mM NaCl was described as an interesting tool to promote the oxidative stress in *Scenedesmus* sp., which increased lipid content up to 33 % and 25 % in batch grown cultures and after a two-stage cultivation with duration of 3 days, respectively. As an acclimatization process to resist the

osmotic shock promoted by the salinity variation, the stressed cells showed a different lipid composition than the untreated cells, namely higher content of neutral lipids (75-76 % vs 67 %) and reduction of glycolipid fraction (7-11 % vs 17 %) which reduced the permeability and fluidity of the cell membrane [202].

Overall, cultures enriched with salt concentrations of 5 to 25 mM NaCl, KCl, MgCl2 or $CaCl_2$ produced a lower biomass content than control cultures of *Chlorella* sp. (0 mM), while in *Desmodemus* sp. a slight increase of biomass was only described with 20-25 mM of KCl and, specially, with the 25 mM of $CaCl_2$. The increasing salt concentrations reduced the chlorophyll content of both species, with a more pronounced effect on *Chlorella* sp. Moreover, the authors highlighted the positive effect of $CaCl_2$ treated cultures on the final lipid content and composition, suggesting the important role of Ca^{2+} in the signaling pathway for lipid production. Supplementation of *Chlorella* sp. with 25 mM $CaCl_2$ increased the lipid and oleic acid content up to 40 % and 64 %, respectively, whereas the *Desmodemus* sp. treated with 5 mM $CaCl_2$ reached 45 % of lipid content and 53 % of oleic acid [203].

The importance of salinity in improving biomass production and, consequently, its fucoxanthin content was described in two halotolerants and four marine microalgae [204]. According to species, the higher content of fucoxanthin in the marine microalgae *Chaetoceros muelleri, Pheodactylum tricornutum, Chrysotila carterae* and *Tisochrysis lutea* ranged from 1.04 to 2.92 mg g^{-1} AFDW, and were achieved when grown at lower NaCl concentrations (35 to 45‰, ppt). Regarding the halotolerants species, the maximum content of fucoxanthin in *Amphora* sp. was 1.21 mg g^{-1} AFDW at 85‰, while the *Navicula* sp, was 1.49 mg g^{-1} AFDW at 75‰. These values were strictly dependent of the saline conditions applied, whose values in the halotolerant species dropped up to 80 % of the optimal fucoxanthin content under non-optimal NaCl concentrations. Significant productivity losses (>90%) were also described for the marine species when grown at salinity levels > 45‰ [204]. On the other hand, the raise of NaCl concentration from 0 to 400 mM reduced, in dose dependent manner, the photosynthetic activity in cultures of freshwater *Scenedesmus* sp, decreasing the chlorophyll from 10.53 to 1.84 ug.mL^{-1} and carotenoids from 1.36 to 0.41 ug.mL^{-1}, respectively [202].

2.5.3 Illumination

Considered as the most limiting factor to photosynthesis in the ocean [205], without the light energy the photoautotrophs are disabled to produce the indispensable chemical energy - adenosine triphosphate (ATP) and the reduced form of nicotinamide adenine dinucleotide phosphate (NADPH) - to reduce CO_2 for

further carbohydrates synthesis [206]. Furthermore, this abiotic factor exerts an important role in the modulation of several enzymatic processes, that affect the cell growth as well as the biochemical composition, such as the elongation of FAs and their partition in different lipid classes [207].

Several studies have pointed out the importance of the light intensity on Pavlovophyceae species [69,70,110,186,208]. Regardless the dilution rate tested, the increase of light intensity from 75 to 120 $\mu E.m^{-2}.s^{-1}$ positively affected the cell growth and the lipid content in continuous cultures of *D. lutheri*, while the variation in EPA content was mainly attributed to the different dilution rates and CO_2 levels [208]. Growth rates of eleven haptophytes increased significantly with increasing light intensities from 60 to 350 $\mu mol\ photons \cdot m^{-2} \cdot s^{-1}$ [110]. The lipid content of *D. lutheri* supplemented with $NaHCO_3$ increased at higher irradiances (100–340 $\mu mol\ photons \cdot m^{-2} \cdot s^{-1}$) compared to growth-limiting irradiance (20 $\mu mol\ photons \cdot m^{-2} \cdot s^{-1}$), while the growth rate was favored by the intermediate irradiation (0.173-0.181 d^{-1}) compared to the upper and lower irradiation level (0.111-0.145 d^{-1}) [185]. Opposite trend was stated in other study with this species, with a ≈2-fold decrease on the lipid content when illumination increased from 9 to 30 $W.m^{-2}$ [69]. The increase of light intensity from 9 to 19 Wm^{-2} in *D. lutheri* promoted an accentuated gain of the TAG fraction from 23 to 78 % TFA. The content of some polar lipids associated with cell membranes or thylakoids showed a negative correlation with the increase in illumination from 9 to 30 Wm-2, such as the decreasing content of MGDG (≈18-fold), PGs (≈3-fold) and BLs (≈2-fold) [69]. Similar trends between TAG and PL were verified in *D. lutheri* cultures [70].

The variations in lipid classes through the different light intensities promote changes in fatty acid composition. With increasing irradiances, there was an increase of TAG content in *D. lutheri*, which had as dominant fatty acids C14:0, C16:0 and C16:1(n-7). At low light intensities was reported an increased accumulation of lipids in photosynthetic membranes and the predominance of C20:5(n-3) and C18:4(n-3) [69]. Similar trends were stated in the mid-exponential growth phase of *D. lutheri*, with increasing content of EPA under low illumination and higher SFA and DHA at high intensities [185]. In nitrate-limited cultures of *D. lutheri* grown at 12 °C, the highest level of EPA (20.5%) and DHA (9.6%) were attained at 40 and 200 $\mu mol\ photons \cdot m^{-2} \cdot s^{-1}$, respectively [70].

The light intensity also proved to be able to stimulate the accumulation and/or the partition of different LC-PUFA from PL to TAG fraction, a mechanism reported in a limited number of species beyond the *D. lutheri* [77]. The partitioning of EPA and DHA into TAGs in nitrate-limited cultures was influenced by light intensity, with the highest EPA content (14.7 $mg\text{-}g^{-1}$ AFDW) achieved at low light intensity, while the highest DHA content was reached at high light intensity (6.9 $mg\text{-}g^{-1}$ AFDW) [70]. Guihéneuf et al. [207], suggested

that low illumination induced the gene expression of desaturases and elongases, such as Δ17 desaturation, Δ5-elongation and Δ4-desaturation, which are the main responsible for the higher level of FA unsaturation, and thus the higher levels of EPA and DHA. Similarly, the authors also suggested that this modulatory role extends to the gene expression of enzymes, acyltransferases, which are responsible for the possible partition of EPA into TAG at low irradiance [207].

The variation in light intensity also affects the pigment profile and content of microalgae. Normally, the chlorophyll content of microalgae, as well as some polar lipids present in the thylakoid membranes, decreased with increasing illumination due to a down-regulation of chloroplast activity [69]. The cellular Chl *a* content of *D. lutheri* was higher when cultured at reduced irradiance (20 µmol photons·m^{-2}·s^{-1}) [185]. The increase from 40 to 200 µmol photons·m^{-2}·s^{-1} decreased the total pigments content regardless the temperature and nutrient conditions. Increased illumination had an opposite effect between the fraction of chlorophylls and the carotenoids, with the latter increasing its content, mainly due to the increased concentration of the photoprotective pigments β-carotene and diadinoxanthin [70].

Pigment patterns of eleven haptophytes were evaluated at three different illumination levels (60, 110 and 350 µmol photons m^{-2}·s^{-1}) [110]. The authors suggested as the main trends the decrease in the pigment ratios of chlorophyll *c*/chlorophyll *a* and fucoxanthin/chlorophyll *a* with increasing light. In fact, the highest light intensity does not promote an increase of photoprotective carotenoids. The authors highlighted the effect of the light in chlorophyll *c* pool and fucoxanthin pool, where the former was mainly composed of chlorophyll c_3 at low light, while chlorophyll c_2 was predominant at higher light intensities [110].

In addition to the effect of intensity, several studies have evaluated the effect of light quality on microalgae. *D. lutheri* cells treated with UV-C radiation at 100 mJ.m^2 had doubled their sterols content (20.3 mg.g^{-1} DW) [209]. UV-C radiation generated oxidative stress, inducing the overproduction of sterols, such as poriferasterol, epicampesterol, methylergostenol, fungisterol, dihydrochondrillasterol and chondrillasterol to restore the membrane integrity and quench the ROS [209]. Furthermore, UV-C radiation (10 mJ.cm^2) raised the EPA level up to 12.6 % of TFA in *D. lutheri* [210]. However, opposite trends were described in *D. lutheri* when exposed to UV-A and UV-B radiation [211]. The growth softened and the chlorophyll *a* content slightly decreased after 8 days of UV treatment, while photochemical efficiency of *D. lutheri* reduced significantly (22-40%) after UV radiation. The UV treatment led to a reduction of 20 % in EPA and 16 % in DHA levels after 8 days, which was probably attributed to FAs peroxidation, decreasing the presence of EPA and DHA in glycolipids and phospholipids, respectively. *Odontella aurita,* on the other

hand, proved to be a more resistant species since its biochemical composition did not change after UV exposure [211].

According to the species-specific pigment composition of microalgae, application of light-emitting diodes (LED) as illumination source has been highlighted as a promising and cost-effective approach to improve the microalgae growth and, depending on the optimal light wavelength, modulate the production of important bioactives. Kim et al. [212] implemented a two-stage growth system using different LED wavelengths. In the first stage, the highest biomass contents of *D. lutheri, P. cruentum* and *C. vulgaris* were achieved by blue (465 nm), green (520 nm) and red (625 nm) LED wavelengths, respectively. In the second stage, the LED wavelength was changed to yellow in *D. lutheri*, green in *C. vulgaris* and red in *P. cruentum* which promoted the highest lipid and PUFA content. *Botryococcus braunii* grown with the combination of 80 % red and 20 % blue LED illumination achieved the highest lipid content and the highest level of PUFA [213]. This strategy also proved useful for maximizing the cell growth and boost the accumulation of fucoxanthin on *Odontella aurita* grown in a photobioreactor with a red:blue light ratio of 8:2 [214].

2.5.4 Nitrogen

Several studies have pointed out nitrogen as a crucial macronutrient for microalgae, with a marked impact on the metabolic behavior of microalgae, which can vary according to its source and its level in the culture medium. For instance, it's widely accepted that nitrogen limitation decreases the cellular content of thylakoid membrane, promotes the phospholipid hydrolysis and activates acyl hydrolase to degrade glycolipids. Consequently, these changes may rise the intracellular content of fatty acid acyl-CoA, which in nitrogen-depleted conditions are converted by the diacylglycerol acyltransferase into TAG, increasing the lipid and TAG content in microalgae [215].

Regardless the importance of temperature and light, the nutrient composition, namely the depletion of nitrogen, was the main driver to regulate the synthesis of TFA in *D. lutheri*. This condition promoted a 1.6- to 3.7-fold increase in the level of TAG, whose composition reached the maximum EPA and DHA contents [70]. Similar behavior was described in the same species, supplemented with different bicarbonate concentrations, whose TAG percentage increased from 29–42 % of TFA to 54–74 % after N-depletion. This condition induced alterations in TFA profile, namely an increase of SFA and MUFA through the increment of C16:0 and C16:1 n-7, and at same time reduced proportion of PUFA, such as C18:4 n-3, EPA and DHA [216].

Several nitrogen sources have been used for microalgae growth, such as $NaNO_3$, KNO_3, $CO(NH_2)_2$, NH_4Cl, NH_4NO_3, NH_4HCO_3, CH_3COONH_4, glycine, and yeast extract [184,217,218]. The appropriate N source to maximize biomass production is species-specific. *Pavlova* spp. produced the highest biomass content with KNO_3 [184,217], whereas *Tetraselmis* sp. with yeast extract produced 1.5 times more biomass compared to the inorganic nitrate sources [218].

Moreover, the nitrogen concentration should be tailored to the individual needs of each microalgal growth. The optimal nitrate supplementation for *D. lutheri* and *P. cruentum* was 160 $mg.L^{-1}$ of $NaNO_3$, whereas *C. vulgaris* achieved the highest biomass with 240 $mg.L^{-1}$ of $NaNO_3$ [212]. The authors suggested that highest nitrate concentration was inhibitory to the cells, probably, due to increased activity of nitrate reductase that led to the accumulation of inhibitory compounds such as ammonia and nitrite. The effect of culture medium composed of different N sources, such as ammonium and nitrate, was evaluated on *D. lutheri* cultures. The authors found diauxic growth of *D. lutheri* with a higher affinity for ammonium and lower cell densities compared to the best formulation, which was solely composed of nitrate [132].

The use of potassium nitrate, ammonium chloride and urea produced no significant differences in n-3 LC-PUFA production in *Diacronema lutheri*, with EPA content ranging from 0.63 to 1.24 $mg.L^{-1}$, and DHA content from 0.38 to 0.70 $mg.L^{-1}$ [217]. The nitrate and/or phosphate replete or deplete conditions did not result in considerable differences on sterol content of *D. lutheri*, whose values ranged from 5 to 7.6 $mg.g\ DW^{-1}$ [200]. The effect of KNO_3 and Na_2HPO_4 on *N. oculata, T. suecica, I. galbana* and *D. lutheri,* overall, showed that biomass production was favored by increasing nitrate up to 120-150 $g.L^{-1}$ and phosphate concentration up to 12-15 $g.L^{-1}$. The highest lipid content, which according to the species ranged from 23.8 to 37.1 %, was reached with lower KNO_3 and PO_4 concentration, namely 10-70 $g.L^{-1}$ and 4-7 $g.L^{-1}$, respectively [219]. Likewise, the medium with highest N supplementation (1.76 mmol $N.L^{-1}$) promoted the highest specific growth rates and cell densities of *T. subcordiformis, N. oculata* and *P. viridis* which presented the lowest lipid content among the nitrogen concentrations tested (1.76 - 0 mmol $N.L^{-1}$). *N. oculata* and *P. viridis* with 0.22 mmol $N.L^{-1}$ had the highest lipid content, mostly composed by neutral lipids, and the FA profile enriched with SFA (e.g. C16:0) and lower levels of PUFA (e.g. EPA) relative to the enriched N conditions [220].

According to Thiyagarajan et al. [221], the different levels of PUFA in the haptophytes *Isochrysis* sp. and *Pavlova* sp. are modulated by the fatty acid gene expression Δ6-elongase gene and Δ5-desaturase gene, respectively, under nitrogen stress. Under nitrogen replete conditions (500 $mg.L^{-1}$) the Δ5-desaturase gene expression in *Pavlova* sp. was improved 3.3-fold compared to control (100 $mg.L^{-1}$), whereas the Δ6-

elongase expression was 1.7-fold improved either by repletion or depletion of nitrogen. Both species had the highest gene expression in the initial logarithmic phase. Thus, the authors proved that the concentration of this nutrient in the medium, besides being decisive for the final lipid content, is critical in determining the unsaturation level of the fatty acids [221].

The N source also had an impact on pigment composition. *Pavlova* sp. grown with $NaNO_3$ produced the highest fucoxanthin content, 12.74 $mg.g^{-1}$ DW, increasing from 1.5 to 2.3 times compared to the other nitrogen sources (KNO_3, $CO(NH_2)_2$, NH_4Cl) [184]. Under low light and N-depleted conditions, *D. lutheri* decreased its production of photosynthetic pigments (Chl *a*, Chl *c* and fucoxanthin) and increased β-car content. On the other hand, at higher illumination, N-depletion resulted in an increase in diatoxanthin+diadinoxanthin pigments while the β-car level decreased [70]. The lower nitrogen concentration and higher carbon content of the Ben-Amotz medium were suggested to be primarily responsible for the 30 % increase in carotenoid accumulation and higher carotenoid/chlorophyll *a* ratio in *Dunaliella salina* grown outdoors [222].

2.5.5 Phosphorus

Phosphorus is of utmost importance for cells considering the high content of this macronutrient and its wide distribution in various cellular components. Among the molecules with the highest phosphorus content are those with structural action in cell membranes (e.g. glycerophospholipids), molecules acting as energy storage (e.g. polyphosphate) as well as molecules involved in signaling pathways such as ATP (Blank 2012). Phosphorus content in biomass of microalgae ranged from 1 % [224], when cultured in the limiting P conditions, to 3.85 % when cultured in the luxury P conditions [225]. Luxury P uptake occurs in phosphorus-replete environments, with phosphorus accumulating in the form of polyphosphate. This can be used in cellular metabolism or as a storage compound that will promote the growth of microalgae once the external environment presents phosphorus-limiting concentrations [224,226].

Several growth models have been proposed to explain the relationship between microalgae growth, the concentration of phosphate in extracellular media, and its uptake and accumulation within the cell. Normally, phosphate uptake is carried out by several transporters in cell membrane, which, according to the species and phosphorus supply, leads to different affinities and uptake rates [226]. The addition of phosphate spikes in *D. lutheri* cells increased up to three times the maximum uptake rates of this nutrient, compared to the cells under steady-state uptake conditions, leading the authors to suggest the existence of multiple phosphate uptake systems in *D. lutheri* [227].

According to Terry [228], the phosphate uptake in *D. lutheri* demonstrated inhibitory effects on the uptake of nitrate. This partial inhibition of nitrate uptake was reported over a wide range of N:P ratios, with this behavior being most pronounced at the highest N:P ratios (P-limiting conditions) and in cells with the highest growth rates. *D. lutheri* when exposed to high concentrations of both nutrients demonstrated similar uptake rates of N and P, despite the forty-fold smaller requirement of P. In nutrient rich conditions, the cellular quota of P increased many times higher than the P required (6-fold), whereas the maximum storage of N was doubled. Increasing P uptake capacity as external P supply increases has also been reported in *Scenedesmus* sp [229]. The preference for the phosphate uptake could be developed as an adaptative mechanism that allowed the microalgae to take advantage, and thus grow successfully in natural environments (e.g., open sea) where phosphate concentration is limited [228]. The ability to grow under P starved conditions was confirmed when *D. lutheri* achieved similar cell density when grown with N:P ratios of 9.8 and 125. The authors also argued that phosphorus starvation induced a decrease in N uptake, which is likely related to a decrease in ATP content that is crucial for N assimilation by cells [71].

The external P concentration affected the distribution of this nutrient in the main storage pools of microalgae cells. Namely, low P concentration promoted greater storage of inorganic phosphorus and organic phosphorus in extracellular polymeric substances and intracellular polymeric substances, respectively. On the other hand, *Scenedesmus* sp. grown under P-rich conditions resulted in the uptake of large amounts of inorganic phosphorus by intracellular polymeric substances which were then converted into organic phosphorus [229]. The ability to use the P stored in cell reserves under external phosphate deprivation to produce microalgae biomass increased in nine marine microalgae, which according to species the phosphate use efficiency was improved up to 7-fold. Depending to the species the authors also assumed that the internal P cell quota and the contents of betaine lipids and phospholipids performed an important regulatory role in the luxury phosphate uptake [230].

As stated under N-starvation conditions, depletion of phosphorus also leads to a similar decrease in photosynthetic activity of PSII and reduced the MGDG/DGDGD ratio on thylakoid membranes. The content of pigments, soluble proteins and soluble carbohydrates were negatively affected in phosphorus-starved cells, although to a lesser extent when compared to N-starved cells. Similarly, stress conditions of P and N reduced the C20:5 content in FA composition of polar lipids, whereas a marked increase of C14:0, C16:0, C16:1 and C20:5 was reported in neutral lipids of *D. lutheri*, with the variation on C20:5 being the result of membrane polar lipids recycling [71].

Phosphorus stress has been seen as an important modulator of lipid composition on microalgae. Batch cultured *Scenedesmus* sp showed a decrease >40 % in biomass production with the decreasing concentrations of phosphorus from 50 to 0.5 $mg.L^{-1}$, whereas the lipid content in the same conditions rise from 22.3 to 42 %. In order to achieve the highest lipid content without impaired the microalgae growth, the authors suggested the limited addition of phosphorus (2 $mg.L^{-1}$) every 48h, which promoted a lipid content of 41 % and a lipid productivity 84.2 % higher than the control conditions. The major modifications of P limitation in lipid composition were the increment on neutral lipids and saturated fatty acids and a reduction in phospholipids proportion [231]. A similar trend was observed in the freshwater microalga *Chlorella* sp. where lipid content and lipid productivity were higher with limited phosphorus concentrations, a behavior corroborated by decreased lipid accumulation after feeding the microalgae with external phosphorus in the late growth phase. The phosphorus-deprived conditions also increased the content of neutral lipids and replaced the phospholipids by phosphorus-free glycolipids and sulfolipids [232].

In addition, the phosphate supply also affected the pigment composition, and therefore the color of the cultures. *Nannochloropsis gaditana* grown in phosphate limiting conditions enhanced the production of valuables carotenoids such as violaxanthin, zeaxanthin and cantaxanthin [233]. The highest accumulation of carotenoids (4.32 $mg.g^{-1}$ DW) in *P. pinguis* was reached under low phosphorus supply, probably as a result of a protective mechanism against oxidative stress. This pigment content promoted yellowish cultures, instead of the brown color when grown under nutrient-rich conditions [128]. Phosphorus depletion allowed a 1.6-fold increase in total carotenoid content of *Tetraselmis marina*, but a two-stage cultivation with phosphorus supplementation raised the carotenoid content up to 2.2 times compared to control conditions [234]. Generally, the chlorophyll content did not follow the trend for carotenoids, and its composition decreased independently of the phosphorus supplementation used [234].

2.5.6 Micronutrients - minerals and vitamins

Culture media have a wide variety of nutrients that are present in smaller concentration but play a critical role in microalgae growth and biochemical composition. Thus, efficient control and implementation of biomass production to achieve bioactive metabolites of interest for potential industrial applications, requires a thorough understanding of the effect and importance of these micronutrients, such as minerals and vitamins, in order to optimize and tailor the cultivation process to the desired microalgae [132,235].

Despite the mineral composition of microalgae is variable according to the species, growth media and growth stage, it is predominantly composed by minerals such iron, calcium, magnesium, phosphorus

(see Chapter 2.5.5), sodium, potassium and trace elements like as aluminum, copper, manganese, strontium, zinc, barium, chromium, cobalt and vanadium [236–238]. Usually, the mineral content is estimated by the ash determination, and its value in marine and freshwater microalgae can range from low ash level (<10%), such as the *Nannochloropsis granulata, Botryococcus braunii, Chlorella sp.* [236] and *Pavlova sp.* [239], to moderate level (14-17%) as described in *Phaeodactylum tricornutum, Neochloris oleoabundans* and *Tetraselmis chuii* [236].

The ability of microalgae to accumulate some of these minerals with important biological functions has been known for a long time, reason why microalgae biomass has been widely used as an important fish feed [240] and a valuable and promising nutritional source for human diet [237]. On the other hand, it has been shown that microalgae exhibit a high metabolic plasticity showing high tolerance and robust growth in wastewater rich in minerals labeled as harmful and toxic to the environment (heavy metals). The efficient accumulation of these heavy metals in microalgae biomass presents them as an alternative bioremediation tool to treat polluted waters [241,242].

Despite the diversity of micronutrients present in culture medium formulations, not all of them have the same degree of importance for cell growth and photosynthetic activity. The micronutrients requirements are variable according to microalgae species, as described to *Botryococcus braunii* (Fe>Mn>Mo>Ni) [243], and *Symbiodinium kawagutii* (Fe>Zn>Mn>Cu>Ni>Co) [244]. Each of these micronutrients has a specific activity at the cellular level, namely a structural, catalytic, physiological and/or regulatory function [245]. For instance, magnesium is associated to the synthesis of ROS and protein production. Mg is reported as important cofactor and allosteric regulator of over 300 enzymes, among which stands out ribulose-1,5-bisphosphate carboxylase/oxygenase (Rubisco) whose activity, and consequently photosynthetic rate, is strongly reduced when exposed to Mg-deficient conditions [246]. Considered the third most limiting nutrient for plant growth, iron plays an important role in the synthesis of chlorophyll, which is why about 80 % of this nutrient is found in photosynthetic cells. It is also an important cofactor in hormone synthesis and is involved in other biological processes, such as DNA synthesis and nutrient uptake [247]. Calcium is present intracellularly in large quantities, acting as a crucial messenger in signal transduction when eukaryotic cells are exposed to external variations. Cytosolic calcium variations promote an appropriate cellular response through efficient protein regulation [248]. Copper acts as an important cofactor that regulates the activity of valuable metalloproteins such as plastocyanin, cytochrome *c* oxidase, and multicopper oxidase, which are involved in redox homeostasis and photosynthetic activity of microalgae [249]. Similarly, zinc also affects the photosynthesis acting as a cofactor of carbonic

anhydrase, an enzyme responsible by the interconversion of CO_2 to HCO_3, which regulate the CO_2 supply to Rubisco enzyme [250]. A full description of the activities and functions of the remaining micronutrients in photosynthetic organisms was reviewed extensively elsewhere [245,251].

Although they are seen as essential minerals, it is important to tailor the concentrations of these minerals to the cellular requirements. Some works have reported the toxic nature of these minerals at high concentrations, that strongly impaired physiological and biochemical processes of microalgae, leading to growth inhibition [252,253], as a result of lipid peroxidation and oxidative stress induced by ROS [254]. In addition, the evaluation of tolerance to these nutrients must consider the species-specific sensitivity as well as the effect of growing conditions, such as cell density [253] and interactive effects with other nutrients [255]. For example, it was reported an increase of Cu toxicity in *Selenastrum gracile* grown in phosphorus limited conditions [255].

Beyond the mineral nutrient, vitamins are others trace elements with important role for photoautotrophic microalgae. According to Brown et al. [256], the vitamin content of four microalgae is composed by vitamin A, B_1, B_2 B_6, B_7, B_{12}, C and E. The variation of some vitamins between the species analyzed and the culture conditions assessed ranged from 2- to 10-fold. Vitamin C was the most prominent vitamin ranging from to 1.3 to 3.0 $mg.g^{-1}$, whereas cobalamin (B_{12}) and biotin (B_7) did not exceed 2 $ug.g^{-1}$ [256].

Microalgae have a vitamin auxotrophic nature, which means that the vitamins required to sustain cell growth are obtained exogenously. In the ocean where vitamins availability is low, microalgae acquire these nutrients from prokaryotes possibly by symbiotic interaction, with the microalgae supplying the carbon product from photosynthesis in exchange for the vitamins of bacterial origin [257]. As proposed by Nef et al. [258], in a survey of nineteen haptophyte species, a B_{12} auxotrophic phylum, the authors suggested that the preferred source for dealing with deficiency of this vitamin is cobalamin-producing bacteria, either by cell lysis or excretion. However, other mechanisms were also described such as the uptake and assimilation of methionine for protein synthesis, the end product of the B_{12} cofactor-dependent enzyme, as well as the regulation of cobalamin-dependent cellular processes under B_{12}-limited conditions [258]. When external vitamin B_1 conditions did not meet the cellular needs of some haptophytes, these microalgae demonstrated the ability to utilize precursors of this vitamin as an alternative source, such as the pyrimidine compound 4-amino-5-hydroxymethyl-2-methylpyrimidine, which even allowed for superior growth rates compared to vitamin B_1 [259].

Several authors have reported as a key growth factor for microalgae the addition, in a species-dependent combination, of vitamin, B_1, B_7 and B_{12} to the growth medium. For instance, in a survey of 306 microalgae

species from seven different phylum, 51 %, 22 %, and 5 % required the supplementation of cobalamin, thiamine, and biotin, respectively [260]. These vitamins develop a crucial role on microalgae metabolism acting as an important cofactor of several enzymatic processes. For instance, vitamin B_{12} regulates enzymes involved in protein production (methionine synthase), DNA synthesis (class II ribonucleotide reductase) and in TCA cycle by reverse isomerization of methylmalonyl-CoA to succinyl-CoA (methylmalonyl-CoA-mutase) [258]. Vitamin B_1 is phosphorylated to thiamine pyrophosphate (TPP) acting as a critical cofactor in carbohydrate and amino acid metabolism. Thiamine-dependent enzymes are associated to TCA cycle being responsible by the conversion of pyruvate into acetyl-CoA (pyruvate dehydrogenase) and conversion of α- ketoglutarate into succinyl-CoA (oxoglutarate dehydrogenase). Vitamin B_1 also impacts catabolic reactions in the pentose phosphate pathway and the Calvin-Benson cycle through the regulation of transketolase [261]. Vitamin B_7 enables the carboxylase enzymes involved in carbon dioxide metabolism, which mediate cellular processes such as gluconeogenesis, fatty acid synthesis, and branched-chain amino acid catabolism [262].

Several research have addressed the effect of these micronutrients on Pavlovophyceae species. The importance of mineral composition for the growth of *D. lutheri* was described by Carvalho et al. [132]. Among the growth conditions evaluated, the authors identified the lower concentration of toxic micronutrients (e.g. copper and molybdenum), the higher concentration of the chemical EDTA chelator - which complexes heavy metals and reduces their toxicity to the cells - and the chemical form of the micronutrients as the main reasons for improved cell density [132]. Carvalho et al. [217] reported growth inhibition of *D. lutheri* grown in sulfur or vitamin B_{12} deprived conditions, as well as a significant reduction of cell density in the absence of iron, calcium or manganese. On the other hand, the lack of boron promoted higher growth compared to the control medium. Regarding FA content, the same authors reported an increase in EPA and DHA content in the absence of boron, molybdenum or copper, while the absence of calcium decreased the content of both FAs [217]. The haptophyte *Tisochrysis lutea,* produced ten times less biomass when grown in the absence of vitamin B_{12} [258]. Supplementation of *P. viridis* cultures with 3.0 $mg.L^{-1}$ of Cu^{2+} and 6.5 $mg.L^{-1}$ of Zn^{2+} inhibited the cell growth (17.67 % and 14.16 %, respectively). Although the effect of copper was more significant, both metals promoted an increase in oxidative stress with increasing concentrations of these micronutrients. Namely, both metals increased catalase activity, glutathione content, and lipid peroxidation, which in turn led to a reduction in chlorophyll content. Copper also induced a marked increase in glutathione peroxidase and superoxide dismutase activity [263]. The response of *P. viridis* to Co^{2+} and Mn^{2+} supplementation was also evaluated. In contrast

to Mn^{2+}, a strong inhibitory effect of Co^{2+} on cell growth was confirmed at all tested concentrations (10-200 µmol.L^{-1}), which can reach 75%. The oxidative stress promoted by the addition of Co^{2+} was also expressed by a marked decrease in protein content, as well as a significant increase in lipid peroxidation and in the activity of enzymes and antioxidant compounds [264]. Similarly, the use of the highest iron concentrations (≥ 1.2 mmol.L^{-1}) in *T. subcordiformis, N. oculata* and *P. viridis* led to a significant decrease in the growth rates of these microalgae. Furthermore, increasing the iron concentration from $1.2x10^{-2}$ to 12 mmol.L^{-1} promoted an increase in the neutral/polar lipid ratio, which in the case of *P. viridis* rose from 31 to 47 %. Depending on the species, the use of the higher iron concentration led to a positive variation of SFA, between 3 and 26 %, while the PUFA content was reduced between 4 and 37 %. In *P.viridis*, this variation in FAs led to a decrease in EPA content from 14-15 % to 11 %, as well as the absence of DHA [265]. The optimization study that evaluated the effect of iron and two other nutrients (PO_4 and NO_3) on growth parameters and lipid content of four microalgae, among them *D. lutheri*, showed in general that biomass production was increased under high levels of Fe (4–5 g.L^{-1}), PO_4 (12–15 g.L^{-1}) and NO_3 (120–150 g.L^{-1}), while deficient levels of Fe (2 g.L^{-1}), but especially PO_4 (4-7 g.L^{-1}) and NO_3 (10-70 g.L^{-1}) had a positive impact on lipid content [219]. Kanamoto et al. [184], suggested as a likely reason for the growth inhibition of *Pavlova* sp. in the absence seawater the lack of the micronutrients Mg^{2+} and Ca^{2+}.

2.6 PAVLOVOPHYCEAE AS A PROMISING AND VALUABLE SOURCE OF HIGH ADDED VALUE PRODUCTS

2.6.1 Haptophyta

Haptophyta is a diverse phylum with more than 300 species of microalgae identified [266,267], part of which is unknown in terms of their cultivation conditions, and are distributed among the classes Rappephyceae, Pavlovophyceae and Coccolithophyceae, with the latter class as the most representative. [268,269]. Emerging as a distinct taxonomic group 829 million years ago [270], countless species of haptophytes remain to be identified, catalogued and characterized morphologically [271,272] .

The haptophytes are mainly found in oceanic and coastal waters and possess an important effect on the economy, climate and the earth's biogeochemical cycles. They are well known for extreme and periodical phenomenon around the world (microalgae blooms), some of them with negative impact in the economy and the marine life [267,273]. Regarding the marine ecosystems, pigment and genomic analyzes have shown that haptophytes are the main source of chlorophyll *a* in the global ocean's photic layer (30-50%), overcoming the diatoms and cyanobacteria as the main photosynthetic agent in the ocean [274].

Haptophytes have as a common feature, a unique pigment profile in which the presence of chlorophyll *a* and *c* stands out, but above all, the existence of some carotenoids, *e.g.* the carotenoid 19'-hexanoyloxifucoxanthin (19-HFx), which is only found among haptophytes and can be considered as an important taxonomic marker [274,275]. Others pigments commonly found are β-carotene, diadinoxanthin, diatoxanthin and fucoxanthin [111].

Morphologically, this phylum is characterized by the existence of two flagella (heterodynamic/homodynamic and equal/unequal in length), body scales (mineralized, organic or siliceous) on the plasma membrane and a characteristic haptonema between the flagella [3,268,276]. Haptonema's main role is to avoid obstacles and to collect and aggregate food particles [277,278]. Haptophytes can take different forms, such as non-motile single cells, non-motile colonies of single cells, motile single cells or colonial flagellates, with the cell ranging from 2 μm to macroscopic colonies [267,268].

2.6.2 Pavlovophyceae

2.6.2.1 Taxonomy

Initially named Pavlovea, was proposed by Cavalier-Smith in 1993 [279] as a new class in the phylum Haptophyta, according with their ultrastructural data and phylogenetic information. The class was renamed Pavlovophyceae and taxonomic classification was later corroborated by 18S rRNA analysis of different haptophytes, in which a 6 % molecular divergence was identified between species of the classes Pavlovophyceae and Coccolithophyceae [280]. Several phylogenetic studies have been carried out to understand the evolution and the divergent times of haptophytes. Multigene analysis of nuclear and plastid genes the molecular clock estimated that the divergence between both haptophyte classes occurred in the early Cambrian (543 Ma), and the subsequent division of Pavlovophyceae class into four genera occurred between 230 and 103 Ma [270]. In fact, it is usually argued that members of this class represent the primitive state, since they share similar characteristics with the ancestral haptophyte [10,270].

The Pavlovophyceae have thirteen identified species distributed by four genera and can be found in a wide range of habitats, such as the littoral, marine, brackish water and, rarely, in freshwater [280]. *Pavlova* (Butcher 1952) was the first genus identified, presenting the species *Pavlova gyrans* as the phenotypic pattern, basing this classification on significant differences in the place of insertion of the flagella compared to those described in other genera of flagellates [281]. Later and according with the identification of new morphological features the *Diacronema* Prauser and *Exanthemachrysis* Lepailleur

were also erected as new genera. *Diacronema* genus possess a distinctive posterior flagellum, whilst in the *Exanthernachrysis* genus, unlike *Pavlova* genus, the non-motile cells lack external flagellar apparatus, and in the motile cells the flagellar knob-scales are absent [282,283]. Based on the analysis of 18S rDNA of eighteen haptophytes species it was established the fourth genus (*Rebecca* J.C. Green gen. nov) within the Pavlovophyceae, to which the species *Rebecca salina* and *Rebecca helicata* were transferred [279].

Taxonomic reassessment through a morpho-molecular approach involving twenty-nine Pavlovophyceae strains, has confirmed the division into four differentiated clades but with some modifications proposed [280]. Excluding *Pavlova gyrans* and *Pavlova pinguis,* all the analyzed strains have showed a pronounced genetic differentiation. Similar conclusions were stated by Green about the resemblance of morphological characteristics between both species [283]. Thus, the authors hypothesized that these species may form a single cryptic species complex or, on the other hand, *P. gyrans* and *P. pinguis* may be different forms within the same life cycle [280]. However, these possibilities were denied by other phylogenetic analysis, which assume that both species are completely distinct [284]. The complete ultrastructural description of Pavlovophyceae species is fully described elsewhere [280].

2.6.2.2 Biochemical composition

2.6.2.2.1 Pigment

As stated by Lenning et al. [10], and later confirmed by Bendif et al. [280], the Pavlovophyceae strains can be grouped into three types (A-C) according to their pigment signatures. All Pavlovophyceae species share the common pigments chlorophylls *a,* c_1, c_2, MgDVP (Mg-[3,8-divinyl]-phytoporphyrin-132-methylcarboxylate) and the carotenoids Fx, Ddxd, Dtx, and β-β-carotene. This is the simplest composition and when these are the only pigments found the species belong to Type A, which contains *D. lutheri, D. virescens, D. noctivaga, D. ennorea* and *D. vlkianum.* Pavlovophyceae pigment-type B is represented by species such as *P. gyrans*, *P. pinguis* and *P. granifera,* which comprise the pigments of Type A with the addition of a carotenoid (diadinoxanthin like) and a divinyl (DV) form of chlorophyll *c* (cPAV). Species from the Type C present the pigments of Type B and the monovinyl (MV) form of chlorophyll *c,* being this pigment profile typical of only one species (*E. gayraliae)*. The presence of a lower number of pigments and the observation of the MV and DV forms of chlorophyll *c* presents itself as a differentiating aspect compared to the Prymnesiophyceae class. Likewise, the carotenoids 19-HFx, 4-keto-hexanoyloxyfucoxanthin and 4-keto-fucoxanthin that are commonly found in many haptophytes were not detected in the Pavlovophyceae class [10].

2.6.2.2.2 Lipids

Regarding the biochemical composition these microalgae are known to have a distinguishable lipid profile with commercial interest and taxonomic relevance, such as the n-3 PUFAs and a distinctive sterol composition [238]. A high diversity of 4-desmethylsterols, 4-methylsterols and dihydroxysterols were identified in the species of *P. gyrans, D. vlkianum, D. lutheri*, and *P. pinguis* [9,285–288]. Moreover, *D. lutheri* was identified as a high sterol producer, whose content reached 5.1 % DW [199].

The peculiar dihydroxysterols are strictly found in Pavlovales and are a distinctive feature of this order, which is why they are called pavlovols [289]. The pavlovols currently identified in *Pavlova* and *Diacronema* species are 4α-methyl-24β-ethyl-5α-cholestan-3β, 4β-diol (ethylpavlovol) and the 4α, 24β-dimethyl-5α-cholestan-3β, 4β-diol (methylpavlovol) [9,289], which occur exclusively as steryl glycosides [287]. Although Ballantine et al. [290] stated that pavlovols and 4-methyl sterols were only identified in the stationary phase, this conclusion was not confirmed by Volkman et al. [288], who found no significant variation of the two sets of sterols in cultures of *D. lutheri* during different growth phases. The prevalence of dihydroxysterols in the final sterol composition is species-specific, varying, for example, from 0.23 % to 33 % of total sterols [287–289].

Similarly, Pavlovophyceae species have a distinct and more diverse profile of 4-desmethylsterols when compared to other haptophytes, namely the absence of the typical, and sometimes the only 4-desmethylsterol of haptophytes (24-methyl-cholesta-5,22E-dien-3β-ol), and on the other hand the presence of a high concentration of sterols, such as 24-ethyl-cholesta-5,22E-dien-3β-ol and the uncommon 5a-stanols [285,288]. Among the 4-methylsterols, 4α,24-dimethyl-5α-cholestan-3β-ol and, in particular, 4α-methyl-24-ethyl-5α-cholest-22E-en-3β-ol stand out as the most widely distributed and predominant sterols among the different species of the order Pavlovales [9,285,287,288].

As reported between two different strains of *D. lutheri*, the sterol composition as well as the proportion of the different classes in the sterol profile can vary significantly [287,288]. Moreover, manipulation of growth conditions such as temperature [288], UV-C irradiation [208] and the cultivation over a longer period of time [199] induced significant variation in the content and composition of sterols in *D. lutheri*. In addition to their taxonomic importance, these compounds have been of particular interest due to their nutraceutical properties with great application in the food industry and in aquaculture[199,291].

Considering the other lipid classes, the order Pavlovales is distributed by different groups of polar lipids and neutral lipids, as mentioned in Chapter 2.2. The main lipidic classes identified in *D. lutheri* were the

glycolipids MGDG and DGDG, SQDG and acylated steryl glycosides (SG), and the neutral lipids mono-, di- and triacylglycerols (MAG, DAG and TAG, respectively) [35,69], Figure 2-1. PL represent a small percentage (< 5%) and the BL were identified in traceable amounts [69]. Polar lipids such as MGDG, DGDG and PL are preferentially found in chloroplast membranes and thylakoyds. In contrast, non-plastidial membranes of *D. lutheri* are mostly composed by BL, DGCC and DGTA, with DGCC accounting for 63-78 % of these membrane lipids [71].

The total lipid content reported for some Pavlovophyceae species ranged between 3.6 and 66.0 $pg.cell^{-1}$ [292,293], with their lipid classes as well as their fatty acid composition varying according to the culture conditions used and the growth stage of the microalgae. According to Dunstan et al. [293], the lipid classes of *D. lutheri* during the exponential phase are predominantly composed of polar lipids (88 %), while in the stationary phase a marked variation occurs, with polar lipids decreasing to 50-57 % while TAG content increased to 28-35 % [293]. The lipid composition, as well as the fatty acid profile and their distribution, were strongly influenced by the culture conditions employed, such as the nutrient conditions, temperature and light intensity [34,69,192,292], as shown in Chapter 2.5 .

The fatty acid profile of pavlophytes is mainly composed by the SFA C14:0 and C16:0, the MUFA C16:1 and the PUFA C18:4 n-3, C20:5 n-3, C22:6 n-3 [9,126,184,293,294], which can represent about 83-90 % of the total fatty acids [126,294]. Considering the species *D. lutheri* and *P. pinguis*, the fatty acid composition is normally distributed as follows: 46-63 % are PUFAs, 17-23 % are MUFAs and the SFAs represent 22-30 % of TFAs. In terms of PUFA composition, these species can produce a high content of EPA and DHA which represent about 22-29 % and 5-19 % of TFA, respectively, as well as the ability to produce low amounts of the unusual C24-C28 PUFA [184,292]. The total content of EPA and DHA in the biomass is species-specific and can range between 3.9-18 and 2.0-13.2 $mg.g^{-1}$ DW, respectively [9,126]. Furthermore, in some species have been described the lipid remodelling process (see Chapter 2.2.2), in which occurs an increase of DHA, and sometimes EPA, in TAG fraction during the stationary phase [77,293]. For instance, *D. lutheri* incorporated 40% of EPA and 17 % of DHA into the TAG fraction, with the corresponding partition initiated at the middle and at the end of the exponential growth phase, respectively [77].

The high ability to produce PUFAs, and especially the n-3 FAs, make strains like *D. lutheri* and *R. salina* the subject of genetic studies to identify the gene sequences and the enzymes involved in EPA and DHA conversion and, eventually, further heterologous expression [295]. For instance, it was identified in *R. salina* three cDNA sequences (*PsD4Des, PsD5Des* and *PsD8Des*) which encode the three front-end

desaturases Δ4, Δ5 and Δ8-desaturases [296]. A desaturase gene (*Δ 5Des*-Pav) and an elongase gene (*pavELO*) were identified in *Pavlova sp.*, which converts eicosatetraenoic acid to EPA, and EPA to docosapentaenoic acid (C22:5 n-3), respectively [220,297]. The conversion of C22:5 n-3 to DHA in *D. lutheri* is carried on by Δ4-desaturase, encoded by a cDNA sequence named *PlDES1* [298].

2.6.2.2.3 Carbohydrates

Besides the production of lipids as the main energy reserve component, it was also suggested the presence of storage carbohydrate globules with crystalline structure similar to paramylon [1,283,299,300]. However, by ^{13}C solid-state Nuclear Molecular Ressonance (NMR), it was confirmed that the main component of the storage sugar was chrysolaminarin ((1-3)-β-glucan) rather than paramylon [301]. The aqueous extracts produced from *D. lutheri* and *P. gyrans* showed a high carbohydrate content ranging from 57-60 % and 69-84 %, respectively, being mainly composed of glucose (85-100 %mol) [302]. The extracts were fractionated according to their water solubility, resulting in a soluble fraction rich in highly branched (1-3),(1-6)-β-glucans, while the insoluble part consisted of (1-3)-β-glucans [302].

Regarding the cell surface, cellulose and hemicellulose were identified as the main components, with a high content of glucose (43%), and lower amounts (<13%) of galactose, arabinose and xylose in the monosaccharide profile [301]. In the cell wall related polysaccharides of *D. lutheri* about 6 % are the biological important sulfated polysaccharides [303]. Although showing lower anti-adhesive activity than protein- and glycoside-rich extracts, some β-glucan-rich extracts from *D. lutheri* and *P. gyrans* have been suggested as a promising source of anti-adhesive agents that can prevent or mitigate the adhesion of enteropathogens to the host [302].

Representatives of all genera of the family Pavlovophyceae were identified as microalgae capable of producing and releasing polysaccharides into the extracellular environment (exopolysaccharides - EPS). Among the twelve species analyzed, only *D. lutheri* and *D. viridis* were not able to produce EPS, while the EPS producers showed a content from 0.05 to 0.39 $g.L^{-1}$. The EPS produced was mainly composed of two to four monosaccharides: rhamnose, galactose, and glucose in *Diacronema* sp; rhamnose, galactose, arabinose, xylose, or glucose in *Pavlova* spp; and galactose, mannose, xylose, and N-acetyl-glucosamine in *Exanthemachrysis* sp.. *P. gyrans* and especially *Exanthemachrysis* sp have stood out as producers of EPS rich in uronic acid (N-acetylgalactosamine), which represents 11 % and 35 % of their composition, respectively [304].

2.6.2.2.4 Protein

Although the main attribute highlighted in the order Pavlovales is its high n-3 PUFA content, some studies have reported these species as promising source of protein, in which its content can represent 28 % to 66 % DW [237,305–307]. The amino acid (AA) composition of *D. lutheri* was preserved regardless of the harvest time and the culture technique used (batch or semi-continuous), with aspartic acid (8-10 %), glutamic acid (10-12 %) and leucine (8 %) as the major AA [308]. The amino acid composition of *D. lutheri* and *R. salina* was similar, with the predominance (8-11 %) of the aforementioned amino acids, arginine, and alanine [305]. Similar AA profile was identified in *Pavlova* sp. CCMP459 [309]. Due to its high composition of essential amino acids (*e.g.* leucine, arginine and valine), which represents 47 % of total AAs, along with perfect balance between essential AAs and non-essential AAs (ratio = 1), this strain showed to be a promising and high quality live feed for salmonids [237,309].

However, the importance of the protein fraction it's not strictly related with the feed application in aquaculture. The end products from the yeast fermentation using the microalga *D. lutheri* as substrate, exhibited high antioxidant activity and absence of citoxicity in *in vitro* assays [310]. The authors assumed that these effects are linked to increased amounts of hydrophobic amino acids (*e.g* leucine, valine, and alanine) in fermented microalgae. Later, it was confirmed that fermented microalgae increased the activity of alkaline phosphatase and osteocalcin (mineralization regulator) in osteoblastic cells [311]. This behavior was attributed to a hydrophobic rich peptide produced after the fermentation, that was sequenced as Glu-Pro-Gln-Trp-Phe-Leu, suggesting its potential use for medical applications.

2.6.2.2.5 Minerals

According to Ponis et al [238] the ash content of six strains of Pavlovophyceae ranged between 5% to 14 % DW. The ash content in *D. vlkianum* remained unchanged over the entire growth and was positively influenced by the salinity level in the culture medium, increasing from ≈3 % to ≈18 % in DW between salinities of 5 and 50 $g.L^{-1}$ [200]. Considering the mineral composition, *Pavlova* sp. exhibited a high content of potassium, calcium and sodium, amounting about 4 % of the microalgae composition. The trace metals profile was rich in iron, manganese, zinc and copper [237]. On the other, the phosphorus and manganese were the main minerals identified in *D. vlkianum* [312], while *D. lutheri* was mainly composed by sodium and potassium [303].

2.6.2.3 Applications

Given the richness and variability in biochemical composition presented above, some applications (Table 2-2) have been evaluated regarding the use of pavlophytes as an alternative source of n-3 FAs for feed

and food products, biological agent in bioremediation processes, either as feed or a source of bioactive compounds against aquatic pathogens [313–316].

Table 2-2: Potential applications developed using Pavlovophyceae species

Aquaculture		
Species	Potential application	Reference
Pavlova sp	Antimicrobial agent against aquatic pathogens	[236]
Diacronema viridis *Pavlova* sp. (CCMP 1228)	Feed for rotifers (Brachionus plicatilis)	[238]
Diacronema lutheri	Feed for pearl oyster (Pinctada fucata martensii)	[237]
Diacronema lutheri	Feed for Pacific oyster (*Crassostrea gigas*)	[239]
Rebecca salina (CS-49) *Pavlova* sp. (CS-50)	Feed for oysters (Pinctada margaritifera)	[240]
Pavlova sp. AC 250; *Pavlova* sp. AC 248; *Pavlova* sp. AC 251; *Pavlova* sp. AC 538; *Pavlova pinguis*; *Rebecca salina*.	Feed for molluscs (Crassostrea gigas and Pecten maximus)	[141]
Pavlova sp. (*Pavlova* 1800®, Reed Mariculture Inc.)	Feed for giant clam (*Tridacna noae*)	[241]
Pavlova sp. (CCMP 459)	Feed for salmonids (*Salmo salar L.*)	[140]
Pavlova sp. (CCMP 459) and *Pavlova pinguis* (CCMP 609)	Feed for scallops (Placopecten magellanicus)	[212]
Diacronema viridis	Feed for European sea bass (*Dicentrarchus labrax L.*)	[21]
Food industry		
Species	Potential application	Reference
Diacronema lutheri	Yoghurt fortified with lipid extract	[234]
Diacronema vlkianum	Pasta enriched with microalgae biomass	[227]
Bioremediation		
Species	Potential application	Reference
Pavlova sp	Biodegradation of biphenyl compounds	[235]
Diacronema lutheri	Biodegradation of palm oil mill effluent	[242]
Bioenergy		
Species	Potential application	Reference
Diacronema lutheri	Biodiesel production and pellet manufacturing	[247]
Pavlova sp	Bio-oil production by biomass pyrolysis	[248]

Table 2-2 (cont): Potential applications developed using Pavlovophyceae species

Biotechnology/Medical industry/Health ingredient		
Species	Potential application	Reference
Diacronema lutheri	Peptide with protective effect against oxidative stress and inhibitory effect on melanogenesis.	[243]
Diacronema lutheri	Isolation of osteoblast differentiation inducing peptide	[232]
Diacronema lutheri	Antibacterial agent against pathogenic bacteria	[244]
Diacronema vlkianum	Biomass as omega-3 rich food supplement	[245]
Pavlova sp. CCMP459	Source of genetic information for heterologous expression of PUFA synthesizing enzyme	[217]
Diacronema lutheri and *Pavlova gyrans*	Extract with adhesive properties towards enterobacteria *Salmonella enterica*	[223]
Diacronema lutheri	Lipid extract with anti-inflammatory activity in human macrophages	[246]

2.7 CONCLUSIONS

Microalgae exhibit metabolic plasticity that allows them to adapt to a wide range of environmental conditions - light, temperature, and nutrient availability - by changing their biochemical composition to cope with stresses induced by external conditions. These include modifying the composition of FAs and carotenoids responsible for fluidity changes in the cell and thylakoid membranes, as well as varying the production of primary and secondary pigments to withstand, for example, different irradiances, optimizing the light absorption and reducing the ROS content, respectively. Fine control of abiotic factors presents itself as a crucial step to maximize the production of microalgae biomass and its use as a source of valuable metabolites with potential application in several industries. Among them, Pavlovophyceae species have shown a rich composition comprising not only the highly demanding PUFAs and carotenoids (e.g. fucoxanthin, β-carotene) but also an interesting protein/amino acid profile and carbohydrates composition, highlighting this microalgae class as a promising bioresource for food application in aquaculture, supplement/ingredient for food and pharmaceutical products, as well as bioremediation agent for wastewater treatment. However, additional studies are mandatory to evaluate i) the nutritional requirements of microalgae for enhanced biomass and metabolite production, ii) efficient downstream processing techniques to improve extractability and separation of biocompounds for human consumption, and iii) economic analysis of upstream/downstream processing methodologies to provide important

insights to enable cost-effective large-scale biomass production and commercialization of products derived from Pavlovophyceae species.

2.8 REFERENCES

1. Bendif EM, Probert I, Hervé A, Billard C, Goux D, Lelong C, et al. Integrative Taxonomy of the Pavlovophyceae (Haptophyta): A Reassessment. Protist [Internet]. Elsevier GmbH.; 2011;162:738–61. Available from: http://dx.doi.org/10.1016/j.protis.2011.05.001

2. Enzing C, Ploeg M, Barbosa MJ, Sijtsma L. Microalgae-based products for the food and feed sector: an outlook for Europe. JRC Scientific and Policy Reports. European Comission. 2014.

3. Eikrem W, Medlin LK, Henderiks J, Rokitta S, Rost B, Probert I, et al. Haptophyta. Handbook of the Protists: Second Edition. Springer, Cham; 2017. p. 893–953.

4. Dunstan JA, Mitoulas LR, Dixon G, Doherty DA, Hartmann PE, Simmer K, et al. The Effects of Fish Oil Supplementation in Pregnancy on Breast Milk Fatty Acid Composition Over the Course of Lactation: A Randomized Controlled Trial. Pediatr Res. 2007;62:689–94.

5. Fetterman JW, Zdanowicz MM. Therapeutic potential of n-3 polyunsaturated fatty acids in disease. American Journal of Health-System Pharmacy. 2009;66:1169–79.

6. Sadli N, Barrow CJ, McGee S, Suphioglu C. Effect of DHA and CoenzymeQ10 against Aβ- and zinc-induced mitochondrial dysfunction in human neuronal cells. Cellular Physiology and Biochemistry. Cell Physiol Biochem Press; 2013;32:243–52.

7. Fliesler AJ, Anderson RE. Chemistry and metabolism of lipids in the vertebrate retina. Prog Lipid Res. 1983;22:79–131.

8. Serhan CN, Chiang N, van Dyke TE. Resolving inflammation: Dual anti-inflammatory and pro-resolution lipid mediators. Nat Rev Immunol. 2008;8:349–61.

9. Fernandes T, Martel A, Cordeiro N. Exploring Pavlova pinguis chemical diversity: a potentially novel source of high value compounds. Sci Rep. 2020;10:1–11.

10. van Lenning K, Latasa M, Estrada M, Sáez AG, Medlin L, Probert I, et al. Pigment signatures and phylogenetic relationships of the Pavlovophyceae (Haptophyta). J Phycol. 2003;39:379–89.

11. Calder PC. Functional Roles of Fatty Acids and Their Effects on Human Health. Journal of Parenteral and Enteral Nutrition. 2015;39:18S-32S.

12. Poulos A. Complex lipids: a review. Pathology. Elsevier; 1975;7:252.

13. di Pasquale MG. The essentials of essential fatty acids. J Diet Suppl. 2009;6:143–61.

14. Blasbalg TL, Hibbeln JR, Ramsden CE, Majchrzak SF, Rawlings RR. Changes in consumption of omega-3 and omega-6 fatty acids in the United States during the 20th century. American Journal of Clinical Nutrition. 2011;93:950–62.

15. Falk-Petersen S, Sargent JR, Henderson J, Hegseth EN, Hop H, Okolodkov YB. Lipids and fatty acids in ice algae and phytoplankton from the Marginal Ice Zone in the Barents Sea. Polar Biology 1998 20:1 [Internet]. Springer; 1998 [cited 2022 Sep 29];20:41–7. Available from: https://link.springer.com/article/10.1007/s003000050274

16. European Comission. Comission Implementing Regulation (EU) 2017/2470. Official Journal of the European Union. 2017;72–201.

17. European Comission. Commission Implementing Regulation (EU) 2020/1559 . Official Journal of the European Union . 2020;7–16.

18. European Comission. Commission Implementing Regulation (EU) 2020/478. Official Journal ot the European Union. 2020;1–3.

19. European Comission. Commission Implementing Regulation (EU) 2018/1023. Official Journal of the European Union [Internet]. 2018;1–133. Available from: https://ec.europa.eu/food/sites/food/files/safety/docs/novel-food_authorisation_2015_auth-letter_krill-oil_en.pdf

20. Wada H, Murata N. The essential role of phosphatidylglycerol in photosynthesis. Photosynth Res [Internet]. Photosynth Res; 2007 [cited 2022 Sep 29];92:205–15. Available from: https://pubmed.ncbi.nlm.nih.gov/17634751/

21. Guschina IA, Harwood JL. Algal lipids and their metabolism. Algae for Biofuels and Energy [Internet]. Springer Netherlands; 2013 [cited 2022 Sep 30];17–36. Available from: https://link.springer.com/chapter/10.1007/978-94-007-5479-9_2

22. Guschina IA, Harwood JL. Lipids and lipid metabolism in eukaryotic algae. Prog Lipid Res. Pergamon; 2006;45:160–86.

23. Harwood JL, Okanenko AA. Sulphoquinovosyl Diacylglycerol (SQDG) — The Sulpholipid of Higher Plants. Sulphur in Plants [Internet]. Springer, Dordrecht; 2003 [cited 2022 Sep 29];189–219. Available from: https://link.springer.com/chapter/10.1007/978-94-017-0289-8_11

24. Meireles LA, Guedes AC, Malcata FX. Lipid class composition of the microalga Pavlova lutheri: Eicosapentaenoic and docosahexaenoic acids. J Agric Food Chem. 2003;51:2237–41.

25. Gunstone FD, Harwood J. The Lipid Handbook. The Lipid Handbook. CRC Press; 2007;

26. Dembitsky VM. Betaine ether-linked glycerolipids: Chemistry and biology. Prog Lipid Res [Internet]. Elsevier Ltd; 1996 [cited 2022 Sep 29];35:1–51. Available from: https://pubmed.ncbi.nlm.nih.gov/9039425/

27. Fan J, Andre C, Xu C. A chloroplast pathway for the de novo biosynthesis of triacylglycerol in Chlamydomonas reinhardtii. FEBS Lett [Internet]. FEBS Lett; 2011 [cited 2022 Sep 29];585:1985–91. Available from: https://pubmed.ncbi.nlm.nih.gov/21575636/

28. Gurr MI, Harwood JL FK. Lipid Biochemistry. 5th ed. Oxford, Blackwell Science Ltd; 2002. 2002 [cited 2022 Sep 29]; Available from: https://www.wiley.com/en-us/Lipid+Biochemistry%3A+An+Introduction+%2C+5th+Edition-p-9780470774366

29. LaBrant E, Barnes AC, Roston RL. Lipid transport required to make lipids of photosynthetic membranes. Photosynth Res [Internet]. Photosynth Res; 2018 [cited 2022 Sep 29];138:345–60. Available from: https://pubmed.ncbi.nlm.nih.gov/29961189/

30. Froehlich JE, Benning C, Dörmann P. The digalactosyldiacylglycerol (DGDG) synthase DGD1 is inserted into the outer envelope membrane of chloroplasts in a manner independent of the general import pathway and does not depend on direct interaction with monogalactosyldiacylglycerol synthase for DGDG

biosynthesis. J Biol Chem [Internet]. J Biol Chem; 2001 [cited 2022 Sep 29];276:31806–12. Available from: https://pubmed.ncbi.nlm.nih.gov/11429410/

31. Blunsom NJ, Cockcroft S. CDP-Diacylglycerol Synthases (CDS): Gateway to Phosphatidylinositol and Cardiolipin Synthesis. Front Cell Dev Biol. Frontiers Media S.A.; 2020;8:63.

32. Siegenthaler P-A, Trémolières A. Role of Acyl Lipids in the Function of Photosynthetic Membranes in Higher Plants. Lipids in Photosynthesis: Structure, Function and Genetics [Internet]. Springer, Dordrecht; 1998 [cited 2022 Sep 29];145–73. Available from: https://link.springer.com/chapter/10.1007/0-306-48087-5_8

33. Vogel G, Eichenberger W. Betaine Lipids in Lower Plants. Biosynthesis of DGTS and DGTA in Ochromonas danica (Chrysophyceae) and the Possible Role of DGTS in Lipid Metabolism. Plant Cell Physiol [Internet]. Oxford Academic; 1992 [cited 2022 Sep 29];33:427–36. Available from: https://academic.oup.com/pcp/article/33/4/427/1879105

34. Tatsuzawa H, Takizawa E. Changes in lipid and fatty acid composition of Pavlova lutheri. Phytochemistry. 1995;40:397–400.

35. Eichenberger W, Gribi C. Lipids of Pavlova lutheri: cellular site and metabolic role of DGCC. Phytochemistry. 1997;45:1561–7.

36. Hurlock AK, Roston RL, Wang K, Benning C. Lipid trafficking in plant cells. Traffic [Internet]. Traffic; 2014 [cited 2022 Sep 29];15:915–32. Available from: https://pubmed.ncbi.nlm.nih.gov/24931800/

37. Remize M, Brunel Y, Silva JL, Berthon JY, Filaire E. Microalgae n-3 PUFAs Production and Use in Food and Feed Industries. Mar Drugs [Internet]. Mar Drugs; 2021 [cited 2022 Sep 29];19. Available from: https://pubmed.ncbi.nlm.nih.gov/33670628/

38. Oliver DJ, Nikolau BJ, Wurtele ES. Acetyl-CoA—Life at the metabolic nexus. Plant Science. Elsevier; 2009;176:597–601.

39. Harwood JL. Fatty acid biosynthesis. Plant Lipids: biology, utilisation and manipulation. 1sr ed. Blackwell, Oxford.; 2005. p. 27–66.

40. Harwood JL. Recent advances in the biosynthesis of plant fatty acids. Biochim Biophys Acta [Internet]. Biochim Biophys Acta; 1996 [cited 2022 Sep 29];1301:7–56. Available from: https://pubmed.ncbi.nlm.nih.gov/8652653/

41. Salas JJ, Ohlrogge JB. Characterization of substrate specificity of plant FatA and FatB acyl-ACP thioesterases. Arch Biochem Biophys [Internet]. Arch Biochem Biophys; 2002 [cited 2022 Sep 29];403:25–34. Available from: https://pubmed.ncbi.nlm.nih.gov/12061798/

42. Groot PH, Scholte HR, Hülsmann WC. Fatty Acid Activation: Specificity, Localization, and Function. Adv Lipid Res. Elsevier; 1976;14:75–126.

43. Mühlroth A, Li K, Røkke G, Winge P, Olsen Y, Hohmann-Marriott MF, et al. Pathways of lipid metabolism in marine algae, co-expression network, bottlenecks and candidate genes for enhanced production of EPA and DHA in species of Chromista. Mar Drugs [Internet]. Mar Drugs; 2013 [cited 2022 Sep 29];11:4662–97. Available from: https://pubmed.ncbi.nlm.nih.gov/24284429/

44. Domergue F, Spiekermann P, Lerchl J, Beckmann C, Kilian O, Kroth PG, et al. New Insight into Phaeodactylum tricornutum Fatty Acid Metabolism. Cloning and Functional Characterization of Plastidial

and Microsomal Δ12-Fatty Acid Desaturases. Plant Physiol [Internet]. Oxford University Press; 2003 [cited 2022 Sep 29];131:1648. Available from: /pmc/articles/PMC166921/

45. Sato N, Tsuzuki M, Kawaguchi A. Glycerolipid synthesis in Chlorella kessleri 11h - I. Existence of a eukaryotic pathway. Biochim Biophys Acta Mol Cell Biol Lipids [Internet]. Elsevier; 2003 [cited 2022 Sep 29];1633:27–34. Available from: https://pubmed.ncbi.nlm.nih.gov/12842192/

46. Frentzen M, Heinz E, Mckeon TA, Stumpf PK. Specificities and selectivities of glycerol-3-phosphate acyltransferase and monoacylglycerol-3-phosphate acyltransferase from pea and spinach chloroplasts. Eur J Biochem [Internet]. Eur J Biochem; 1983 [cited 2022 Sep 29];129:629–36. Available from: https://pubmed.ncbi.nlm.nih.gov/6825679/

47. Kennedy EP. Biosynthesis of complex lipids. Fed Proc [Internet]. Fed Proc; 1961 [cited 2022 Sep 29];20:934–40. Available from: https://pubmed.ncbi.nlm.nih.gov/14455159/

48. Heinz E, Roughan PG. Similarities and differences in lipid metabolism of chloroplasts isolated from 18:3 and 16:3 plants. Plant Physiol [Internet]. Plant Physiol; 1983 [cited 2022 Sep 29];72:273–9. Available from: https://pubmed.ncbi.nlm.nih.gov/16662992/

49. Frentzen M. Biosynthesis and Desaturation of the Different Diacylglycerol Moieties in Higher Plants. J Plant Physiol. Urban & Fischer; 1986;124:193–209.

50. Li N, Gügel IL, Giavalisco P, Zeisler V, Schreiber L, Soll J, et al. FAX1, a Novel Membrane Protein Mediating Plastid Fatty Acid Export. PLoS Biol [Internet]. Public Library of Science; 2015 [cited 2022 Sep 29];13:e1002053. Available from: https://journals.plos.org/plosbiology/article?id=10.1371/journal.pbio.1002053

51. Bai F, Yu L, Shi J, Li-Beisson Y, Liu J. Long-chain acyl-CoA synthetases activate fatty acids for lipid synthesis, remodeling and energy production in Chlamydomonas. New Phytol [Internet]. New Phytol; 2022 [cited 2022 Sep 29];233:823–37. Available from: https://pubmed.ncbi.nlm.nih.gov/34665469/

52. Li N, Xu C, Li-Beisson Y, Philippar K. Fatty Acid and Lipid Transport in Plant Cells. Trends Plant Sci [Internet]. Trends Plant Sci; 2016 [cited 2022 Sep 29];21:145–58. Available from: https://pubmed.ncbi.nlm.nih.gov/26616197/

53. Smith R, Jouhet J, Gandini C, Nekrasov V, Marechal E, Napier JA, et al. Plastidial acyl carrier protein Δ9-desaturase modulates eicosapentaenoic acid biosynthesis and triacylglycerol accumulation in Phaeodactylum tricornutum. Plant J [Internet]. Plant J; 2021 [cited 2022 Sep 29];106:1247–59. Available from: https://pubmed.ncbi.nlm.nih.gov/33725374/

54. Avidan O, Malitsky S, Pick U. Fatty Acid Production and Direct Acyl Transfer through Polar Lipids Control TAG Biosynthesis during Nitrogen Deprivation in the Halotolerant Alga Dunaliella tertiolecta. Mar Drugs [Internet]. Mar Drugs; 2021 [cited 2022 Sep 29];19. Available from: https://pubmed.ncbi.nlm.nih.gov/34202376/

55. Bates PD, Fatihi A, Snapp AR, Carlsson AS, Browse J, Lu C. Acyl editing and headgroup exchange are the major mechanisms that direct polyunsaturated fatty acid flux into triacylglycerols. Plant Physiol [Internet]. Plant Physiol; 2012 [cited 2022 Sep 29];160:1530–9. Available from: https://pubmed.ncbi.nlm.nih.gov/22932756/

56. Tsugawa H, Satoh A, Uchino H, Cajka T, Arita M, Arita M. Mass Spectrometry Data Repository Enhances Novel Metabolite Discoveries with Advances in Computational Metabolomics. Metabolites

[Internet]. Metabolites; 2019 [cited 2022 Sep 29];9. Available from: https://pubmed.ncbi.nlm.nih.gov/31238512/

57. Huang D, Li DW, Balamurugan S, Zheng JW, Liu WJ, Zou LG, et al. Plastidial and ER Triacylglycerol Biosynthesis in a Growth Phase-Dependent Manner in the Heterokont Nannochloropsis oceanica. Front Mar Sci. Frontiers Media S.A.; 2020;7:104.

58. Riekhof WR, Sears BB, Benning C. Annotation of genes involved in glycerolipid biosynthesis in Chlamydomonas reinhardtii: Discovery of the betaine lipid synthase BTA1Cr. Eukaryot Cell [Internet]. American Society for Microbiology ; 2005 [cited 2022 Sep 29];4:242–52. Available from: https://journals.asm.org/doi/10.1128/EC.4.2.242-252.2005

59. Murakami H, Nobusawa T, Hori K, Shimojima M, Ohta H. Betaine Lipid Is Crucial for Adapting to Low Temperature and Phosphate Deficiency in Nannochloropsis. Plant Physiol [Internet]. Oxford Academic; 2018 [cited 2022 Sep 29];177:181–93. Available from: https://academic.oup.com/plphys/article/177/1/181/6116925

60. Jennings W, Epand RM. CDP-diacylglycerol, a critical intermediate in lipid metabolism. Chem Phys Lipids. Elsevier; 2020;230:104914.

61. Han D, Jia J, Li J, Sommerfeld M, Xu J, Hu Q. Metabolic remodeling of membrane glycerolipids in the microalga Nannochloropsis oceanica under nitrogen deprivation. Front Mar Sci. Frontiers Media S. A; 2017;4:242.

62. John U, Beszteri B, Derelle E, van de Peer Y, Read B, Moreau H, et al. Novel insights into evolution of protistan polyketide synthases through phylogenomic analysis. Protist [Internet]. Protist; 2008 [cited 2022 Sep 29];159:21–30. Available from: https://pubmed.ncbi.nlm.nih.gov/17931970/

63. John U, Beszteri S, GlöCkner G, Singh R, Medlin L, Cembella AD. Genomic characterisation of the ichthyotoxic prymnesiophyte Chrysochromulina polylepis, and the expression of polyketide synthase genes in synchronized cultures. https://doi.org/101080/09670261003746193 [Internet]. Taylor & Francis Group ; 2010 [cited 2022 Sep 29];45:215–29. Available from: https://www.tandfonline.com/doi/abs/10.1080/09670261003746193

64. Anestis K, Kohli GS, Wohlrab S, Varga E, Larsen TO, Hansen PJ, et al. Polyketide synthase genes and molecular trade-offs in the ichthyotoxic species Prymnesium parvum. Science of The Total Environment. Elsevier; 2021;795:148878.

65. Sun XM, Ren LJ, Zhao QY, Ji XJ, Huang H. Enhancement of lipid accumulation in microalgae by metabolic engineering. Biochim Biophys Acta Mol Cell Biol Lipids [Internet]. Biochim Biophys Acta Mol Cell Biol Lipids; 2019 [cited 2022 Sep 29];1864:552–66. Available from: https://pubmed.ncbi.nlm.nih.gov/30308323/

66. Ernst R, Ejsing CS, Antonny B. Homeoviscous Adaptation and the Regulation of Membrane Lipids. J Mol Biol. Academic Press; 2016;428:4776–91.

67. Harayama T, Riezman H. Understanding the diversity of membrane lipid composition. Nature Reviews Molecular Cell Biology 2018 19:5 [Internet]. Nature Publishing Group; 2018 [cited 2022 Sep 29];19:281–96. Available from: https://www.nature.com/articles/nrm.2017.138

68. Sun X lin, Yang S, Wang LY, Zhang QY, Zhao SJ, Meng QW. The unsaturation of phosphatidylglycerol in thylakoid membrane alleviates PSII photoinhibition under chilling stress. Plant Cell Rep [Internet]. Plant

Cell Rep; 2011 [cited 2022 Sep 29];30:1939–47. Available from: https://pubmed.ncbi.nlm.nih.gov/21695527/

69. Guedes AC, Meireles LA, Amaro HM, Malcata FX. Changes in lipid class and fatty acid composition of cultures of Pavlova lutheri, in response to light intensity. JAOCS, Journal of the American Oil Chemists' Society. 2010;87:791–801.

70. Guihéneuf F, Stengel DB. Interactive effects of light and temperature on pigments and n-3 LC-PUFA-enriched oil accumulation in batch-cultivated Pavlova lutheri using high-bicarbonate supply. Algal Res [Internet]. Elsevier B.V.; 2017;23:113–25. Available from: http://dx.doi.org/10.1016/j.algal.2017.02.002

71. Huang B, Mimouni V, Lukomska E, Morant-Manceau A, Bougaran G. Carbon Partitioning and Lipid Remodeling During Phosphorus and Nitrogen Starvation in the Marine Microalga Diacronema lutheri (Haptophyta). J Phycol. 2020;56:908–22.

72. Haines TH, Dencher NA. Cardiolipin: A proton trap for oxidative phosphorylation. FEBS Lett [Internet]. FEBS Lett; 2002 [cited 2022 Sep 29];528:35–9. Available from: https://pubmed.ncbi.nlm.nih.gov/12297275/

73. Li J, Liu LN, Meng Q, Fan H, Sui N. The roles of chloroplast membrane lipids in abiotic stress responses. Plant Signal Behav [Internet]. Plant Signal Behav; 2020 [cited 2022 Sep 29];15. Available from: https://pubmed.ncbi.nlm.nih.gov/32815751/

74. Garnier M, Bougaran G, Pavlovic M, Berard JB, Carrier G, Charrier A, et al. Use of a lipid rich strain reveals mechanisms of nitrogen limitation and carbon partitioning in the haptophyte Tisochrysis lutea. Algal Res. Elsevier; 2016;20:229–48.

75. Huang B, Marchand J, Thiriet-Rupert S, Carrier G, Saint-Jean B, Lukomska E, et al. Betaine lipid and neutral lipid production under nitrogen or phosphorus limitation in the marine microalga Tisochrysis lutea (Haptophyta). Algal Res. Elsevier B.V.; 2019;40.

76. Popko J, Herrfurth C, Feussner K, Ischebeck T, Iven T, Haslam R, et al. Metabolome Analysis Reveals Betaine Lipids as Major Source for Triglyceride Formation, and the Accumulation of Sedoheptulose during Nitrogen-Starvation of Phaeodactylum tricornutum. PLoS One [Internet]. Public Library of Science; 2016 [cited 2022 Sep 29];11:e0164673. Available from: https://journals.plos.org/plosone/article?id=10.1371/journal.pone.0164673

77. Tonon T, Harvey D, Larson TR, Graham IA. Long chain polyunsaturated fatty acid production and partitioning to triacylglycerols in four microalgae. Phytochemistry. 2002;61:15–24.

78. Cañavate JP, Armada I, Hachero-Cruzado I. Interspecific variability in phosphorus-induced lipid remodelling among marine eukaryotic phytoplankton. New Phytol [Internet]. New Phytol; 2017 [cited 2022 Sep 29];213:700–13. Available from: https://pubmed.ncbi.nlm.nih.gov/27605045/

79. Oishi Y, Otaki R, Iijima Y, Kumagai E, Aoki M, Tsuzuki M, et al. Diacylglyceryl-N,N,N-trimethylhomoserine-dependent lipid remodeling in a green alga, Chlorella kessleri. Communications Biology 2022 5:1 [Internet]. Nature Publishing Group; 2022 [cited 2022 Sep 29];5:1–13. Available from: https://www.nature.com/articles/s42003-021-02927-z

80. Sheffer M, Fried A, Gottlieb HE, Tietz A, Avron M. Lipid composition of the plasma-membrane of the halotolerant alga, Dunaliella salina. Biochimica et Biophysica Acta (BBA) - Biomembranes. Elsevier; 1986;857:165–72.

81. Yang M, Kong F, Xie X, Wu P, Chu Y, Cao X, et al. Galactolipid DGDG and Betaine Lipid DGTS Direct De Novo Synthesized Linolenate into Triacylglycerol in a Stress-Induced Starchless Mutant of Chlamydomonas reinhardtii. Plant Cell Physiol [Internet]. Plant Cell Physiol; 2020 [cited 2022 Sep 29];61:851–62. Available from: https://pubmed.ncbi.nlm.nih.gov/32061132/

82. Li-Beisson Y, Beisson F, Riekhof W. Metabolism of acyl-lipids in Chlamydomonas reinhardtii. Plant J [Internet]. Plant J; 2015 [cited 2022 Sep 29];82:504–22. Available from: https://pubmed.ncbi.nlm.nih.gov/25660108/

83. Huang JJ, Lin S, Xu W, Cheung PCK. Occurrence and biosynthesis of carotenoids in phytoplankton. Biotechnol Adv. Elsevier; 2017;35:597–618.

84. Lichtenthaler HK. Biosynthesis, Localization and Concentration of Carotenoids in Plants and Algae. In: Eaton-Rye J., Tripathy B, Sharkey T, editors. Photosynthesis Advances in Photosynthesis and Respiration. Springer, Dordrecht; 2012. p. 95–112.

85. Dembitsky VM, Maoka T. Allenic and cumulenic lipids. Prog Lipid Res. Pergamon; 2007;46:328–75.

86. Yamamoto HY, Bassi R. Carotenoids: Localization and Function. Oxygenic Photosynthesis: The Light Reactions Advances in Photosynthesis and Respiration. Dordrecht: Springer; 1996. p. 539–63.

87. Ren Y, Sun H, Deng J, Huang J, Chen F. Carotenoid Production from Microalgae: Biosynthesis, Salinity Responses and Novel Biotechnologies. Mar Drugs [Internet]. Multidisciplinary Digital Publishing Institute (MDPI); 2021 [cited 2022 Sep 30];19. Available from: /pmc/articles/PMC8708220/

88. Lamers PP, van de Laak CCW, Kaasenbrood PS, Lorier J, Janssen M, de Vos RCH, et al. Carotenoid and fatty acid metabolism in light-stressed Dunaliella salina. Biotechnol Bioeng. 2010;106:638–48.

89. Abe K, Hattori H, Hirano M. Accumulation and antioxidant activity of secondary carotenoids in the aerial microalga Coelastrella striolata var. multistriata. Food Chem [Internet]. 2007;100:656–61. Available from: https://www.sciencedirect.com/science/article/pii/S0308814605009222

90. Kato S, Ozasa K, Maeda M, Tanno Y, Tamaki S, Higuchi-Takeuchi M, et al. Carotenoids in the eyespot apparatus are required for triggering phototaxis in Euglena gracilis. Plant Journal. Blackwell Publishing Ltd; 2020;101:1091–102.

91. Lohscheider JN, Río Bártulos C. Plastoglobules in algae: A comprehensive comparative study of the presence of major structural and functional components in complex plastids. Mar Genomics [Internet]. Mar Genomics; 2016 [cited 2022 Sep 30];28:127–36. Available from: https://pubmed.ncbi.nlm.nih.gov/27373732/

92. Frank HA, Young AJ, Britton G, Codgell RJ. The Photochemistry of Carotenoids. 1st ed. Dordrecht: Springer ; 1999.

93. Kreimer G. The green algal eyespot apparatus: A primordial visual system and more? Curr Genet [Internet]. Springer; 2009 [cited 2022 Sep 30];55:19–43. Available from: https://link.springer.com/article/10.1007/s00294-008-0224-8

94. Paniagua-Michel J, Olmos-Soto J, Ruiz MA. Pathways of Carotenoid Biosynthesis in Bacteria and Microalgae. In: Barredo JL, editor. Microbial Carotenoids from Bacteria and Microalgae Methods in Molecular Biology. Totowa, NJ: Humana Press; 2012. p. 1–12.

95. Shumskaya M, Bradbury LMT, Monaco RR, Wurtzela ET. Plastid localization of the key carotenoid enzyme phytoene synthase is altered by isozyme, allelic variation, and activity. Plant Cell [Internet]. Plant

Cell; 2012 [cited 2022 Sep 30];24:3725–41. Available from: https://pubmed.ncbi.nlm.nih.gov/23023170/

96. Couso I, Vila M, Vigara J, Cordero BF, Vargas MÁ, Rodríguez H, et al. Synthesis of carotenoids and regulation of the carotenoid biosynthesis pathway in response to high light stress in the unicellular microalga Chlamydomonas reinhardtii. https://doi.org/101080/096702622012692816 [Internet]. Taylor & Francis Group ; 2012 [cited 2022 Sep 30];47:223–32. Available from: https://www.tandfonline.com/doi/abs/10.1080/09670262.2012.692816

97. Joyard J, Ferro M, Masselon C, Seigneurin-Berny D, Salvi D, Garin J, et al. Chloroplast proteomics and the compartmentation of plastidial isoprenoid biosynthetic pathways. Mol Plant [Internet]. Mol Plant; 2009 [cited 2022 Sep 30];2:1154–80. Available from: https://pubmed.ncbi.nlm.nih.gov/19969518/

98. Ferro M, Brugière S, Salvi D, Seigneurin-Berny D, Court M, Moyet L, et al. AT_CHLORO, a comprehensive chloroplast proteome database with subplastidial localization and curated information on envelope proteins. Mol Cell Proteomics [Internet]. Mol Cell Proteomics; 2010 [cited 2022 Sep 30];9:1063–84. Available from: https://pubmed.ncbi.nlm.nih.gov/20061580/

99. Douce R, Joyard J. Biosynthesis of Thylakoid Membrane Lipids. Oxygenic Photosynthesis: The Light Reactions [Internet]. Springer, Dordrecht; 1996 [cited 2022 Sep 30];69–101. Available from: https://link.springer.com/chapter/10.1007/0-306-48127-8_6

100. Banerjee A, Sharkey TD. Methylerythritol 4-phosphate (MEP) pathway metabolic regulation. Nat Prod Rep [Internet]. Nat Prod Rep; 2014 [cited 2022 Sep 30];31:1043–55. Available from: https://pubmed.ncbi.nlm.nih.gov/24921065/

101. Schwender J, Gemünden C, Lichtenthaler HK. Chlorophyta exclusively use the 1-deoxyxylulose 5-phosphate/2-C-methylerythritol 4-phosphate pathway for the biosynthesis of isoprenoids. Planta [Internet]. Planta; 2001 [cited 2022 Sep 30];212:416–23. Available from: https://pubmed.ncbi.nlm.nih.gov/11289606/

102. Tamaki S, Mochida K, Suzuki K. Diverse Biosynthetic Pathways and Protective Functions against Environmental Stress of Antioxidants in Microalgae. Plants (Basel) [Internet]. Plants (Basel); 2021 [cited 2022 Sep 30];10. Available from: https://pubmed.ncbi.nlm.nih.gov/34205386/

103. Varela JC, Pereira H, Vila M, León R. Production of carotenoids by microalgae: Achievements and challenges. Photosynth Res [Internet]. Kluwer Academic Publishers; 2015 [cited 2022 Sep 30];125:423–36. Available from: https://link.springer.com/article/10.1007/s11120-015-0149-2

104. Schüler LM, Schulze PSC, Pereira H, Barreira L, León R, Varela J. Trends and strategies to enhance triacylglycerols and high-value compounds in microalgae. Algal Res. Elsevier; 2017;25:263–73.

105. Ota S, Morita A, Ohnuki S, Hirata A, Sekida S, Okuda K, et al. Carotenoid dynamics and lipid droplet containing astaxanthin in response to light in the green alga Haematococcus pluvialis. Scientific Reports 2018 8:1 [Internet]. Nature Publishing Group; 2018 [cited 2022 Sep 30];8:1–10. Available from: https://www.nature.com/articles/s41598-018-23854-w

106. Lafarga T, Clemente I, Garcia-Vaquero M. Carotenoids from microalgae. Carotenoids: Properties, Processing and Applications. Academic Press; 2020;149–87.

107. Berger R, Liaaen-Jensen S, McAlister V, Guillard RRL. Carotenoids of Prymnesiophyceae (Haptophyceae). Biochem Syst Ecol. 1977;5:71–5.

108. Fawley MW, Morton SJ, Stewart KD, Mattox KR. Evidence for a common evolutionary origin of light-harvesting fucoxanthin chlorophyll a/c protein complexes of Pavlova gyrans (Prymnesiophycceae) and Phaeodactylum tricornutum (Bacillariophyceae). J. Phycol. 1987.

109. Seoane S, Zapata M, Orive E. Growth rates and pigment patterns of haptophytes isolated from estuarine waters. J Sea Res [Internet]. Elsevier B.V.; 2009;62:286–94. Available from: http://dx.doi.org/10.1016/j.seares.2009.07.008

110. Zapata M, Jeffrey SW, Wright SW, Rodríguez F, Garrido JL, Clementson L. Photosynthetic pigments in 37 species (65 strains) of Haptophyta: Implications for oceanography and chemotaxonomy. Mar Ecol Prog Ser. 2004;270:83–102.

111. Goss R, Latowski D. Lipid Dependence of Xanthophyll Cycling in Higher Plants and Algae. Front Plant Sci. Frontiers Media S.A.; 2020;11:455.

112. Kihara S, Hartzler DA, Savikhin S. Oxygen concentration inside a functioning photosynthetic cell. Biophys J [Internet]. Biophys J; 2014 [cited 2022 Sep 30];106:1882–9. Available from: https://pubmed.ncbi.nlm.nih.gov/24806920/

113. Tardy F, Havaux M. Thylakoid membrane fluidity and thermostability during the operation of the xanthophyll cycle in higher-plant chloroplasts. Biochim Biophys Acta [Internet]. Biochim Biophys Acta; 1997 [cited 2022 Sep 30];1330:179–93. Available from: https://pubmed.ncbi.nlm.nih.gov/9408171/

114. Lepetit B, Volke D, Gilbert M, Wilhelm C, Goss R. Evidence for the existence of one antenna-associated, lipid-dissolved and two protein-bound pools of diadinoxanthin cycle pigments in diatoms. Plant Physiol [Internet]. Plant Physiol; 2010 [cited 2022 Sep 30];154:1905–20. Available from: https://pubmed.ncbi.nlm.nih.gov/20935178/

115. Bojko M, Olchawa-Pajor M, Goss R, Schaller-Laudel S, Strzałka K, Latowski D. Diadinoxanthin de-epoxidation as important factor in the short-term stabilization of diatom photosynthetic membranes exposed to different temperatures. Plant Cell Environ. Blackwell Publishing Ltd; 2019;42:1270–86.

116. Togarcheti SC, Padamati RB. Comparative Life Cycle Assessment of EPA and DHA Production from Microalgae and Farmed Fish. Clean Technologies. MDPI AG; 2021;3:699–710.

117. Santigosa E, Brambilla F, Milanese L. Microalgae oil as an effective alternative source of epa and dha for gilthead seabream (Sparus aurata) aquaculture. Animals. MDPI AG; 2021;11.

118. Capelli B, Bagchi D, Cysewski GR. Synthetic astaxanthin is significantly inferior to algal-based astaxanthin as an antioxidant and may not be suitable as a human nutraceutical supplement. Nutrafoods. Springer Science and Business Media LLC; 2013;12:145–52.

119. Credence Research. Algae Products Market Size, Analysis, Trends, Growth And Forecast To 2027 [Internet]. [cited 2022 Apr 11]. Available from: https://www.credenceresearch.com/report/algae-products-market

120. Fernandes AS, Nascimento TC, Pinheiro PN, Vendruscolo RG, Wagner R, de Rosso V v., et al. Bioaccessibility of microalgae-based carotenoids and their association with the lipid matrix. Food Research International. Elsevier Ltd; 2021;148.

121. BCC Research. Carotenoids Market Size, Share & Growth Analysis Report [Internet]. [cited 2022 Apr 11]. Available from: https://www.bccresearch.com/market-research/food-and-beverage/the-global-market-for-carotenoids.html

122. Borowitzka MA. High-value products from microalgae-their development and commercialisation. J Appl Phycol. 2013. p. 743–56.

123. Hu I-C. Production of potential coproducts from microalgae. Biofuels from Algae. Elsevier; 2019. p. 345–58.

124. Zhu Y, Cheng J, Min Z, Yin T, Zhang R, Zhang W, et al. Effects of fucoxanthin on autophagy and apoptosis in SGC-7901cells and the mechanism. J Cell Biochem. Wiley-Liss Inc.; 2018;119:7274–84.

125. Zhang Y, Xu W, Huang X, Zhao Y, Ren Q, Hong Z, et al. Fucoxanthin ameliorates hyperglycemia, hyperlipidemia and insulin resistance in diabetic mice partially through IRS-1/PI3K/Akt and AMPK pathways. J Funct Foods. Elsevier Ltd; 2018;48:515–24.

126. Patil V, Källqvist T, Olsen E, Vogt G, Gislerød HR. Fatty acid composition of 12 microalgae for possible use in aquaculture feed. Aquaculture International. 2007;15:1–9.

127. Fernandes T, Cordeiro N. Effects of phosphorus-induced changes on the growth, nitrogen uptake, and biochemical composition of Pavlova pinguis and Hemiselmis cf. andersenii. J Appl Phycol. Springer Science and Business Media LLC; 2022;

128. Suh SS, Kim SJ, Hwang J, Park M, Lee TK, Kil EJ, et al. Fatty acid methyl ester profiles and nutritive values of 20 marine microalgae in Korea. Asian Pac J Trop Med. Elsevier (Singapore) Pte Ltd; 2015;8:191–6.

129. Haas S, Bauer JL, Adakli A, Meyer S, Lippemeier S, Schwarz K, et al. Marine microalgae Pavlova viridis and Nannochloropsis sp. as n-3 PUFA source in diets for juvenile European sea bass (Dicentrarchus labrax L.). J Appl Phycol. 2016;28:1011–21.

130. Rodolfi L, Zittelli GC, Bassi N, Padovani G, Biondi N, Bonini G, et al. Microalgae for oil: Strain selection, induction of lipid synthesis and outdoor mass cultivation in a low-cost photobioreactor. Biotechnol Bioeng. 2009;102:100–12.

131. Carvalho AP, Malcata FX. Effect of culture media on production of polyunsaturated fatty acids by Pavlova lutheri. Cryptogam Algol. 2000;21:59–71.

132. Gao F, Sá M, Cabanelas ITD, Wijffels RH, Barbosa MJ. Improved fucoxanthin and docosahexaenoic acid productivities of a sorted self-settling Tisochrysis lutea phenotype at pilot scale. Bioresour Technol. Elsevier Ltd; 2021;325.

133. Gao F, Teles (Cabanelas, ITD) I, Ferrer-Ledo N, Wijffels RH, Barbosa MJ. Production and high throughput quantification of fucoxanthin and lipids in Tisochrysis lutea using single-cell fluorescence. Bioresour Technol. Elsevier Ltd; 2020;318.

134. di Lena G, Casini I, Lucarini M, Lombardi-Boccia G. Carotenoid profiling of five microalgae species from large-scale production. Food Research International. Elsevier Ltd; 2019;120:810–8.

135. Bhattacharjya R, Singh PK, Mishra B, Saxena A, Tiwari A. Phycoprospecting the nutraceutical potential of Isochrysis sp as a source of aquafeed and other high-value products. Aquac Res. Blackwell Publishing Ltd; 2021;52:2988–95.

136. di Lena G, Casini I, Lucarini M, Lombardi-Boccia G. Carotenoid profiling of five microalgae species from large-scale production. Food Research International. Elsevier Ltd; 2019;120:810–8.

137. Janssen JH, Kastenhofer J, de Hoop JA, Lamers PP, Wijffels RH, Barbosa MJ. Effect of nitrogen addition on lipid productivity of nitrogen starved Nannochloropsis gaditana. Algal Res. 2018;33:125–32.

138. Song Z, Lye GJ, Parker BM. Morphological and biochemical changes in Phaeodactylum tricornutum triggered by culture media: Implications for industrial exploitation. Algal Res. Elsevier B.V.; 2020;47.

139. Hashemi A, Moslemi M, Pajoum Shariati F, Delavari Amrei H. Beta-carotene production within Dunaliella salina cells under salt stress condition in an indoor hybrid helical-tubular photobioreactor. Canadian Journal of Chemical Engineering. Wiley-Liss Inc.; 2020;98:69–74.

140. García-González M, Moreno J, Manzano JC, Florencio FJ, Guerrero MG. Production of Dunaliella salina biomass rich in 9-cis-β-carotene and lutein in a closed tubular photobioreactor. J Biotechnol. 2005;115:81–90.

141. Chuang LT, Bülbül U, Wen PC, Glew RH, Ayaz FA. Fatty Acid Composition of 12 Fish Species from the Black Sea. J Food Sci. 2012;77.

142. Mazzeo T, N'Dri D, Chiavaro E, Visconti A, Fogliano V, Pellegrini N. Effect of two cooking procedures on phytochemical compounds, total antioxidant capacity and colour of selected frozen vegetables. Food Chem. 2011;128:627–33.

143. Peet M, Stokes C. Omega-3 Fatty Acids in the Treatment of Psychiatric Disorders. 2005;65:1051–9.

144. Fotuhi M, Mohassel P, Yaffe K. Fish consumption, long-chain omega-3 fatty acids and risk of cognitive decline or Alzheimer disease: A complex association. Nat Clin Pract Neurol. 2009;5:140–52.

145. EFSA Panel on Dietetic Products N and A (NDA). Scientific Opinion on the Tolerable Upper Intake Level of eicosapentaenoic acid (EPA), docosahexaenoic acid (DHA) and docosapentaenoic acid (DPA). EFSA Journal. Wiley-Blackwell Publishing Ltd; 2012;10.

146. Judge MP, Harel O, Lammi-Keefe CJ. Maternal consumption of a docosahexaenoic acid-containing functional food during pregnancy: Benefit for infant performance on problem-solving but not on recognition memory tasks at age 9 mo. American Journal of Clinical Nutrition. 2007;85:1572–7.

147. Swanson D, Block R, Mousa SA. Omega-3 Fatty Acids EPA and DHA: Health Benefits Throughout Life. Advances in Nutrition: An International Review Journal. 2012;3:1–7.

148. Simopoulos AP. Symposium: Role of poultry products in enriching the human diet with n-3 PUFA. Poult Sci. 2000;79:961–70.

149. Simopoulos AP. Evolutionary aspects of diet: The omega-6/omega-3 ratio and the brain. Mol Neurobiol. 2011;44:203–15.

150. Simopoulos A P. The importance of the ratio of omega-6/omega-3 essential fatty acids. Biomedicine and Pharmacotherapy. 2002;56:365–79.

151. BCC Research. Global Omega 3 Market Size and Growth Forecast to 2025 [Internet]. [cited 2022 Apr 11]. Available from: https://www.bccresearch.com/partners/verified-market-research/global-omega-3-market-size-and-forecast.html

152. Taylor P, Ganesan B, Brothersen C, Mcmahon DJ, Ganesan B, Brothersen C. Fortification of Foods with Omega-3 Polyunsaturated Fatty Acids Fortification of Foods with Omega-3. 2014;37–41.

153. Ander BP, Dupasquier CMC, Prociuk MA, Pierce GN. Polyunsaturated fatty acids and their effects on cardiovascular disease. Exp Clin Cardiol. 2003;8:164–72.

154. Lopes FG, Oliveira KA, Lopes RG, Poluceno GG, Simioni C, Pescador GDS, et al. Anti-cancer effects of fucoxanthin on human glioblastoma cell line. Anticancer Res. International Institute of Anticancer Research; 2020;40:6799–815.

155. Terasaki M, Maeda H, Miyashita K, Mutoh M. Induction of Anoikis in Human Colorectal Cancer Cells by Fucoxanthinol. Nutr Cancer. Routledge; 2017;69:1043–52.

156. Enăşescu DA, Moisescu MG, Imre M, Greabu M, Ripszky Totan A, Stanescu-Spinu I, et al. Lutein treatment effects on the redox status and metalloproteinase–9 (MMP-9) in oral cancer squamous cells—are there therapeutical hopes? Materials. MDPI AG; 2021;14.

157. Aoi W, Naito Y, Takanami Y, Ishii T, Kawai Y, Akagiri S, et al. Astaxanthin improves muscle lipid metabolism in exercise via inhibitory effect of oxidative CPT I modification. Biochem Biophys Res Commun. 2008;366:892–7.

158. Chiang YF, Chen HY, Chang YJ, Shih YH, Shieh TM, Wang KL, et al. Protective effects of fucoxanthin on high glucoseand 4-hydroxynonenal (4-HNE)-induced injury in human retinal pigment epithelial cells. Antioxidants. MDPI; 2020;9:1–15.

159. Huang YM, Dou HL, Huang FF, Xu XR, Zou ZY, Lin XM. Effect of supplemental lutein and zeaxanthin on serum, macular pigmentation, and visual performance in patients with early age-related macular degeneration. Biomed Res Int. Hindawi Publishing Corporation; 2015;2015.

160. Ikeda Y, Tsuji S, Satoh A, Ishikura M, Shirasawa T, Shimizu T. Protective effects of astaxanthin on 6-hydroxydopamine-induced apoptosis in human neuroblastoma SH-SY5Y cells. J Neurochem. 2008;107:1730–40.

161. Ito N, Seki S, Ueda F. The protective role of astaxanthin for UV-induced skin deterioration in healthy people—a randomized, double-blind, placebo-controlled trial. Nutrients. MDPI AG; 2018;10.

162. Pistelli L, Sansone C, Smerilli A, Festa M, Noonan DM, Albini A, et al. Mmp-9 and il-1β as targets for diatoxanthin and related microalgal pigments: Potential chemopreventive and photoprotective agents. Mar Drugs. MDPI AG; 2021;19.

163. Régnier P, Bastias J, Rodriguez-Ruiz V, Caballero-Casero N, Caballo C, Sicilia D, et al. Astaxanthin from Haematococcus pluvialis prevents oxidative stress on human endothelial cells without toxicity. Mar Drugs. MDPI AG; 2015;13:2857–74.

164. Regu GM, Kim H, Kim YJ, Paek JE, Lee G, Chang N, et al. Association between dietary carotenoid intake and bone mineral density in Korean adults aged 30–75 years using data from the fourth and fifth korean national health and nutrition examination surveys (2008–2011). Nutrients. MDPI AG; 2017;9.

165. Yang UJ, Park TS, Shim SM. Protective effect of chlorophyllin and lycopene from water spinach extract on cytotoxicity and oxidative stress induced by heavy metals in human hepatoma cells. Journal of Toxicology and Environmental Health - Part A: Current Issues. 2013;76:1307–15.

166. Zhang L, Wang H, Fan Y, Gao Y, Li X, Hu Z, et al. Fucoxanthin provides neuroprotection in models of traumatic brain injury via the Nrf2-ARE and Nrf2-autophagy pathways. Sci Rep. Nature Publishing Group; 2017;7.

167. Wang N, Wang D, Luo G, Zhou J, Tan Z, Du Y, et al. Lutein attenuates excessive lipid accumulation in differentiated 3T3-L1 cells and abdominal adipose tissue of rats by the SIRT1-mediated pathway. International Journal of Biochemistry and Cell Biology. Elsevier Ltd; 2021;133.

168. AbuMweis S, Jew S, Tayyem R, Agraib L. Eicosapentaenoic acid and docosahexaenoic acid containing supplements modulate risk factors for cardiovascular disease: a meta-analysis of randomised placebo-control human clinical trials. Journal of Human Nutrition and Dietetics. Blackwell Publishing Ltd; 2018;31:67–84.

169. Chan SSM, Luben R, Olsen A, Tjonneland A, Kaaks R, Lindgren S, et al. Association between high dietary intake of the n-3 polyunsaturated fatty acid docosahexaenoic acid and reduced risk of Crohn's disease. Aliment Pharmacol Ther. Blackwell Publishing Ltd; 2014;39:834–42.

170. John S, Luben R, Shrestha SS, Welch A, Khaw KT, Hart AR. Dietary n-3 polyunsaturated fatty acids and the aetiology of ulcerative colitis: A UK prospective cohort study. Eur J Gastroenterol Hepatol. 2010;22:602–6.

171. Miles EA, Calder PC. Influence of marine n-3 polyunsaturated fatty acids on immune function and a systematic review of their effects on clinical outcomes in rheumatoid arthritis. British Journal of Nutrition. 2012.

172. Nauroth JM, Liu YC, van Elswyk M, Bell R, Hall EB, Chung G, et al. Docosahexaenoic acid (DHA) and docosapentaenoic acid (DPAn-6) algal oils reduce inflammatory mediators in human peripheral mononuclear cells in vitro and paw edema in vivo. Lipids. 2010;45:375–84.

173. Merendino N, Costantini L, Manzi L, Molinari R, D'Eliseo D, Velotti F. Dietary ω-3 polyunsaturated fatty acid DHA: A potential adjuvant in the treatment of cancer. Biomed Res Int. 2013.

174. Echeverría F, Valenzuela R, Catalina Hernandez-Rodas M, Valenzuela A. Docosahexaenoic acid (DHA), a fundamental fatty acid for the brain: New dietary sources. Prostaglandins Leukot Essent Fatty Acids. Churchill Livingstone; 2017. p. 1–10.

175. Matsuoka YJ, Sawada N, Mimura M, Shikimoto R, Nozaki S, Hamazaki K, et al. Dietary fish, n-3 polyunsaturated fatty acid consumption, and depression risk in Japan: a population-based prospective cohort study. Transl Psychiatry. 2017;7:e1242.

176. Chung RWS, Leanderson P, Lundberg AK, Jonasson L. Lutein exerts anti-inflammatory effects in patients with coronary artery disease. Atherosclerosis. Elsevier Ireland Ltd; 2017;262:87–93.

177. Hwang PA, Phan NN, Lu WJ, Hieu BTN, Lin YC. Low-molecular-weight fucoidan and high-stability fucoxanthin from brown seaweed exert prebiotics and anti-inflammatory activities in Caco-2 cells. Food Nutr Res. Co-Action Publishing; 2016;60.

178. Lin KH, Hsu CY, Huang YP, Lai JY, Hsieh W bin, Huang MY, et al. Chlorophyll-related compounds inhibit cell adhesion and inflammation in human aortic cells. J Med Food. 2013;16:886–98.

179. Park JS, Chyun JH, Kim YK, Line LL, Chew BP. Astaxanthin decreased oxidative stress and inflammation and enhanced immune response in humans [Internet]. 2010. Available from: http://www.nutritionandmetabolism.com/content/7/1/18

180. Okada T, Nakai M, Maeda H, Hosokawa M, Sashima T, Miyashita K. Suppressive effect of neoxanthin on the differentiantion of 3t3-L1. J Oleo Sci. 2008;57:345–52.

181. Hu C, Li M, Li J, Zhu Q, Liu Z. Variation of lipid and fatty acid compositions of the marine microalga Pavlova viridis (Prymnesiophyceae) under laboratory and outdoor culture conditions. World J Microbiol Biotechnol. 2008;24:1209–14.

182. Durmaz Y, Donato M, Monteiro M, Gouveia L, Nunes ML, Gama Pereira T, et al. Effect of temperature on α-tocopherol, fatty acid profile, and pigments of Diacronema vlkianum (Haptophyceae). Aquaculture International. 2009;17:391–9.

183. Kanamoto A, Kato Y, Yoshida E, Hasunuma T, Kondo A. Development of a Method for Fucoxanthin Production Using the Haptophyte Marine Microalga Pavlova sp. OPMS 30543. Marine Biotechnology [Internet]. Springer US; 2021;23:331–41. Available from: https://doi.org/10.1007/s10126-021-10028-5

184. Guihéneuf F, Mimouni V, Ulmann L, Tremblin G. Combined effects of irradiance level and carbon source on fatty acid and lipid class composition in the microalga Pavlova lutheri commonly used in mariculture. J Exp Mar Biol Ecol. Elsevier B.V.; 2009;369:136–43.

185. Carvalho AP, Malcata FX. Kinetic modeling of the autotrophic growth of Pavlova lutheri: Study of the combined influence of light and temperature. Biotechnol Prog. 2003;19:1128–35.

186. Béchet Q, Laviale M, Arsapin N, Bonnefond H, Bernard O. Modeling the impact of high temperatures on microalgal viability and photosynthetic activity. Biotechnol Biofuels. BioMed Central; 2017;10:1–11.

187. Mathur S, Agrawal D, Jajoo A. Photosynthesis: Response to high temperature stress. J Photochem Photobiol B. Elsevier B.V.; 2014;137:116–26.

188. Barten R, Djohan Y, Evers W, Wijffels R, Barbosa M. Towards industrial production of microalgae without temperature control: The effect of diel temperature fluctuations on microalgal physiology. J Biotechnol [Internet]. Elsevier B.V.; 2021;336:56–63. Available from: https://doi.org/10.1016/j.jbiotec.2021.06.017

189. Volkman JK, Kearney P, Jeffrey SW. A new source of 4-methyl sterols and 5α(H)-stanols in sediments: prymnesiophyte microalgae of the genus Pavlova. Org Geochem. 1990;15:489–97.

190. Zheng S, Zou S, Feng T, Sun S, Guo X, He M, et al. Low temperature combined with high inoculum density improves alpha-linolenic acid production and biochemical characteristics of Chlamydomonas reinhardtii. Bioresour Technol. Elsevier Ltd; 2022;126746.

191. Han F, Pei H, Hu W, Han L, Zhang S, Ma G. Effect of high-temperature stress on microalgae at the end of the logarithmic phase for the efficient production of lipid. Environmental Technology (United Kingdom) [Internet]. Taylor & Francis; 2016;37:2649–57. Available from: https://doi.org/10.1080/09593330.2016.1158867

192. Carvalho AP, Monteiro CM, Malcata FX. Simultaneous effect of irradiance and temperature on biochemical composition of the microalga Pavlova lutheri. J Appl Phycol. 2009;21:543–52.

193. Srirangan S, Sauer ML, Howard B, Dvora M, Dums J, Backman P, et al. Interaction of temperature and photoperiod increases growth and oil content in the marine microalgae Dunaliella viridis. PLoS One. 2015;10:1–32.

194. Liu BH, Lee YK. Secondary carotenoids formation by the green alga Chlorococcum sp. J Appl Phycol. 2000;12:301–7.

195. Munns R, Termaat A. Whole-plant responses to salinity. Aust J Plant Physiol. 1986;13:143–60.

196. Cañavate JP, Fernández-Díaz C. Salinity induces unique changes in lipid classes and fatty acids of the estuarine haptophyte Diacronema vlkianum. Eur J Phycol [Internet]. Taylor & Francis; 2021;00:1–21. Available from: https://doi.org/10.1080/09670262.2021.1970234

197. Neelam S, Subramanyam R. Alteration of photochemistry and protein degradation of photosystem II from Chlamydomonas reinhardtii under high salt grown cells. J Photochem Photobiol B. 2013;124:63–70.

198. Shah SMU, Che Radziah C, Ibrahim S, Latiff F, Othman MF, Abdullah MA. Effects of photoperiod, salinity and pH on cell growth and lipid content of Pavlova lutheri. Ann Microbiol. 2014;64:157–64.

199. Ahmed F, Zhou W, Schenk PM. Pavlova lutheri is a high-level producer of phytosterols. Algal Res [Internet]. Elsevier B.V.; 2015;10:210–7. Available from: http://dx.doi.org/10.1016/j.algal.2015.05.013

200. Cañavate JP, Fernández-Díaz C. Salinity induces unique changes in lipid classes and fatty acids of the estuarine haptophyte Diacronema vlkianum. Eur J Phycol [Internet]. Taylor & Francis; 2021;00:1–21. Available from: https://doi.org/10.1080/09670262.2021.1970234

201. Pancha I, Chokshi K, Maurya R, Trivedi K, Patidar SK, Ghosh A, et al. Salinity induced oxidative stress enhanced biofuel production potential of microalgae Scenedesmus sp. CCNM 1077. Bioresour Technol. Elsevier Ltd; 2015;189:341–8.

202. Srivastava G, Nishchal, Goud V V. Salinity induced lipid production in microalgae and cluster analysis (ICCB 16-BR_047). Bioresour Technol. Elsevier Ltd; 2017;242:244–52.

203. Ishika T, Moheimani NR, Bahri PA, Laird DW, Blair S, Parlevliet D. Halo-adapted microalgae for fucoxanthin production: Effect of incremental increase in salinity. Algal Res. 2017;28:66–73.

204. Ryther JH. Photosynthesis in the Ocean as a Function of Light Intensity. Limonogy and oceanography. 1956;1:61–70.

205. Wimalasekera R. Effect of Light Intensity on Photosynthesis. In: Ahmad P, Ahanger MA, Alyemeni MN, Alam P, editors. Photosynthesis, Productivity and Environmental Stress. John Wiley & Sons Ltd; 2020. p. 65–73.

206. Guihéneuf F, Mimouni V, Tremblin G, Ulmann L. Light intensity regulates LC-PUFA incorporation into lipids of Pavlova lutheri and the final desaturase and elongase activities involved in their biosynthesis. J Agric Food Chem. 2015;63:1261–7.

207. Carvalho AP, Malcata FX. Optimization of ω-3 fatty acid production by microalgae: Crossover effects of CO2 and light intensity under batch and continuous cultivation modes. Marine Biotechnology. 2005;7:381–8.

208. Ahmed F, Schenk PM. UV–C radiation increases sterol production in the microalga Pavlova lutheri. Phytochemistry [Internet]. Elsevier Ltd; 2017;139:25–32. Available from: http://dx.doi.org/10.1016/j.phytochem.2017.04.002

209. Adarme-Vega TC. Optimisation of microalgal growth conditions for production of eicosapentaenoic acid (EPA). University of Queensland; 2014.

210. Guihéneuf F, Fouqueray M, Mimouni V, Ulmann L, Jacquette B, Tremblin G. Effect of UV stress on the fatty acid and lipid class composition in two marine microalgae Pavlova lutheri (Pavlovophyceae) and Odontella aurita (Bacillariophyceae). J Appl Phycol. 2010;22:629–38.

211. Kim SH, Sunwoo IY, Hong HJ, Awah CC, Jeong GT, Kim SK. Lipid and unsaturated fatty acid productions from three microalgae using nitrate and light-emitting diodes with complementary LED

wavelength in a two-phase culture system. Bioprocess Biosyst Eng [Internet]. Springer Berlin Heidelberg; 2019;42:1517–26. Available from: https://doi.org/10.1007/s00449-019-02149-y

212. Kurt, Ekinci K, Uysal. The effect of LEDs on the growth and fatty acid composition of Botryococcus braunii. Renew Energy [Internet]. Elsevier Ltd; 2022;186:66–73. Available from: https://doi.org/10.1016/j.renene.2021.12.142

213. Zhang H, Gong P, Cai Q, Zhang C, Gao B. Maximizing fucoxanthin production in Odontella aurita by optimizing the ratio of red and blue light-emitting diodes in an auto-controlled internally illuminated photobioreactor. Bioresour Technol [Internet]. Elsevier Ltd; 2022;344:126260. Available from: https://doi.org/10.1016/j.biortech.2021.126260

214. Takagi M, Watanabe K, Yamaberi K, Yoshida T. Limited feeding of potassium nitrate for intracellular lipid and triglyceride accumulation of Nannochloris sp. UTEX LB1999. Appl Microbiol Biotechnol. 2000;54:112–7.

215. Guihéneuf F, Stengel DB. LC-PUFA-enriched oil production by microalgae: Accumulation of lipid and triacylglycerols containing n-3 LC-PUFA is triggered by nitrogen limitation and inorganic carbon availability in the marine haptophyte Pavlova lutheri. Mar Drugs. 2013;11:4246–66.

216. Carvalho AP, Pontes I, Gaspar H, Malcata FX. Metabolic relationships between macro- and micronutrients, and the eicosapentaenoic acid and docosahexaenoic acid contents of Pavlova lutheri. Enzyme Microb Technol. 2006;38:358–66.

217. Kim G, Mujtaba G, Lee K. Effects of nitrogen sources on cell growth and biochemical composition of marine chlorophyte tetraselmis sp. For lipid production. Algae. 2016;31:257–66.

218. Usman Shah SM, Abdullah MA. Effects of macro/micronutrients on green and brown microalgal cell growth and fatty acids in photobioreactor and open-tank systems. Biocatal Agric Biotechnol [Internet]. Elsevier Ltd; 2018;14:10–7. Available from: https://doi.org/10.1016/j.bcab.2018.01.011

219. Huang X, Huang Z, Wen W, Yan J. Effects of nitrogen supplementation of the culture medium on the growth, total lipid content and fatty acid profiles of three microalgae (Tetraselmis subcordiformis, Nannochloropsis oculata and Pavlova viridis). J Appl Phycol. 2013;25:129–37.

220. Thiyagarajan S, Arumugam M, Kathiresan S. Identification and Functional Characterization of Two Novel Fatty Acid Genes from Marine Microalgae for Eicosapentaenoic Acid Production. Appl Biochem Biotechnol. Applied Biochemistry and Biotechnology; 2020;190:1371–84.

221. Borovkov AB, Gudvilovich IN, Avsiyan AL, Lantushenko AO. Light supply and mineral nutrition conditions as optimization factors for outdoor mass culture of carotenogenic microalga Dunaliella salina. Aquac Res. 2021;52:6098–106.

222. Blank LM. The cell and P: From cellular function to biotechnological application. Curr Opin Biotechnol. 2012. p. 846–51.

223. Powell N, Shilton AN, Pratt S, Chisti Y. Factors influencing luxury uptake of phosphorus by microalgae in waste stabilization ponds. Environ Sci Technol. 2008;42:5958–62.

224. Powell N, Shilton A, Chisti Y, Pratt S. Towards a luxury uptake process via microalgae - Defining the polyphosphate dynamics. Water Res. Elsevier Ltd; 2009;43:4207–13.

225. Dyhrman ST. Nutrients and Their Acquisition: Phosphorus Physiology in Microalgae. The Physiology of Microalgae. Springer International Publishing; 2016. p. 155–83.

226. Laws EA, Pei S, Bienfang P, Grant S, Sunda WG. Phosphate-limited growth of pavlova lutheri (prymnesiophyceae) in continuous culture: Determination of growth-rate-limiting substrate concentrations with a sensitive bioassay procedure. J Phycol. 2011;47:1089–97.

227. Terry KL. Nitrate and Phosphate Uptake Interactions in a Marine Prymnesiophyte. J Phycol. 1982;18:79–86.

228. Wu Q, Guo L, Li X, Wang Y. Effect of phosphorus concentration and light/dark condition on phosphorus uptake and distribution with microalgae. Bioresour Technol. NLM (Medline); 2021;340:125745.

229. Cañavate JP, Armada I, Hachero-Cruzado I. Aspects of phosphorus physiology associated with phosphate-induced polar lipid remodelling in marine microalgae. J Plant Physiol. Elsevier GmbH; 2017;214:28–38.

230. Yang F, Xiang W, Li T, Long L. Transcriptome analysis for phosphorus starvation-induced lipid accumulation in Scenedesmus sp. Sci Rep. Nature Publishing Group; 2018;8.

231. Liang K, Zhang Q, Gu M, Cong W. Effect of phosphorus on lipid accumulation in freshwater microalga Chlorella sp. J Appl Phycol. Kluwer Academic Publishers; 2013;25:311–8.

232. Forján E, Garbayo I, Casal C, Vílchez C. Enhancement of carotenoid production in Nannochloropsis by phosphate and sulphur limitation. Communicating Current Research and Educational Topics and Trends in Applied Microbiology [Internet]. 2007. p. 356–64. Available from: https://www.researchgate.net/publication/229026176

233. Dahmen-Ben Moussa I, Chtourou H, Karray F, Sayadi S, Dhouib A. Nitrogen or phosphorus repletion strategies for enhancing lipid or carotenoid production from Tetraselmis marina. Bioresour Technol. Elsevier Ltd; 2017;238:325–32.

234. Aslam A, Rasul S, Bahadar A, Hossain N, Saleem M, Hussain S, et al. Effect of micronutrient and hormone on microalgae growth assessment for biofuel feedstock. Sustainability (Switzerland). MDPI AG; 2021;13.

235. Tibbetts SM, Milley JE, Lall SP. Chemical composition and nutritional properties of freshwater and marine microalgal biomass cultured in photobioreactors. J Appl Phycol. Kluwer Academic Publishers; 2015;27:1109–19.

236. Santhakumaran P, Ayyappan SM, Ray JG. Nutraceutical applications of twenty-five species of rapid-growing green-microalgae as indicated by their antibacterial, antioxidant and mineral content. Algal Res. Elsevier B.V.; 2020;47.

237. Tibbetts SM, Patelakis SJJ. Apparent digestibility coefficients (ADCs) of intact-cell marine microalgae meal (Pavlova sp. 459) for juvenile Atlantic salmon (Salmo salar L.). Aquaculture [Internet]. Elsevier B.V.; 2022;546:737236. Available from: https://doi.org/10.1016/j.aquaculture.2021.737236

238. Ponis E, Probert I, Véron B, le Coz JR, Mathieu M, Robert R. Nutritional value of six Pavlovophyceae for Crassostrea gigas and Pecten maximus larvae. Aquaculture. 2006;254:544–53.

239. Fabregas J, Herrero C. Marine microalgae as a potential source of minerals in fish diets. Aquaculture. 1986;51:237–43.

240. León-Vaz A, León R, Giráldez I, Vega JM, Vigara J. Impact of heavy metals in the microalga Chlorella sorokiniana and assessment of its potential use in cadmium bioremediation. Aquatic Toxicology. Elsevier B.V.; 2021;239.

241. Bauenova MO, Sadvakasova AK, Mustapayeva ZO, Kokociński M, Zayadan BK, Wojciechowicz MK, et al. Potential of microalgae Parachlorella kessleri Bh-2 as bioremediation agent of heavy metals cadmium and chromium. Algal Res. Elsevier B.V.; 2021;59.

242. Song L, Qin JG, Su S, Xu J, Clarke S, Shan Y. Micronutrient requirements for growth and hydrocarbon production in the oil producing green Alga Botryococcus braunii (Chlorophyta). PLoS One. 2012;7.

243. Rodriguez IB, Ho TY. Trace metal requirements and interactions in Symbiodinium kawagutii. Front Microbiol. Frontiers Media S.A.; 2018;9.

244. Fox JM, Zimba P v. Minerals and trace elements in microalgae. Microalgae in Health and Disease Prevention. Elsevier; 2018. p. 177–93.

245. Farhat N, Elkhouni A, Zorrig W, Smaoui A, Abdelly C, Rabhi M. Effects of magnesium deficiency on photosynthesis and carbohydrate partitioning. Acta Physiol Plant. Polish Academy of Sciences; 2016.

246. Rout GR, Sahoo S. Role of iron in plant growth and metabolism. Reviews in Agricultural Science. United Graduate School of Agricultural Science; 2015;3:1–24.

247. Chen H, Zhang Y, He C, Wang Q. Ca2+ signal transduction related to neutral lipid synthesis in an oil-producing green alga Chlorella sp. C2. Plant Cell Physiol. Oxford University Press; 2014;55:634–44.

248. Kong L, Price NM. Identification of copper-regulated proteins in an oceanic diatom,: Thalassiosira oceanica 1005. Metallomics. Royal Society of Chemistry; 2020;12:1106–17.

249. Sültemeyer D. Carbonic anhydrase in eukaryotic algae: characterization, regulation, and possible function during photosynthesis. Canadian Journal of Botany [Internet]. 1998;962–72. Available from: www.nrcresearchpress.com

250. Maathuis FJM, Diatloff E. Roles and functions of plant mineral nutrients. In: Maathuis F, editor. Plant Mineral Nutrients Methods in Molecular Biology (Methods and Protocols). Totowa, NJ: Humana Press; 2013. p. 1–21.

251. Monteiro CM, Fonseca SC, Castro PML, Malcata FX. Toxicity of cadmium and zinc on two microalgae, Scenedesmus obliquus and Desmodesmus pleiomorphus, from Northern Portugal. J Appl Phycol. Kluwer Academic Publishers; 2011;23:97–103.

252. Debelius B, Forja JM, DelValls Á, Lubián LM. Toxicity and bioaccumulation of copper and lead in five marine microalgae. Ecotoxicol Environ Saf. 2009;72:1503–13.

253. Sabatini SE, Juárez ÁB, Eppis MR, Bianchi L, Luquet CM, Ríos de Molina M del C. Oxidative stress and antioxidant defenses in two green microalgae exposed to copper. Ecotoxicol Environ Saf. 2009;72:1200–6.

254. Rocha GS, Lombardi AT, Melão M da GG. Influence of phosphorus on copper toxicity to Selenastrum gracile (Reinsch) Korshikov. Ecotoxicol Environ Saf. Academic Press; 2016;128:30–5.

255. Brown MR, Mular M, Miller I, Farmer C, Trenerry & C. The vitamin content of microalgae used in aquaculture. J Appl Phycol. 1999.

256. Croft MT, Lawrence AD, Raux-Deery E, Warren MJ, Smith AG. Algae acquire vitamin B12 through a symbiotic relationship with bacteria. Nature. Nature Publishing Group; 2005;438:90–3.

257. Nef C, Jung S, Mairet F, Kaas R, Grizeau D, Garnier M. How haptophytes microalgae mitigate vitamin B12 limitation. Sci Rep. 2019;9:1–11.

258. Gutowska MA, Shome B, Sudek S, McRose DL, Hamilton M, Giovannoni SJ, et al. Globally important haptophyte algae use exogenous pyrimidine compounds more efficiently than thiamin. mBio. 2017;8.

259. Croft MT, Warren MJ, Smith AG. Algae need their vitamins. Eukaryot Cell. 2006. p. 1175–83.

260. Higgins BT, Wang Q, Du S, Hennebelle M, Taha AY, Fiehn O, et al. Impact of thiamine metabolites and spent medium from Chlorella sorokiniana on metabolism in the green algae Auxenochlorella protothecoides. Algal Res. Elsevier B.V.; 2018;33:197–208.

261. Cui H, Wang Y, Zhang H, Wang Y, Qin S. Genome-Wide Analysis of Biotin Biosynthesis in Eukaryotic Photosynthetic Algae. Plant Mol Biol Report. 2012;30:421–32.

262. Li M, Hu C, Zhu Q, Chen L, Kong Z, Liu Z. Copper and zinc induction of lipid peroxidation and effects on antioxidant enzyme activities in the microalga Pavlova viridis (Prymnesiophyceae). Chemosphere. 2006;62:565–72.

263. Li M, Zhu Q, Hu C wei, Chen L, Liu Z li, Kong Z ming. Cobalt and manganese stress in the microalga Pavlova viridis (Prymnesiophyceae): Effects on lipid peroxidation and antioxidant enzymes. Journal of Environmental Sciences. 2007;19:1330–5.

264. Huang X, Wei L, Huang Z, Yan J. Effect of high ferric ion concentrations on total lipids and lipid characteristics of Tetraselmis subcordiformis, Nannochloropsis oculata and Pavlova viridis. J Appl Phycol. 2014;26:105–14.

265. Edvardsen B, Egge ES, Vaulot D. Diversity and distribution of haptophytes revealed by environmental sequencing and metabarcoding – a review. Perspectives in Phycology. 2016;3:77–91.

266. Jordan RW, Chamberlain AHL. Biodiversity among haptophyte algae. Biodivers Conserv. 1997;6:131–52.

267. Saezl AG, Probert I, Young JR, Edvardsen B, Eikrem W, Medlin LK. A review of the phylogeny of the Haptophyta. In: Thierstein HR, Young JR, editors. Coccolithophores. Berlin, Heidelberg: Springer; 2004. p. 251–69.

268. Kawachi M, Nakayama T, Kayama M, Nomura M, Miyashita H, Bojo O, et al. Rappemonads are haptophyte phytoplankton. Current Biology [Internet]. Elsevier Ltd.; 2021;31:2395-2403.e4. Available from: https://doi.org/10.1016/j.cub.2021.03.012

269. Liu H, Aris-Brosou S, Probert I, De Vargas C. A time line of the environmental genetics of the haptophytes. Mol Biol Evol. 2010;27:161–76.

270. Gran-Stadniczeñko S, Šupraha L, Egge ED, Edvardsen B. Haptophyte Diversity and Vertical Distribution Explored by 18S and 28S Ribosomal RNA Gene Metabarcoding and Scanning Electron Microscopy. Journal of Eukaryotic Microbiology. 2017;64:514–32.

271. Simon M, López-García P, Moreira D, Jardillier L. New haptophyte lineages and multiple independent colonizations of freshwater ecosystems. Environ Microbiol Rep. 2013;5:322–32.

272. Peperzak L, Poelman M. Mass mussel mortality in The Netherlands after a bloom of Phaeocystis globosa (prymnesiophyceae). J Sea Res. 2008;60:220–2.

273. Liu H, Probert I, Uitz J, Claustre H, Aris-Brosou S, Frada M, et al. Extreme diversity in noncalcifying haptophytes explains a major pigment paradox in open oceans. Proc Natl Acad Sci U S A. 2009;106:12803–8.

274. Inouye I. Systematics of haptophyte algae in Asia-Pacific waters. Algae (Kor. J. Phycol). 1997. p. 247–261.

275. Tsuji Y, Yoshida M. Biology of Haptophytes: Complicated Cellular Processes Driving the Global Carbon Cycle. In: Hirakawa Y, editor. Advances in Botanical Research Secondary Endosymbioses. 1st ed. Academic Press; 2017. p. 219–61.

276. Kawachi M, Inouye I. Functional roles of the haptonema and the spine scales in the feeding process of Chrysochromulina spinifera (Fournier) Pienaar et Norris (Haptophyta=Prymnesiophyta). Phycologia. 1995;34:193–200.

277. Kawachi M, Inouye I, Maeda O, Chihara M. The haptonema as a food-capturing device: observations on Chrysochromulina hirta (Prymnesiophyceae). Phycologia. 1991;30:563–73.

278. Cavalier-Smith T. Kingdom protozoa and its 18 phyla. Microbiol Rev. 1993;57:953–94.

279. Edvardsen B, Eikrem W, Green JC, Andersen RA, Moon-Van Der Staay SY, Medlin LK. Phylogenetic reconstructions of the haptophyta inferred from 18S ribosomal DNA sequences and available morphological data. Phycologia. 2000;39:19–35.

280. Bendif EM, Probert I, Hervé A, Billard C, Goux D, Lelong C, et al. Integrative Taxonomy of the Pavlovophyceae (Haptophyta): A Reassessment. Protist. Elsevier GmbH.; 2011;162:738–61.

281. Butcher RW. Contributions to our knowledge of the smaller marine algae. Journal of the Marine Biological Association of the United Kingdom. 1952;31:175–91.

282. Gayral P, Fresnel J. Exanthemachrysis gayralie Lepailleur (Prymnesiophyceae, Pavlovales) ultrastructure et discussion taxinomique. Protistologia. 1979;15:271–82.

283. Green JC. The fine structure of Pavlova pinguis Green and a preliminary survey of the order Pavlovales (Prymnesiophyceae). British Phycological Journal. 1980;15:151–91.

284. Xiaodong Z, Shuang Y, Jun S, Yanlong Q, Jing W, Haijiao L. The first record of Pavlova pinguis (Pavlovophyceae, Haptophyta) in China seas. Acta Oceanologica Sinica. 2018;37:28–32.

285. Volkman JK, Farmer CL, Barrett SM, Sikes EL. Unusual dihydroxysterols as chemotaxonomic markers for microalgae from the order Pavlovales (Haptophyceae). J Phycol. 1997;33:1016–23.

286. Rauter AP, Filipe MM, Prata C, Noronha JP, Sampayo MAM, Justino J, et al. A new dihydroxysterol from the marine phytoplankton Diacronema sp. Fitoterapia. 2005;76:433–8.

287. Véron B, Dauguet JC, Billard C. Sterolic biomarkers in marine phytoplankton. i. free and conjugated sterols of pavlova lutheri (haptophyta). Eur J Phycol. 1996;31:211–5.

288. Volkman JK, Kearney P, Jeffrey SW. A new source of 4-methyl sterols and 5α(H)-stanols in sediments: prymnesiophyte microalgae of the genus Pavlova. Org Geochem. 1990;15:489–97.

289. Gladu PK, Patterson GW, Wikfors GH, Lusby WR. Free and combined sterols of Pavlova gyrans. Lipids. 1991;26:656–9.

290. Ballantine JA, Lavis A, Morris RJ. Sterols of the phytoplankton—effects of illumination and growth stage. Phytochemistry. Pergamon; 1979;18:1459–66.

291. Milke LM, Bricelj VM, Parrish CC. Biochemical characterization and nutritional value of three Pavlova spp. in unialgal and mixed diets with Chaetoceros muelleri for postlarval sea scallops, Placopecten magellanicus. Aquaculture. 2008;276:130–42.

292. Mansour MP, Frampton DMF, Nichols PD, Volkman JK, Blackburn SI. Lipid and fatty acid yield of nine stationary-phase microalgae: Applications and unusual C24-C28 polyunsaturated fatty acids. J Appl Phycol. 2005;17:287–300.

293. Dunstan GA, Volkman JK, Barrett SM, Garland CD. Changes in the lipid composition and maximisation of the polyunsaturated fatty acid content of three microalgae grown in mass culture. J Appl Phycol. 1993;5:71–83.

294. Volkman JK, Dunstan GA, Jeffrey SW, Kearney PS. Fatty acids from microalgae of the genus Pavlova. Phytochemistry. 1991;30:1855–9.

295. Kaewsuwan S, Bunyapraphatsara N, Cove DJ, Quatrano RS, Chodok P. High level production of adrenic acid in Physcomitrella patens using the algae Pavlova sp. Δ5-elongase gene. Bioresour Technol. 2010;101:4081–8.

296. Zhou XR, Robert SS, Petrie JR, Frampton DMF, Mansour MP, Blackburn SI, et al. Isolation and characterization of genes from the marine microalga Pavlova salina encoding three front-end desaturases involved in docosahexaenoic acid biosynthesis. Phytochemistry. 2007;68:785–96.

297. Pereira SL, Leonard AE, Huang YS, Chuang L Te, Mukerji P. Identification of two novel microalgal enzymes involved in the conversion of the ω3-fatty acid, eicosapentaenoic acid, into docosahexaenoic acid. Biochemical Journal. 2004;384:357–66.

298. Tonon T, Harvey D, Larson TR, Graham IA. Identification of a very long chain polyunsaturated fatty acid Δ4-desaturase from the microalga Pavlova lutheri. FEBS Lett. 2003;553:440–4.

299. Van der Veer J, Leewis RJ. Pavlova ennorea sp. nov., a haptophycean alga with a dominant palmelloid phase, from England. Acta Botanica Neerlandica. 1977;26:159–76.

300. Kiss JZ, Triemer RE. A comparative study of the storage carbohydrate granules from Euglena (Euglenida) and Pavlova (Prymnesiida). J Protozool. 1988;35:237–41.

301. Arnold AA, Genard B, Zito F, Tremblay R, Warschawski DE, Marcotte I. Identification of lipid and saccharide constituents of whole microalgal cells by 13C solid-state NMR. Biochim Biophys Acta Biomembr. Elsevier B.V.; 2015;1848:369–77.

302. Machado TWM, Rodrigues JM, Moro TR, Duarte MER, Noseda MD. Marine microalgae biomolecules and their adhesion capacity to Salmonella enterica sv. Typhimurium. Applied Sciences (Switzerland). 2020;10.

303. Bernaerts TMM, Gheysen L, Kyomugasho C, Jamsazzadeh Kermani Z, Vandionant S, Foubert I, et al. Comparison of microalgal biomasses as functional food ingredients: Focus on the composition of cell wall related polysaccharides. Algal Res [Internet]. Elsevier; 2018;32:150–61. Available from: https://doi.org/10.1016/j.algal.2018.03.017

304. Gaignard C, Laroche C, Pierre G, Dubessay P, Delattre C, Gardarin C, et al. Screening of marine microalgae: Investigation of new exopolysaccharide producers. Algal Res [Internet]. Elsevier; 2019;44:101711. Available from: https://doi.org/10.1016/j.algal.2019.101711

305. Brown MR. The amino-acid and sugar composition of 16 species of microalgae used in mariculture. J Exp Mar Biol Ecol. 1991;145:79–99.

306. Fradique M, Batista AP, Nunes MC, Gouveia L, Bandarra NM, Raymundo A. Isochrysis galbana and Diacronema vlkianum biomass incorporation in pasta products as PUFA's source. LWT - Food Science and Technology [Internet]. Elsevier Ltd; 2013;50:312–9. Available from: http://dx.doi.org/10.1016/j.lwt.2012.05.006

307. Brown MR, McCausland MA, Kowalski K. The nutritional value of four Australian microalgal strains fed to Pacific oyster Crassostrea gigas spat. Aquaculture. 1998;165:281–93.

308. Brown MR, Garland CD, Jeffrey SW, Jameson ID, Leroi JM. The gross and amino acid compositions of batch and semi-continuous cultures of Isochrysis sp. (clone T.ISO), Pavlova lutheri and Nannochloropsis oculata. J Appl Phycol. 1993;5:285–96.

309. Tibbetts SM, Patelakis SJJ, Whitney-Lalonde CG, Garrison LL, Wall CL, MacQuarrie SP. Nutrient composition and protein quality of microalgae meals produced from the marine prymnesiophyte Pavlova sp. 459 mass-cultivated in enclosed photobioreactors for potential use in salmonid aquafeeds. J Appl Phycol. 2020;32:299–318.

310. Qian ZJ, Jung WK, Kang KH, Ryu B, Kim SK, Je JY, et al. In vitro antioxidant activities of the fermented marine microalga pavlova lutheri (haptophyta) with the yeast hansenula polymorpha. J Phycol. 2012;48:475–82.

311. Qian ZJ, Ryu B, Kang KH, Heo SJ, Kang DH, Bae SY, et al. Cellular properties of the fermented microalgae pavlova lutheri and its isolated active peptide in osteoblastic differentiation of MG-63 cells. Mol Med Rep. 2018;17:2044–50.

312. Batista AP, Gouveia L, Bandarra NM, Franco JM, Raymundo A. Comparison of microalgal biomass profiles as novel functional ingredient for food products. Algal Res. Elsevier B.V.; 2013;2:164–73.

313. Robertson RC, Gracia Mateo MR, O'Grady MN, Guihéneuf F, Stengel DB, Ross RP, et al. An assessment of the techno-functional and sensory properties of yoghurt fortified with a lipid extract from the microalga Pavlova lutheri. Innovative Food Science and Emerging Technologies [Internet]. Elsevier B.V.; 2016;37:237–46. Available from: http://dx.doi.org/10.1016/j.ifset.2016.03.017

314. Shimoda K, Hamada H. Bioremediation of Bisphenol a and Benzophenone by Glycosylation with Immobilized Marine Microalga Pavlova sp. Environ Health Insights. 2009;3:89–94.

315. George S, Chellappan A, Antonykennady ER, Thangamani P, Markose S, Ponuswamy G, et al. Effect of algal antimicrobials on selected aquatic pathogens and characterization of bioactive compounds. J Appl Pharm Sci. 2020;10:122–33.

316. Yamamoto S, Tsutsui T, Saguchi T, Tsutsui N, Yoshimatsu T. Effect of different microalgal diets on the growth performance of Japanese pearl oyster Pinctada fucata martensii broodstock. Aquac Res. 2020;51:4809–13.

317. Rehberg-Haas S, Meyer S, Lippemeier S, Schulz C. A comparison among different Pavlova sp. products for cultivation of Brachionus plicatilis. Aquaculture [Internet]. Elsevier B.V.; 2015;435:424–30. Available from: http://dx.doi.org/10.1016/j.aquaculture.2014.10.029

318. Ponis E, Parisi G, Chini Zittelli G, Lavista F, Robert R, Tredici MR. Pavlova lutheri: Production, preservation and use as food for Crassostrea gigas larvae. Aquaculture. 2008;282:97–103.

319. Martínez-Fernández E, Southgate PC. Use of tropical microalgae as food for larvae of the black-lip pearl oyster Pinctada margaritifera. Aquaculture. 2007;263:220–6.

320. Braley RD, Militz TA, Southgate PC. Comparison of three hatchery culture methods for the giant clam Tridacna noae. Aquaculture. Elsevier B.V; 2018;495:881–7.

321. Shah SMU, Ahmad A, Othman MF, Abdullah MA. Enhancement of Lipid Content in Isochrysis Galbana and Pavlova Lutheri Using Palm Oil Mill Effluent as an Alternative Medium. Chem Eng Trans. 2014;37:733–8.

322. Oh GW, Ko SC, Heo SY, Nguyen VT, Kim G, Jang CH, et al. A novel peptide purified from the fermented microalga Pavlova lutheri attenuates oxidative stress and melanogenesis in B16F10 melanoma cells. Process Biochemistry [Internet]. Elsevier Ltd; 2015;50:1318–26. Available from: http://dx.doi.org/10.1016/j.procbio.2015.05.007

323. Bashir KMI, Lee JH, Petermann MJ, Shah AA, Jeong SJ, Kim MS, et al. Estimation of Antibacterial properties of Chlorophyta, Rhodophyta and Haptophyta Microalgae Species. Microbiology and Biotechnology Letters. 2018;46:225–33.

324. De Mello-Sampayo C, Paterna A, Polizzi A, Duarte D, Batista I, Pinto R, et al. Evaluation of marine microalga Diacronema vlkianum biomass fatty acid assimilation in Wistar rats. Molecules. 2017;22:1–14.

325. Robertson RC, Guihéneuf F, Bahar B, Schmid M, Stengel DB, Fitzgerald GF, et al. The anti-inflammatory effect of algae-derived lipid extracts on lipopolysaccharide (LPS)-stimulated human THP-1 macrophages. Mar Drugs. 2015;13:5402–24.

326. Álvarez P, Pérez L, Salgueiro JL, Cancela Á, Sánchez Á, Ortiz L. Bioenergy Use from Pavlova lutheri Microalgae. Int J Environ Res. 2017;11:281–9.

327. Aysu T, Ola O, Maroto-Valer MM, Sanna A. Effects of titania based catalysts on in-situ pyrolysis of Pavlova microalgae. Fuel Processing Technology. 2017;166:291–8.

CHAPTER 3 FULL OPTIMIZATION OF *PAVLOVA GYRANS* BIOMASS PRODUCTION AND FATTY ACIDS PROFILE USING A TWO-STEP APPROACH

3.1 INTRODUCTION

Long-chain omega-3 fatty acids, especially the docosahexaenoic acid (DHA – C22:6 n-3) and eicosapentaenoic acid (EPA – C20:5 n-3) are essential fatty acids with important benefits for human and animal health. Several works have highlighted the importance of their supplementation in human diet, mainly due to their antioxidant and anti-inflammatory properties and protective effect against various diseases such as cancer, cardiovascular diseases (CVD), inflammatory diseases (*e.g.* rheumatoid arthritis), or mental disorders related to human aging, as the case of Alzheimer's [1–3]. In addition, an adequate uptake of n-3 fatty acids during pregnancy and childhood has been linked to substantial enhancement of visual and cognitive function of children [4]. Scarcely produced by the organism due to the absence or inefficient enzymatic machinery, that enables the elongation and desaturation of α-linolenic acid (ALA; C18:3 n-3) into EPA and/or DHA, humans must source these fatty acids (FAs) through dietary supplementation [5].

According to the European Food Safety Authority (EFSA), adults should have a daily intake of 250 to 500 mg of EPA and DHA [6]. Actually, human nutritional supplementation is mostly accomplished by ingestion of fish and seafood products. However, these products have not been able to meet the growing demand for such FAs and it is estimated that the current market only provides 30 % of the EPA and DHA needed for human consumption [7]. Moreover, Western countries have been warned about the consequences of dietary changes occurred in the last decades as consequence of a diet enriched with omega-6 fatty acids. Contrary to omega-3 FAs, those FAs are the precursors of pro-inflammatory lipid mediators responsible for the development of mortal diseases, such as cancer and CVD [8]. Thus, with an annual growth rate of 14.7 % and an estimated market value of US$ 9.8 billion by 2025, it is crucial the development and implementation of new sources of omega-3 FAs [9]. However, the global market of EPA/DHA is dealing with some constraints, namely (i) the fish stocks in the oceans are overexploited, (ii) fish quality and quantity as a source of omega-3 FAs is seasonal, (iii) the fish produced through aquaculture have shown lower EPA/DHA content due to the use of nutritionally poor feeds as substituents of the scarce fishmeal or oil fish, and (iv) the fact that the use of high trophic level organisms as primary source of omega-3 FAs results in considerable losses of EPA/DHA due to inefficient retention and elongation of these fatty acids [7,10]. Therefore, the utilization of microalgae has been pointed out as a promising alternative source. These microorganisms possess, as advantage, a rapid and controlled growth, higher plasticity allowing for their cultivation under a wide range of environmental conditions, and higher productivities of high-added compounds, such as omega-3 FAs and pigments [11]. Furthermore, unlike fish products, the

efficient control of microalgae culture conditions makes them a safe source for human consumption due to the absence of contaminants such as dioxins, methyl mercury, and polychlorinated biphenyls [12].

Several oleaginous microalgae (lipid content > 20 % w/w of dry weight (DW)) have been identified as a potential source of lipids for biotechnological applications, which according to the algae species, nutrient conditions, and growth phase, can reach a lipid content of 53.2 %DW with an omega-3 FAs content that can vary from 0.06 to 9.32 %DW [13,14]. Among them, the class Pavlovophyceae – composed of thirteen microalgae species, most of them inhabiting littoral and brackish waters, and mainly used in aquaculture [15,16] – has been pointed out as a promising source of EPA and DHA for nutraceutical and pharmaceutical applications. Unlike other widely used classes of microalgae (*e.g.* Eustigmatophyceae, Chlorophyceae or Bacillariophyceae), these haptophytes have an interesting fatty acid profile comprising high concentrations of EPA and DHA that can reach 18.0 %DW and 13.2 %DW, respectively [17]. Furthermore, species such as *Diacronema lutheri* showed the particular ability to partition 40 % EPA and 17 % of DHA from the polar fraction into TAG fraction (storage oils) during the stationary phase of growth, which can be seen as an advantage for further extraction and separation of these omega-3 FAs [18,19]. Moreover, the high contents of high-added value compounds with important biological activities, such as carotenoids (*e.g.*, fucoxanthin), very long chain alcohols, and bioactive sterols (5 % DW), the adequate composition of essential amino acids, and the absence of cell wall, made them a suitable option for human diet and feed due to its greater bioactivity, digestibility and bioacessibility [12,20–23]. To meet the increasing market demand for these high nutritional species, a thorough understanding of the effects of cultivation conditions on biomass production and biochemical profile is fundamental to successfully implement large-scale production of these strains in a cost-effective manner. For example, Cañavate et al. [24] evaluated *Diacronema vlkianum* under different salinities and reported an increase of 2.4 days in the lag phase when salinity increased from 5 to 35 ppt, and absence of growth for 5 days under salinity 50 ppt. Maximum cell densities of *D. vlkanium* were reached at salinity 20 and 35 ppt and its nutritional value was negatively affected when placed at higher salinities due to a decreased EPA and DHA content [24]. Light intensity was shown to modulate the FAs profile of *D. lutheri*, presenting the highest content of EPA at lower irradiance whereas higher light intensities promoted an increase of both DHA and saturated fatty acids [25]. The same authors also reported an improvement on the cell density and lipid content when *D. lutheri* was supplemented with sodium acetate and sodium bicarbonate [25]. The latter carbon source, along with high pH and nitrogen depletion conditions, triggered the accumulation of EPA and DHA on triacylglycerols of *D. lutheri* [26]. Concerning the effect of nutrients on biomass production, the growth of *D. lutheri* was inhibited when cultured in the absence of sulfur or vitamin B_{12} and strongly

reduced in growth media with the absence of iron, calcium or manganese [27]. The same study also showed that the micronutrients boron, molybdenum and copper, unlike to calcium, promoted a decrease in EPA and DHA content [27]. Other works have attested the effects of additional abiotic factors on Pavlovophyceae species, such as the nitrogen source [21] and concentration [26,28], phosphorus [29,30], copper [31,32], molybdenum [31], zinc [32], cobalt and manganese [33], and iron [34].

While the vast majority of research involving Pavlovophyceae species addressed the influence of a limited number of abiotic factors, the aim of this study was to carry out a complete evaluation of the growth conditions on biomass production and FAs profile of the microalga *Pavlova gyrans*. To our knowledge, this is the first study where the growth conditions of this strain were fully optimized regarding its biomass production. The research was divided into three stages: i) the identification of the most significant variables through a Placket-Burman (PB) design, among the seventeen tested; ii) response surface optimization using a rotatable central composite design (RCCD) with the variables identified in PB design; iii) optimization of the $NaNO_3$ concentration with further validation test.

3.2 MATERIALS AND METHODS

3.2.1 Microalga and inoculum preparation

The non-axenic microalga strain *Pavlova gyrans* (RCC1553) was grown in 2 L flat bottom flask with Walne's medium (500 $mg.L^{-1}$ $NaNO_3$) and salinity of 30 psu under continuous aeration with a mixture of air and CO_2 (8 $mL.min^{-1}$ – Alicat Scientific, USA) to maintain the pH value in the range of 8.0 ± 0.5. *P. gyrans* were grown at room temperature and under continuous illumination (100 µmol photons m^{-2} s^{-1}). The remaining nutrients concentration used in the inoculum preparation were those used in Level 0 conditions, presented in Table 3-1.

3.2.2 Experimental design

3.2.2.1 Plackett-Burman design

In the current study, the PB design was used to assess the effect of 17 independent variables on biomass growth of *P. gyrans* [35]. Each variable was tested at three different levels, as presented in Table 3-1, accounting for 24 experiments with a unique combination of the 17 variables and the addition of six replicates at Level 0 – as central points – to evaluate the repeatability of the microalgae growth. Except for $NaNO_3$, the nutrients concentration at Level 0 represents the usual composition of Walne's medium [36]. In addition, and according to the conclusions obtained in other works with Pavlovophyceae species

[37,38], it was also decided to evaluate the effect of $NaHCO_3$ on the biomass production of *P. gyrans*. Table 3-2 displays the experimental matrix design for the seventeen abiotic factors evaluated in biomass growth of *P. gyrans.* The PB assays were performed in 1 L bubble column reactors (6.5 cm diameter and 43 cm high) using the inoculum as previously described. Individual stock solutions of the variables x_5 to x_{17} were prepared, sterilized by filtration (0.2 µm) and added to each reactor to meet the concentration described in Table 3-1. The remaining medium components and materials were sterilized by autoclave.

Table 3-1: the abiotic factors and the respective levels tested in Plackett-Burman experiments the abiotic factors and the respective levels tested in Plackett-Burman experiments

Abiotic factor		**Level -1**	**Level 0**	**Level 1**
Inoculum size ($g.L^{-1}$)	x_1	0.1	0.2	0.3
Salinity (psu)	x_2	20	30	40
Light intensity ($\mu mol.photons.m^{-2}.s^{-1}$)	x_3	150	450	750
Air flow ($mL.min^{-1}$)	x_4	600	800	1000
$NaNO_3$ ($mg.L^{-1}$)	x_5	250	500	750
$NaH_2PO_4.H_2O$ ($mg.L^{-1}$)	x_6	10	20	30
$Na_2H_2EDTA.2H_2O$ ($mg.L^{-1}$)	x_7	22.5	45	67.5
H_3BO_3 ($mg.L^{-1}$)	x_8	16.8	33.6	50.4
$FeCl_3.6H_2O$ ($mg.L^{-1}$)	x_9	0.65	1.3	1.95
$MnCl_2.4H_2O$ ($\mu g.L^{-1}$)	x_{10}	180	360	540
$NaHCO_3$ ($mg.L^{-1}$)	x_{11}	170	652	1134
$ZnCl_2$ ($\mu g.L^{-1}$)	x_{12}	10.25	21	31.75
$CoCl_2.6H_2O$ ($\mu g.L^{-1}$)	x_{13}	10	20	30
$(NH_4)_6Mo_7O_{24}.4H_2O$ ($\mu g.L^{-1}$)	x_{14}	4.5	9	13.5
$CuSO_4.5H_2O$ ($\mu g.L^{-1}$)	x_{15}	10	20	30
Thiamin ($\mu g.L^{-1}$)	x_{16}	50	100	150
Cyanocobalamin ($\mu g.L^{-1}$)	x_{17}	2.5	5	7.5

The salinity in each reactor was adjusted using a concentrated stock solution of sea salt and quantified by a salinity refractometer (Hanna HI96822). All experiments were performed at room temperature (25 ± 2 °C) under constant illumination, being the photosynthetically active radiation (PAR) measured at two points on the outer surface of the reactor (bottom and top) with a LI-250A light meter (LI-COR quantum sensor Q44069). Cultures were continuously air bubbled with different airflows (Table 3-1), which were supplemented with 6 $mL.min^{-1}$ of CO_2 to control the pH (8.0 ± 0.5).

3.2.2.2 Rotatable central composite design (RCCD)

After the identification of the most significant independent variables for the biomass production of *P. gyrans*, a RCCD was designed to determine the optimum growth conditions. The variables selected for optimization were the light intensity (x_3), $NaNO_3$ (x_5), $NaH_2PO_4.H_2O$ (x_6), and $CuSO_4.5H_2O$ (x_{13}). Although the effect of $NaH_2PO_4.H_2O$ was not considered significant in the PB design, this variable was also selected for

optimization considering that its *p*-value was close to the 10 % significance level ($p < 0.10$), but also considering its biological importance for microalgae cultivation [29,39–41].

Table 3-2: the twenty-seven trials combination of the RCCD with the real and coded values (within parentheses) of the independent variables: light intensity (µmol.photons.m^{-2}.s^{-1}), $NaNO_3$ (mg.L^{-1}), $NaH_2PO_4.H_2O$ (mg.L^{-1}) and $CuSO_4.5H_2O$ (µg.L^{-1})

#A	Light intensity (x_3)	$NaNO_3$ (x_5)	$NaH_2PO_4.H_2O$ (x_6)	$CuSO_4.5H_2O$ (x_{15})
1	350 (-1)	750 (-1)	20 (-1)	5 (-1)
2	650 (1)	750 (-1)	20 (-1)	5 (-1)
3	350 (-1)	1250 (1)	20 (-1)	5 (-1)
4	650 (1)	1250 (1)	20 (-1)	5 (-1)
5	350 (-1)	750 (-1)	40 (1)	5 (-1)
6	650 (1)	750 (-1)	40 (1)	5 (-1)
7	350 (-1)	1250 (1)	40 (1)	5 (-1)
8	650 (1)	1250 (1)	40 (1)	5 (-1)
9	350 (-1)	750 (-1)	20 (-1)	15 (1)
10	650 (1)	750 (-1)	20 (-1)	15 (1)
11	350 (-1)	1250 (1)	20 (-1)	15 (1)
12	650 (1)	1250 (1)	20 (-1)	15 (1)
13	350 (-1)	750 (-1)	40 (1)	15 (1)
14	650 (1)	750 (-1)	40 (1)	15 (1)
15	350 (-1)	1250 (1)	40 (1)	15 (1)
16	650 (1)	1250 (1)	40 (1)	15 (1)
17	200 (-2)	1000 (0)	30 (0)	10 (0)
18	800 (2)	1000 (0)	30 (0)	10 (0)
19	500 (0)	500 (-2)	30 (0)	10 (0)
20	500 (0)	1500 (2)	30 (0)	10 (0)
21	500 (0)	1000 (0)	10 (-2)	10 (0)
22	500 (0)	1000 (0)	50 (2)	10 (0)
23	500 (0)	1000 (0)	30 (0)	0 (-2)
24	500 (0)	1000 (0)	30 (0)	20 (2)
25	500 (0)	1000 (0)	30 (0)	10 (0)
26	500 (0)	1000 (0)	30 (0)	10 (0)
27	500 (0)	1000 (0)	30 (0)	10 (0)

Thus, to optimize biomass production based on these four factors (k=4), a 2^4 factorial design without replicates (r=1) with 8 axial points and 3 replicates at the central point (cp) was performed, totaling 27 trials (Table 3-2). The different results produced in RCCD were fitted to a second order model by a multiple linear regression in order to predict the different responses (Y) related to microalgae growth performance and its biochemical composition, using following equation:

$$Y = \beta_o + \sum_j \beta_j X_j + \sum_{i<j} \beta_{ij} X_i X_j + \sum_j \beta_{jj} X_j^2 + \varepsilon$$

where X_i and X_j are the coded values for the independent variables, β_0 is the intercept coefficient, β_i is the linear coefficient, β_{ii} is the quadratic coefficient and ε is the error of the model [35]. The levels ($-\alpha$, -1, 0, 1, $+\alpha$) attributed for each factor were based on the outcomes of PB design and are presented in Table 3-3. The inoculum size (x_1), air flow (x_4), and $NaHCO_3$ concentration (x_{11}) were fixed at Level -1, whereas all the other variables that have shown non-significant effects in the PB matrix were set at Level 0 to not limit the microalgae growth due to nutrient deficiency. The cultivation procedures adopted were the same described for the PB experiments.

3.2.2.3 Optimization of $NaNO_3$ concentration

Considering that the optimal $NaNO_3$ concentration was not reached through the RCCD, a set of experiments was performed in order to find out the most suitable conditions for biomass production. Briefly, *P. gyrans* was grown under four different $NaNO_3$ concentrations: 1500, 2000, 2500, and 3000 $mg.L^{-1}$. The other three variables evaluated in 3.2.2.2 were set at their optimal values: 700 $\mu mol.photons.m^{-2}.s^{-1}$ for light intensity, 40 $mg.L^{-1}$ of $NaH_2PO_4.H_2O$ and 6 $\mu g.L^{-1}$ of $CuSO_4.5H_2O$. The remaining abiotic factors was used as defined in 3.2.2.2. Each condition was tested in triplicate using the procedures already reported (Section 3.2.2.1).

3.2.2.4 Validation test

The optimized growth conditions obtained after 3.2.2.2 and 3.2.2.3 were compared with the conventional Walne's medium formulation. In addition, two more formulations were tested (Table 3-4). One formulation (Lvl-1) aimed at understanding if the non-significant variables determined in the PB design could be used at Level -1, instead of Level 0 (Table 3-1), in the subsequent optimization steps. Another assay evaluated the importance of vitamin supplementation in the optimized growth conditions, in which no vitamins were added to the culture medium (Vit-). In order to eliminate the trace concentration of vitamins, the inoculum was washed twice under sterilized conditions. This process consisted of centrifuging the biomass (4000 RPM, 15 min, 5 °C; Centurion Pro-Analytical CR7000, Chichester, UK) with further resuspension in autoclaved saline solution (30 psu). All conditions were performed in triplicate.

Table 3-3: the abiotic factors and their respective levels tested in RCCD experiments

	-2 (-α)	**-1**	**0**	**1**	**2 (+α)**
Light intensity ($\mu mol.photons.m^{-2}.s^{-1}$), x_3	200	350	500	650	800
$NaNO_3$ ($mg.L^{-1}$), x_5	500	750	1000	1250	1500
$NaH_2PO_4.H_2O$ ($mg.L^{-1}$), x_6	10	20	30	40	50
$CuSO_4.5H_2O$ ($\mu g.L^{-1}$), x_{15}	0	5	10	15	20

3.2.3 Growth analysis

The microalgal growth was monitored every 2 days by optical density (750 nm; Synergy HT, BioTek Instruments, Inc., U.S.A.) and its value converted to ash-free dry weight (AFDW), using the calibration curve previously determined: $\mathrm{AFDW(g.L^{-1})} = 0.8991 \times \mathrm{OD_{750}}$+0.0054, R^2 =0.99. The AFDW was determined by the vacuum filtration of 10 mL of culture samples using pre-weighted glass filters (VWR) and their combustion in a muffle furnace (Nabertherm, Bremem, Germany) at 500 °C overnight. After filtration, the samples were washed twice with 20 mL of ammonium formate (0.5 $mol.L^{-1}$), dried at 105 °C in a convection oven (WTCBinder, Germany) during 24 h and weighed. The dried filters were then re-combusted at 500 °C overnight and re-weighed to determine the ash-free dry weight.

The AFDW determined along the *P. gyrans* growth was used to assess the biomass production parameters. The mean volumetric biomass productivity (P_X) was calculated using the equation:

$$P_X = \frac{AFDW_{t1} - AFDW_{t0}}{t_1 - t_0},$$

where t_0 represents the beginning of the growth (0 days) and t_1 was assumed as the first point of stationary phase. The maximum biomass (X_{max}) produced was also calculated in the time t_1. The experiments were stopped once reached the stationary phase and full stabilization of the AFDW. The biomass was centrifuged at 5 °C (4000 RPM; 20 min - Centurion Pro-Analytical CR7000, Chichester, UK). The pellet was stored at -20 °C and later freeze-dried for biochemical characterization.

3.2.4 Biochemical characterization

3.2.4.1 Protein quantification

The protein content of *P. gyrans* was performed by elemental analysis of C, H, and N using a Vario el III (Vario EL, Elementar Analyser system, GmbH, Hanau, Germany) [42]. As reported by Lourenço et al. [43], the percentage of protein per dry weight was achieved after multiplying the total nitrogen (N) content by the conversion factor 4.78. The samples of the RCCD are presented as the mean of two replicates with deviation values representing the maximum and minimum values. The remaining values are presented as the mean values and standard deviation of three replicates.

3.2.4.2 Total lipids

The extraction and quantification of the *P. gyrans* lipids was carried out by the Folch method described by Couto et al. [44], with some modifications. Briefly, 10 mg of *P. gyrans* biomass and 2 mL of

dichloromethane:methanol (2:1 v/v) solution were added to a glass tube. The suspension was homogenized by vortexing 2 min. After the extraction, the suspension was centrifuged at 2000 RPM for 10 min and the organic phase was collected for a new glass tube. The biomass residue was extracted two more times, until there was no more pigmentation in the solvent. The combined organic phases collected in the new glass tube were dried under a stream of nitrogen gas. The dried lipid extract was washed to remove the non-lipid contaminants. First, it was added 2 mL of dichloromethane and 1 mL of methanol, followed by 2 min vortexing for complete re-solubilization. Then, 0.75 mL of water were added and the mixture was vortexed during 2 min. The extracts were centrifuged at 2000 RPM for 10 min to separate the phases, with the lower phase (organic) being collected and transferred to a new glass tube. The remaining aqueous extract was re-extracted two more times. The combined organic phases were dried under nitrogen stream. The final dried lipid extract was re-suspended in dichloromethane, transferred to a pre-weighed vial, dried with nitrogen, weighed, and stored at -20 °C. The total lipids were determined using three replicates for each growth condition and presented as the percentage of dry weight of *P. gyrans* biomass.

Table 3-4: combination of abiotic factors used in the validation experiments: optimized conditions, Opt, control/Walne's medium, Con, medium without vitamins, Vit-, and assay with the non-significant abiotic factors of the Plackett-Burman design defined at Level-1, Lvl-1

Variable	Opt	Lvl-1	Vit-	Con
Light intensity (µmol.photons.$m^{-2}.s^{-1}$)	700	700	700	700
$NaNO_3$ ($mg.L^{-1}$)	1500	1500	1500	100
$CuSO_4.5H_2O$ ($\mu g.L^{-1}$)	6	6	6	20
$NaH_2PO_4.H_2O$ ($mg.L^{-1}$)	40	40	40	20
$Na_2H_2EDTA.2H_2O$ ($mg.L^{-1}$)	45 (0)	22.5 (-1)	45 (0)	45 (0)
H_3BO_3 ($mg.L^{-1}$)	33.6 (0)	16.8 (-1)	33.6 (0)	33.6 (0)
$FeCl_3.6H_2O$ ($mg.L^{-1}$)	1.3 (0)	0.65 (-1)	1.3 (0)	1.3 (0)
$MnCl_2.4H_2O$ ($\mu g.L^{-1}$)	360 (0)	180 (-1)	360 (0)	360 (0)
$ZnCl_2$ ($\mu g.L^{-1}$)	21 (0)	10.25 (-1)	21 (0)	21 (0)
$CoCl_2.6H_2O$ ($\mu g.L^{-1}$)	20 (0)	10 (-1)	20 (0)	20 (0)
$(NH_4)_6Mo_7O_{24}.4H_2O$ ($\mu g.L^{-1}$)	9 (0)	4.5 (-1)	9 (0)	9 (0)
Thiamine ($\mu g.L^{-1}$)	100 (0)	50 (-1)	-	100 (0)
Cyanocobalamin ($\mu g.L^{-1}$)	5 (0)	2,5 (-1)	-	5 (0)
$NaHCO_3$ ($mg.L^{-1}$)	170 (-1)	170 (-1)	170 (-1)	-
Salinity (psu)	30 (0)	20 (-1)	30 (0)	30 (0)
Air flow ($mL.min^{-1}$)	600 (-1)	600 (-1)	600 (-1)	600 (-1)
Inoculum size ($g.L^{-1}$)	0.1 (-1)	0.1 (-1)	0.1 (-1)	0.1 (-1)

3.2.4.3 Fatty acid analysis by gas chromatography-mass spectrometry (GC-MS)

The transesterification of the total lipid extracts of *P. gyrans* was carried out according to the methodology described by Couto et al. [44]. The fatty acid analysis was carried out on an Agilent 6890 N gas chromatograph connected to an Agilent 5973 mass spectrometer (Agilent, Santa Clara, CA, USA), operating with electron impact ionization (70 eV). The remaining settings and conditions of operation were used as defined by Couto et al. [44]. The fatty acids were identified using commercial standards through the comparison of the retention time and the spectral fragmentation patterns. The relative abundance of each fatty acid was determined by the equation:

$$\%FA = \frac{A_{FA}}{A_{TFA}} \times 100$$

where A_{FA} is the integrated area of a single fatty acid and A_{TFA} is the total area of all the fatty acids identified.

3.2.5 Nutritional indices: hypocholesterolemic index *(HI)*, atherogenic index *(AI)*, and thrombogenic index *(TI)*

The hypocholesterolemic *(HI)*, atherogenic *(AI)*, and thrombogenic *(TI)* indices were calculated from the fatty acid composition (% TFA) according to the following equations:

$$HI = \frac{(C18{:}1 + \ C18{:}2 + C18{:}3 + C18{:}4 + C20{:}5 + C22{:}5 + C22{:}6)}{C14{:}0 + \ C16{:}0}$$

$$AI = \frac{(C12{:}0 + 4 \times C14{:}0 + C16{:}0)}{(\sum MUFA + \sum PUFA)}$$

$$TI = \frac{(C14{:}0 + C16{:}0 + C18{:}0)}{(0.5 \times \sum MUFA + 0.5 \times \sum n-6\ PUFA + 3 \times \sum n-3\ PUFA) + (\frac{\sum n-3}{\sum n-6})}$$

where MUFA and PUFA are the monosaturated and polyunsaturated fatty acids, respectively [45,46].

3.2.6 Statistical analysis

The significant variables in the PB design were selected using a 90 % confidence level (p< 0.10). The second order models of RCCD were obtained using a 90 % confidence level (p< 0.10) and the quality of the fitted model was statistically evaluated by analysis of variance (ANOVA) and coefficient determination (R^2). PB and RCCD analysis was performed with the online software Protimiza Experimental Design (http://experimental-design.protimiza.com.br/). The experiments performed in triplicate and their

biochemical properties were analyzed by differences among means using one-way ANOVA followed by Tukey's multiple comparison test at 95 % confidence level (software: GraphPad Prism version 8.0.2).

3.3 RESULTS AND DISCUSSION

3.3.1 Identification of significant factors for biomass productivity of *P. gyrans* (PB design)

The biomass productivities achieved in the Plackett-Burman design are presented in Table 3-5, whereas the calculated effects, standard errors, and *p*-value of the seventeen variables assessed are described in Table 3-6**.** Among the thirty assays performed, the X_{max} ranged from 0.81 to 2.16 g AFDW.L^{-1}. The biomass productivity varied between 0.072 and 0.256 g.L^{-1}.d^{-1}, which resulted in the identification of three independent variables ($p < 0.1$) that greatly affected the growth of *P. gyrans*: light intensity, $NaNO_3$, and $CuSO_4.5H_2O$.

Light intensity was identified as the most significant abiotic factor ($p < 0.001$) showing a positive calculated effect, meaning that the biomass productivity increased at higher light intensities in the range 150-750 μmol.photons.m^{-2}.s^{-1}. In fact, light intensity has a pivotal role in the photosynthesis process of microalgae, which supplies energy for further production of ATP and NADPH (chemical energy) that will be used to fix carbon dioxide and generate biomolecules for the biomass production [47]. Although tested in a lower illumination range, Seoane et al. were able to confirm the positive effect of light on the growth kinetics of eleven haptophytes, including *P. gyrans*, whose specific growth rate has increased ≈3-fold when the light intensity increased from 60/110 to 350 μmol.photons.m^{-2}.s^{-1} [48].

The second most important variable was $NaNO_3$ ($p = 0.001$), with the increase from 250 mg.L^{-1} to 750 mg.L^{-1} favoring the biomass production (positive effect). In fact, nitrogen is of the utmost importance for microalgae considering its wide distribution in molecules such as proteins, DNA, and RNA [49]. In addition, the efficient control and dosage of nitrogen in the culture medium has been described as an important factor for the regulation of the total lipid content as well as the fatty acid profile [50]. The importance of $NaNO_3$ was confirmed in *Pavlova* sp., whose biomass doubled when using a growth medium supplemented with 400 mg.L^{-1} $NaNO_3$ instead of the values commonly used in f/2 and Walne's medium (75-100 mg.L^{-1} $NaNO_3$) [21]. In contrast, the increase on biomass production of *Diacronema lutheri* was positively affected by $NaNO_3$ until 160 mg.L^{-1}, with the above concentration values decreasing its growth performance [28].

On the other hand, the last significant variable, CuSO4.5H2O (p = 0.073), was the only one with a negative effect over *P. gyrans*, which means that the growth performance was hindered when the microalgae were subject to higher concentrations of copper. This micronutrient is an important cofactor for several metalloproteins in microalgae that are responsible for maintaining redox homeostasis and photosynthesis; however, when excessively supplied, it can be toxic to microalgae, leading to inhibition or even cell death [51].

Table 3-5: the experiments of PB matrix design with coded values of the seventeen abiotic factors and the respective response for mean volumetric biomass productivity (P_x, g AFDW.L^{-1}.d^{-1}), and maximum biomass produced (X_{max}, g AFDW.L^{-1}) calculated in beginning of stationary phase (t), during the *P. gyrans* growth

	Variable (x)																	y		
#E$_i$	1	2	3	4	5	6	7	8	9	10	11	12	13	14	15	16	17	**t**	P_x	X_{max}
1	+	-	-	-	-	+	-	+	-	-	+	+	-	-	+	+	-	6	0.133	1.09
2	+	+	-	-	-	-	+	-	+	-	-	+	+	-	-	+	+	6	0.109	1.20
3	+	+	+	-	-	-	-	+	-	+	-	-	+	+	-	-	+	6	0.150	1.21
4	+	+	+	+	-	-	-	-	+	-	+	-	-	+	+	-	-	4	0.135	0.86
5	+	+	+	+	+	-	-	-	-	+	-	+	-	-	+	+	-	8	0.175	1.67
6	-	+	+	+	+	+	-	-	-	-	+	-	+	-	-	+	+	8	0.256	2.15
7	+	-	+	+	+	+	+	-	-	-	-	+	-	+	-	-	+	8	0.209	1.96
8	-	+	-	+	+	+	+	+	-	-	-	-	+	-	+	-	-	10	0.121	1.31
9	+	-	+	-	+	+	+	+	+	-	-	-	-	+	-	+	-	6	0.247	1.79
10	+	+	-	+	-	+	+	+	+	+	-	-	-	-	+	-	+	6	0.110	0.87
11	-	+	+	-	+	-	+	+	+	+	+	-	-	-	-	+	-	6	0.203	1.32
12	-	-	+	+	-	+	-	+	+	+	+	+	-	-	-	-	+	6	0.150	1.01
13	+	-	-	+	+	-	+	-	+	+	+	+	+	-	-	-	-	8	0.138	1.41
14	+	+	-	-	+	+	-	+	-	+	+	+	+	+	-	-	-	16	0.116	2.16
15	-	+	+	-	-	+	+	-	+	-	+	+	+	+	+	-	-	6	0.134	0.91
16	-	-	+	+	-	-	+	+	-	+	-	+	+	+	+	+	-	6	0.123	0.85
17	+	-	-	+	+	-	-	+	+	-	+	-	+	+	+	+	+	14	0.101	1.71
18	-	+	-	-	+	+	-	-	+	+	-	+	-	+	+	+	+	12	0.099	1.30
19	+	-	+	-	-	+	+	-	-	+	+	-	+	-	+	+	+	6	0.131	1.10
20	-	+	-	+	-	-	+	+	-	-	+	+	-	+	-	+	+	10	0.077	0.87
21	-	-	+	-	+	-	-	+	+	-	-	+	+	-	+	-	+	6	0.178	1.18
22	-	-	-	+	-	+	-	-	+	+	-	-	+	+	-	+	-	8	0.096	0.87
23	-	-	-	-	+	-	+	-	-	+	+	-	-	+	+	-	+	10	0.140	1.48
24	-	-	-	-	-	-	-	-	-	-	-	-	-	-	-	-	-	10	0.072	0.81
25	0	0	0	0	0	0	0	0	0	0	0	0	0	0	0	0	0	8	0.162	1.48
26	0	0	0	0	0	0	0	0	0	0	0	0	0	0	0	0	0	8	0.158	1.49
27	0	0	0	0	0	0	0	0	0	0	0	0	0	0	0	0	0	8	0.161	1.47
28	0	0	0	0	0	0	0	0	0	0	0	0	0	0	0	0	0	8	0.151	1.38
29	0	0	0	0	0	0	0	0	0	0	0	0	0	0	0	0	0	8	0.156	1.46
30	0	0	0	0	0	0	0	0	0	0	0	0	0	0	0	0	0	8	0.162	1.47

This greater sensitivity of *P. gyrans* to copper was also described in works with other haptophytes. A toxicity exposure assessment study with five marine microalgae described the haptophyte *Isochrysis galbana* as a sensitive species to copper due to its low EC_{50} value [52]. According to Li et al. the increasing supplementation from 0 to 3 $mg.L^{-1}$ leads to an oxidative stress on *Pavlova viridis*, which may inhibit the microalgae growth and trigger the protective mechanisms such as antioxidant enzymes [32]. Although the data from Table 3-6 excluded $NaH_2PO_4.H_2O$ concentration from the key factors involved in the biomass production of *P. gyrans*, this variable was also selected along with light, $NaNO_3$, and $CuSO_4.5H_2O$ for further study and optimization through the RCCD. The main reasons for that option were the relative statistical importance ($p = 0.13$) and, mostly, the widely known biological role played by phosphorus in microalgae growth and composition [27,39,53]. Thus, in order to not limit the growth of *P. gyrans* in the RCCD, a new concentration range of $NaH_2PO_4.H_2O$ was set according to its calculated effect, as presented in Table 3-6. For that reason, the remaining growth conditions (not-significant variables), except for $NaHCO_3$, inoculum size and airflow (Level -1), were set at Level 0 in RCCD.

Table 3-6: statistical parameters of the independent variables assessed in the Placket-Burman design for the biomass productivity of *P. gyrans* ($p < 0.10$)

Factor	Effect	Standard error	t-calc	p-value	Significant
Mean	0.142	0.005	27.724	0.000	-
Light intensity	0.065	0.010	6.346	0.000	Yes
$NaNO_3$	0.047	0.010	4.587	0.001	Yes
$CuSO_4.5H_2O$	-0.020	0.010	-1.980	0.073	Yes
$NaH_2PO_4.H_2O$	0.017	0.010	1.638	0.130	No
Curvature	0.033	0.023	1.446	0.176	No
$(NH_4)_6Mo_7O_{24}.4H_2O$	-0.012	0.010	-1.214	0.250	No
$MnCl_2.4H_2O$	-0.012	0.010	-1.149	0.275	No
$ZnCl_2$	-0.010	0.010	-0.986	0.345	No
Inoculum size	0.009	0.010	0.855	0.411	No
$CoCl_2.6H_2O$	-0.008	0.010	-0.790	0.446	No
Thiamine	0.008	0.010	0.790	0.446	No
$Na_2H_2EDTA.2H_2O$	0.007	0.010	0.660	0.523	No
Salinity	-0.003	0.010	-0.269	0.793	No
$NaHCO_3$	0.002	0.010	0.204	0.842	No
Air flow	-0.002	0.010	-0.171	0.867	No
Cyanocobalamin	0.001	0.010	0.138	0.892	No
H_3BO_3	0.001	0.010	0.122	0.905	No
$FeCl_3.6H_2O$	0.000	0.010	-0.024	0.981	No

3.3.2 Rotatable central composite design (RCCD)

3.3.2.1 Biomass growth analysis

The evaluation of the optimal conditions for biomass production of *P. gyrans* were carried out using a RCCD with the variables previously identified: light intensity (x_3), $NaNO_3$ (x_5), $NaH_2PO_4.H_2O$ (x_6), and $CuSO_4.5H_2O$ (x_{15}) (Table 3-2). The twenty-seven experiments were analyzed for biomass productivity (P_x) and maximum AFDW reached (X_{max}). The biomass productivity ranged from 0.165 to 0.262 g AFDW.L^{-1}d^{-1}, whereas the maximum biomass concentration varied between 1.30 and 2.34 g AFDW.L^{-1} Table 3-7**.** Overall, the productivities achieved in the RCCD were higher and less variable compared to the PB design (0.077 to 0.256 g AFDW.L^{-1}d^{-1}), demonstrating the importance of the selected variables and their effects on the growth performance. The values here reported for X_{max} in *P. gyrans* are higher than those described for *P. pinguis* (1.54 g DW.L^{-1}), *D. lutheri* (<0.2 g DW.L^{-1}) and *Pavlova sp*. OPMS 30543 (0.92 g DW.L^{-1}) under non-optimized conditions; however, the values of the present study are in accordance with the biomass productions *Pavlova sp*. OPMS 30543 (2.20 g DW.L^{-1}) at large scale [21]. Similarly, the biomass productivities of *P. gyrans* were 4- to 8-fold higher than those produced by *P. pinguis* under different phosphorus supplementation on f/2-Si medium [39].

As described in Table 3-8, and only using the significant terms ($p < 0.1$), these responses were used to calculate the regression coefficients and to generate a one-order model for P_x and a second-order model for X_{max}, each one as a function of coded independent variables, where x_3, x_5, x_6, and x_{15} represent the coded values for light intensity, $NaNO_3$, $NaH_2PO_4.H_2O$, and $CuSO_4.5H_2O$, respectively. The analysis of variance (ANOVA) was carried out to assess the model fitness. The mathematical model generated for the dependent variable P_x, Table 3-8, showed a low value of R^2 (32.0 %), which makes impossible the production of contour curves. As reported by Sadahira et al. [54], the inability to produce the contour curves for P_x may be explained by the lower range of values obtained for this dependent variable compared to the range of values for X_{max} and even compared to the range of values obtained for P_x in the PB design. Thus, under such narrow range, it is impossible to explain the significance of the independent variables on P_x, which hinders the generation of the respective contour curves and their corresponding analysis [54]. On the other hand, from the ANOVA analysis of X_{max} it was obtained a satisfactory R^2 (84.1%) as well as $F_{calc}>F_{tab}$, which allowed the generation of the second-order model and the subsequent contour curves, as presented in Figure 3-1.

Table 3-7: results obtained in the RCCD assays for the response variables: volumetric biomass productivity (P_x - g.L^{-1}.d^{-1}), maximum biomass produced (X_{max} - g.L^{-1}), total lipids (%w.w^{-1}), total saturated fatty acids (∑SFA %TFA), total monosaturated fatty acids (∑MUFA %TFA), total polyunsaturated fatty acids (∑PUFA %TFA), total omega-3 fatty acids (∑n-3 %TFA), eicosapentaenoic acid (EPA %TFA) and docosahexaenoic acid (DHA %TFA), and protein content (%w.w^{-1}). The values are the mean and standard deviation of three different analysis (n=3), with the exception for the protein content whose values are the mean of two different analysis (n=2) with the deviation representing the maximum and minimum values

#E	P_x (g.L^{-1}.d^{-1})	X_{max} (g.L^{-1})	Total lipids (%w.w^{-1})	∑SFA (%TFA)	∑MUFA (%TFA)	∑PUFA (%TFA)	∑n-3 FA (%TFA)	EPA (%TFA)	DHA (%TFA)	Protein content (%w.w^{-1})
1	0.262	1.57	21.95±3.02	48.80±1.31	18.22±0.23	32.98±1.12	26.63±0.90	16.79±0.72	5.11±0.17	18.37±0.13
2	0.196	1.57	20.75±2.17	62.23±1.40	22.73±0.62	15.05±1.42	11.79±1.18	6.62±0.55	3.52±0.43	19.64±0.04
3	0.240	1.92	20.53±1.25	43.29±1.69	18.63±1.31	38.08±0.84	32.26±0.63	19.28±1.11	6.80±0.28	27.30±0.47
4	0.249	1.99	20.76±0.69	63.64±2.78	20.73±1.21	15.63±1.64	12.60±1.25	7.11±0.72	3.75±0.41	29.91±0.52
5	0.205	1.64	28.34±2.85	44.65±0.27	20.44±0.16	34.92±0.11	27.80±0.08	17.67±0.16	5.40±0.09	18.04±0.29
6	0.167	1.67	24.57±2.02	56.88±0.48	25.50±0.09	17.62±0.56	13.98±0.50	8.99±0.43	3.06±0.31	17.79±0.37
7	0.239	1.91	25.66±1.80	46.37±1.72	19.65±1.26	33.97±2.21	27.80±2.29	18.35±2.27	4.74±0.07	28.49±0.21
8	0.211	2.11	22.09±0.41	62.78±2.30	22.68±0.84	14.54±1.59	11.54±1.18	7.33±0.70	2.79±0.33	25.23±0.35
9	0.217	1.30	22.81±1.49	45.82±1.79	18.54±0.37	35.64±2.02	29.43±1.75	18.84±1.10	5.31±0.47	22.51±0.31
10	0.255	1.53	19.95±1.90	68.95±2.05	18.59±1.10	12.46±1.34	9.49±0.98	5.35±0.65	2.84±0.29	15.61±0.20
11	0.215	1.72	20.04±1.08	42.40±4.73	18.33±0.64	39.28±4.10	33.14±3.57	20.14±2.37	5.52±0.66	37.57±0.28
12	0.228	1.82	20.87±0.77	61.26±3.57	21.95±1.36	16.79±2.69	13.47±2.25	6.70±0.84	4.86±1.28	33.25±1.02
13	0.183	1.46	24.12±1.29	44.93±2.23	21.01±0.49	34.06±2.04	27.67±1.68	16.80±1.08	6.26±0.36	24.65±0.66
14	0.166	1.66	25.23±1.76	58.76±0.11	25.28±0.40	15.96±0.51	12.36±0.36	7.70±0.31	2.86±0.08	17.43±0.34

Table 3-7 (cont.): results obtained in the RCCD assays for the response variables: volumetric biomass productivity (P_x - $g.L^{-1}.d^{-1}$), maximum biomass produced (X_{max} - $g.L^{-1}$), total lipids (%w.w^{-1}), total saturated fatty acids (∑SFA %TFA), total monosaturated fatty acids (∑MUFA %TFA), total polyunsaturated fatty acids (∑PUFA %TFA), total omega-3 fatty acids (∑n-3 %TFA), eicosapentaenoic acid (EPA %TFA) and docosahexaenoic acid (DHA %TFA), and protein content (%w.w^{-1}). The values are the mean and standard deviation of three different analysis (n=3), with the exception for the protein content whose values are the mean of two different analysis (n=2) with the deviation representing the maximum and minimum values

#E	P_x ($g.L^{-1}.d^{-1}$)	X_{max} ($g.L^{-1}$)	Total lipids (%w/w)	∑SFA (%TFA)	∑MUFA (%TFA)	∑PUFA (%TFA)	∑n-3 FA (%TFA)	EPA (%TFA)	DHA (%TFA)	Protein content (%w/w)
15	0.165	1.65	17.59±1.31	44.15±2.98	22.59±0.22	33.26±3.10	27.38±2.82	16.39±2.09	4.30±0.80	35.47±0.94
16	0.220	1.76	22.46±1.38	60.76±1.49	23.72±0.23	15.52±1.42	12.26±1.18	7.52±0.59	2.99±0.42	28.65±0.09
17	0.209	1.67	24.46±0.97	45.54±0.80	18.69±0.44	35.76±0.83	29.44±0.73	18.72±0.58	5.27±0.14	27.73±0.03
18	0.234	1.87	23.38±2.10	61.65±2.68	23.45±0.87	14.91±1.81	12.05±1.50	7.64±0.97	2.89±0.42	19.71±0.02
19	0.222	1.33	23.27±2.30	59.28±1.84	23.02±0.55	17.69±1.48	13.48±1.13	8.67±0.78	3.06±0.22	14.51±0.10
20	0.234	2.34	17.45±1.28	56.37±0.53	23.21±0.80	20.42±0.28	16.11±0.25	9.73±0.13	4.27±0.17	28.61±1.83
21	0.227	1.36	18.73±2.51	59.50±0.85	22.77±0.35	17.72±0.59	13.97±0.52	7.74±0.37	4.08±0.30	37.71±0.63
22	0.245	1.96	24.22±2.72	61.10±4.12	20.23±2.49	18.67±2.37	14.31±1.96	8.83±1.08	3.68±0.68	18.53±0.21
23	0.225	1.80	23.09±2.61	42.47±0.24	18.89±0.34	38.64±0.57	32.07±0.44	20.13±0.31	6.17±0.08	24.41±0.41
24	0.199	1.59	21.17±0.95	39.09±0.92	20.06±0.78	40.85±0.89	33.80±0.72	20.32±0.51	6.91±0.16	32.09±0.87
25	0.234	1.87	21.16±0.07	64.60±0.63	22.56±0.35	12.84±0.35	9.70±0.32	6.09±0.14	2.37±0.17	21.45±0.30
26	0.240	1.92	21.90±2.30	59.47±2.51	22.04±0.98	18.49±1.56	14.17±1.19	9.28±0.74	3.16±0.37	22.14±0.61
27	0.236	1.89	22.10±1.46	56.71±1.73	22.83±0.06	20.46±1.78	16.07±1.49	10.08±0.68	4.04±0.74	23.52±0.19

Although copper supplementation was reduced in this second optimization step, the increasing concentration of this micronutrient led to reduced biomass production of *P. gyrans*, as in the PB design. This behavior was more noticeable at higher concentrations (20 $\mu g.L^{-1}$), being responsible by a reduction of about 0.3-0.4 g $AFDW.L^{-1}$ when compared with the optimal copper concentration range, < 12 $\mu g.L^{-1}$, shown in Figure 3-1. These results highlight the harmful effects of copper on *P. gyrans*, which is in accordance with the works of other Pavlovophyceae species [27,32]. According to Purbonegoro et al., there was a reduction in cell density of *Pavlova* sp. when supplemented with 13 $\mu g.L^{-1}$ copper, which was followed by a dramatic decrease when this concentration increased to 98 $\mu g.L^{-1}$ [55].

Concentration ranges from 0 to 12 $\mu g.L^{-1}$ of $CuSO_4.5H_2O$ and from 24 to 49 $mg.L^{-1}$ of $NaH_2PO_4.H_2O$ led to the optimal X_{max} of *P. gyrans*. Figure 3-1a) suggests that the tolerance or toxicity of copper on *P. gyrans* is linked to the phosphate concentration in the medium, and it is augmented under lower phosphate values. Similar evidence was observed in *Selenastrum gracile* [56]. The authors argued that under P replete conditions there is an increase of intracellular polyphosphate granules, which successfully bind to copper and decrease its toxicity. On the other hand, the limitation of phosphate in culture media changes the composition of membrane lipids as well as increases the membrane permeability of microalgae, which enables copper absorption [56].

Table 3-8: analysis of variance (ANOVA) with the percentage of explained variance (R^2), Fcalculated and Ftabulated, at 10% significance level, for the responses mean volumetric biomass productivity (P_x) and maximum biomass (X_{max})

P_x (g AFDW.L^{-1}.d^{-1}) = 0.22 - 0.01x_6 + 0.01x_3 x_{15}		
R^2 (%)	F_{calc}	F_{tab}
32.0	5.66	2.54
X_{max} (g AFDW.L^{-1}) = 1.82 + 0.06x_3 + 0.19x_5 + 0.07x_6 - 0.05x_6^2 - 0.08x_{15} - 0.04x_{15}^2		
R^2 (%)	F_{calc}	F_{tab}
84.1	17.59	2.09

P_x: $F_{tab\ 2;\ 24;\ 0.10} = 2.54$ X_{max}: $F_{tab\ 6;\ 20;\ 0.10} = 2.09$

Concerning the effect of light intensity on X_{max}, regardless the interaction with the other variables (x_5, x_6, and x_{15}), its increase always promoted higher growth of *P. gyrans*, showing that there was no apparent photoinhibition under the conditions tested (Figure 3-1b, 1c, 1f). The adequacy of light intensity is of the utmost importance for maintaining photosynthetic activity in microalgae. While low light intensity leads to low biomass production, light energy supply above the photosynthetic capacity of the microalgae can irreversibly damage Photosystem II and the enzymes involved in CO_2 fixation (photoinhibition), leading to decreased growth kinetics [57]. From Figure 3-1b), 1c), and 1f), the light conditions considered ideal for

X_{max} should be above 650 µmol.photons.m^{-2}.s^{-1}. However, this feature is highly species-dependent; *D. lutheri*, for instance, has been reported having higher growth performance under medium light irradiance (100 µmol.photons.m^{-2}.s^{-1}) instead of low and high illumination (20 and 340 µmol.photons.m^{-2}.s^{-1}) [25]. On the other hand, Varshney et al. reported an high light tolerance until 700 µmol.photons.m^{-2}.s^{-1} of *Acutodesmus* sp., with the highest growth rate at 500 µmol.photons.m^{-2}.s^{-1} [58].

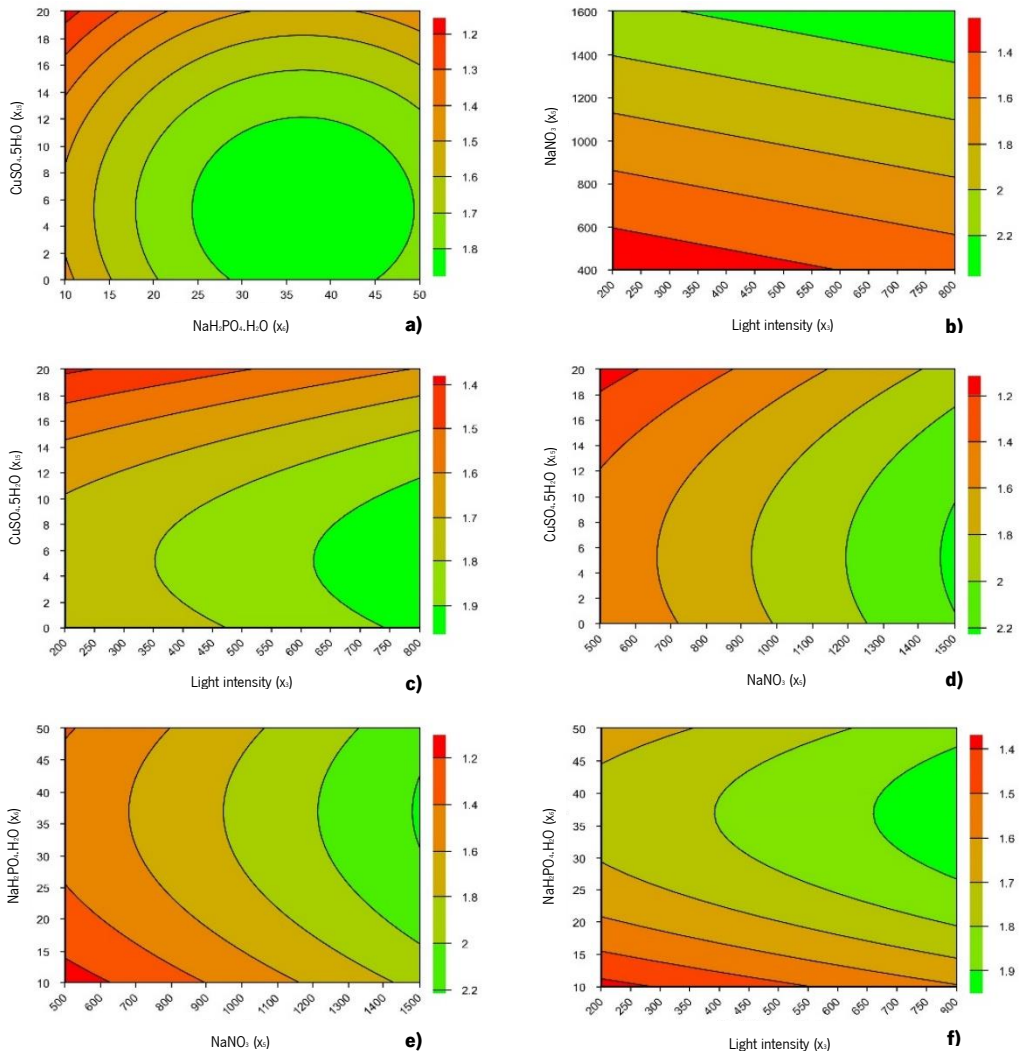

Figure 3-1: contour curves for dependent variable X_{max}, illustrating the interactions between $CuSO_4.5H_2O$ and $NaH_2PO_4.H_2O$, (a), $NaNO_3$ and light intensity, (b), $CuSO_4.5H_2O$ and light intensity, (c), $CuSO_4.5H_2O$ and $NaNO_3$, (d), $NaH_2PO_4.H_2O$ and $NaNO_3$, (e), and $NaH_2PO_4.H_2O$ and light intensity, (f)

Despite not considered as a significant independent variable in PB design, the addition of $NaH_2PO_4.H_2O$ to the RCCD greatly affected the biomass produced by *P. gyrans*. In fact, the increased range of values in RCCD allowed understanding that the biomass production was favored by the higher values of phosphorus, with the optimum values ranging from 27 to 47 mg.L^{-1}. Similarly, *P. pinguis* grown under higher loadings of phosphorus was also shown to result in higher biomass production and productivity in previous studies [39]. This might be explained by the important role that phosphorus availability plays in

the electron receptors and donators of Photosystem II, which, under limitation, may hinder photosynthesis and cell yield [59,60].

A similar trend was presented for $NaNO_3$, with the higher X_{max} reached at the highest nitrate concentration (≈ 1500 $mg.L^{-1}$). However, contrary to the other independent variables, it was not possible to figure out with confidence its optimal condition. Conversely to the described for *Diacronema lutheri*, the high supplementation of $NaNO_3$ in *P. gyrans* did not induce an inhibitory effect, generally associated to the nitrate reductase, which produces ammonia and nitrite that can severely compromise biomass growth [28]. According to Figure 3-1d) and 1e), there is only a slight indication that the optimal range of $NaNO_3$ starts at 1500 $mg.L^{-1}$. Thus, a complementary study using a one-factor at a time approach was conducted to assess the single effect of $NaNO_3$ on biomass growth of *P. gyrans* (Section 3.3.3).

3.3.2.2 Biochemical characterization

3.3.2.2.1 Lipid and protein content

The biomass produced from RCCD was analyzed concerning its lipid and protein contents (Table 3-7)**.** The lipid content varied between 17.45 % (trial 20) and 28.34 % (trial 5), whereas the protein content ranged from 15.61 % (trial 10) to 37.71 % (trial 21). For both dependent variables, protein and lipid content, all the independent variables (x_3, x_5, x_6, and x_{15}) were statistically significant ($p < 0.1$), as described in Table 9. Considering the analysis of variance in Table 9 (R^2 and $F_{calc}>F_{tab}$), the second-order models achieved were considered adequate for the responses "total lipids" and "protein content" [54]. Thus, these models were used to produce the contour curves illustrated in Figure 3-2**.**

According to Figure 3-2 a-f), it was possible to identify a well-defined trend relating the lipid content of *P. gyrans* and the independent variables and/or their interactions. Briefly, the total lipids increase with decreasing concentration of $NaNO_3$ (x_5), with a common optimal region on Figure 3-2b) ,d) and f) for concentration values below 600 $mg.L^{-1}$. This result is aligned with the other studies which pointed out that nitrogen limitation on growth medium was the main triggering factor for storage compounds (*e.g.*, lipids and carbohydrates) [61]. Several microalgae (*e.g.*, *Pavlova, Nitzschia*, and *Scenedesmus*) are reported to attain higher lipid contents when cultured with lower nitrogen supplementation [62–64]. Under nitrogen depleted conditions, oleaginous microalgae have the ability, through genetic overexpression, to reallocate the carbon precursors for protein and carbohydrate synthesis into glycerolipid production, increasing, in turn, the content of neutral lipids – mainly as TAG fatty acids – in the biomass [65,66].

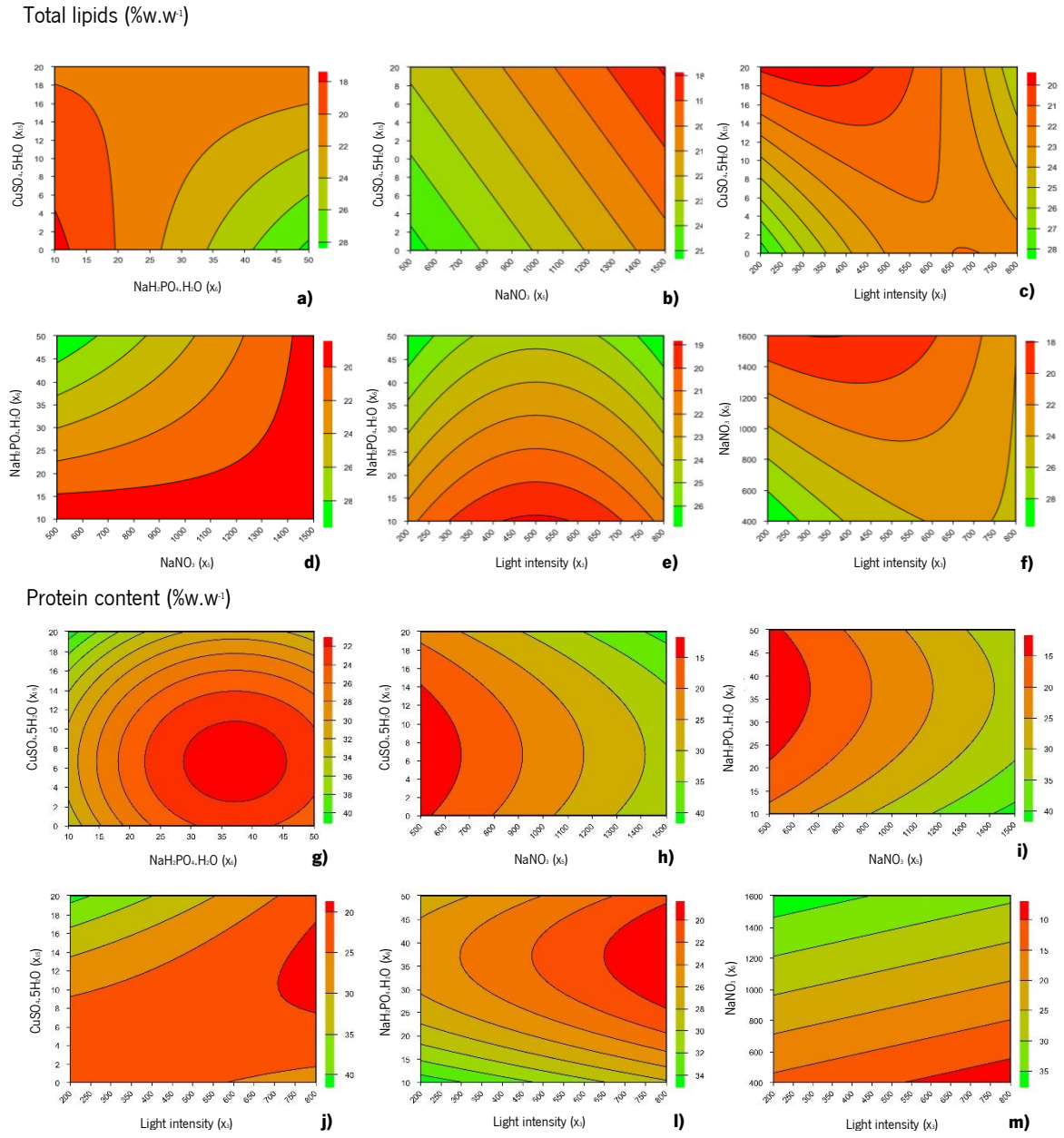

Figure 3-2: contour curves from RCCD for the dependent variable total lipids (% w.w^{-1}), a-f), illustrating the interactions between $CuSO_4.5H_2O$ and $NaH_2PO_4.H_2O$, (a), $CuSO_4.5H_2O$ and $NaNO_3$, (b), $CuSO_4.5H_2O$ and light intensity, (c), $NaH_2PO_4.H_2O$ and $NaNO_3$, (d), $NaH_2PO_4.H_2O$ and light intensity, (e), and $NaNO_3$ and light intensity, (f). Contour curves for protein content (% w.w^{-1}), g-m), illustrating the interactions between $CuSO_4.5H_2O$ and $NaH_2PO_4.H_2O$, (g), $CuSO_4.5H_2O$ and $NaNO_3$, (h), $NaH_2PO_4.H_2O$ and $NaNO_3$, (i), $CuSO_4.5H_2O$ and light intensity, (j), $NaH_2PO_4.H_2O$ and light intensity, l), $NaNO_3$ and light intensity, m)

The opposite behavior was found for $NaH_2PO_4.H_2O$ (x_6) (Figure 3-2a), d) and e)), with increased lipid accumulation at higher concentrations of phosphorus in the medium composition, reaching the higher lipid content where $NaH_2PO_4.H_2O$ ranged from 45 to 50 mg.L^{-1}. This is not in accordance with lipid content of *P. pinguis* achieved under different phosphorus supplementation [39]. However, and as illustrated in Figure 3-2d), some authors have argued that a high supply of phosphorus in microalgae cultures, together with nitrogen deficiency, could be the "real trigger" for lipid accumulation. The luxurious phosphorus uptake during nitrogen starvation can be stored as polyphosphate granules, which can be further used

for the generation of metabolic energy (ATP) [67]. This supplemental energy will be important for the efficient uptake and fixation of inorganic carbon, through the CO_2-concentrating mechanism (CCM), which is the main pathway responsible for the lipid synthesis in microalgae [67,68].

On the other hand, and as previously described for the X_{max}, copper concentration (x_{15}) exerted a negative impact on lipid accumulation. As described in Figure 3-2c), and particularly in Figure 3-2a) and b), lipid accumulation was quite interesting at very low levels of this micronutrient (0 - 2 μg.L^{-1}), which may be linked with the higher X_{max} produced at lower concentrations of $CuSO_4.5H_2O$ (Figure 1). That is, in growth conditions that enhanced the biomass production, like those with low levels of copper (Figure 3-1), it might be expected a more efficient consumption and depletion of nutrients, such as $NaNO_3$, which in turn may be responsible for triggering lipid accumulation.

Regarding the importance of light intensity (x_3), it was noteworthy its quadratic effect and the interaction of this factor with the other independent variables over the total lipids of *P. gyrans*. Namely, the existence of two distinct regions with high lipid content was visible when assessing the interaction between x_5 and x_3 (Figure 3-2e)). This behavior was not verified when the lipid content depended on the interaction between light intensity and $CuSO_4.5H_2O$ or $NaNO_3$ (Figure 3-2c) and f)), in which the region with higher lipid accumulation was represented by the assays with light intensity lower than ≈300 μmol.photons.m^{-2}.s^{-1}. Guihéneuf et al. reported the highest lipid content of *D. lutheri*, collected in the exponential phase, at 340 μmol.photons.m^{-2}.s^{-1} [25]. However, their results comprised a narrower illumination range (20-340 μmol.photons.m^{-2}.s^{-1}) than that used in this work. The effect of light on lipid content has been described as a species-dependent feature. *Scenedesmus* showed a minor impact on its lipid content under an illumination range from 200 to 1500 μmol.photons.m^{-2}.s^{-1} [69,70], whereas, under 600 μmol.photons.m^{-2}.s, the lipid synthesis was incremented in microalgae *C. emersonii, P. beijerinckii*, *and P. kessleri* [71]. Such diverse effects of light could also be dependent of the nutritional conditions applied, namely the nutrient starvation of microalgae.

The effects of the dependent variables on the protein content are illustrated in the contour curves of Figure 3-2g-m). Copper concentration positively affected the protein content of *P. gyrans*. Although the copper levels tested in RCCD were lower than those reported by Li et al. [32], the increase in Cu supplementation is linked to the generation of free radicals that upregulate the production of antioxidant enzymes involved in the protection mechanism, such as catalase, glutathione peroxidase, and superoxide dismutase, increasing the protein content in microalgae. On the other hand, as shown in Figure 3-1, the lower growth

performance under higher copper conditions possibly did not result in nutritional deficiencies that would have stressed *P. gyrans*, enabling protein production rather than accumulation of reserve compounds.

As the nutrient replete medium will not stimulate or stress microalgae to initiate the accumulation of the reserve compounds, this might justify the presence of high contents of protein. Contrary to the lipid content, the increasing concentration of $NaNO_3$ increased the protein content of *P. gyrans*. Depending of the interaction between $NaNO_3$ and the remaining independent variables (Figure 3-2h), i) and m)), the contour curves analysis suggests that a protein content of 40 %w/w can be reached in the range of 1400-1500 mg.L^{-1} of sodium nitrate, which is somehow expected since nitrogen is a vital compound for protein and glycerolypid synthesis [65]. Similarly, the protein content of *Nannochloropsis* was reduced 2.3-fold when cultured in nitrogen-depleted conditions, an opposite trend of that observed for the storage compounds – lipids and carbohydrates [65]. Even when supplying nitrogen to nitrogen-starved cultures of *Nannochloropsis gaditana*, it was verified an increase in protein content from 0.7 g.L^{-1} to 1.1 g.L^{-1}, attesting that the addition of nitrogen was mainly used for protein synthesis [72].

High light intensity decreased the protein content, which only exceed the 32 %w/w under low and medium light intensities, namely, from 200 to ≈ 400 µmol.photons.m^{-2}.s^{-1} (Figure 3-2j), l) and m)). A similar effect was described in *Scenedesmus* and *Dunaliella salina*, whose protein content decreased with increasing light intensities from 50 to 400 µmol.photons.m^{-2}.s^{-1} [69] and from 100 to 600 W, respectively [73]. As reported in Figure 3-1, X_{max} of *P. gyrans* was positively correlated with light intensity. So, under these conditions it is expected a superior nutrient consumption, which limits the nitrogen availability (Figure 3-2m)) and might hinder protein synthesis at higher illumination [74]. In addition, the high light intensity could stress the microalgae, driving the utilization of energy resources towards the accumulation of storage products [73,74].

Concerning the $NaH_2PO_4.H_2O$, it was concluded that, generally, the use of larger concentrations of phosphorus lead to a decrease in the protein content of *P. gyrans*. In fact, Figure 3-2g) ,i) and l) suggest that higher concentrations of this compound (> 35 % w/w) were only reached when growth medium was supplemented with a lower concentration of phosphorus (10 - 20 mg.L^{-1}). Greater supply of phosphorus – from 50 to 250 mg.L^{-1} – also promoted a decrease in protein content of *A. platensis* grown with 42 and 60 µ$Em^{-2}s^{-1}$, being the lowest protein level obtained under limited phosphorus conditions (10 mg.L^{-1}) [75]. Considering that all trials were stopped in the stationary phase, where nitrogen availability for *P. gyrans* should be limited, lower protein synthesis with increasing phosphorus supplementation might be possibly

linked to the preference for lipid accumulation under these growth conditions, as previously reported [67,68].

3.3.2.2.2 Fatty acid analysis

The fatty acid profile (%TFA) of *P. gyrans* obtained from the RCCD is presented in Table 3-7. In order to simplify the statistical analysis, the evaluation of the four independent variables on fatty acid composition was performed on EPA and DHA abundance, with the remaining responses being represented by the different classes of fatty acids according to their degree of (in)saturation, namely saturated (SFA), monounsaturated (MUFA) and polyunsaturated (PUFA) fatty acids, as well as omega-3 fatty acid content (Table 3-7).

In addition to the key role played in growth performance, the manipulation of abiotic factors during microalgae growth has also been highlighted as a key strategy that strongly influences and alters the biochemical composition of these microorganisms. This influence is quite obvious in Table 3-7, in which it can be seen that different combinations of light intensity, $NaH_2PO_4.H_2O$, $NaNO_3$, and $CuSO_4.5H_2O$ led to a wide range of values, for example, for PUFA (12.46 - 40.85 %TFA), SFA (39.09 - 68.95 %TFA) or EPA content (5.35 - 20.32 %TFA).

Using the set of responses and the respective significant terms ($p < 0.1$), a mathematical model with coded independent variables was generated for each dependent variable of Table 3-7. According to the ANOVA, and apart from MUFA, all dependent variables related to fatty acid composition showed a high R^2 value and respected the $F_{calc}>F_{tab}$ condition, attesting the fitness of all second-order models (Table 3-9). The contour curves of the response DHA and EPA (%FA/TFA) are presented in Figure 3-3.

According to Figure 3-3, the growth conditions tested promoted a significant impact on the EPA content, whose value ranged between 5.35 and 20.32 % TFA. The variation in DHA levels occurred in a narrower range of values, varying between 2.37 and 6.91 % TFA. Several authors have identified and discussed the effects of the aforementioned abiotic factors on the fatty acid composition of microalgae. However, most of them adopted a univariate approach, which makes it impossible to identify possible interactions between abiotic factors, as well as to compare these results with those obtained in the present study for *P. gyrans* [76].

Production of EPA and DHA were strongly reduced with increasing light intensities, especially at medium and high irradiances. According to Guihéneuf et al., increasing the light intensity from 20 to 340 $\mu mol.photons.m^{-2}.s^{-1}$ significantly reduced the content of n-3 fatty acid and PUFA – mainly EPA – in *P.*

lutheri [25]. However, and contrary to the results reported here, the authors stated that the highest DHA content was achieved with higher irradiance.

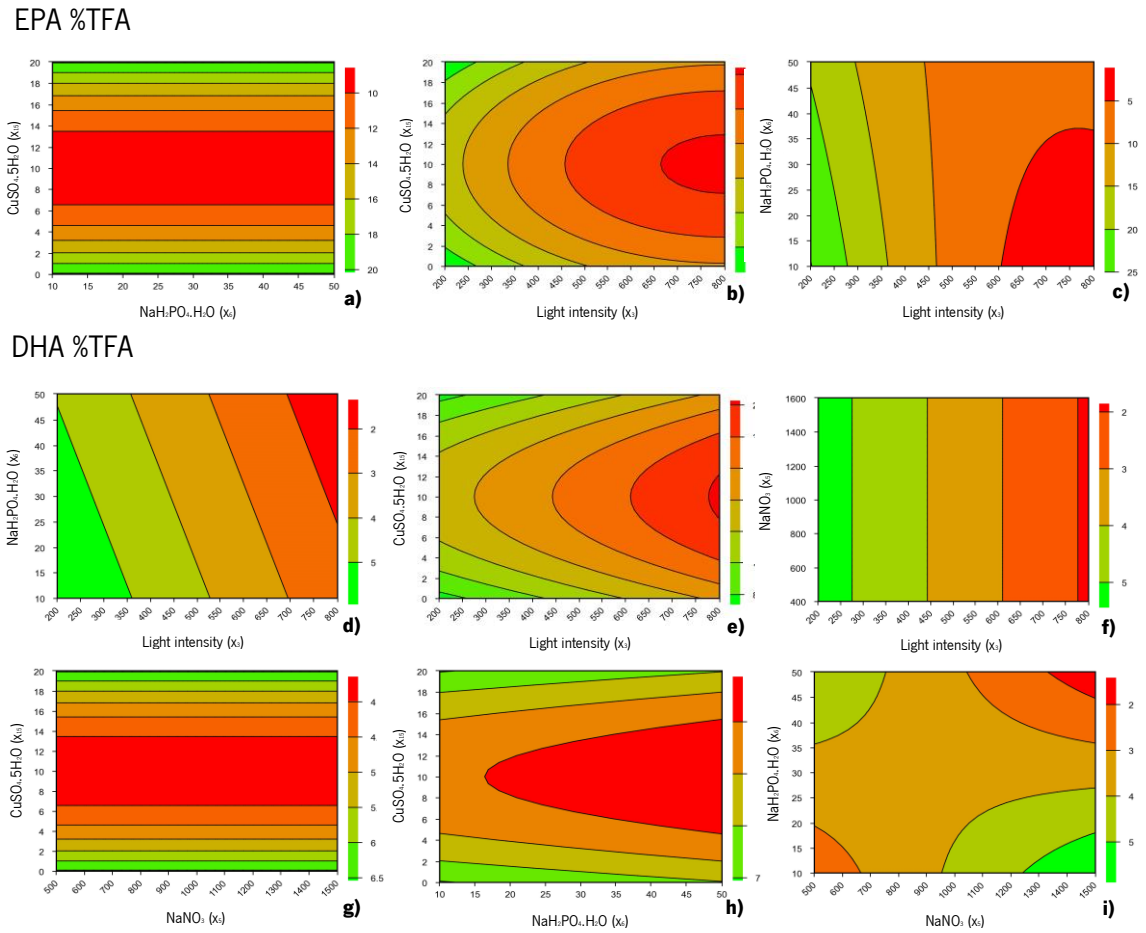

Figure 3-3: contour curves from RCCD for the dependent variable EPA %TFA, a-c), illustrating the interactions between $CuSO_4.5H_2O$ and $NaH_2PO_4.H_2O$, a), $CuSO_4.5H_2O$ and light intensity, b), and $NaH_2PO_4.H_2O$ and light intensity, c). Contour curves for DHA %TFA, d-i), illustrating the interactions between $NaH_2PO_4.H_2O$ and light intensity, d), $CuSO_4.5H_2O$ and light intensity, e), $NaNO_3$ and light intensity, f), $CuSO_4.5H_2O$ and $NaNO_3$, (h), $CuSO_4.5H_2O$ and $NaH_2PO_4.H_2O$, h), and $NaH_2PO_4.H_2O$ and $NaNO_3$, i)

Similarly, the study on the interactive effects between temperature and light showed a negative impact of light intensity on PUFA and EPA levels of *D. lutheri* harvested in exponential and stationary phase, while for DHA the variation was smaller, and the trend varied according to growth temperature [37]. This negative correlation between PUFA content and increase of light intensity is a well-known trend widely described in several microalgae species. High light intensities are linked to a decreased unsaturation degree of the fatty acids from the different lipid classes. Guedes et al. described that increasing illumination enables a shift in fatty acids composition of polar and neutral lipids of *D. lutheri* [77]. At higher irradiances, there was an enhanced triacylglycerols accumulation, which are mainly composed of saturated residues, having the authors also described a reduction in the unsaturation degree of fatty acids from the polar fraction, such as monogalactosylacylglycerols, digalactosylacylglycerols, and acylated steryl

glycosides [77]. For both fatty acids, the $NaNO_3$ variable showed no significant effect ($p > 0.10$), with only its interaction with $NaH_2PO_4.H_2O$ being significant on DHA production ($p < 0.10$) – Table 3-7. In fact, when interacting with $NaH_2PO_4.H_2O$, the highest DHA content (> 5 %) was achieved using high $NaNO_3$ concentrations (≈ >1250 $mg.L^{-1}$) and the lowest phosphorus concentrations, as shown in Figure 3-3i).

According to the calculated coefficients (Table 3-9), there was a negative correlation between phosphorus supply and the DHA level of *P. gyrans*. This result is in agreement with the variation of the DHA content of *P. pinguis*, whose content suffered a slight decrease when increasing the phosphorus loading from 36.60 $\mu mol.L^{-1}$ to 72.40 $\mu mol.L^{-1}$ [39]. However, the effect of phosphorus on PUFA production is dependent on several factors, such as the species of microalgae, the combined effects of the culture conditions, and the concentration of phosphorus in the culture medium, which hinders the comparison of results.

Table 3-9: analysis of variance (ANOVA) with the percentage of explained variance (R^2), $F_{calculated}$ and $F_{tabulated}$, at 10% significance level, for the responses: total lipids (% $w.w^{-1}$), protein content (% $w.w^{-1}$), saturated fatty acids (SFA %TFA), monosaturated fatty acids (MUFA %TFA), polyunsaturated fatty acids (PUFA %TFA), total of omega-3 fatty acids (n-3 FA %TFA), eicosapentaenoic acid (EPA %TFA) and docosahexaenoic acid (DHA %TFA)

	R^2	F_{calc}	F_{tab*}
Total lipids (%w.w^{-1}) = 21.61 + 0.64x_3^2 - 1.22x_5 + 1.39x_6 - 0.64 x_{15} + 0.57 x_3x_5 + 0.77 x_3x_{15} - 0.70 x_5x_6 - 0.68 x_6x_{15}	84.25	12.04	2.04
Protein content (%w.w^{-1}) = 22.36 - 1.71 x_3 + 5 x_5 - 1.95 x_6 + 1.37 x_6^2 + 1.91 x_{15} + 1.40 x_{15}^2 - 1.60 x_3 x_{15}	84.44	14.73	2.06
SFA %TFA = 59.62 + 6.96 x_3 - 1.49 x_3^2 - 4.69 x_{15}^2 + 1.50 x_5 x_6	88.20	41.10	2.22
MUFA %TFA = 21.94 + 1.39 x_3 + 0.75 x_6 - 0.67 x_{15}^2	58.50	10.81	2.34
PUFA %TFA = 18.07 - 8.35 x_3 + 1.83 x_3^2 + 5.43 x_{15}^2	91.97	87.83	2.34
∑ n-3 FA %TFA = 14.06 - 7.06 x_3 + 1.71 x_3^2 + 4.76 x_{15}^2	91.27	80.11	2.34
EPA %TFA = 8.60 - 4.55 x_3 + 1.13 x_3^2 + 2.89 x_{15}^2 + 0.73 x_3 x_6	92.29	65.85	2.22
DHA %TFA = 3.65 - 0.90 x_3 - 0.25 x_6 + 0.72 x_{15}^2 - 0.43 x_5 x_6	82.39	25.84	2.22

*Significance level of 10%

Huang et al. reported that limited supply of phosphorus promoted changes in the lipid composition of microalgae, namely increasing content of neutral lipids (TAG) with a concomitant decrease of polar lipids (*e.g.*, phospholipids) [29]. Comparing to phosphorus-repleted conditions, the limitation of this nutrient seems not to significantly influence DHA levels in polar lipids, with a slight decrease occurring in glycolipids, phospholipids, and betaine lipids in *D. lutheri* [29]; however, this trend was observed in

glycolipids of *Tisochrysis lutea* [78]. Similarly, no clear trend was found between DHA content and the combined effect of different N and P supplies in *D. lutheri* [27].

Copper, on the other hand, showed a quadratic effect for both FAs, reaching their highest contents at the limits of the tested values range. This result is partially in line with those reported by Carvalho et al. whose medium formulation absent of copper improved the DHA and EPA content of *D. lutheri* [27]. Several studies have pointed out that thylakoid membranes are prone to oxidative damage when subject to higher copper concentrations, which leads to lipid peroxidation of the fatty acids and diminishes the PUFA content of microalgae [32,55,79]. However, these works have tested a wider range of copper concentrations than described here with *P. gyrans*, which makes fatty acids degradation for the highest copper condition tested (20 $\mu g.L^{-1}$) unlikely, as confirmed in Figure 3-3. Considering the biomass production (Figure 3-1), the lowest EPA and DHA composition was achieved at intermediate copper concentrations (Figure 3-3), i.e., close to the range of values where *P. gyrans* produced the highest biomass levels (X_{max}). Thus, the EPA and DHA content might be indirectly affected by the copper content through its influence on the growth performance of microalgae, which determines the nutritional properties of the *P. gyrans* growth conditions and, consequently, its biochemical composition [26].

3.3.3 Effect of $NaNO_3$ concentration on biomass productivity and biochemical composition of *P. gyrans*

3.3.3.1 Biomass growth analysis

The outcomes derived from the RCCD showed that the optimal range of $NaNO_3$ concentration for maximum biomass production by *P. gyrans* was barely identified in the respective contour curves (Figure 3-1). For that reason, an univariate approach was implemented to evaluate the single effect of the independent variable x_5, whereas the remaining variables were fixed, according to Figure 3-1, at their optimal value, namely 700 $\mu mol.photons.m^{-2}.s^{-1}$, 40 $mg.L^{-1}$ and 6 $\mu g.L^{-1}$ for light intensity (x_3), $NaH_2PO_4.H_2O$ (x_6) and $CuSO_4.5H_2O$ (x_{15}) concentrations, respectively. The growth profile and kinetics analysis are described in Figure 3-4 and Table 3-10, respectively. Overall, slower growth could be visualized from the sixth day onwards for the conditions with higher $NaNO_3$ supplementation, with the lowest level showing the highest X_{max} and biomass productivity at day 10 (Table 3-10), despite not statistically significant ($p > 0.05$). Thus, attending to the results in Figure 3-1 and Figure 3-4, both data indicated the 1500 $mg.L^{-1}$ as the theorical optimal level of the independent variable x_5 for the validation test.

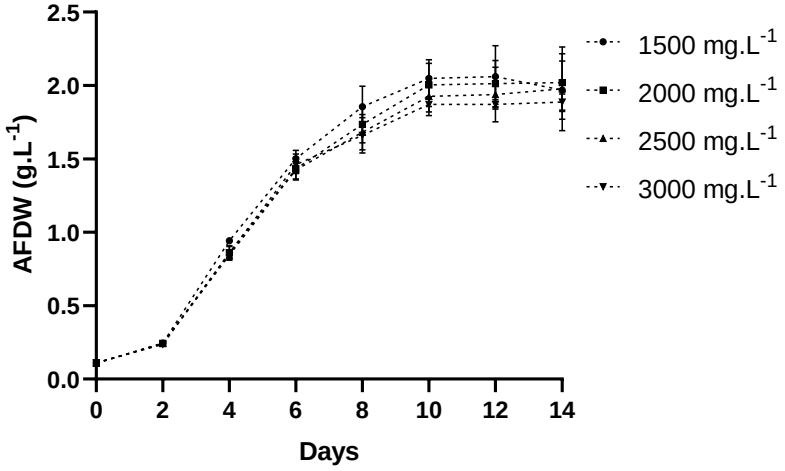

Figure 3-4: ash-free dry weight (AFDW g.L^{-1}) of *P. gyrans* grown under different concentrations of $NaNO_3$

3.3.3.2 Lipid and protein content

The total lipid and total protein content are presented in Table 3-10**.** The lipid content decreased from 22.80 % w.w^{-1} – at 1500 mg.L^{-1} $NaNO_3$ – to 20.57 % w.w^{-1} – at 3000 mg.L^{-1} $NaNO_3$ – with no statiscal significance ($p > 0.05$). The values here reported are in accordance with the range of values described in RCCD – Figure 3-2b), d) and f). These lower total lipids content under the N replete conditions proved, once again, the key role of nitrogen availability on lipid accumulation of microalgae [62–64].

Table 3-10: values of maximum biomass produced (X_{max}, g AFDW.L^{-1}) and volumetric biomass productivity (P_x, g AFDW.L^{-1}.d^{-1}) at the beginning of the stationary phase (10 d), protein content (% w.w^{-1}), total lipids (% w.w^{-1}) and fatty acids composition (expressed in % of TFA) of *P. gyrans* cultivated with 1500, 2000, 2500, and 3000 mg.L^{-1} of $NaNO_3$. Values are the mean and standard deviation of three replicates (n=3). Different letters indicate significant differences in the fatty acids or the fatty acids class between the $NaNO_3$ treatments (one-way ANOVA, $p < 0.05$, followed by the Tukey's test)

	$NaNO_3$ (mg.L^{-1})			
	1500	**2000**	**2500**	**3000**
X_{max}	2.05±0.13^{a}	2.00±0.15^{a}	1.93±0.13^{a}	1.87±0.05^{a}
P_x	0.205±0.013^{a}	0.200±0.015^{a}	0.193±0.013^{a}	0.187±0.005^{a}
Protein content	38.06±3.77^{a}	44.24±3.51^{ac}	47.81±2.16^{bc}	42.89±1.36^{ac}
Total lipids	22.80±2.50^{a}	22.10±1.13^{a}	21.63±2.10^{a}	20.57±1.79^{a}
Fatty acid (% TFA)				
C20:5 n-3	23.86±1.32^{a}	23.61±2.91^{a}	25.2±2.48^{a}	24.31±1.60^{a}
C22:6 n-3	10.84±0.36^{a}	11.07±3.16^{a}	12.04±1.12^{a}	13.23±0.94^{a}
Σ SFA	28.34±1.80^{a}	29.87±7.00^{a}	26.04±1.95^{a}	25.98±0.63^{a}
Σ MUFA	20.19±0.58^{a}	18.91±1.70^{a}	18.81±1.67^{a}	18.83±2.02^{a}
Σ PUFA	51.48±2.29^{a}	51.22±8.71^{a}	55.15±2.84^{a}	55.19±2.63^{a}
Σ n-3	42.68±1.38^{a}	43.04±7.45^{a}	46.25±1.81^{a}	46.04±2.46^{a}

Saturated fatty acids (SFA), monosaturated fatty acids (MUFA), polyunsaturated fatty acids (PUFA), omega-3 fatty acids (n-3), omega-6 fatty acids (n-6) eicosapentaenoic acid (EPA), docosahexaenoic acid (DHA) and total fatty acids (TFA).

Concerning the protein content, its value varied from 38.06 % w.w^{-1} (at 1500 mg.L^{-1} $NaNO_3$) to 47.81 % w.w^{-1} (at 2500 mg.L^{-1} $NaNO_3$), with the difference being significant ($p < 0.05$) only among these two trials.

As showed in Figure 3-2, similar (high) contents of protein were reached when *P. gyrans* was cultured under great supply of $NaNO_3$. The data in Table 3-10 confirm that the carbon fixed during photosynthesis under high nitrogen supply, was mainly used for *de novo* protein synthesis, rather than the production of storage compounds such as neutral lipids [72].

3.3.3.3 Fatty acids analysis

The effect of $NaNO_3$ concentration – from 1500 to 3000 $mg.L^{-1}$ – on fatty acids profile of *P. gyrans* is presented in Table 3-10. The whole set of experiments showed a very similar fatty acids composition, with non-significant variations ($p > 0.05$) of EPA, DHA, and the FAs classes. Under high $NaNO_3$ supplementation, stands out the production of PUFA, which exceed 50 % TFA in all conditions tested. Regarding DHA level, there was a slight increase – from 10.84 % to 13.23 % TFA – with increasing $NaNO_3$ concentrations. Similar trend was observed for EPA, which value ranged from 23.61 to 25.20 % TFA (at 2500 $mg.L^{-1}$).

3.3.4 Validation test

3.3.4.1 Biomass growth analysis

In order to validate the optimal conditions of the independent variables x_3, x_5, x_6, and x_{15}, described in Section 0 and Section 3.3.3, a validation assay was performed – Figure 3-5. The main goal was to validate the mathematical model developed (Table 3-8) and to compare the growth performance of *P. gyrans* in the optimal formulation with the control conditions (Walne's medium), Table 3-4. Supplementary assays were also carried out to evaluate: i) the impact of vitamins absence and ii) if all the non-significant variables identified in PB design could be set at their minimum level. Due to practical issues, the assay with control conditions (Walne's medium) was also conducted under the optimal light intensity (700 $\mu mol.photons.m^{-2}.s^{-1}$).

Table 3-11 and Figure 3-5 show that a very distinctive growth profile of *P. gyrans* was reached with the optimized abiotic factors. While the optimized conditions allowed a constant growth from day 2 to 10, reaching a maximum biomass of 2.26 g $AFDW.L^{-1}$ ($p < 0.05$), in all the other experiments, *P. gyrans* ceased its growth at day 4, with the control reaching 0.59 g $AFDW.L^{-1}$ (Table 3-11). The two-step statistical approach adopted here yielded a significant 3.8-fold improvement in biomass production of *P. gyrans* (Table 3-11). Considering that both trials were performed at the same light intensity, this result seems to be related to the increased supplementation of $NaNO_3$ and $NaH_2PO_4.H_2O$, limitation of $CuSO_4.5H_2O$ in the

growth medium and, to a lesser extent, probably due to the addition of an extra source of inorganic carbon ($NaHCO_3$) [26].

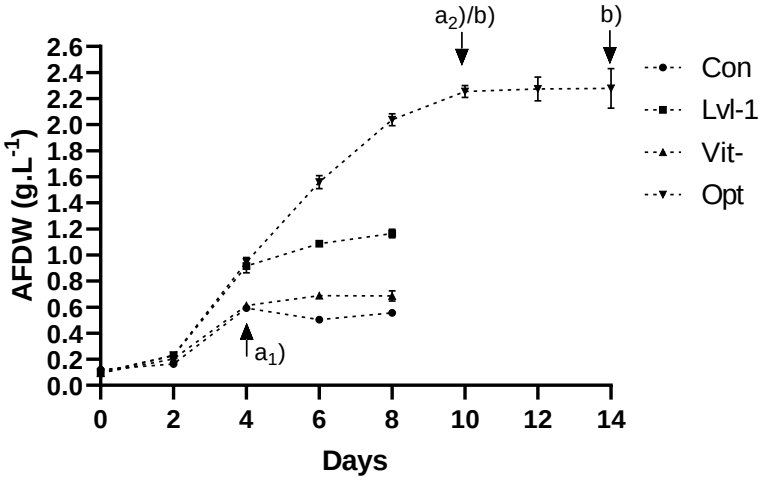

Figure 3-5: growth of *P. gyrans*, ash-free dry weight (g AFDW.L^{-1}), in the validation assays: optimized conditions, Opt, control/Walne's medium, Con, medium without vitamins, Vit-, and assay with the abiotic factors considered non- significant in Plackett-Burman design fixed at Level -1, Lvl-1. Data from sampling time a1) and a2) were used in the biomass growth analysis. Samples b) in Opt assay were used in lipid analysis

Using the coded values for the independent variables, the mathematical models (Table 3-8 and Table 3-9) were used to predict the response values for X_{max}, total proteins, total lipids, EPA and DHA (%FA/TFA). The predicted values, as well as the associated errors between the experimental and predicted data, are displayed in Table 3-12**.** Due to their low relative error, the predicted value for X_{max} (RE -3.69%) and total protein (RE 0.60%) are in accordance with the experimental values, attesting the fitness of the model. On the other hand, the deviation from the experimental values for total lipids, and especially for EPA and DHA, was higher, accounting for relative errors of 22.10 %, 64.39 %, and 82.54 %, respectively.

Table 3-11: values of maximum biomass produced (X_{max}) and volumetric biomass productivity (P_x) at the beginning of the stationary phase (t_x) for the *P. gyrans* grown in the validation assays: optimized conditions, Opt, control/Walne's medium, Con, medium without vitamins, Vit-, and assay with the abiotic factors considered non-significant in Plackett-Burman design fixed at Level -1, Lvl-1. Values are the mean and standard deviation of three replicates (n=3). Different letters indicate significant differences between the validation assays (one-way ANOVA, $p < 0.05$, followed by the Tukey's test). Gain was calculated as the ratio of $X_{max}/X_{maxcontrol}$

	t_x (d)	P_x (g AFDW.L^{-1}.d^{-1})	X_{max} (g AFDW.L^{-1})	Gain
Con	4	$0.148 \pm 0.003^{\alpha}$	0.59 ± 0.01^{a}	1.0
Lvl-1	4	$0.229 \pm 0.013^{\beta}$	0.92 ± 0.05^{b}	1.5
Vit-	4	$0.153 \pm 0.001^{\alpha}$	0.61 ± 0.01^{a}	1.0
Opt	10	$0.225 \pm 0.005^{\beta}$	2.26 ± 0.05^{c}	3.8

The assay without vitamins showed the crucial role played by these nutrients on *P. gyrans*. Its growth was severely delayed after the second day and ceased by the fourth day with a maximum biomass produced similar to the control ($p > 0.05$) (Table 3-11). Additionally, it was also possible to confirm the negative

effects of vitamin depletion in *P. gyrans*, thanks to the development of an unusual greenish color instead of the common brown or yellow color (Figure 3-6). The inability to grow in vitamin-free environments, are in accordance with the described for other haptophytes: *D. lutheri* [27] and *T. lutea* [80]. Haptophytes are considered vitamin B_{12} (cyanocobalamin) auxotrophs due to the absence of the cobalamin-independent isoform of methionine synthase, which negatively affects the protein synthesis on microalgae under privation of B_{12} [80]. The lower growth here reported for *P. gyrans* may be attributed to the residual concentrations within the cell, considering that no culture acclimation was done before the assay, or due to the residual content of vitamin B_{12} present in the natural sea salt used in the medium formulation [80].

Table 3-12: experimental and predicted values, as well as the relative errors *(%RE = 100 x (Exp-Pred)/Exp),* for the responses maximum biomass produced (X_{max}), protein content, total lipids, eicosapentaenoic acid (EPA) and docosahexaenoic acid (DHA), achieved under the optimal conditions defined for validation of the mathematical models produced

Response	Experimental	Predicted	%RE
X_{max} (AFDW g.L^{-1})	2.26 ± 0.05	2.34	-3.69
Protein content (%w.w^{-1})	30.76 ± 4.37	30.58	0.60
Total lipids (%w.w^{-1})	28.30 ± 0.95	22.05	22.10
EPA (%TFA)	20.69 ± 1.61	7.37	64.39
DHA (%TFA)	10.33 ± 0.30	1.80	82.54

Regarding the Lvl-1 assay, these conditions produced the second highest maximum biomass produced at the end of the exponential phase, with a significative difference from the remaining conditions tested ($p < 0.05$) – Table 3-11 and Figure 3-5. Despite being presented in PB design as independent variables with no significant effects on X_{max} ($p > 0.10$), reducing these eleven abiotic factors at the same time inhibited *P. gyrans* growth from the fourth day onwards. Similarly, in previous studies, the mineral limitation in the culture medium negatively affected biomass production of *D. lutheri*, especially when deprived of Ca, Fe, Mn, Zn or Co [27].

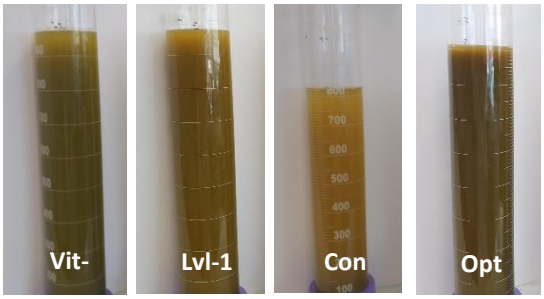

Figure 3-6: appearance of the *P. gyrans* cultures of the validation assays: optimized conditions, Opt, control/Walne's medium, Con, medium without vitamins, Vit-, and assay with the abiotic factors considered non-significant in Plackett-Burman design fixed at Level -1, Lvl-1

Furthermore, it is well known the key role developed by some of these nutrients as important cofactors for enzymatic processes involved in protein synthesis, carbon fixation, and chlorophyll production in microalgae [81,82], which may be severely affected under mineral limited conditions.

3.3.4.2 Biochemical analyses

3.3.4.2.1 Lipid and protein content

P. gyrans from the validation assays reached a protein content of 45.86, 42.11, 30.76, and 10.59 % w.w^{-1} under the growth conditions of Vit-, Lvl-1, Opt, and Con, respectively (Figure 3-7). The assays Vit- and Lvl-1 had similar protein amounts, with significant differences ($p < 0.05$) for Opt and Con. In addition to increasing biomass production, the optimized growth conditions also allowed a 3-fold increase on protein content compared to the control ($p < 0.05$). The range of values reported in the validation tests are in accordance with the protein contents obtained in medium formulations with high nitrogen supply (Chapter 3.3.2.2.1) and follow the trend described in Figure 3-2 for such conditions. Despite the variety of formulations, the highest values of protein were achieved in the assays that shared the optimal value of nitrogen, phosphorus, and copper.

In terms of lipid content, the experiments Lvl-1, Opt, and Con, showed the highest value, ranging from 26.73 to 28.3 % w.w^{-1} (Figure 3-7). The absence of vitamins in *P. gyrans* culture led to a significant decrease compared to the other conditions ($p < 0.05$), totaling only 19.83 % w.w^{-1}. The effect of time was also assessed in the lipid content and fatty acid profile of the optimum growth conditions – Figure 3-7 and Table 3-13. For that, two different samples were taken throughout the *P. gyrans* growth: one was taken in the transition between exponential and stationary phase (10 days) and the second one at the end of the microalgae growth (14 days) – sample b) in Figure 3-5**.** Increasing the sampling time 4 days, enabled an increment of 5 % in the lipid content ($p < 0.05$) of *P. gyrans*, which reached 28.3 % w.w^{-1} at end of the growth.

Considering the calculated coefficients of the model obtained for lipid and protein content (Table 3-9), we can suggest that the sharp variations for both compounds may be mainly attributed to the supply of nitrogen (x_5) and phosphorus (x_6). As previously mentioned, nitrogen concentration has been described as one of the main factors responsible for modulating the production of protein, lipids, and carbohydrates. The replete or limited conditions of N acts as a switch that promotes cell division and protein synthesis or store the carbon photosynthetically fixed as neutral lipids, respectively [65].

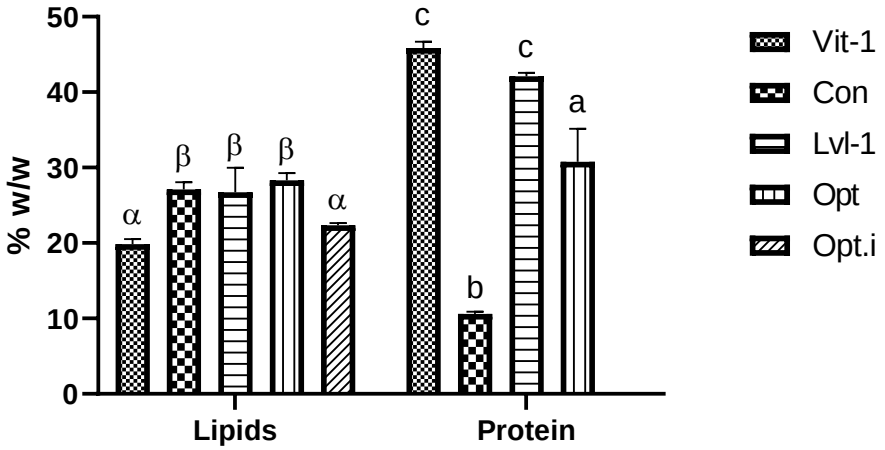

Figure 3-7: Values of the total lipids (% w.w $^{-1}$) and protein content (% w.w $^{-1}$) for the *P. gyrans* grown in the validation assays. Values are the mean and standard deviation of three assays (n=3). Different letters indicate significant differences between the validation assays (one-way ANOVA, $p < 0.05$, followed by the Tukey's test)

3.3.4.2.2 Fatty acids analysis

The fatty acids profiles of *P. gyrans'* biomass produced in the validation experiment are presented in Table 3-13**.** In general, thirteen fatty acids (> 1% TFA) were identified in *P. gyrans*, of which five stand out most prominently (> 10 % TFA): C14:0, C16:0, C16:1 n-7, C20:5 n-3 and C22:6 n-3. Among these, and despite the different growth conditions, it was possible to verify a common feature of *P. gyrans*: the high level of both EPA and DHA – which reached the maximum value of 27.03 % and 11.65 % TFA, respectively. Also, the fatty acids profile of *P. gyrans* here described is in accordance with other microalgae species, such *as P. viridis* [64], *P. pinguis* [20] and *D. lutheri* [37]. The optimal growth conditions produced noticeable differences compared to the control. The modifications carried out on abiotic factors, mainly those on $NaNO_3$, $NaH_2PO_4.H_2O$, and $CuSO_4.5H_2O$ concentrations, overall resulted in a significant increase ($p < 0.05$) on total PUFA content (≈10% TFA) and n-3 fatty acids (≈12% TFA), with a concomitant decrease of ≈11 % in total SFA ($p < 0.05$). Particularly, it was evident a substantial improvement in the DHA content, which raised from 5.73 to 10.33 % TFA ($p < 0.05$), with a similar trend for EPA – increased from 17.09 to 20.69 % TFA ($p > 0.05$).

Regarding the evolution of the fatty acids profile of Opt between the onset of stationary phase and its end, no significant variation was notable, except for the total MUFA ($p < 0.05$), that increased with the culture aging. Despite not being statistically relevant, two fatty acids presented the same order of variation (4 %) but with opposite trends among both sampling times. That is, the earlier sampling has an increased content of EPA, whereas the C16:1 n-7 was more pronounced at 14 days.

Table 3-13: fatty acids composition, expressed in % of TFA and mg.g^{-1} dry weight, of *P. gyrans* from the validation assays: optimized conditions at day 10 (Opt.i) and 14 (Opt), control/Walne's medium, Con, medium without vitamins, Vit-, and assay with the abiotic factors considered non-significant in Plackett-Burman design fixed at Level -1, Lvl-1. Values are the mean and standard deviation of three replicates (n=3). Different letters indicate significant differences in the fatty acid or the fatty acids class between the treatments (one-way ANOVA, $p < 0.05$, followed by the Tukey's test)

Fatty acid %TFA	Opt.i (10 d)	Opt (14 d)	Con	Vit-1	Lvl-1
C14:0	11.33 ±0.47	10.57 ±0.89	11.55 ±1.36	8.87 ±1.13	9.41 ±0.91
C16:0	17.73 ±0.21	19.32 ±2.63	29.62 ±2.96	20.25 ±2.15	17.73 ±0.21
C16:1 n-7	13.92 ±1.94	17.88 ±1.52	17.1 ±1.49	8.83 ±0.58	14.21 ±0.50
C16:2 n-4	1.02 ±0.05	0.99 ±0.36	0.39 ±0.05	0.66 ±0.04	0.96 ±0.15
C18:0	3.46 ±0.63	2.75 ±0.32	2.21 ±0.40	7.45 ±1.39	3.38 ±0.86
C18:1 n-9	0.85 ±0.06	1.15 ±0.09	1.59 ±0.22	1.05 ±0.20	1.13 ±0.13
C18:1 n-7	1.11 ±0.51	1.21 ±0.15	0.81 ±0.14	4.13 ±0.83	1.82 ±0.13
C18:2 n-6	1.74 ±0.52	1.24 ±0.26	2.03 ±0.37	0.28 ±0.05	2.16 ±0.16
C18:3 n-3	0.78 ±0.03	0.69 ±0.15	0.42 ±0.05	0.67 ±0.17	1.18 ±0.13
C18:4 n-3	7.04 ±0.80	6.56 ±0.62	3.25 ±0.46	7.77 ±0.97	6.70 ±0.33
C20:5 n-3	24.33 ±1.03^{ac}	20.69 ±1.61^{ad}	17.09 ±1.65^{bd}	27.03 ±2.41^{ce}	23.37 ±0.51^{ae}
C22:5 n-6	7.36 ±0.82	6.60 ±0.11	8.21 ±0.99	4.30 ±0.29	6.32 ±0.52
C22:6 n-3	9.30 ±0.80^{a}	10.33 ±0.30^{ad}	5.73 ±0.62^{b}	8.71 ±0.80^{a}	11.65 ±0.83^{cd}
Σ SFA	32.53 ±1.03^{ac}	32.65 ±2.25^{ac}	43.37 ±2.25^{b}	36.57 ±2.46^{a}	30.51 ±1.36^{c}
Σ MUFA	15.88 ±2.29^{ac}	20.24 ±1.35^{b}	19.5 ±1.62^{ab}	14.01 ±1.28^{cd}	17.16 ±0.44^{abd}
Σ PUFA	51.59 ±1.54^{a}	47.11 ±3.24^{a}	37.13 ±3.5^{b}	49.42 ±3.45^{a}	52.33 ±1.59^{a}
Σ n-3	41.46 ±0.47^{ac}	38.27 ±2.57^{a}	26.49 ±2.33^{b}	44.19 ±3.20^{cd}	42.89 ±1.08^{ad}
Σ n-6	9.10 ±1.35	7.84 ±0.36	10.25 ±1.24	4.57 ±0.32	8.47 ±0.66
n-3/n-6	4.62 ±0.72	4.88 ±0.15	2.59 ±0.1	9.66 ±0.32	5.08 ±0.28

The composition of *P. gyrans* grown with limited micronutrients presented a similar fatty acids profile to the optimal conditions. Although the lower concentration of a high number of nutrients hindered the growth of *P. gyrans*, this change in culture conditions did not greatly affect the fatty acids composition. In fact, the comparison between the Opt, Lvl-1, and Con assay, allows us assuming that the production of fatty acids by *P. gyrans* was strongly dependent on the individual or combined availability of nitrogen, phosphorus, and copper.

The amount of nitrogen available has been reported as a crucial factor involved in lipids and fatty acids modelling in microalgae. In N replete conditions, microalgae are not stressed, preventing lipid membrane remodeling, in which an increased accumulation of neutral lipids (*e.g.* TAGs), at the expense of polar lipids, is promoted. Polar lipids are the main components of photosynthetic membranes in microalgae, which are the main sink of PUFAs and may explain the relative high levels of EPA and DHA, as well the lower content of SFA on *P. gyrans* [26,64].

The trial without supplementation of both vitamins presented the highest value of EPA compared to Con and the Opt (14 d) ($p < 0.05$). Furthermore, there were also described important variations in other five fatty acids (statistical analysis not presented). Namely, the Vit- had the lowest level of C16:1 n-7, C18:2 n-6, and C22:5 n-6, which decreased 1.6-2.0-fold, 4.4-7.7-fold, and 1.5-1.9-fold, respectively. Conversely, there was an increase of 2.2-3.4 times in C18:0 and 2.3-5.1 times in C18:1 n-7.

3.3.4.3 Nutritional indices

Microalgae have been highlighted as a promising source of important bioactives for nutraceutical applications. This importance is partially linked to their ability to produce high levels of PUFA that have proved their biological importance as anti-inflammatory and antioxidant compounds in several illnesses, such as some related to the cardiovascular system and mental development [2,3]. However, to reach that goal, an extensive work must be done in order to identify microalgae species with suitable fatty acids composition, and mostly to identify the respective adequate growth conditions for the biomass produced to meet the appropriate nutritional indices for human applications [45].

Taking into account the fatty acids composition of *P. gyrans*, the impact of the validation conditions on its nutritional value was estimated by the calculation of the hypocholesterolemic (*HI*), atherogenic (*AI*), and thrombogenic indices (*TI*) (Figure 3-8). These indices allow to categorize food products according to their healthiness for human diet, especially the likelihood to develop cardiovascular disease (CVD), which is usually associated with the accumulation of lipid plaques in the circulatory system (atherogenicity), clot

formation in the blood vessels (thrombogenicity), and the cholesterol increase in blood (hypocholesterolemia) [46]. In general, a fatty acids composition rich in saturated residues, in opposition to unsaturated FAs, has pro-atherogenic, pro-thrombogenic, and hypercholesterolemic activity, promoting high *AI* and *TI* indices, and reduced *HI* index, which may lead to increased CVD risk [46,83]. Similarly, several studies have highlighted the detrimental effect of Western diet for human health because of the massive increase (> 15 times) of pro-inflammatory n-6 FA intake, over the anti-inflammatory n-3 FA, which have been linked to the development of inflammatory diseases, cancer, and CVD [8].

The main outcome of the present work was the significant ($p < 0.05$) variation achieved in the values of *AI*, *TI* and *HI*: compared to Con experiment, whose biomass produced the highest values for *AI* (1.34) and *TI* (0.45), and the lowest for *HI* (0.96), *P. gyrans* produced under the optimal conditions (Opt) yielded 0.93, 0.24, and 1.63 for *AI*, *TI*, and *HI*, respectively. This variation amongst the nutritional indices arises from the considerable increase of the SFA C16:0 (29.62 % TFA) in Con (Table 3-13), a fatty acid considered pro-atherogenic, pro-thrombogenic, and hypercholesterolemic, in opposition to *P. gyrans* biomass enriched with n-3 FA (38.27 % TFA) and PUFA (47.11 % TFA) from Opt [46]. Similarly, the ratio ∑n-3/∑n-6 % TFA almost doubled in the optimal conditions of *P. gyran*s (4.88) when compared to the control (2.59).

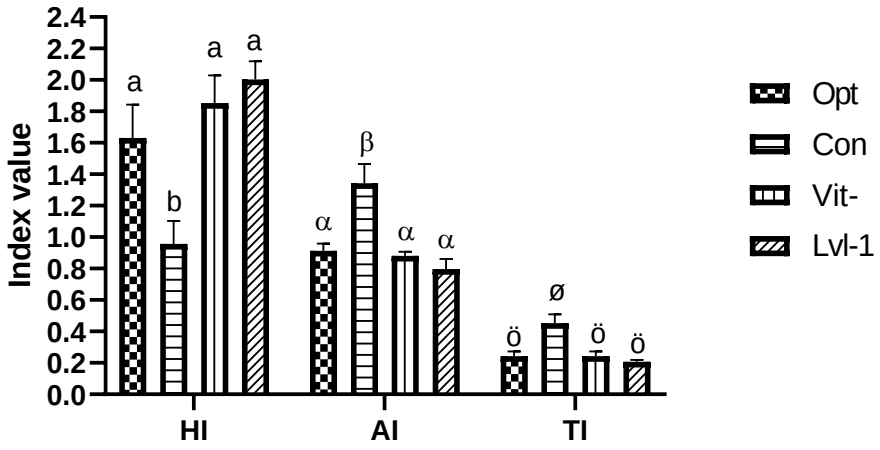

Figure 3-8: hypocholesterolemic index *(HI),* atherogenic index *(AI)*, and thrombogenic index *(TI)* of *P. gyrans* produced in the validation assays under the optimized conditions at day 10, Opt.i, and 14, Opt, control/Walne's medium, Con, medium without vitamins, Vit-, and assay with the abiotic factors considered non-significant in Plackett-Burman design fixed at Level -1, Lvl-1. Values are the mean and standard deviation of three assays (n=3). Different letters indicate significant differences in the fatty acid or the fatty acids class between the treatments (one-way ANOVA, $p < 0.05$, followed by the Tukey's test)

The nutritional values here reported for the optimal conditions of *P. gyrans* are in accordance with other microalgae. Aussant et al. assessed the nutritional value of eight microalgae species and stated that the

average values for *AI*, *TI*, and *HI* indices ranged from 0.492 – 1.424, 0.197 – 0.836, and 0.523 – 2.014, respectively [45]. *HI* index of *P. pinguis* grown under different levels of nitrogen varied from 1.28 to 2.16 [84]. Thus, considering that a healthy diet should be characterized by high intake of n-3 fatty acids, low values of *AI* and *TI*, and relatively high values of *HI* [8,83], *P. gyrans* cultured at their optimum conditions presents itself as a potential source of healthy lipids for human consumption, mostly due to its ability to produce high contents of EPA and DHA.

3.4 CONCLUSIONS

In this work, a two-step statistical approach was used to optimize the growth performance of *Pavlova gyrans*. Plackett-Burman design assessed the effect of seventeen abiotic factors and allowed identifying the independent variables light intensity, $NaNO_3$, and $CuSO_4.5H_2O$ as the most significant abiotic factors ($p < 0.10$) in the biomass productivity of the microalgae, the value of which ranged from 0.072 to 0.256 $g.L^{-1}.d^{-1}$. $NaNO_3$ and light intensity were positively correlated with the biomass productivity, whereas copper showed a negative impact. These variables, along with $NaH_2PO_4.H_2O$ (positive effect), were further used in a rotatable central composite design to optimize the maximum biomass produced and the responses obtained were applied to fit mathematical models to predict the dependent variables X_{max}, total lipids, protein content, and the relative abundance of EPA and DHA. The biomass productivity and the maximum biomass concentration achieved ranged from 0.165 to 0.262 g $AFDW.L.^{-1}d^{-1}$, and from 1.30 to 2.34 g $AFDW.L.^{-1}$, respectively. The models generated allowed understanding the impact of the independent variables and their interactions in growth performance of *P. gyrans* and its biochemical composition. Compared to control conditions (Walne's medium), the maximum biomass produced increased 3.8-fold under the optimal growth conditions, with a significant improvement in biochemical composition ($p < 0.05$), namely increasing the protein content (30.76 % $w.w^{-1}$) and the levels of PUFA (47.11 % TFA), n-3 fatty acids (38.27 % TFA), and the DHA (10.33 % TFA). EPA level was also increased to 20.69 % TFA ($p > 0.05$). Due to this fatty acids' composition, *P. gyrans* grown under the defined optimal conditions presented very interesting nutritional indices, which indicate this strain as a promising potential source of healthy lipids for the human diet.

3.5 REFERENCES

1. Peet M, Stokes C. Omega-3 Fatty Acids in the Treatment of Psychiatric Disorders. 2005;65:1051–9.

2. Kris-Etherton PM, Harris WS, Appel LJ. Fish consumption, fish oil, omega-3 fatty acids, and cardiovascular disease. Circulation. 2002;106:2747–57.

3. Fotuhi M, Mohassel P, Yaffe K. Fish consumption, long-chain omega-3 fatty acids and risk of cognitive decline or Alzheimer disease: A complex association. Nature Clinical Practice Neurology. 2009;5:140–52.

4. Judge MP, Harel O, Lammi-Keefe CJ. Maternal consumption of a docosahexaenoic acid-containing functional food during pregnancy: Benefit for infant performance on problem-solving but not on recognition memory tasks at age 9 mo. American Journal of Clinical Nutrition. 2007;85:1572–7.

5. Taylor P, Ganesan B, Brothersen C, Mcmahon DJ, Ganesan B, Brothersen C. Fortification of Foods with Omega-3 Polyunsaturated Fatty Acids Fortification of Foods with Omega-3. 2014;37–41.

6. EFSA Panel on Dietetic Products N and A (NDA). Scientific Opinion on the Tolerable Upper Intake Level of eicosapentaenoic acid (EPA), docosahexaenoic acid (DHA) and docosapentaenoic acid (DPA). EFSA Journal. Wiley-Blackwell Publishing Ltd; 2012;10.

7. Hamilton HA, Newton R, Auchterlonie NA, Müller DB. Systems approach to quantify the global omega-3 fatty acid cycle. Nature Food. Springer Nature; 2020;1:59–62.

8. Simopoulos A P. The importance of the ratio of omega-6/omega-3 essential fatty acids. Biomedicine and Pharmacotherapy. 2002;56:365–79.

9. BCC Research. Global Omega 3 Market Size and Growth Forecast to 2025 [Internet]. [cited 2022 Apr 11]. Available from: https://www.bccresearch.com/partners/verified-market-research/global-omega-3-market-size-and-forecast.html

10. Glencross BD, Tocher DR, Matthew C, Gordon Bell J. Interactions between dietary docosahexaenoic acid and other long-chain polyunsaturated fatty acids on performance and fatty acid retention in post-smolt Atlantic salmon (Salmo salar). Fish Physiology and Biochemistry. Kluwer Academic Publishers; 2014;40:1213–27.

11. Guihéneuf F, Mimouni V, Tremblin G, Ulmann L. Light intensity regulates LC-PUFA incorporation into lipids of Pavlova lutheri and the final desaturase and elongase activities involved in their biosynthesis. Journal of Agricultural and Food Chemistry. 2015;63:1261–7.

12. Tibbetts SM, Patelakis SJJ, Whitney-Lalonde CG, Garrison LL, Wall CL, MacQuarrie SP. Nutrient composition and protein quality of microalgae meals produced from the marine prymnesiophyte Pavlova sp. 459 mass-cultivated in enclosed photobioreactors for potential use in salmonid aquafeeds. Journal of Applied Phycology. 2020;32:299–318.

13. Slocombe SP, Zhang Q, Ross M, Anderson A, Thomas NJ, Lapresa Á, et al. Unlocking nature's treasure-chest: Screening for oleaginous algae. Scientific Reports. Nature Publishing Group; 2015;5:1–17.

14. Reitan KI, Øie G, Jørgensen H, Wang X. Chemical composition of selected marine microalgae, with emphasis on lipid and carbohydrate production for potential use as feed resources. Journal of Applied Phycology [Internet]. Springer Netherlands; 2021;33:3831–42. Available from: https://doi.org/10.1007/s10811-021-02586-x

15. Bendif EM, Probert I, Hervé A, Billard C, Goux D, Lelong C, et al. Integrative Taxonomy of the Pavlovophyceae (Haptophyta): A Reassessment. Protist [Internet]. Elsevier GmbH.; 2011;162:738–61. Available from: http://dx.doi.org/10.1016/j.protis.2011.05.001

16. Volkman JK, Dunstan GA, Jeffrey SW, Kearney PS. Fatty acids from microalgae of the genus Pavlova. Phytochemistry. 1991;30:1855–9.

17. Patil V, Källqvist T, Olsen E, Vogt G, Gislerød HR. Fatty acid composition of 12 microalgae for possible use in aquaculture feed. Aquaculture International. 2007;15:1–9.

18. Grima EM, Medina AR, Giménez AG, Pérez JAS, Camacho FG, Sánchez JLG. Comparison Between Extraction of Lipids and Fatty Acids from Microalgal Biomass. Journal of the American Oil Chemists' Society. 1994;71:955–9.

19. Tonon T, Harvey D, Larson TR, Graham IA. Long chain polyunsaturated fatty acid production and partitioning to triacylglycerols in four microalgae. Phytochemistry. 2002;61:15–24.

20. Fernandes T, Martel A, Cordeiro N. Exploring Pavlova pinguis chemical diversity: a potentially novel source of high value compounds. Scientific Reports. 2020;10:1–11.

21. Kanamoto A, Kato Y, Yoshida E, Hasunuma T, Kondo A. Development of a Method for Fucoxanthin Production Using the Haptophyte Marine Microalga Pavlova sp. OPMS 30543. Marine Biotechnology [Internet]. Springer US; 2021;23:331–41. Available from: https://doi.org/10.1007/s10126-021-10028-5

22. Tibbetts SM, Patelakis SJJ. Apparent digestibility coefficients (ADCs) of intact-cell marine microalgae meal (Pavlova sp. 459) for juvenile Atlantic salmon (Salmo salar L.). Aquaculture [Internet]. Elsevier B.V.; 2022;546:737236. Available from: https://doi.org/10.1016/j.aquaculture.2021.737236

23. Ahmed F, Zhou W, Schenk PM. Pavlova lutheri is a high-level producer of phytosterols. Algal Research [Internet]. Elsevier B.V.; 2015;10:210–7. Available from: http://dx.doi.org/10.1016/j.algal.2015.05.013

24. Cañavate JP, Fernández-Díaz C. Salinity induces unique changes in lipid classes and fatty acids of the estuarine haptophyte Diacronema vlkianum. European Journal of Phycology [Internet]. Taylor & Francis; 2021;00:1–21. Available from: https://doi.org/10.1080/09670262.2021.1970234

25. Guihéneuf F, Mimouni V, Ulmann L, Tremblin G. Combined effects of irradiance level and carbon source on fatty acid and lipid class composition in the microalga Pavlova lutheri commonly used in mariculture. Journal of Experimental Marine Biology and Ecology. Elsevier B.V.; 2009;369:136–43.

26. Guihéneuf F, Stengel DB. LC-PUFA-enriched oil production by microalgae: Accumulation of lipid and triacylglycerols containing n-3 LC-PUFA is triggered by nitrogen limitation and inorganic carbon availability in the marine haptophyte Pavlova lutheri. Marine Drugs. 2013;11:4246–66.

27. Carvalho AP, Pontes I, Gaspar H, Malcata FX. Metabolic relationships between macro- and micronutrients, and the eicosapentaenoic acid and docosahexaenoic acid contents of Pavlova lutheri. Enzyme and Microbial Technology. 2006;38:358–66.

28. Kim SH, Sunwoo IY, Hong HJ, Awah CC, Jeong GT, Kim SK. Lipid and unsaturated fatty acid productions from three microalgae using nitrate and light-emitting diodes with complementary LED wavelength in a two-phase culture system. Bioprocess and Biosystems Engineering [Internet]. Springer Berlin Heidelberg; 2019;42:1517–26. Available from: https://doi.org/10.1007/s00449-019-02149-y

29. Huang B, Mimouni V, Lukomska E, Morant-Manceau A, Bougaran G. Carbon Partitioning and Lipid Remodeling During Phosphorus and Nitrogen Starvation in the Marine Microalga Diacronema lutheri (Haptophyta). Journal of Phycology. 2020;56:908–22.

30. Terry KL. Nitrate and Phosphate Uptake Interactions in a Marine Prymnesiophyte. Journal of Phycology. 1982;18:79–86.

31. Carvalho AP, Malcata FX. Effect of culture media on production of polyunsaturated fatty acids by Pavlova lutheri. Cryptogamie, Algologie. 2000;21:59–71.

32. Li M, Hu C, Zhu Q, Chen L, Kong Z, Liu Z. Copper and zinc induction of lipid peroxidation and effects on antioxidant enzyme activities in the microalga Pavlova viridis (Prymnesiophyceae). Chemosphere. 2006;62:565–72.

33. LI M, ZHU Q, HU C wei, CHEN L, LIU Z li, KONG Z ming. Cobalt and manganese stress in the microalga Pavlova viridis (Prymnesiophyceae): Effects on lipid peroxidation and antioxidant enzymes. Journal of Environmental Sciences. 2007;19:1330–5.

34. Huang X, Wei L, Huang Z, Yan J. Effect of high ferric ion concentrations on total lipids and lipid characteristics of Tetraselmis subcordiformis, Nannochloropsis oculata and Pavlova viridis. Journal of Applied Phycology. 2014;26:105–14.

35. Rodrigues MI, Iemma AF. Experimental design and process optimization. 1st Edition. Experimental Design and Process Optimization. CRC Press; 2014.

36. Andersen RA, editor. Algal Culturing Techniques. Elsevier Academic Press; 2005.

37. Guihéneuf F, Stengel DB. Interactive effects of light and temperature on pigments and n-3 LC-PUFA-enriched oil accumulation in batch-cultivated Pavlova lutheri using high-bicarbonate supply. Algal Research [Internet]. Elsevier B.V.; 2017;23:113–25. Available from: http://dx.doi.org/10.1016/j.algal.2017.02.002

38. Guihéneuf F, Ulmann L, Tremblin G, Mimouni V. Light-dependent utilization of two radiolabelled carbon sources, sodium bicarbonate and sodium acetate, and relationships with long chain polyunsaturated fatty acid synthesis in the microalga Pavlova lutheri (Haptophyta). European Journal of Phycology. 2011;46:143–52.

39. Fernandes T, Cordeiro N. Effects of phosphorus-induced changes on the growth, nitrogen uptake, and biochemical composition of Pavlova pinguis and Hemiselmis cf. andersenii. Journal of Applied Phycology. Springer Science and Business Media LLC; 2022;

40. Dahmen-Ben Moussa I, Chtourou H, Karray F, Sayadi S, Dhouib A. Nitrogen or phosphorus repletion strategies for enhancing lipid or carotenoid production from Tetraselmis marina. Bioresource Technology. Elsevier Ltd; 2017;238:325–32.

41. Cañavate JP, Armada I, Hachero-Cruzado I. Aspects of phosphorus physiology associated with phosphate-induced polar lipid remodelling in marine microalgae. Journal of Plant Physiology. Elsevier GmbH; 2017;214:28–38.

42. Pereira H, Páramo J, Silva J, Marques A, Barros A, Maurício D, et al. Scale-up and large-scale production of Tetraselmis sp. CTP4 (Chlorophyta) for CO2 mitigation: From an agar plate to 100-m3 industrial photobioreactors. Scientific Reports. Nature Publishing Group; 2018;8.

43. Lourenço SO, Barbarino E, Lavín PL, Lanfer Marquez UM, Aidar E. Distribution of intracellular nitrogen in marine microalgae: Calculation of new nitrogen-to-protein conversion factors. European Journal of Phycology. 2004;39:17–32.

44. Couto D, Melo T, Conde TA, Costa M, Silva J, Domingues MRM, et al. Chemoplasticity of the polar lipid profile of the microalgae Chlorella vulgaris grown under heterotrophic and autotrophic conditions. Algal Research. Elsevier B.V.; 2021;53.

45. Aussant J, Guihéneuf F, Stengel DB. Impact of temperature on fatty acid composition and nutritional value in eight species of microalgae. Applied Microbiology and Biotechnology. Springer Verlag; 2018;102:5279–97.

46. Chen J, Liu H. Nutritional indices for assessing fatty acids: A mini-review. International Journal of Molecular Sciences. MDPI AG; 2020. p. 1–24.

47. Wimalasekera R. Effect of Light Intensity on Photosynthesis. In: Ahmad P, Ahanger MA, Alyemeni MN, Alam P, editors. Photosynthesis, Productivity and Environmental Stress. John Wiley & Sons Ltd; 2020. p. 65–73.

48. Seoane S, Zapata M, Orive E. Growth rates and pigment patterns of haptophytes isolated from estuarine waters. Journal of Sea Research [Internet]. Elsevier B.V.; 2009;62:286–94. Available from: http://dx.doi.org/10.1016/j.seares.2009.07.008

49. Su Y. Revisiting carbon, nitrogen, and phosphorus metabolisms in microalgae for wastewater treatment. Science of the Total Environment. Elsevier B.V.; 2021.

50. Janssen JH, Kastenhofer J, de Hoop JA, Lamers PP, Wijffels RH, Barbosa MJ. Effect of nitrogen addition on lipid productivity of nitrogen starved Nannochloropsis gaditana. Algal Research. 2018;33:125–32.

51. Kong L, Price NM. Identification of copper-regulated proteins in an oceanic diatom,: Thalassiosira oceanica 1005. Metallomics. Royal Society of Chemistry; 2020;12:1106–17.

52. Debelius B, Forja JM, DelValls Á, Lubián LM. Toxicity and bioaccumulation of copper and lead in five marine microalgae. Ecotoxicology and Environmental Safety. 2009;72:1503–13.

53. Blank LM. The cell and P: From cellular function to biotechnological application. Current Opinion in Biotechnology. 2012. p. 846–51.

54. Sadahira MS, Rodrigues MI, Akhtar M, Murray BS, Netto FM. Effect of egg white protein-pectin electrostatic interactions in a high sugar content system on foaming and foam rheological properties. Food Hydrocolloids. Elsevier; 2016;58:1–10.

55. Purbonegoro T, Suratno, Puspitasari R, Husna NA. Toxicity of copper on the growth of marine microalgae Pavlova sp. and its chlorophyll-a. IOP Conference Series: Earth and Environmental Science. Institute of Physics Publishing; 2018.

56. Rocha GS, Lombardi AT, Melão M da GG. Influence of phosphorus on copper toxicity to Selenastrum gracile (Reinsch) Korshikov. Ecotoxicology and Environmental Safety. Academic Press; 2016;128:30–5.

57. Simkin AJ, Kapoor L, Doss CGP, Hofmann TA, Lawson T, Ramamoorthy S. The role of photosynthesis related pigments in light harvesting, photoprotection and enhancement of photosynthetic yield in planta. Photosynthesis Research. Springer Science and Business Media B.V.; 2022.

58. Varshney P, Sohoni S, Wangikar PP, Beardall J. Effect of high CO2 concentrations on the growth and macromolecular composition of a heat- and high-light-tolerant microalga. Journal of Applied Phycology. Springer Netherlands; 2016;28:2631–40.

59. Wu Q, Guo L, Li X, Wang Y. Effect of phosphorus concentration and light/dark condition on phosphorus uptake and distribution with microalgae. Bioresour Technol. NLM (Medline); 2021;340:125745.

60. Jiao Y, Ouyang HL, Jiang YJ, Kong XZ, He W, Liu WX, et al. Effects of phosphorus stress on the photosynthetic and physiological characteristics of Chlorella vulgaris based on chlorophyll fluorescence and flow cytometric analysis. Ecological Indicators. Elsevier B.V.; 2017;78:131–41.

61. Tan KWM, Lin H, Shen H, Lee YK. Nitrogen-induced metabolic changes and molecular determinants of carbon allocation in Dunaliella tertiolecta. Scientific Reports. Nature Publishing Group; 2016;6.

62. Cao Z, Shen X, Wang X, Zhu B, Pan K, Li Y. Effect of Nitrogen Concentration on the Alkalophilic Microalga Nitzschia sp. NW129-a Promising Feedstock for the Integrated Production of Lipids and Fucoxanthin in Biorefinery. Front Mar Sci. Frontiers Media S.A.; 2022;8.

63. Xin L, Hong-ying H, Ke G, Ying-xue S. Effects of different nitrogen and phosphorus concentrations on the growth, nutrient uptake, and lipid accumulation of a freshwater microalga Scenedesmus sp. Bioresource Technology. 2010;101:5494–500.

64. Huang X, Huang Z, Wen W, Yan J. Effects of nitrogen supplementation of the culture medium on the growth, total lipid content and fatty acid profiles of three microalgae (Tetraselmis subcordiformis, Nannochloropsis oculata and Pavlova viridis). Journal of Applied Phycology. 2013;25:129–37.

65. Jia J, Han D, Gerken HG, Li Y, Sommerfeld M, Hu Q, et al. Molecular mechanisms for photosynthetic carbon partitioning into storage neutral lipids in Nannochloropsis oceanica under nitrogen-depletion conditions. Algal Research. Elsevier; 2015;7:66–77.

66. Li J, Han D, Wang D, Ning K, Jia J, Wei L, et al. Choreography of Transcriptomes and Lipidomes of Nannochloropsis Reveals the Mechanisms of Oil Synthesis in Microalgae. Source: The Plant Cell. 2014.

67. Chu F, Cheng J, Li K, Wang Y, Li X, Yang W. Enhanced Lipid Accumulation through a Regulated Metabolic Pathway of Phosphorus Luxury Uptake in the Microalga Chlorella vulgaris under Nitrogen Starvation and Phosphorus Repletion. ACS Sustainable Chemistry and Engineering. American Chemical Society; 2020;8:8137–47.

68. Chu FF, Chu PN, Shen XF, Lam PKS, Zeng RJ. Effect of phosphorus on biodiesel production from Scenedesmus obliquus under nitrogen-deficiency stress. Bioresource Technology. Elsevier Ltd; 2014;152:241–6.

69. Liu J, Yuan C, Hu G, Li F. Effects of light intensity on the growth and lipid accumulation of microalga Scenedesmus sp. 11-1 under nitrogen limitation. Applied Biochemistry and Biotechnology. 2012;166:2127–37.

70. Breuer G, Lamers PP, Martens DE, Draaisma RB, Wijffels RH. Effect of light intensity, pH, and temperature on triacylglycerol (TAG) accumulation induced by nitrogen starvation in Scenedesmus obliquus. Bioresource Technology. Elsevier Ltd; 2013;143:1–9.

71. Takeshita T, Ota S, Yamazaki T, Hirata A, Zachleder V, Kawano S. Starch and lipid accumulation in eight strains of six Chlorella species under comparatively high light intensity and aeration culture conditions. Bioresource Technology. Elsevier Ltd; 2014;158:127–34.

72. Janssen JH, Kastenhofer J, de Hoop JA, Lamers PP, Wijffels RH, Barbosa MJ. Effect of nitrogen addition on lipid productivity of nitrogen starved Nannochloropsis gaditana. Algal Research. Elsevier B.V.; 2018;33:125–32.

73. Sui Y, Harvey PJ. Effect of light intensity and wavelength on biomass growth and protein and amino acid composition of dunaliella salina. Foods. MDPI AG; 2021;10.

74. Nzayisenga JC, Farge X, Groll SL, Sellstedt A. Effects of light intensity on growth and lipid production in microalgae grown in wastewater. Biotechnology for Biofuels. BioMed Central Ltd.; 2020;13.

75. Markou G, Chatzipavlidis I, Georgakakis D. Effects of phosphorus concentration and light intensity on the biomass composition of Arthrospira (Spirulina) platensis. World Journal of Microbiology and Biotechnology. 2012;28:2661–70.

76. Conceição D, Lopes RG, Derner RB, Cella H, do Carmo APB, Montes D'Oca MG, et al. The effect of light intensity on the production and accumulation of pigments and fatty acids in Phaeodactylum tricornutum. Journal of Applied Phycology. Springer; 2020;32:1017–25.

77. Guedes AC, Meireles LA, Amaro HM, Malcata FX. Changes in lipid class and fatty acid composition of cultures of Pavlova lutheri, in response to light intensity. JAOCS, Journal of the American Oil Chemists' Society. 2010;87:791–801.

78. Huang B, Marchand J, Thiriet-Rupert S, Carrier G, Saint-Jean B, Lukomska E, et al. Betaine lipid and neutral lipid production under nitrogen or phosphorus limitation in the marine microalga Tisochrysis lutea (Haptophyta). Algal Research. Elsevier B.V.; 2019;40.

79. Sabatini SE, Juárez ÁB, Eppis MR, Bianchi L, Luquet CM, Ríos de Molina M del C. Oxidative stress and antioxidant defenses in two green microalgae exposed to copper. Ecotoxicology and Environmental Safety. 2009;72:1200–6.

80. Nef C, Jung S, Mairet F, Kaas R, Grizeau D, Garnier M. How haptophytes microalgae mitigate vitamin B12 limitation. Scientific Reports. 2019;9:1–11.

81. Rout GR, Sahoo S. Role of iron in plant growth and metabolism. Reviews in Agricultural Science. United Graduate School of Agricultural Science; 2015;3:1–24.

82. Farhat N, Elkhouni A, Zorrig W, Smaoui A, Abdelly C, Rabhi M. Effects of magnesium deficiency on photosynthesis and carbohydrate partitioning. Acta Physiologiae Plantarum. Polish Academy of Sciences; 2016.

83. Attia YA, Al-Harthi MA, Korish MA, Shiboob MM. Fatty acid and cholesterol profiles and hypocholesterolemic, atherogenic, and thrombogenic indices of table eggs in the retail market. Lipids in Health and Disease. BioMed Central Ltd.; 2015;14.

84. Fernandes T, Cordeiro N. High-value lipids accumulation by Pavlova pinguis as a response to nitrogen-induced changes. Biomass and Bioenergy. Elsevier Ltd; 2022;158.

CHAPTER 4 IDENTIFICATION AND OPTIMIZATION OF THE KEY ABIOTIC FACTORS INVOLVED IN CAROTENOID PRODUCTION OF THE MARINE MICROALGA *PAVLOVA GYRANS*

4.1 INTRODUCTION

Carotenoids are the pigments responsible for the yellow, orange, and red colors in nature, such those presented by microalgae, bacteria, and plants [1], with over 1110 natural carotenoids identified in 683 organisms [2]. They are characterized by their lipophilic nature and a 40 carbon atoms structure composed of isoprene units [3]. According to their chemical composition, carotenoids can be classified as xanthophylls or carotenes, depending on if they present an oxygenic functional group attached or are solely composed of hydrocarbons, respectively [1].

Carotenoids have been highlighted as high-added value products due to their biological activity and coloring properties, which make them of great interest for biotechnological and industrial applications [4]. Several biological functions in human health have been described for this class of pigments, including antioxidant and anticancer activity, provitamin A, prevention of heart disease, visual and cognitive development in children, improvement of the immune system, and benefits in weight control and obesity [5]. Most of these functions are associated with the antioxidant properties of carotenoids due to their ability to quench singlet oxygen and reactive oxygen species, which is strongly dependent of the pigments' chemical composition. Singlet oxygen quenching is linked to a higher number of conjugated double bonds in molecular structure, being at least 9 double bonds needed to exert protective effects against photosensitization [6]. Furthermore, the functional group and chain structure of carotenoids may also affect their oxygen quenching ability [7].

Humans are not able to naturally synthesize carotenoids and their needs are only met through proper nutrition. Thus, considering their biological relevance along with the consumers' awareness for a healthy lifestyle, there has been an increasing demand for carotenoids in recent decades, estimating a compound annual growth rate of 5.7 % and a potential global market value of 2.7 billion US$ by 2027 [8]. Cheaper production of chemically synthetized colorants makes them attractive, however, they represent a high environmental impact and health concerns raised when used as ingredient for human consumption [9]. Furthermore, synthetic carotenoids are not a viable option, since they have significantly lower bioactivity compared to the natural carotenoids. According to Capelli et al. [10], the natural astaxanthin from *Haematococcus pluvialis* presented an oxygen quenching and a free radical elimination 50x and 20x stronger, respectively, against its synthetic form.

Driven by the increased consumers demand for products labelled as natural and produced through sustainable processes, several alternative sources have been proposed [11]. Among them, microalgae are presented as one of the most promising. These microorganisms are widespread in aquatic and even

in terrestrial habitats (lichens) and are known for their high photosynthetic activity, fast growth, and metabolic plasticity. They possess a rich composition, which can include several bioactive pigments, polyunsaturated fatty acids and/or high protein content [12–14]. Several species have been commercially explored as producers of carotenoids, being the most well-known examples *Haematococcus pluvialis* and *Dunaliella salina*, which can produce 6% and 10% of their dry weight (DW) as astaxanthin and βCar, respectively [15,16].

Nevertheless, the differentiated properties of natural carotenoids, along with challenging implementation of microalgae production at industrial scale, contributed to their increasing market value, which can reach 1500 US$.kg^{-1} for βCar or even 42000 US$.kg^{-1} for Fx [17]. Thus, to improve the cost-effectiveness of the process several research studies have been developed with the aim of identifying new microalgae species enriched in carotenoid, assessing growth conditions to improve biomass production, as well as developing strategies to increase the accumulation of carotenoids [13,18–27].

Microalgae species from the Pavlovophyeceae class have been commonly used over the last decades as feed product for fish, crustaceans, and bivalves [28,29]. Constituted by thirteen species, this class of haptophytes is widely distributed in coastal, brackish waters and, at a lesser extent, in freshwater [30]. Over the past years, these microalgae have been seen as a promising source of bioactive compounds for industries other than aquaculture, such as food and pharmaceutical industries or even wastewater management [31–35]. Firstly, the commercial interest of Pavlovophyeceae species relied on their ability to produce large lipids contents enriched with the high valuable eicosapentaenoic acid (EPA) and docosahexaenoic acid (DHA), which can account for 3.49 and 2.01 mg g^{-1} of its DW, respectively [36]. However, these microalgae also present an interesting composition of sterols, essential amino acids, higher digestibility due to the absence of cell wall and a valuable carotenoids profile composed of diadinoxanthin (Ddx), diatoxanthin (Dtx), βCar and, mostly, Fx (51-68% of total carotenoids) [34,36–38]. As previously mentioned, carotenoids – and particularly Fx – have been highlighted and highly demanded due to its potential anti-obesity, anti-cancer, and anti-diabetic effect [39–41].

Regarding the effect of growth conditions, Seoane et al. [42] described a negative impact of the increasing light intensity on fucoxanthin:chlorophyll *a* ratio of *Pavlova gyrans*. Similar approach was performed with *Diacronema lutheri*, where the combined effect of temperature and illumination was evaluated [43]. In a screening study involving *Pavlova* strains with further optimization of growth conditions, *Pavlova* sp. OPMS 30543 was grown in outdoor conditions producing 4.88 mg.L^{-1}.day^{-1} of Fx [44]. In addition, the low phosphorus [45] and high nitrogen [46] levels was found to promote the carotenoid accumulation in

Pavlova pinguis, reaching 4.32 and 2.91 mg g^{-1} DW, respectively. Under non-optimized conditions Tibbetts et al. [47] stated that Fx content of the *Pavlova* sp. CCMP strain 459 was 0.36 g/100 g of its dry weight, whereas in a food grade *Diacronema lutheri* extract it represented 26 % of the total pigments [32].

The present study aims to optimize the carotenoids accumulation of the microalga *Pavlova gyrans* through a multivariate approach. To the authors' knowledge, and unlike other haptophytes and diatoms, few studies were found related to the optimization of their growth conditions to maximize the carotenoids content, despite the potential of Pavlovophyeceae species as carotenoid sources. Seventeen abiotic factors were tested and their effects calculated in order to identify the most significant variables on the TCar, Fx and βCar. Additionally, other pigments such as Dtx and Ddx, as well chlorophylls, were analyzed presenting complementary information regarding *Pavlova gyrans'* potential for pigments and bioactive compounds production. Considering the calculated effects, several growth conditions were formulated and validated against the control conditions. Moreover, the most significant abiotic factors were also validated against the optimum growth conditions for biomass production of *P. gyrans*, which were determined in CHAPTER 3.

4.2 MATERIALS AND METHODS

4.2.1 Microalga and inoculum preparation

The non-axenic microalga strain *Pavlova gyrans* (RCC1553) was obtained from the Roscoff Culture Collection (Roscoff, France). It was maintained in Walne's medium (500 mg.L^{-1} $NaNO_3$), at Level 0 (Table 4-1), under salinity of 30 psu. The inoculum was up-scaled to 2 L flat bottom flask, in which was bubbled with a mixture of air and CO_2 (8 mL.min^{-1} – Alicat Scientific, USA) to keep the pH value in the range of 8.0 ± 0.5. The cultures were grown at room temperature and irradiated with 100 µmol photons m^{-2} s^{-1} over 24 h.

4.2.2 Screening of the abiotic factors for carotenoids production by *P. gyrans* using a Plackett-Burman design

The experimental design adopted to assess the impact of abiotic factors over *P. gyrans* carotenoids composition is described in Table 4-1. Each abiotic factor was evaluated at three different levels: -1, 0, and 1. The corresponding combinations of the growth conditions are presented in Table 4-2. Briefly, seventeen abiotic factors were assessed through a Plackett-Burman design (PB), composed of 24 individual combinations and 4 central points (assays 25-28), totaling 28 assays [48]. All independent

variables were set at Level 0 in the central points, which allowed evaluating the repeatability of the carotenoids' composition of *P. gyrans*. The experiments were carried out in 1 L bubble column reactors (6.5 cm diameter and 43 cm high) at room temperature and continuously illuminated and aerated with filtered air (0.2 µm).

Table 4-1: the seventeen abiotic factors, and respective levels, assessed in the carotenoids composition of *P. gyrans* through the Plackett-Burman experimental design

Abiotic factor		Level		
		-1	0	1
x_1	Inoculum size (AFDW g.L^{-1})	0.1	0.2	0.3
x_2	Salinity (psu)	20	30	40
x_3	Light intensity (µmol.photons.m^{-2}.s^{-1})	150	450	750
x_4	Air flow (mL.min^{-1})	600	800	1000
x_5	$NaNO_3$ (mg.L^{-1})	250	500	750
x_6	$NaH_2PO_4.H_2O$ (mg.L^{-1})	10	20	30
x_7	$Na_2H_2EDTA.2H_2O$ (mg.L^{-1})	22.5	45	67.5
x_8	H_3BO_3 (mg.L^{-1})	16.8	33.6	50.4
x_9	$FeCl_3.6H_2O$ (mg.L^{-1})	0.65	1.3	1.95
x_{10}	$MnCl_2.4H_2O$ (µg.L^{-1})	180	360	540
x_{11}	$NaHCO_3$ (mg.L^{-1})	170	652	1134
x_{12}	$ZnCl_2$ (µg.L^{-1})	10.25	21	31.75
x_{13}	$CoCl_2.6H_2O$ (µg.L^{-1})	10	20	30
x_{14}	$(NH_4)_6Mo_7O_{24}.4H_2O$ (µg.L^{-1})	4.5	9	13.5
x_{15}	$CuSO_4.5H_2O$ (µg.L^{-1})	10	20	30
x_{16}	Thiamin (µg.L^{-1})	50	100	150
x_{17}	Cyanocobalamin (µg.L^{-1})	2.5	5	7.5

Microalgal growth was monitored by optical density (750 nm) every 2 days, being this value subsequently converted to ash-free dry weight (AFDW) using the following calibration curve: $\mathrm{AFDW(g.L^{-1})} = 0.8991 \times \mathrm{OD_{750}} + 0.0054$, $R^2 = 0.99$. The pH was monitored and maintained to 8.0 ± 0.5 (Hanna HI 2210, Padova, Italy) by continuous injection of CO_2 (6 mL.min^{-1}). The experiments were stopped once the stationary growth phase was attained and the cultures were centrifuged at 4000 rpm for 20 min (Centurion Pro-Analytical CR7000, Chichester, United Kingdom). The pellets were recovered and stored at -20 °C, and further at -80 °C for lyophilization.

4.2.3 Validation test

The calculated effects and corresponding statistical significance of the PB design enabled the identification of the most relevant growth conditions for each carotenoid assessed and the sum of all carotenoids (mg.g^{-1}) in *P. gyrans*. That information was used to define tailored growth conditions for the carotenoid of interest, in which the carotenoids' yields were evaluated and validated in two different sets

of experiments (V1 and V2). The full composition of the growth conditions used in both sets of experiments is described in Table 4-3. The first set (V1) aimed at validating the optimum conditions defined in PB design for the dependent variables Fx, TCar, and βCar, against the control conditions (Con - Walne's medium). For practical reasons, the variables inoculum size (x_1), light intensity (x_3), and air flow (x_4) in the control assay were the same of the remaining experiments. The non-significant abiotic factors ($p > 0.10$) for Fx, βCar and TCar were set at Level -1.

Table 4-2: coded values of each independent variable used in the twenty-eight experiments, #E, performed in the Plackett-Burman design

	Independent variable (*x*)																
#E	1	2	3	4	5	6	7	8	9	10	11	12	13	14	15	16	17
1	1	-1	-1	-1	-1	1	-1	1	-1	-1	1	1	-1	-1	1	1	-1
2	1	1	-1	-1	-1	-1	1	-1	1	-1	-1	1	1	-1	-1	1	1
3	1	1	1	-1	-1	-1	-1	1	-1	1	-1	-1	1	1	-1	-1	1
4	1	1	1	1	-1	-1	-1	-1	1	-1	1	-1	-1	1	1	-1	-1
5	1	1	1	1	1	-1	-1	-1	-1	1	-1	1	-1	-1	1	1	-1
6	-1	1	1	1	1	1	-1	-1	-1	-1	1	-1	1	-1	-1	1	1
7	1	-1	1	1	1	1	1	-1	-1	-1	-1	1	-1	1	-1	-1	1
8	-1	1	-1	1	1	1	1	1	-1	-1	-1	-1	1	-1	1	-1	-1
9	1	-1	1	-1	1	1	1	1	1	-1	-1	-1	-1	1	-1	1	-1
10	1	1	-1	1	-1	1	1	1	1	1	-1	-1	-1	-1	1	-1	1
11	-1	1	1	-1	1	-1	1	1	1	1	1	-1	-1	-1	-1	1	-1
12	-1	-1	1	1	-1	1	-1	1	1	1	1	1	-1	-1	-1	-1	1
13	1	-1	-1	1	1	-1	1	-1	1	1	1	1	1	-1	-1	-1	-1
14	1	1	-1	-1	1	1	-1	1	-1	1	1	1	1	1	-1	-1	-1
15	-1	1	1	-1	-1	1	1	-1	1	-1	1	1	1	1	1	-1	-1
16	-1	-1	1	1	-1	-1	1	1	-1	1	-1	1	1	1	1	1	-1
17	1	-1	-1	1	1	-1	-1	1	1	-1	1	-1	1	1	1	1	1
18	-1	1	-1	-1	1	1	-1	-1	1	1	-1	1	-1	1	1	1	1
19	1	-1	1	-1	-1	1	1	-1	-1	1	1	-1	1	-1	1	1	1
20	-1	1	-1	1	-1	-1	1	1	-1	-1	1	1	-1	1	-1	1	1
21	-1	-1	1	-1	1	-1	-1	1	1	-1	-1	1	1	-1	1	-1	1
22	-1	-1	-1	1	-1	1	-1	-1	1	1	-1	-1	1	1	-1	1	-1
23	-1	-1	-1	-1	1	-1	1	-1	-1	1	1	-1	-1	1	1	-1	1
24	-1	-1	-1	-1	-1	-1	-1	-1	-1	-1	-1	-1	-1	-1	-1	-1	-1
25	0	0	0	0	0	0	0	0	0	0	0	0	0	0	0	0	0
26	0	0	0	0	0	0	0	0	0	0	0	0	0	0	0	0	0
27	0	0	0	0	0	0	0	0	0	0	0	0	0	0	0	0	0
28	0	0	0	0	0	0	0	0	0	0	0	0	0	0	0	0	0

The second set of validation experiments (V2) was devised to understand if the variables identified as being the most significant in the PB design could trigger the accumulation of carotenoids in *P. gyrans* when cultured under the optimum growth conditions (Opt) for biomass production, as described in

CHAPTER 3. Briefly, Opt (Table 4-3) presents the optimal values for the abiotic factors: light intensity (x_3), $NaNO_3$ (x_5), $NaH_2PO_4.H_20$ (x_6), and $CuSO_4.5H_2O$ (x_{15}).

Regarding the non-significant independent variables identified in the PB matrix for biomass production, inoculum size (x_1), airflow (x_4), and $NaHCO_3$ concentration (x_{11}) were set at Level -1, while the remaining abiotic factors were set at Level 0. In addition to the assay Opt, that was used as control, this formulation was modified to promote the accumulation of all carotenoids (TCar), and fucoxanthin (Fx1ph and Fx2ph) Table 4-3. Regarding Fx, two different strategies were applied. In the assay Fx1ph, the whole growth of *P. gyrans* was performed under the same light intensity (150 µmol.photons.m^{-2}.s^{-1}).

Table 4-3: Levels of the abiotic factors used in the validation experiments. In V1, Walne's medium (control - Con) was compared to the maximized conditions for accumulation of fucoxanthin (Fx), β-carotene (βCar), and the sum of all carotenoids analyzed (TCar). The set V2 validated the maximized conditions for TCar and fucoxanthin accumulation using the optimized growth conditions for P. gyrans' biomass production (Opt). Two strategies for fucoxanthin production were evaluated: 150 µmol.photons.m^{-2}.s^{-1} during the entire growth (Fx1ph) and a two-phase growth (Fx2ph) using 700 µmol.photons.m^{-2}.s^{-1} in the first 8 days and 150 µmol.photons.m^{-2}.s^{-1} in the last 2 days (stationary phase). Bold numbers represent the most significant variables and their values according to the calculated effects in Plackett-Burman. Underlined numbers represent the optimum growth conditions achieved for the maximal biomass production of *P. gyrans*

	V1				**V2**			
	Con	**Fx**	**βCar**	**TCar**	**Opt**	**Fx1ph**	**Fx2ph**	**TCar**
Inoculum size (AFDW g.L^{-1})	0.1	0.1	0.1	0.1	0.1	0.1	0.1	0.1
Salinity (psu)	30	20	20	**20**	30	30	30	**20**
Light intensity (µmol.photons.m-2.s-1)	150	**150**	150	**150**	700	**150**	**700/ 150**	**150**
Air flow (mL.min^{-1})	600	600	600	600	600	600	600	600
$NaNO_3$ (mg.L^{-1})	100	**750**	**750**	**750**	1500	**1500**	**1500**	**1500**
$NaH_2PO_4.H_2O$ (mg.L^{-1})	20	10	10	10	40	40	40	40
$Na_2H_2EDTA.2H_2O$ (mg.L^{-1})	45	22.5	22.5	22.5	45	45	45	45
H_3BO_3 (mg.L^{-1})	33.6	16.8	16.8	16.8	33.6	33.6	33.6	33.6
$FeCl_3.6H_2O$ (mg.L^{-1})	1.3	0.65	**1.95**	**1.95**	1.3	1.3	1.3	**1.95**
$MnCl_2.4H_2O$ (µg.L^{-1})	360	180	180	180	360	360	360	360
$NaHCO_3$ (mg.L^{-1})	-	170	170	170	170	170	170	170
$ZnCl_2$ (µg.L^{-1})	21	10.25	10.25	10.25	21	21	21	21
$CoCl_2.6H_2O$ (µg.L^{-1})	20	10	10	**30**	20	20	20	**30**
$(NH_4)6Mo_7O_{24}.4H_2O$ (µg.L^{-1})	9	4.5	4.5	4.5	9	9	9	9
$CuSO_4.5H_2O$ (µg.L^{-1})	20	10	10	10	6	6	6	6
Thiamin (µg.L^{-1})	100	50	50	50	100	100	100	100
Cyanocobalamin (µg.L^{-1})	5	2.5	2.5	2.5	5	5	5	5

On the other hand, and according to the light intensity used, the growth in the Fx2ph experiment was divided into two phases. First, *P. gyrans* was grown at the optimal light intensity for biomass production (700 µmol.photons.m^{-2}.s^{-1}) until the end of the exponential growth phase; in the second phase, lasting 2 days, the light intensity was reduced to 150 µmol.photons.m^{-2}.s^{-1} to increase the Fx content of *P. gyrans*. Since $NaNO_3$ showed a positive effect on Fx and TCar, and the concentration defined in the maximized

growth conditions for biomass production was higher than those set in the PB design, the second validation experiments were supplemented with 1500 $mg.L^{-1}$ of $NaNO_3$. All experiments were performed in triplicate.

4.2.4 Biomass characterization

4.2.4.1 Pigment extraction, identification, and quantification by HPLC-DAD

Pigment analysis was conducted as described by Sanz et al. [49] with some modifications. Carotenoids were extracted from 10 mg of freeze-dried biomass in a screw cap glass tube with 3 mL of cold extraction solution (90 % acetone, 0.1 % BHT). Tubes were kept in ice and protected from light during all steps. Samples were left extracting for 15 min to allow acetone penetrating in microalgae structures, then they were vortexed for 30 s followed by 5 min in an ultrasonic bath. Extracts were centrifuged for 15 min at 2000 rpm (Hettich Mikro 120, Tuttlingen, Germany) and the supernatant was collected. The pellet was re-extracted until it was colorless. From the total extract, 1 mL was syringe filtered (0.22 µm nylon) to an amber vial, and received 0.3 mL of ultra-pure H_2O to avoid incompatibility of solvents in the HPLC-DAD [50].

The extracts were analyzed in a Shimadzu Nexera X2 system equipped with a 30AD liquid chromatograph, a SIL-30AC autosampler, a CTO-20AC column oven, a SPD-M20A diode array detector, and a CBM-20A Communication Bus Module. The pigments separation was performed through an ACE C18 PFP column 150 mm x 4.6 mm, 3 µm particle size (Advanced Chromatography Technologies, Aberdeen, Scotland) at 40 °C. The mobile phase was a mixture of methanol:225 mM ammonium acetate (82:18, v:v) as eluent A and ethanol as eluent B. The gradient followed the indications of Sanz et al. [49] with some modifications: 96%:4% eluent A:eluent B (0-16 min), 62%:38% eluent A:eluent B (16-22 min), 62%:38% eluent A:eluent B (22-28 min), 28%:72% eluent A:eluent B (28-35 min), 20%:80% eluent A:eluent B (35-45 min), 20%:80% eluent A:eluent B (45-50 min) and 96%:4% eluent A:eluent B (50-55 min). The flow rate was 1 $mL.min^{-1}$, the run duration 55 min, and the injection volume 20 µL. All reagents used in pigment extraction and chromatography analysis were HPLC grade. Identification of the extracted pigments was accomplished by comparison of the retention times and absorption spectra with commercial standards. Standards for chlorophyll *a*, chlorophyll c_1, chlorophyll c_2, fucoxanthin, all-*trans*-β-carotene, diadinoxanthin, and diatoxanthin were obtained from DHI (Hørsholm, Denmark). The identification of α-carotene (αCar) was done only by absorption spectra and retention time. All analysis were performed in triplicate.

4.2.4.2 Biomass and carotenoids productivity of P. gyrans

Volumetric productivity of the carotenoids (P_C) and the biomass (P_X) produced by *P. gyrans* was calculated using the following equations:

$$P_C(\mathrm{mg.L^{-1}.d^{-1}}) = \frac{C_i \times (X_{tf} - X_{t0})}{t_f}$$

$$P_X\ (\mathrm{g.L^{-1}.d^{-1}}) = \frac{X_{tf} - X_0}{t_t}$$

where C_i is the carotenoid content, mg.g^{-1}, and X is the ash-free dry weight, g.L^{-1}, of the sampling time, days, at the end (t_f) and the beginning (t_0) of *P. gyrans* growth.

4.2.5 Statistical analysis

The abiotic factors defined in the PB design as the most significant in the carotenoids production of *P. gyrans* were identified using a 90 % confidence level ($p < 0.10$), in order to avoid excluding any important independent variable. The statistical analysis was performed with the online software Protimiza Experimental Design (http://experimental-design.protimiza.com.br/). The validation tests were evaluated for differences between means using one-way ANOVA followed by Tukey's multiple comparison test at 95 % confidence level (GraphPad Prism version 8.0.2).

4.3 RESULTS AND DISCUSSION

4.3.1 Plackett-Burman design

As referred in CHAPTER 3, the biomass productivity of *P. gyrans* through the Plackett-Burman design ranged from 0.072 g.L^{-1}.d^{-1} (#24) to 0.256 g.L^{-1}.d^{-1} (#6). The statistical evaluation pointed out the significant effects ($p < 0.10$) of light intensity, sodium nitrate and copper in the growth performance of *P. gyrans*.

Regarding the pigments composition of *P. gyrans*, the chromatogram achieved during the preliminary tests (Figure 4-1), overall, allowed to confirm the pigment profile commonly described for this species and other Pavlovophyceae species [37,38,51]. Eight pigments were identified: three chlorophylls and five carotenoids. Despite the identification of chlorophylls *a*, c_1 and c_2, they were not quantified because the goal of this work was to study the ability of *P. gyrans* to accumulate carotenoid pigments, reason why statistics and discussion are focused on carotenoids. Among the carotenoids, it was possible to identify fucoxanthin (Fx), diadinoxanthin (Ddx), diatoxanthin (Dtx), β-carotene (βCar) and α-carotene (αCar),

which match to the carotenoid composition described in other strains of *P. gyrans* [51]. As stated by Lenning et al. and Bendif et al. [30,38] the pigment signatures are a valuable tool in the phylogenetic analysis. According to their pigment composition, the Pavlovophyceae species was grouped in three different clades, which share the same composition: chlorophyll *a, c*$_1$*, c*$_2$, Mg-divinyl protochlorophyllide, Fx, Ddx, Dtx and βCar. *P. gyrans* belongs to the strains with pigment type B, along with *P. pinguis* and P. granifera, which presented as distinguishable feature two unknown pigments: Unk-1 (Ddx-like carotenoid) and chl *c*$_{PAV}$ (divinyl form of chl *c*) [30,38] which were not quantified in the present study.

According to their role on microalgae, these pigments can be classified as primary pigments – if they are part of the light-harvesting complexes, located in thylakoid membranes, and are involved in light capture and photosynthetic activity [52] – or secondary pigments – those with a photoprotective role, whose production is triggered under stressful growth conditions. Among the pigments present in *P. gyrans,* chlorophylls *a*, *c*$_1$, and *c*$_2$, as well as Fx, have photosynthetic activity, while Ddx, Dtx, and βCar act as a photoprotective agents [43].

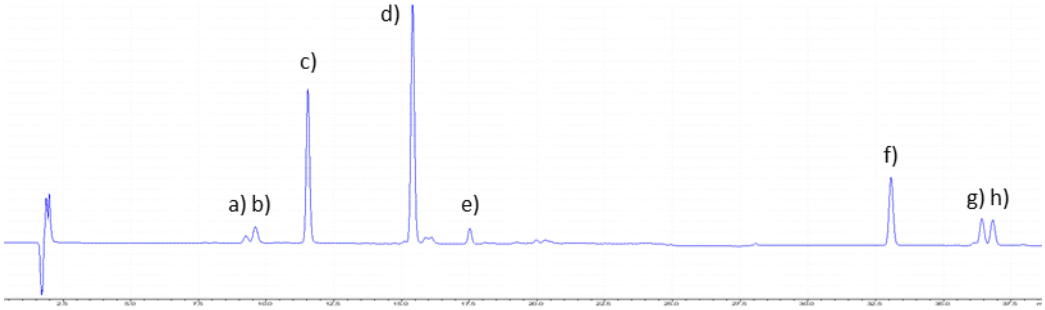

Figure 4-1: typical chromatogram of *P. gyrans* pigments: a) chlorophyll *c*$_2$ (RT: 9.02 min, λ_{max}: 447, 584, 633 nm); b) chlorophyll *c*$_1$ (RT: 9.35 min, λ_{max}: 441, 580, 633 nm); c) fucoxanthin (RT: 11.22 min, λ_{max}: 453 nm); d) diadinoxanthin (RT: 15.01 min, λ_{max}: 446, 475 nm); e) diatoxanthin (RT: 17.09 min, λ_{max}: 451, 479 nm); f) chlorophyll *a* (RT: 32.75 min, λ_{max}: 432, 618, 664 nm); g) α-carotene (RT: 35.97 min, λ_{max}: 448, 471 nm); h) β-carotene (RT: 36.45 min, λ_{max}: 452, 477 nm)

The influence of the twenty-eight abiotic factor combinations tested on the carotenoids' composition of *P. gyrans* is present in Table 4-4. Fx content ranged from 3.409 mg.g^{-1} DW in assay #13 to 0.401 mg.g^{-1} DW in assay #3. The extreme values for Ddx were obtained in the assays #13 and #3 with 1.068 and 0.113 mg.g^{-1} DW, respectively, whereas the Dtx content varied from 0.091 (#4) to 1.678 mg.g^{-1} DW (#17). Regarding the carotene production, the highest values of βCar and αCar were 0.491 (#11) and 0.545 mg.g^{-1} DW (#9) while the lowest were 0.151 (#27) and 0.114 mg.g^{-1} DW (#18). Finally, and summing all the carotenoids previously mentioned, the total carotenoids content ranged from 6.743 (#13) to 1.017 mg.g^{-1} DW (#4). The wide variation achieved for each carotenoid, as well as its total content, represents well the key role of the growth conditions and nutrient availability in microalgae metabolism, which in this case had as main outcome a diversified carotenoids' composition.

Data from Table 4-4 were used to calculate the effect of each independent variable (abiotic factor) on the accumulation of each carotenoid (dependent variable) using a statistical significance lower than 10% to identify the most significant independent factors (Table 4-5). Fx production by *P. gyrans* was promoted by decreasing light intensity ($p < 0.001$) and increasing $NaNO_3$ ($p = 0.006$), which means that these variables had a negative and positive effect on this carotenoid, respectively. These variables also had a similar impact on Ddx content, together with salinity, whose lower values increased the accumulation of Ddx ($p = 0.031$). Results showed that βCar was positively correlated with higher supplementation of $NaNO_3$ ($p = 0.046$) and $FeCl_3.6H_2O$ ($p = 0.062$), whereas for αCar none of the independent variables was statistically significant within the tested ranges ($p > 0.10$). Dtx was identified as the carotenoid with the highest number of significant variables (7), namely, $NaHCO_3$ ($p = 0.005$), $NaNO_3$ ($p = 0.015$), $CoCl_2.6H_2O$ ($p = 0.033$), and inoculum size ($p = 0.043$) had a calculated positive effect. On the other hand, the increase of light intensity ($p < 0.001$), salinity ($p = 0.007$), and $NaH_2PO_4.H_2O$ ($p = 0.028$) presented a negative impact in the production of Dtx. Concerning the sum of all carotenoids of *P. gyrans*, three abiotic factors with statistical importance were identified: light intensity ($p < 0.001$), $NaNO_3$ ($p = 0.001$), and $FeCl_3.6H_2O$ ($p = 0.038$). As already mentioned for individual carotenoids, nitrogen and copper concentrations in the medium were positively correlated with total carotenoids content, in contrast to the light intensity.

In order to avoid excluding any important variable, the nutrient $CoCl_2.6H_2O$ and the salinity level of the medium were also considered significant variables, given the closeness of their p-values ($p = 0.103 – 0.104$) to the statistical significance threshold adopted. Among the dependent variables assessed, only Fx, Dtx, and TCar presented a significant curvature ($p < 0.10$), meaning that the optimal value for these carotenoids was reached within the range of abiotic factors tested.

Overall, the abiotic factors here identified with a marked effect on the carotenoid composition of *P. gyrans* are in accordance with described in literature, and their effects are discussed below.

Table 4-4: carotenoids composition, $mg.g^{-1}$, of *P. gyrans* produced in the Plackett-Burman design

#E	Fucoxanthin	Diatoxanthin	Diadinoxanthin	β-carotene	α-carotene	Total carotenoids
1	1.670 ± 0.047	0.707 ± 0.014	0.427 ± 0.005	0.342 ± 0.005	0.413 ± 0.008	3.587 ± 0.052
2	1.942 ± 0.008	0.620 ± 0.002	0.341 ± 0.003	0.257 ± 0.002	0.265 ± 0.002	3.426 ± 0.018
3	0.401 ± 0.002	0.093 ± 0.000	0.113 ± 0.000	0.277 ± 0.001	0.242 ± 0.060	1.127 ± 0.003
4	0.444 ± 0.000	0.091 ± 0.000	0.113 ± 0.000	0.231 ± 0.002	0.137 ± 0.002	1.017 ± 0.004
5	0.933 ± 0.007	0.183 ± 0.002	0.184 ± 0.001	0.387 ± 0.001	0.421 ± 0.001	2.107 ± 0.011
6	1.417 ± 0.024	0.190 ± 0.001	0.282 ± 0.014	0.285 ± 0.015	0.342 ± 0.019	2.517 ± 0.023
7	0.570 ± 0.008	0.200 ± 0.001	0.194 ± 0.001	0.278 ± 0.013	0.193 ± 0.008	1.437 ± 0.023
8	2.161 ± 0.017	0.334 ± 0.003	0.554 ± 0.007	0.174 ± 0.009	0.245 ± 0.011	3.468 ± 0.045
9	0.765 ± 0.002	0.257 ± 0.001	0.410 ± 0.003	0.482 ± 0.003	0.545 ± 0.004	2.460 ± 0.013
10	1.118 ± 0.011	0.331 ± 0.006	0.207 ± 0.006	0.289 ± 0.007	0.338 ± 0.008	2.282 ± 0.035
11	0.846 ± 0.013	0.184 ± 0.003	0.167 ± 0.051	0.491 ± 0.009	0.461 ± 0.005	2.149 ± 0.027
12	0.482 ± 0.002	0.323 ± 0.001	0.247 ± 0.001	0.225 ± 0.008	0.194 ± 0.008	1.471 ± 0.016
13	3.409 ± 0.068	1.474 ± 0.017	1.068 ± 0.005	0.396 ± 0.002	0.395 ± 0.003	6.743 ± 0.078
14	1.896 ± 0.035	0.798 ± 0.009	0.393 ± 0.015	0.210 ± 0.007	0.221 ± 0.008	3.518 ± 0.022
15	0.469 ± 0.004	0.258 ± 0.003	0.183 ± 0.001	0.244 ± 0.004	0.230 ± 0.004	1.385 ± 0.014
16	0.421 ± 0.10	0.415 ± 0.011	0.237 ± 0.007	0.191 ± 0.002	0.191 ± 0.002	1.454 ± 0.023
17	3.290 ± 0.015	1.678 ± 0.008	0.991 ± 0.007	0.312 ± 0.003	0.286 ± 0.003	6.557 ± 0.036
18	3.351 ± 0.024	0.476 ± 0.003	0.767 ± 0.005	0.206 ± 0.003	0.114 ± 0.001	4.915 ± 0.036
19	0.467 ± 0.033	0.134 ± 0.010	0.154 ± 0.009	0.250 ± 0.020	0.173 ± 0.014	1.178 ± 0.086
20	1.850 ± 0.024	0.488 ± 0.007	0.375 ± 0.006	0.195 ± 0.005	0.213 ± 0.007	3.121 ± 0.044
21	0.799 ± 0.006	0.242 ± 0.002	0.322 ± 0.002	0.463 ± 0.004	0.642 ± 0.005	2.468± 0.013
22	1.651 ± 0.167	0.401 ± 0.049	0.600 ± 0.074	0.285 ± 0.046	0.352 ± 0.056	3.290 ± 0.363
23	1.599 ± 0.213	0.836 ± 0.127	0.526 ± 0.072	0.233 ± 0.041	0.322 ± 0.048	3.515 ± 0.499
24	1.656 ± 0.005	0.375 ± 0.001	0.526 ± 0.002	0.189 ± 0.002	0.228 ± 0.002	2.975 ± 0.007
25	0.837 ± 0.020	0.122 ± 0.002	0.443 ± 0.004	0.292 ± 0.001	0.332 ± 0.010	2.025 ± 0.025
26	0.762 ± 0.004	0.218 ± 0.001	0.326 ± 0.001	0.180 ± 0.012	0.207 ± 0.014	1.693 ± 0.019
27	0.695 ± 0.011	0.237 ± 0.004	0.278 ± 0.004	0.151 ± 0.008	0.182 ± 0.006	1.543 ± 0.032
28	0.957 ± 0.073	0.186 ± 0.016	0.182 ± 0.014	0.324 ± 0.045	0.387 ± 0.052	2.037 ± 0.200

4.3.1.1 Light intensity

Light plays a crucial role in photosynthetic organisms, providing the energy needed for the carbon fixation that will be metabolized for further biocompounds synthesis and cell growth. Microalgae present a variety of pigments whose intracellular concentrations vary according to external illumination to optimize the photosynthetic capacity. Chlorophylls and fucoxanthin maximize light harvesting in different environments/ranges of wavelengths, whereas the other carotenoids are protective agents when the light absorption exceeds the microalgae needs, avoiding photodamage and photoinhibition [53]. Similarly to the results here reported for *P. gyrans*, increasing light intensity in nitrogen-stressed cells of *D. lutheri* contributed to a sharp decrease (> 50 %) in total carotenoids content [43]. These authors argued that, at higher light intensities, the N-starvation condition triggered the accumulation of Ddx and Dtx, mainly at the expense of βCar. Similarly, *P. gyrans* grown under three different illumination levels (60, 110, 350 μmol photons m^{-2} s^{-1}) achieved the lowest fucoxanthin/chlorophyll *a* ratio and greater growth rates with increasing light intensity. Higher light intensity led to an overall decrease in pigment content, both in photosynthetic and photoprotective pigments [42]. The haptophyte *Tisochrysis lutea* and the diatoms *Phaeodactylum tricornutum* and *Odontella aurita* also improved their Fx content at lower irradiances [54,55]. As reported for the haptophyte *Emiliania huxleyi*, the photoacclimation process has as the main goal to optimize photosynthesis efficiency by changing the composition of the light harvesting complex (LHC). At low light intensity, this is reached by increasing the amounts of photosynthetic pigments and proteins LHCF [56]. LHC of *P. gyrans* is composed by a Fx-Chl *a*/*c*-protein complex [52], which explains the negative effect of the light intensity over the pigments composition here reported.

4.3.1.2 Nitrogen

Regarding the $NaNO_3$, a comparable trend was described for the Fx content of *Pavlova* OPMS 30543, whose value increased in culture medium supplemented with higher levels of nitrate [44]. Such trend was also stated in other microalgae genus like *Nitzschia* [57], *Phaeodactylum* [55] and *Odontella* [58]. Likewise, the total carotenoids content of *P. pinguis* had a substantial increase (58 times) when the nitrogen supplementation changed from 140 μmol.L^{-1} to 1752 μmol.L^{-1} $NaNO_3$ [46]. There is some structural resemblance between *P. gyrans* and *P. tricornutum*, specially regarding the light-harvesting complexes [52]. Longworth et al. [59] verified that nitrogen-stressed *P. tricornutum* cells showed a significant reduction in the photosynthetic pathway due to the lower abundance of enzymes responsible for carbon fixation, as well less presence of proteins and pigments in the photosynthetic apparatus.

Table 4-5: calculated effects for each carotenoid, mg.g^{-1}, of *P. gyrans* from the Plackett-Burman experimental design. Bold numbers represent the abiotic factors with p-values considered statistically significant ($p < 0.10$)

	Fucoxanthin		**Diatoxanthin**		**Diadinoxanthin**		**β-carotene**		**α-carotene**		**Total Carotenoids**	
	Effect	*p*-value	Effect	*p*-value	Effect	*p*-value	Effect	*p*-value	Effect	*p*-value	Effect	*p*-value
Mean	1.402	**0.000**	0.462	**0.000**	0.391	**0.000**	0.287	**0.000**	0.299	**0.000**	2.840	**0.000**
Curvature	-1.177	**0.052**	-0.543	**0.020**	-0.167	0.365	-0.101	0.291	-0.043	0.784	-2.032	**0.023**
Inoculum size	0.020	0.923	0.170	**0.043**	-0.016	0.816	0.044	0.226	0.008	0.894	0.226	0.441
Salinity	0.002	0.993	-0.250	**0.007**	-0.169	**0.031**	-0.033	0.352	-0.059	0.335	-0.509	**0.103**
Light intensity	-1.467	**0.000**	-0.496	**0.000**	-0.347	**0.001**	0.060	0.113	0.032	0.598	-2.219	**0.000**
Air flow	0.155	0.457	0.094	0.227	0.060	0.387	-0.033	0.357	-0.046	0.450	0.230	0.433
$NaNO_3$	0.703	**0.006**	0.218	**0.015**	0.195	**0.017**	0.079	**0.046**	0.101	0.114	1.295	**0.001**
$NaH_2PO_4.H_2O$	-0.128	0.534	-0.189	**0.028**	-0.045	0.511	-0.029	0.410	-0.037	0.538	-0.429	0.160
$Na_2H_2EDTA.2H_2O$	-0.200	0.341	-0.002	0.977	-0.046	0.508	0.006	0.871	-0.002	0.974	-0.244	0.406
H_3BO_3	-0.182	0.385	0.051	0.501	-0.041	0.550	0.034	0.341	0.068	0.267	-0.070	0.808
$FeCl_3.6H_2O$	0.291	0.177	0.132	0.102	0.121	0.101	0.072	**0.062**	0.063	0.304	0.680	**0.038**
$MnCl_2.4H_2O$	-0.041	0.842	0.017	0.816	-0.005	0.945	-0.001	0.977	-0.026	0.658	-0.056	0.846
$NaHCO_3$	0.175	0.402	0.269	**0.005**	0.039	0.569	-0.005	0.879	-0.032	0.590	0.446	0.146
$ZnCl_2$	0.167	0.422	0.107	0.175	0.008	0.908	-0.009	0.804	-0.015	0.800	0.258	0.381
$CoCl_2.6H_2O$	0.251	0.239	0.182	**0.033**	0.091	0.202	-0.017	0.629	0.001	0.992	0.508	**0.104**
$(NH_4)6Mo_7O_{24}.4H_2O$	-0.019	0.927	0.075	0.330	0.035	0.607	-0.050	0.173	-0.089	0.156	-0.048	0.868
$CuSO_4.5H_2O$	-0.011	0.956	0.023	0.753	-0.004	0.949	-0.021	0.558	-0.012	0.845	-0.025	0.931
Thiamin	0.302	0.163	0.031	0.674	0.041	0.553	0.039	0.275	0.033	0.586	0.446	0.146
Cyanocobalamin	0.078	0.703	0.011	0.883	-0.029	0.675	-0.029	0.410	-0.043	0.478	-0.012	0.967

The reason for that relies on its chemical composition, which possesses a high content of nitrogen. Therefore, to maximize the nitrogen availability for protein synthesis indispensable for cell subsistence, stressed cells down-regulate the photosynthetic pathway, causing a decrease in their pigments [59].

4.3.1.3 Salinity

Some research has been conducted to explore the effect of salinity level on the carotenoid production in microalgae. Under salinity stress, microalgae tend to increase the intracellular composition of the signaling molecules, such as calcium and reactive oxygen species (ROS) [60]. By reacting with macromolecules (*e.g.*, DNA, proteins), ROS can severely impair the cell metabolism or even lead to death. In order to counteract ROS action, the cell activates antioxidant defense mechanisms, which may involve increased production of antioxidant compounds, such as the enzymes superoxide dismutase and catalase, carotenoids, or γ-aminobutyric acid (a non-protein amino acid regulated by cytoplasmic Ca^{2+} concentration) [60,61]. Overall, salinity stress has been especially highlighted as a key factor responsible for causing the accumulation of carotenoids in several microalgae from the genus *Dunaliella* [62–64], *Chlorella* [65], *Desmodemus* [66], and *Haematococcus* [60]. For instance, *Dunaliella tertiolecta* grown under extreme salinities (3 M) was shown to have a marked increase – at cellular basis – of βCar, although the negative impact in the microalgae growth performance [62]. *Desmodesmus* sp. also presented a total carotenoid content 2.7-fold higher when subjected to salt stress conditions [66].

However, the TCar of *P. gyrans* (Table 4-5) had a negative impact promoted by salinity. Despite the different salinity range tested, the Fx content of marine species *Tisochrysis lutea* and *P. tricornutum* also presented a significant drop when grown with increasing salinities beyond the optimal level (35-45 ‰) [67]. The authors also discussed that, although the suboptimal salinity levels tested led to stressful conditions for the photosynthetic apparatus of the cells, the impact on photosynthetic pigment production (*e.g.*, fucoxanthin) remains unclear. Similarly, the carotenoids and chlorophyll *a* content of *Nannochloropsis oculata* increased with the salinity reduction from 35 to 25 $g.L^{-1}$ during growth [68]. This particular evidence points out the species-dependent behavior of each microalga for the same abiotic factor.

4.3.1.4 Iron

Iron is an important micronutrient for several cellular processes, such as DNA synthesis, respiration, and photosynthesis. It is a crucial cofactor for enzymatically mediated processes, which allow the physiological and chemical balance (*e.g.*, redox reactions, nitrogen assimilation, uptake mechanisms), as well as a key nutrient for chlorophyll synthesis and chloroplasts stability [69]. The deficient supply of iron in

Chlamydomonas reinhardtii induced the remodeling of LHCI, by processing and up- or down regulation of its pigment-binding proteins, with a concomitant decrease of excitation energy efficiency to the photosystem I [70]. In addition, iron also regulates the catalase and peroxidase enzymes, which play an important role in the antioxidant mechanism against ROS [70,71]. In this work, the increasing concentrations of iron within the range tested showed a positive effect on carotenoids accumulation of *P. gyrans*. Kosakowska et al. [72] reported a similar trend in *P. tricornutum*, whose cells were grown in a range of 0.001 to 10 μmol.L^{-1} Fe^{3+}, with higher concentrations promoting the highest contents of chlorophyll *a*, c_1 + c_2, Fx, Ddx, and βcarotene. The authors also noticed that the iron-deficient cells presented a marked decrease of its βCar, a conclusion that is in line with *P. gyrans* considering the relevance (p = 0.062) achieved for $FeCl_3.6H_2O$ (Table 4-5)**.**

4.3.1.5 Cobalt

Cobalt is an important micronutrient for microalgae, mainly due to its role as structural molecule involved in the synthesis of the important cofactor cobalamin, which in turn influences the enzymatic processes responsible for nitrogen fixation [73]. However, when supplied at higher concentrations, this heavy metal can be harmful for microalgae as consequence of the increasing oxidative stress [74], a phenomenon always described as species-dependent. In the present work, cobalt had a positive impact on TCar, Dtx, and αCar content of *P. gyrans.* Indeed, the increasing accumulation of protective carotenoids (*e.g.*, Dtx) under higher cobalt concentrations might be seen as the response of *P. gyrans* against the likely production of ROS during electron acceptor-donor interactions of cobalt [75]. The supplementation of cobalt at low levels proved to be successful for microalgae growth and carotenogenesis in *Spirulina platensis* [76]*, Monoraphidium minutum*, and *Nitzchia perminuta* [77]*.* Although the decreasing content in both classes of pigments, the authors also highlighted the superior stability of carotenoids at higher cobalt levels, in contrast to chlorophyll [77]. For practical reasons, only three responses (those allowing to maximise Fx, βCar, and TCar) were considered in the validation assays. The aim was to confirm the high potential of *P. gyrans* as a carotenoid producer, in particular of the commercially important and demanded βCar and, mostly, Fx. Considering the interconnected and dependent production of Dtx and Ddx (xanthophyll cycle), the individual validation of these carotenoids was passed over in favor of TCar.

4.3.2 Validation tests

4.3.2.1 Growth analysis

The culture conditions applied in the validation assays are presented in Table 4-3. The growth performance of *P. gyrans* under the validation conditions of set V1 is presented in Figure 4-2. Despite the

decreasing concentration in ten nutrients, *P. gyrans* grown in the assay Fx, βCar, and TCar had longer growth and higher X_{max} values when compared to the control medium (Con), as shown in Table 4-6.

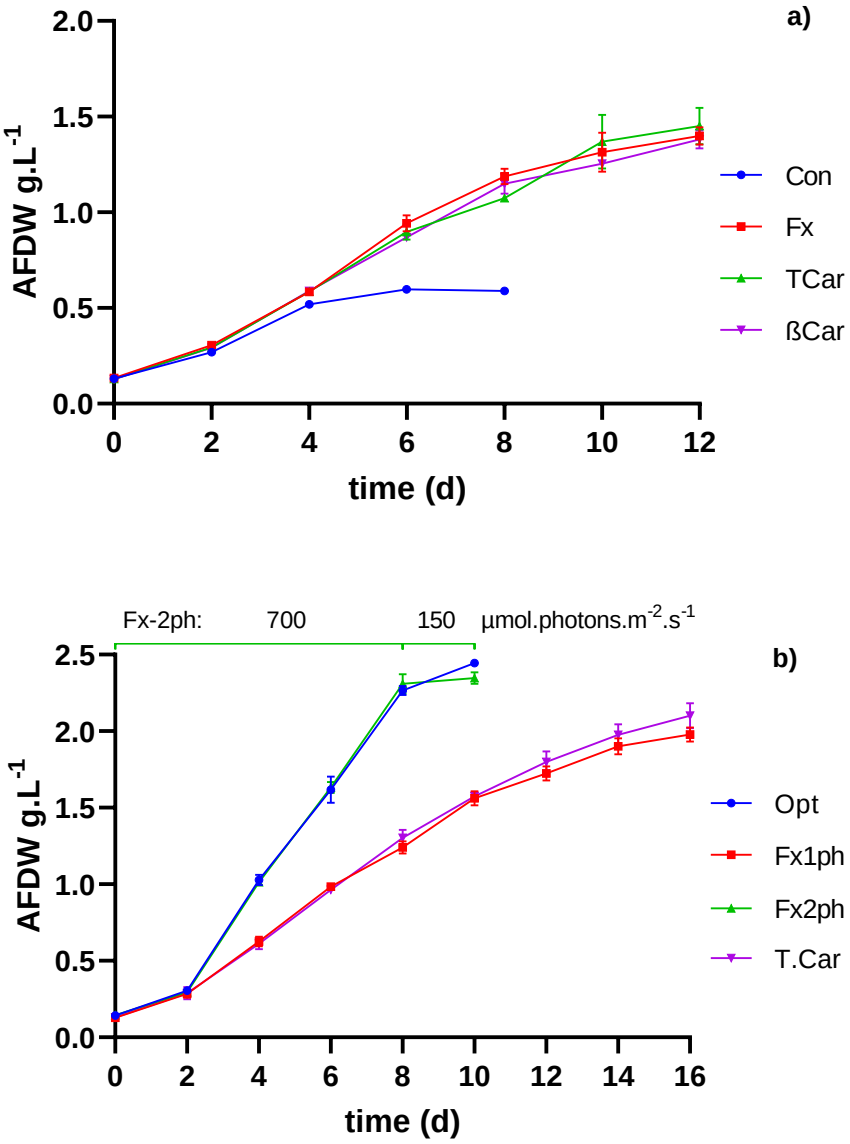

Figure 4-2: Growth profile of *P. gyrans* cultivated with the modified medium for the validation experiments V1 (a): Walne's medium (Con) and the maximized conditions for accumulation of fucoxanthin (Fx), β-carotene (βCar), and the sum of all carotenoids analyzed (TCar). In V2 (b) was assessed the optimized growth conditions for P. gyrans' biomass production (Opt) and the maximized growth conditions for TCar and fucoxanthin: 150 µmol.photons.m^{-2}.s^{-1} during the entire growth (Fx1ph) or using 700 µmol.photons.m^{-2}.s^{-1} in the first 8 days and 150 µmol.photons.m^{-2}.s^{-1} in the last 2 days (Fx2ph). The experiments were performed in triplicate and the error bars represent the mean values and standard deviation

Among the same seventeen abiotic factors, nitrogen supplementation, along with light intensity and copper, were identified in CHAPTER 3 as the most important factors in biomass production of *P. gyrans*. As the Fx, βCar, and TCar maximization assays share the same levels of $NaNO_3$ (7.5 times higher than Con) and copper (2 times lower than Con), the ≈2-fold increase in final X_{max} and P_x may be explained by the variation in these growth conditions.

Regarding the validation set V2, it was verified that *P. gyrans* grown in the assay Opt.V2 and Fx2ph.V2 showed significantly higher X_{max} and P_x compared to the experiments Fx1ph.V2 and TCar.V2 (Table 4-6). The improved biomass production in Opt.V2 and Fx2ph.V2 may be related to the higher illumination, which was used during the whole growth and until the end of the exponential growth phase, respectively. In fact, light intensity stood out as the most significant variable in CHAPTER 3 aimed at optimizing biomass production of *P. gyrans*, in which its optimal value was defined as 700 μmol.photons.m^{-2}.s^{-1}, the same used in Opt.V2 and Fx2ph.V2. As shown in Figure 4-2, increasing the light intensity from 150 to 700 μmol.photons. m^{-2}.s^{-1} was responsible for shortening by 6 days the growth of P. gyrans, which almost doubled its volumetric productivity (Table 4-6). Several works have described the increase in the growth performance with light intensity [42,78]. Light is an important factor for photosynthetic microorganisms, being responsible for the supply of energy that will be fixed and converted to chemical energy, which will fuel the metabolism and microalgae growth [79].

4.3.2.2 Carotenoids composition

Carotenoids composition of *P. gyrans* produced in the validation experiments is described in Figure 4-3. Although the growth conditions tested were primarily aimed at maximizing Fx, βCar, and TCar content, the results obtained for Dtx, Ddx, and αCar were also presented in all experiments.

Regarding the Fx content, in validation set V1 it was seen that Con.V1 produced 2.010 mg.g^{-1} DW, nearly half of the concentration achieved in the remaining experiments (Fx.V1, TCar.V1, and βCar.V1). The Fx values between Fx.V1, TCar.V1, and βCar.V1 were similar ($p > 0.05$), which can be justified by using the same level of the most significant variables for this carotenoid (light intensity and $NaNO_3$).

Similarly, in validation set V2, the control experiment (Opt) presented the lowest level of Fx, with 2.154 mg.g^{-1} DW ($p < 0.05$). The two approaches carried out to improve Fx accumulation in *P. gyrans* were succeeded, with Fx2ph.V2 and Fx1ph.V2 reaching 3.294 and 4.879 mg.g^{-1} DW, respectively. Although the Fx content produced was lower than that achieved in the assays performed strictly at low light intensity, the approach tested on Fx2ph.V2 promoted a 1.5-fold increase in Fx concentration compared to Opt, without compromising biomass production (Figure 4-2 and Table 4-6). In opposition to V1, *P. gyrans* grown under TCar.V2 conditions promoted the highest Fx content ($p < 0.05$), whose value reached 6.153 mg.g^{-1} DW. Such increase might be explained by a richer nutrient composition in V2, among which the notable increase in the $NaNO_3$ level (1500 vs 750 mg.L^{-1}) stands out.

Table 4-6: Average of three independent experiments, represented as mean ± standard deviation, of the maximum biomass produced, *Xmax*, and volumetric biomass productivity, *Px*, of *P. gyrans* grown in the validation experiments from the sets V1 and V2. In V1, Walne's medium (Con) was compared to the maximized conditions for accumulation of fucoxanthin (Fx), β-carotene (βCar), and the sum of all carotenoids analyzed (TCar). In V2 the maximized conditions for TCar and fucoxanthin - 150 µmol.photons.m^{-2}.s^{-1} during the entire growth (Fx1ph) or using 700 µmol.photons. m^{-2}.s^{-1} in the first 8 days and 150 µmol.photons. m^{-2}.s^{-1} in the last 2 days (Fx2ph) - were compared with the optimized growth conditions for *P. gyrans'* biomass production (Opt). Values with different superscript letters are significantly different ($p < 0.05$)

	X_{max} (g AFDW.L^{-1})	P_X (g AFDW.L^{-1}.d^{-1})
Con.V1	0.590 ± 0.010^{a}	0.057 ± 0.001^{a}
Fx.V1	1.400 ± 0.046^{b}	0.106 ± 0.003^{b}
βCar.V1	1.451 ± 0.096^{b}	0.110 ± 0.008^{b}
TCar.V1	1.380 ± 0.048^{b}	0.104 ± 0.004^{b}
Opt.V2	2.445 ± 0.010^{A}	0.230 ± 0.002^{A}
Fx1ph.V2	1.979 ± 0.048^{B}	0.132 ± 0.004^{B}
Fx2ph.V2	2.347 ± 0.037^{A}	0.220 ± 0.004^{A}
TCar.V2	2.102 ± 0.081^{B}	0.123 ± 0.006^{B}

Ddx presented a similar trend to that of Fx. In V1 set, all the conditions tested yielded higher Ddx contents than the control conditions ($p < 0.05$), which values ranged from 1.273 to 3.368 mg.g^{-1} DW. In the V2 set, Opt showed, once again, the lowest content of Ddx (1.938 mg.g^{-1} DW), with a significant increase in the accumulation of this carotenoid occurring as light intensity decreased, reaching its maximum in TCar.V2 (4.573 mg.g-1 DW). With respect to Dtx, the conditions tested in V1 showed no significant differences, with the highest content produced by *P. gyrans* found in Fx.V1 (1.448 mg.g^{-1} DW) and the lowest achieved in βCar (0.758 mg.g^{-1} DW).

Interestingly, the Dtx profile had the opposite trend of the Ddx in V2 set. Dtx values ranged from 0.139 to 0.763 mg.g^{-1} DW, with the highest value being reached under high illumination (Opt.V2) and considered significantly higher than the remaining assays ($p < 0.05$). The relationship between these xantophylls is a well-known process (diadinoxanthin cycle) widely described in several haptophytes and diatoms, that is triggered against the oxidative stress promoted by high light conditions. Through enzyme-mediated processes, microalgae produce Dtx by de-epoxidation of Ddx at high irradiances; conversely, epoxidation of Dtx to Ddx occurs at low light intensities [75]. Due to its higher number of the conjugated double bonds [80], Dtx proved increased performance in scavenging of free radicals and quenching of chlorophyll triple states, protecting and stabilizing the thylakoid membranes under high irradiances and temperatures [12,75].

Among the carotenoids optimized, βCar had the lowest content. There were no significant differences between Con.V1, TCar.V1, and the theorical optimal conditions (βCar.V1) with their contents ranging between 0.455 and 0.629 mg.g^{-1} DW. Fx.V1 produced the lowest value of βCar ($p < 0.05$). Considering

that $FeCl_3.6H_2O$ was identified in the PB design as a key factor for the production of βCar by *P. gyrans*, its concentration may explain the low content of this carotenoid in Fx.V1.

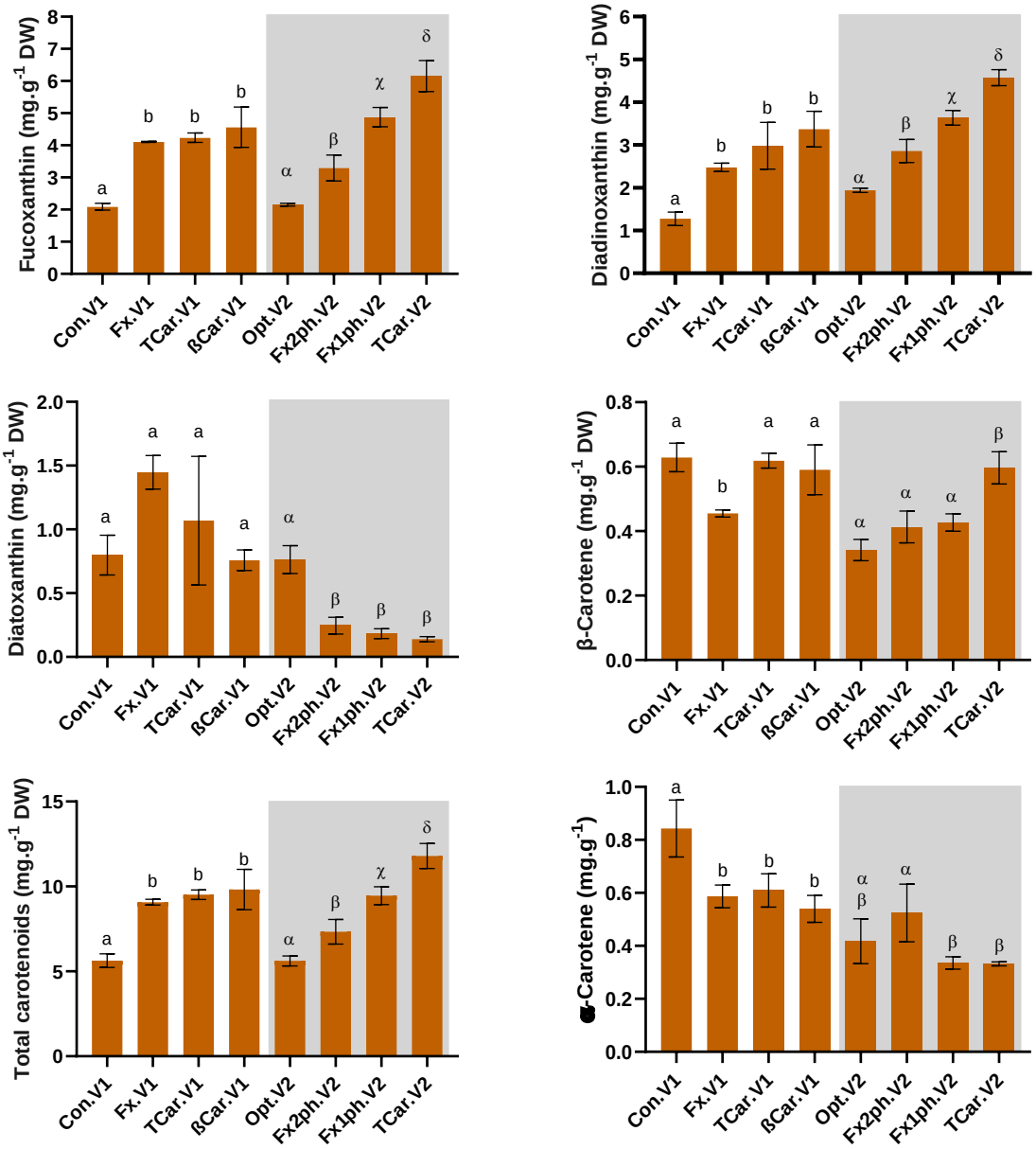

Figure 4-3: carotenoids composition, $mg.g^{-1}$, of *P. gyrans* cultured in validation experiments (V1 and V2). In V1, was evaluated the Walne's medium (Con) and the maximized conditions for accumulation of fucoxanthin (Fx), β-carotene (βCar), and the sum of all carotenoids analyzed (TCar). In V2 (b) was assessed the optimized growth conditions for *P. gyrans'* biomass production (Opt) and the maximized growth conditions for TCar and fucoxanthin: 150 µmol.photons. $m^{-2}.s^{-1}$ during the entire growth (Fx1ph) or using 700 µmol.photons. $m^{-2}.s^{-1}$ in the first 8 days and 150 µmol.photons. $m^{-2}.s^{-1}$ in the last 2 days (Fx2ph). The assays were performed in triplicate, with the bars representing the mean values and the standard deviation. Bars over the grey background represent the values produced by the validation test 2 (V2). Means with different letters within each data set (V1 or V2) are significantly different ($p < 0.05$)

As displayed in Table 4-3, this assay was the only one that showed limited iron concentrations, thus validating the importance of the statistical approach conducted in this work. This observation is also corroborated by the results of V2. Although *P. gyrans* was not tested with culture conditions to increase

the accumulation of βCar, like the βCar.V1, the only assay with a significant increase in this carotenoid was TCar.V2 (0.596 $mg.g^{-1}$ DW), which was also the only assay with a higher iron supplementation (1.95 $mg.L^{-1}$). Regarding the αCar, its value ranged between 0.540-0.843 and 0.322-0.524 $mg.g^{-1}$ DW in the V1 and V2 experiments, respectively.

Considering that the most prominent carotenoids in *P. gyrans* were Fx and Ddx, these carotenoids strongly influenced the TCar content. In fact, TCar content among the assays matched the profile already described for Fx and Ddx. In the set V1, Con produced the lowest content ($p < 0.05$) of total carotenoids, 5.633 $mg.g^{-1}$ DW, whereas in Fx.V1, TCar.V1, and βCar.V1 the range was 9.070-9.820 $mg.g^{-1}$ DW. On the other hand, all the experiments of the set V2 presented significant differences among them ($p < 0.05$). Considering the carotenoids content, whose value ranged from 5.614 to 11.794 $mg.g^{-1}$ DW, the validation experiments can be ranked as TCar.V2 > Fx1ph.V2 > Fx2ph.V2 > Opt.V2. Indeed, the results reported here for TCar validate the findings produced with the statistical approach adopted. In both V1 and V2, the manipulation of the main abiotic factors according to PB (salinity, light intensity, $NaNO_3$, $FeCl_3.6H_2O$, and $CoCl_2.6H_2O$) proved successful, allowing a 1.7- and 2.1-fold increase in the final composition of *P. gyrans*, respectively.

Taking into consideration the assay with the highest yield in carotenoids (TCar.V2), the statistical approach here adopted led to a modified medium with improved production of Fx (6.153 $mg.g^{-1}$ DW) and TCar (11.794 $mg.g^{-1}$ DW). *P. gyrans* grown under those conditions showed a higher content of carotenoids compared to *D. lutheri* (5–6 $mg.g^{-1}$ AFDW) [43] and *P. pinguis* (4.32-2.91 $mg.g^{-1}$ DW) [45,46]. On the other hand, the Fx content of *Pavlova* sp. OPMS 30543, grown under optimized growth conditions, reached 12.88 $mg.g^{-1}$ DW at lab-scale, which rose to 20.86 $mg.g^{-1}$ DW when grown at outdoor conditions [44]. Beyond the Pavlovophyceae, other species are well-known producers of carotenoids, especially Fx. Depending on the cultivation features, the Fx content described for the haptophyte *Tisochrysis lutea* was 5.51–10.73 $mg.g^{-1}$ [54]. The diatoms *Phaeodactylum tricornutum* [55], *Odontella* autira [58] and *Nitzschia sp.* [57] were also highlighted as highly productive species, whose Fx content achieved was 42.8, 18.47, 18.18 $mg.g^{-1}$, respectively.

4.3.2.3 Carotenoids productivity

In order to complement the analysis of Section 4.3.2.2, the data from growth performance (Figure 4-2) and the respective carotenoids content (Figure 4-3) were used to calculate carotenoids productivity ($mg.L^{-1}.d^{-1}$) of *P. gyrans* in the validation experiments Figure 4-4. In general, the values obtained for Con.V1 are in line with the previously described in Section 4.3.2.2. The low biomass production, together with the

low content of carotenoids - especially Fx, Ddx, and TCar - made the respective productivity values significantly lower than in the other assays, as presented in Figure 4-4a). Furthermore, the different values of βCar productivity compared between Con.V1 and βCar.V1 should be pointed out. Although βCar.V1 showed a 4-day increase in growth duration, as well as lower βCar content, this assay achieved higher productivity than Con.V1. This improvement was due to the higher X_{max} achieved, which almost doubled in comparison with Con.V1 (Table 4-6). Thus, although βCar.V1 failed to increase βCar content (Figure 4-3), these growth conditions proved advantageous for enhancing its productivity.

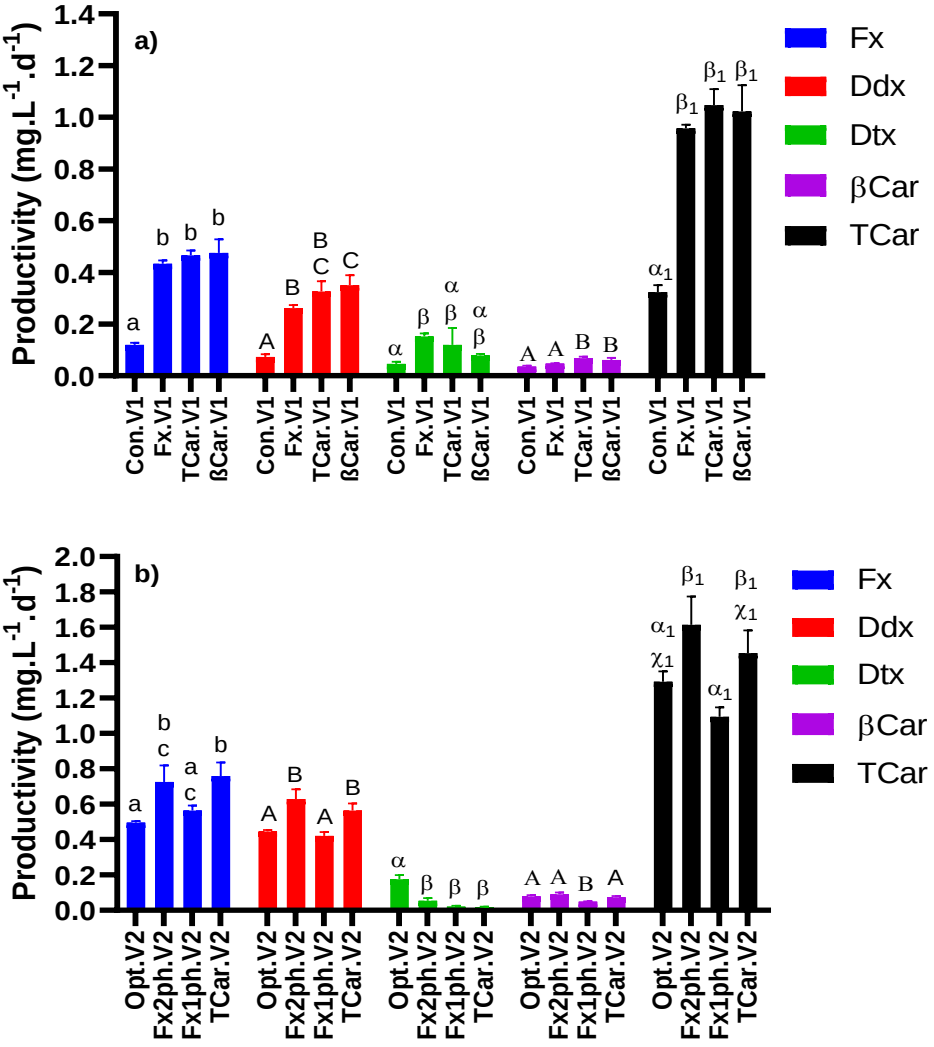

Figure 4-4: volumetric productivities of the carotenoids (fucoxanthin, Fx; diadinoxanthin, Ddx; diatoxanthin, Dtx; β-carotene, βCar; total carotenoids, TCar), mg.L-1.d-1, of P. gyrans grown in validation conditions V1 (a) and V2 (b). In V1, was evaluated the Walne's medium (Con) and the maximized conditions for accumulation of fucoxanthin (Fx), β-carotene (βCar), and the sum of all carotenoids analyzed (TCar). In V2 (b) was assessed the optimized growth conditions for P. gyrans' biomass production (Opt) and the maximized growth conditions for TCar and fucoxanthin: 150 µmol.photons. $m^{-2}.s^{-1}$ during the entire growth (Fx1ph) or using 700 µmol.photons. $m^{-2}.s^{-1}$ in the first 8 days and 150 µmol.photons. $m^{-2}.s^{-1}$ in the last 2 days (Fx2ph). Bars with different superscript letters are significantly different ($p < 0.05$)

In the set V2, it was found that TCar.V2 and Fx2ph.V2 stood out as the most productive conditions for Fx (0.726-0.759 mg.L^{-1}.d^{-1}), Ddx (0.564-0.629 mg.L^{-1}.d^{-1}), and TCar (1.454-1.615 mg.L^{-1}.d^{-1}). The management of light intensity (Fx2ph.V2) throughout *P. gyrans* growth resulted in important gains in productivity for Fx and TCar, ranking the Fx2ph.V2 as the second and first most productive assay, respectively. Thus, the reduction from 700 to 150 µmol photons m^{-2} s^{-1} in the last 2 days of growth can be seen as an interesting strategy for the maximization of *P. gyrans'* biomass production, along with higher productivity for the biologically important carotenoids.

These findings are corroborated by the normalized productivities to the standard growth conditions (Con.V1), presented in Figure 4-5. Except for the data of Dtx from Fx1ph.V2 and TCar.V2 assays, all conditions tested promoted substantial gains in carotenoids productivities (Pt/Pc > 1). However, the experiments whose growth conditions are a combination of the optimum abiotic factors for both biomass production and Fx and TCar synthesis (TCar.V2 and Fx2ph.V2) must be highlighted. The productivity was strongly improved with respect to Fx (6.0-6.3-fold), Ddx (7.8-8.6-fold), and TCar (4.5-5.0-fold) content in both experiments compared to control.

As shown for *P. gyrans*, the productivity value is highly dependent on the growth conditions, as well as the microalgae species under analysis. Looking at the pigment fucoxanthin, its maximum productivity value achieved with *P. gyrans* (0.759 mg.L^{-1}.d^{-1}) is within the range described for other species that were studied as a fucoxanthin source, such as *Chaetoceros muelleri* (0.072 mg.L^{-1}.d^{-1}) [67], *P. tricornutum* (0.041 - 2.3 mg.L^{-1}.d^{-1}) [55,67], but on the other hand, it falls short of the productivity described for *Nitzschia* sp. (1.44 mg.L^{-1}.d^{-1}) [57] and *Tisochrysis lutea* (4.71 mg.L^{-1}.d^{-1}) [54].

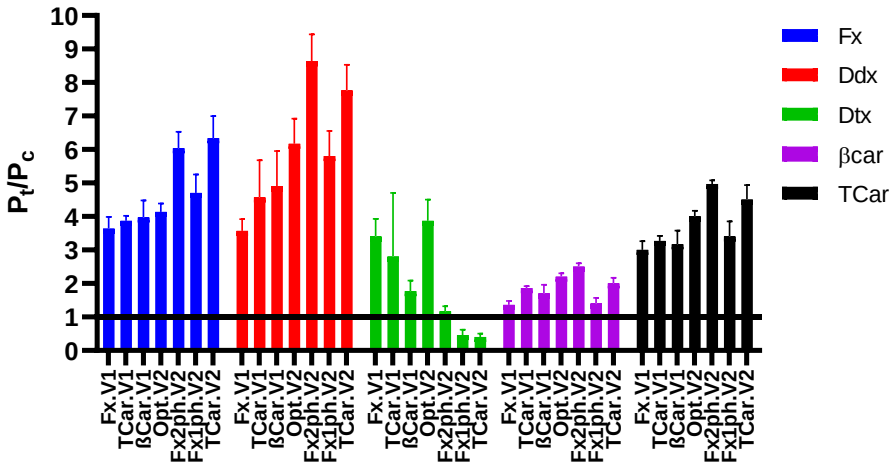

Figure 4-5: normalized values of the volumetric productivities of carotenoids (fucoxanthin, Fx; diadinoxanthin, Ddx; diatoxanthin, Dtx; β-carotene, βcar; total carotenoids, TCar) for the modified media formulated in V1 and V2 *(Pt)* against the control condition Con.V1 (*Pc*). Pt/Pc =1. In V1, was evaluated the Walne's medium (Con) and the maximized conditions for accumulation of fucoxanthin (Fx), β-carotene (βCar), and the sum of all carotenoids analyzed (TCar). In V2 (b) was assessed the optimized growth conditions for *P. gyrans'* biomass production (Opt) and the maximized growth conditions for TCar and fucoxanthin: 150 µmol.photons.m^{-2}.s^{-1} during the entire growth (Fx1ph) or using 700 µmol.photons. m^{-2}.s^{-1} in the first 8 days and 150 µmol.photons. m^{-2}.s^{-1} in the last 2 days (Fx2ph)

4.4 CONCLUSIONS

In this work, a multivariate approach was implemented to identify, among seventeen abiotic factors, those with a significant effect on carotenoids' composition of *P. gyrans* ($p < 0.10$). The pigments profile was composed of three chlorophylls (*a, c_1 and c_2*) and five carotenoids (fucoxanthin (Fx), diadinoxanthin (Ddx), diatoxanthin (Dtx), β-carotene (βCar), and α-carotene (αCar)). The study focused on the key abiotic factors related to the maximization of Fx, βCar, and the total carotenoids (TCar). Fx content of *P. gyrans* was mainly affected by the light intensity and $NaNO_3$ concentration, whereas TCar content was influenced by light intensity, $NaNO_3$, salinity, cobalt, and iron ($p < 0.10$). The manipulation of the key abiotic factors proved successful due to the generalized increase in Fx and TCar. The highest Fx (6.153 $mg.g^{-1}$ DW) and TCar (11.794 $mg.g^{-1}$ DW) contents were achieved in the same experiment, in which the key variables were set to increase the total carotenoids content. This work represents the first study involving a full optimization of *P. gyrans* growth conditions with the aim of improving its carotenoids composition. The results obtained confirm that *P. gyrans* is a promising source of fucoxanthin and other carotenoids for further industrial production.

4.5 REFERENCES

1. Frank HA, Cogdell RJ. Light capture in photosynthesis. Comprehensive Biophysics. Elsevier Inc.; 2012. p. 94–114.

2. Yabuzaki J. Carotenoids Database: Structures, chemical fingerprints and distribution among organisms. Database. Oxford University Press; 2017;2017.

3. Lafarga T, Clemente I, Garcia-Vaquero M. Carotenoids from microalgae. Carotenoids: Properties, Processing and Applications. Elsevier; 2020. p. 149–87.

4. Bogacz-Radomska L, Harasym J. β-Carotene-properties and production methods. Food Quality and Safety. Oxford University Press; 2018. p. 69–74.

5. Eggersdorfer M, Wyss A. Carotenoids in human nutrition and health. Arch Biochem Biophys. Academic Press Inc.; 2018. p. 18–26.

6. Mathews-Roth MM, Wilson T, Fujimori E, Krinsky NI. Carotenoid chromophore length and protection against photosensitization. Photochem Photobiol. Pergamon Press; 1974;19:217–22.

7. Hirayama O, Nakamura K, Hamada S, Kobayasi Y. Singlet Oxygen Quenching Ability of Naturally Occurring Carotenoids. 1994.

8. BCC Research. Carotenoids Market Size, Share & Growth Analysis Report. 2022.

9. Aruldass CA, Dufossé L, Ahmad WA. Current perspective of yellowish-orange pigments from microorganisms- a review. J Clean Prod. Elsevier Ltd; 2018. p. 168–82.

10. Capelli B, Bagchi D, Cysewski GR. Synthetic astaxanthin is significantly inferior to algal-based astaxanthin as an antioxidant and may not be suitable as a human nutraceutical supplement. Nutrafoods. Springer Science and Business Media LLC; 2013;12:145–52.

11. Foong LC, Loh CWL, Ng HS, Lan JCW. Recent development in the production strategies of microbial carotenoids. World J Microbiol Biotechnol. Springer Science and Business Media B.V.; 2021.

12. Bojko M, Olchawa-Pajor M, Goss R, Schaller-Laudel S, Strzałka K, Latowski D. Diadinoxanthin de-epoxidation as important factor in the short-term stabilization of diatom photosynthetic membranes exposed to different temperatures. Plant Cell Environ. Blackwell Publishing Ltd; 2019;42:1270–86.

13. Bhattacharjya R, Singh PK, Mishra B, Saxena A, Tiwari A. Phycoprospecting the nutraceutical potential of Isochrysis sp as a source of aquafeed and other high-value products. Aquac Res. Blackwell Publishing Ltd; 2021;52:2988–95.

14. Guedes AC, Amaro HM, Malcata FX. Microalgae as sources of carotenoids. Mar Drugs. MDPI AG; 2011. p. 625–44.

15. Lamers PP, van de Laak CCW, Kaasenbrood PS, Lorier J, Janssen M, de Vos RCH, et al. Carotenoid and fatty acid metabolism in light-stressed Dunaliella salina. Biotechnol Bioeng. 2010;106:638–48.

16. Chekanov K, Lobakova E, Selyakh I, Semenova L, Sidorov R, Solovchenko A. Accumulation of astaxanthin by a new Haematococcus pluvialis strain BM1 from the white sea coastal rocks (Russia). Mar Drugs. MDPI AG; 2014;12:4504–20.

17. Hu I-C. Production of potential coproducts from microalgae. Biofuels from Algae. Elsevier; 2019. p. 345–58.

18. Zhang H, Gong P, Cai Q, Zhang C, Gao B. Maximizing fucoxanthin production in Odontella aurita by optimizing the ratio of red and blue light-emitting diodes in an auto-controlled internally illuminated photobioreactor. Bioresour Technol [Internet]. Elsevier Ltd; 2022;344:126260. Available from: https://doi.org/10.1016/j.biortech.2021.126260

19. Maglie M, Baldisserotto C, Guerrini A, Sabia A, Ferroni L, Pancaldi S. A co-cultivation process of Nannochloropsis oculata and Tisochrysis lutea induces morpho-physiological and biochemical variations potentially useful for biotechnological purposes. Available from: www.ccap.ac.uk

20. Abe K, Hattori H, Hirano M. Accumulation and antioxidant activity of secondary carotenoids in the aerial microalga Coelastrella striolata var. multistriata. Food Chem. 2007;100:656–61.

21. Hashemi A, Moslemi M, Pajoum Shariati F, Delavari Amrei H. Beta-carotene production within Dunaliella salina cells under salt stress condition in an indoor hybrid helical-tubular photobioreactor. Canadian Journal of Chemical Engineering. Wiley-Liss Inc.; 2020;98:69–74.

22. Fernandes AS, Nascimento TC, Pinheiro PN, Vendruscolo RG, Wagner R, de Rosso V v., et al. Bioaccessibility of microalgae-based carotenoids and their association with the lipid matrix. Food Research International. Elsevier Ltd; 2021;148.

23. di Lena G, Casini I, Lucarini M, Lombardi-Boccia G. Carotenoid profiling of five microalgae species from large-scale production. Food Research International. Elsevier Ltd; 2019;120:810–8.

24. Xi Y, Wang J, Chu Y, Chi Z, Xue S. Effects of different light regimes on Dunaliella salina growth and β-carotene accumulation. Algal Res. Elsevier B.V.; 2020;52.

25. Přibyl P, Cepák V, Kaštánek P, Zachleder V. Elevated production of carotenoids by a new isolate of Scenedesmus sp. Algal Res. Elsevier B.V.; 2015;11:22–7.

26. Narang PK, Dey J, Mahapatra SR, Roy R, Kushwaha GS, Misra N, et al. Genome-based identification and comparative analysis of enzymes for carotenoid biosynthesis in microalgae. World J Microbiol Biotechnol. Springer Science and Business Media B.V.; 2022;38.

27. Song Z, Lye GJ, Parker BM. Morphological and biochemical changes in Phaeodactylum tricornutum triggered by culture media: Implications for industrial exploitation. Algal Res. Elsevier B.V.; 2020;47.

28. Brown MR. The amino-acid and sugar composition of 16 species of microalgae used in mariculture. J Exp Mar Biol Ecol. 1991;145:79–99.

29. Emdadi D, Berland B. Variation in lipid class composition during batch growth of Nannochloropsis salina and Pavlova lutheri. Mar Chem. 1989;26:215–25.

30. Bendif EM, Probert I, Hervé A, Billard C, Goux D, Lelong C, et al. Integrative Taxonomy of the Pavlovophyceae (Haptophyta): A Reassessment. Protist [Internet]. Elsevier GmbH.; 2011;162:738–61. Available from: http://dx.doi.org/10.1016/j.protis.2011.05.001

31. Fradique M, Batista AP, Nunes MC, Gouveia L, Bandarra NM, Raymundo A. Isochrysis galbana and Diacronema vlkianum biomass incorporation in pasta products as PUFA's source. LWT - Food Science and Technology [Internet]. Elsevier Ltd; 2013;50:312–9. Available from: http://dx.doi.org/10.1016/j.lwt.2012.05.006

32. Robertson RC, Gracia Mateo MR, O'Grady MN, Guihéneuf F, Stengel DB, Ross RP, et al. An assessment of the techno-functional and sensory properties of yoghurt fortified with a lipid extract from the microalga Pavlova lutheri. Innovative Food Science and Emerging Technologies [Internet]. Elsevier B.V.; 2016;37:237–46. Available from: http://dx.doi.org/10.1016/j.ifset.2016.03.017

33. Bashir KMI, Lee JH, Petermann MJ, Shah AA, Jeong SJ, Kim MS, et al. Estimation of Antibacterial properties of Chlorophyta, Rhodophyta and Haptophyta Microalgae Species. Microbiology and Biotechnology Letters. 2018;46:225–33.

34. Tibbetts SM, Patelakis SJJ. Apparent digestibility coefficients (ADCs) of intact-cell marine microalgae meal (Pavlova sp. 459) for juvenile Atlantic salmon (Salmo salar L.). Aquaculture [Internet]. Elsevier B.V.; 2022;546:737236. Available from: https://doi.org/10.1016/j.aquaculture.2021.737236

35. Shah SMU, Ahmad A, Othman MF, Abdullah MA. Enhancement of Lipid Content in Isochrysis Galbana and Pavlova Lutheri Using Palm Oil Mill Effluent as an Alternative Medium. Chem Eng Trans. 2014;37:733–8.

36. Fernandes T, Martel A, Cordeiro N. Exploring Pavlova pinguis chemical diversity: a potentially novel source of high value compounds. Sci Rep. 2020;10:1–11.

37. Berger R, Liaaen-Jensen S, McAlister V, Guillard RRL. Carotenoids of Prymnesiophyceae (Haptophyceae). Biochem Syst Ecol. 1977;5:71–5.

38. van Lenning K, Latasa M, Estrada M, Sáez AG, Medlin L, Probert I, et al. Pigment signatures and phylogenetic relationships of the Pavlovophyceae (Haptophyta). J Phycol. 2003;39:379–89.

39. Zhang Y, Xu W, Huang X, Zhao Y, Ren Q, Hong Z, et al. Fucoxanthin ameliorates hyperglycemia, hyperlipidemia and insulin resistance in diabetic mice partially through IRS-1/PI3K/Akt and AMPK pathways. J Funct Foods. Elsevier Ltd; 2018;48:515–24.

40. Hitoe S, Shimoda H. Seaweed Fucoxanthin Supplementation Improves Obesity Parameters in Mildly Obese Japanese Subjects. Functional Foods in Health and Disease. 2017;7:246–62.

41. Lopes FG, Oliveira KA, Lopes RG, Poluceno GG, Simioni C, Pescador GDS, et al. Anti-cancer effects of fucoxanthin on human glioblastoma cell line. Anticancer Res. International Institute of Anticancer Research; 2020;40:6799–815.

42. Seoane S, Zapata M, Orive E. Growth rates and pigment patterns of haptophytes isolated from estuarine waters. J Sea Res [Internet]. Elsevier B.V.; 2009;62:286–94. Available from: http://dx.doi.org/10.1016/j.seares.2009.07.008

43. Guihéneuf F, Stengel DB. Interactive effects of light and temperature on pigments and n-3 LC-PUFA-enriched oil accumulation in batch-cultivated Pavlova lutheri using high-bicarbonate supply. Algal Res [Internet]. Elsevier B.V.; 2017;23:113–25. Available from: http://dx.doi.org/10.1016/j.algal.2017.02.002

44. Kanamoto A, Kato Y, Yoshida E, Hasunuma T, Kondo A. Development of a Method for Fucoxanthin Production Using the Haptophyte Marine Microalga Pavlova sp. OPMS 30543. Marine Biotechnology [Internet]. Springer US; 2021;23:331–41. Available from: https://doi.org/10.1007/s10126-021-10028-5

45. Fernandes T, Cordeiro N. Effects of phosphorus-induced changes on the growth, nitrogen uptake, and biochemical composition of Pavlova pinguis and Hemiselmis cf. andersenii. J Appl Phycol. Springer Science and Business Media LLC; 2022;

46. Fernandes T, Cordeiro N. High-value lipids accumulation by Pavlova pinguis as a response to nitrogen-induced changes. Biomass Bioenergy. Elsevier Ltd; 2022;158.

47. Tibbetts SM, Patelakis SJJ, Whitney-Lalonde CG, Garrison LL, Wall CL, MacQuarrie SP. Nutrient composition and protein quality of microalgae meals produced from the marine prymnesiophyte Pavlova sp. 459 mass-cultivated in enclosed photobioreactors for potential use in salmonid aquafeeds. J Appl Phycol. 2020;32:299–318.

48. Rodrigues MI, Iemma AF. Experimental design and process optimization. 1st Edition. Experimental Design and Process Optimization. CRC Press; 2014.

49. Sanz N, García-Blanco A, Gavalás-Olea A, Loures P, Garrido JL. Phytoplankton pigment biomarkers: HPLC separation using a pentafluorophenyloctadecyl silica column. Methods Ecol Evol. British Ecological Society; 2015;6:1199–209.

50. Zapatal M, Garrido L. Influence of Injection Conditions in Reversed-Phase High-Performance Liquid Chromatography of Chlorophylls and Carotenoids. Chromatographia. 1991;31:589–94.

51. Zapata M, Jeffrey SW, Wright SW, Rodríguez F, Garrido JL, Clementson L. Photosynthetic pigments in 37 species (65 strains) of Haptophyta: Implications for oceanography and chemotaxonomy. Mar Ecol Prog Ser. 2004;270:83–102.

52. Fawley MW, Morton SJ, Stewart KD, Mattox KR. Evidence for a common evolutionary origin of light-harvesting fucoxanthin chlorophyll a/c-protein complexes of Pavlova gyrans (Prymnesiophyceae) and Phaeodactylum tricornutum (Bacillariophyceae). J Phycol. 1987;23:377–81.

53. Simkin AJ, Kapoor L, Doss CGP, Hofmann TA, Lawson T, Ramamoorthy S. The role of photosynthesis related pigments in light harvesting, photoprotection and enhancement of photosynthetic yield in planta. Photosynth Res. Springer Science and Business Media B.V.; 2022.

54. Gao F, Sá M, Cabanelas ITD, Wijffels RH, Barbosa MJ. Improved fucoxanthin and docosahexaenoic acid productivities of a sorted self-settling Tisochrysis lutea phenotype at pilot scale. Bioresour Technol. Elsevier Ltd; 2021;325.

55. McClure DD, Luiz A, Gerber B, Barton GW, Kavanagh JM. An investigation into the effect of culture conditions on fucoxanthin production using the marine microalgae Phaeodactylum tricornutum. Algal Res. Elsevier B.V.; 2018;29:41–8.

56. Mckew BA, Davey P, Finch SJ, Hopkins J, Lefebvre SC, Metodiev M v., et al. The trade-off between the light-harvesting and photoprotective functions of fucoxanthin-chlorophyll proteins dominates light acclimation in Emiliania huxleyi (clone CCMP 1516). New Phytologist. 2013;200:74–85.

57. Cao Z, Shen X, Wang X, Zhu B, Pan K, Li Y. Effect of Nitrogen Concentration on the Alkalophilic Microalga Nitzschia sp. NW129-a Promising Feedstock for the Integrated Production of Lipids and Fucoxanthin in Biorefinery. Front Mar Sci. Frontiers Media S.A.; 2022;8.

58. Xia S, Wang K, Wan L, Li A, Hu Q, Zhang C. Production, characterization, and antioxidant activity of fucoxanthin from the marine diatom Odontella aurita. Mar Drugs. MDPI AG; 2013;11:2667–81.

59. Longworth J, Wu D, Huete-Ortega M, Wright PC, Vaidyanathan S. Proteome response of Phaeodactylum tricornutum, during lipid accumulation induced by nitrogen depletion. Algal Res. Elsevier; 2016;18:213–24.

60. Li Q, You J, Qiao T, Zhong D bo, Yu X. Sodium chloride stimulates the biomass and astaxanthin production by Haematococcus pluvialis via a two-stage cultivation strategy. Bioresour Technol. Elsevier Ltd; 2022;344.

61. Ren Y, Sun H, Deng J, Huang J, Chen F. Carotenoid production from microalgae: Biosynthesis, salinity responses and novel biotechnologies. Mar Drugs. MDPI; 2021.

62. Fazeli MR, Tofighi H, Samadi N, Jamalifar H. Effects of salinity on β-carotene production by Dunaliella tertiolecta DCCBC26 isolated from the Urmia salt lake, north of Iran. Bioresour Technol. 2006;97:2453–6.

63. Gonabadi E, Samadlouie HR, Shafafi Zenoozian M. Optimization of culture conditions for enhanced Dunaliella salina productions in mixotrophic culture. Prep Biochem Biotechnol. Taylor and Francis Ltd.; 2022;52:154–62.

64. Ben-Amotz A, Lers A, Avron M. Stereoisomers of β-Carotene and Phytoene in the Alga Dunaliella bardawil. Plant Physiol. 1988;86:1286–91.

65. Campenni' L, Nobre BP, Santos CA, Oliveira AC, Aires-Barros MR, Palavra AMF, et al. Carotenoid and lipid production by the autotrophic microalga Chlorella protothecoides under nutritional, salinity, and luminosity stress conditions. Appl Microbiol Biotechnol. 2013;97:1383–93.

66. Mehariya S, Plöhn M, Leon-Vaz A, Patel A, Funk C. Improving the content of high value compounds in Nordic Desmodesmus microalgal strains. Bioresour Technol. Elsevier BV; 2022;359:127445.

67. Ishika T, Moheimani NR, Bahri PA, Laird DW, Blair S, Parlevliet D. Halo-adapted microalgae for fucoxanthin production: Effect of incremental increase in salinity. Algal Res. 2017;28:66–73.

68. Gu N, Lin Q, Li G, Qin G, Lin J, Huang L. Effect of Salinity Change on Biomass and Biochemical Composition of Nannochloropsis oculata [Internet]. J World Aquac Soc. 2012. Available from: http://www.cmar.csiro.au/microalgae

69. Rout GR, Sahoo S. Role of iron in plant growth and metabolism. Reviews in Agricultural Science. United Graduate School of Agricultural Science; 2015;3:1–24.

70. Naumann B, Stauber EJ, Busch A, Sommer F, Hippler M. N-terminal processing of Lhca3 is a key step in remodeling of the photosystem I-light-harvesting complex under iron deficiency in Chlamydomonas reinhardtii. Journal of Biological Chemistry. 2005;280:20431–41.

71. Leong YK, Chen CY, Varjani S, Chang JS. Producing fucoxanthin from algae – Recent advances in cultivation strategies and downstream processing. Bioresour Technol. Elsevier Ltd; 2022.

72. Kosakowska A, Lewandowska J, Sto´n JS, Burkiewicz K. Qualitative and quantitative composition of pigments in Phaeodactylum tricornutum (Bacillariophyceae) stressed by iron. BioMetals. 2004.

73. Hu X, Wei X, Ling J, Chen J. Cobalt: An Essential Micronutrient for Plant Growth? Front Plant Sci. Frontiers Media S.A.; 2021.

74. Li M, Zhu Q, Hu C wei, Chen L, Liu Z li, Kong Z ming. Cobalt and manganese stress in the microalga Pavlova viridis (Prymnesiophyceae): Effects on lipid peroxidation and antioxidant enzymes. Journal of Environmental Sciences. 2007;19:1330–5.

75. Latowski D, Kuczyńska P, Strzałka K. Xanthophyll cycle - a mechanism protecting plants against oxidative stress. Redox Report. 2011;16:78–90.

76. Bhosale P. Environmental and cultural stimulants in the production of carotenoids from microorganisms. Appl Microbiol Biotechnol. 2004. p. 351–61.

77. El-Sheekh M, El-Naggar A, Osman M, El-Mazaly E. Effect of cobalt on growth, pigments and the photosyntheticelectron transport in Monoraphidium minutum and Nitzchia perminuta. Braz J Plant Physiol. 2003;15:159–66.

78. Varshney P, Sohoni S, Wangikar PP, Beardall J. Effect of high CO2 concentrations on the growth and macromolecular composition of a heat- and high-light-tolerant microalga. J Appl Phycol. Springer Netherlands; 2016;28:2631–40.

79. Wimalasekera R. Effect of Light Intensity on Photosynthesis. In: Ahmad P, Ahanger MA, Alyemeni MN, Alam P, editors. Photosynthesis, Productivity and Environmental Stress. John Wiley & Sons Ltd; 2020. p. 65–73.

80. Enriquez MM, Lafountain AM, Budarz J, Fuciman M, Gibson GN, Frank HA. Direct determination of the excited state energies of the xanthophylls diadinoxanthin and diatoxanthin from Phaeodactylum tricornutum. Chem Phys Lett. 2010;493:353–7.

CHAPTER 5 FINAL REMARKS

5.1 GENERAL CONCLUSIONS

This thesis it was aimed to fully assess the impact of seventeen abiotic factors on *Pavlova gyrans* biomass using a multivariate approach, in order to identify the key parameters and subsequently use them to optimize the growth performance and biochemical composition of this microalga. The biomass optimization was divided in two steps: i) identification of key independent variables using a PB design, and ii) an optimization of the previously identified key factors using a RCCD design. The assays carried out in the RCCD were also characterized by GC-MS and elemental analysis to determine the fatty acid composition, particularly the EPA and DHA fraction, and the protein content, respectively. Similarly, *P. gyrans* biomass from the PB design was also analyzed by HPLC technique to determine its carotenoid content and profile, namely the composition of Fx, Ddx, Dtx, βCar, αCar and the sum of all carotenoids analysed (TCar). Special attention was given to the FX, βCar and TCar, for which the main abiotic factors involved in their production were identified. This information was used to devise tailored growth strategies to maximize the accumulation of these carotenoids. Thus, the main conclusions from this work were:

- The parameters light intensity (µmol.photons.m^{-2}.s^{-1}), $NaNO_3$ (mg.L^{-1}), and $CuSO_4.5H_2O$ (mg.L^{-1}) stood out as the most significant abiotic factors involved in the volumetric biomass productivity of *P. gyrans.*
- The outcomes of the RCCD design allowed to identify and understand the synergistic effects of the independent variables (light intensity, $NaNO_3$, $CuSO_4.5H_2O$ and NaH2PO4.H2O) on the response variables *Xmax*, EPA, DHA, lipid and protein content.
- Statistical model and the corresponding counter curves were generated for *Xmax,* which exhibited a satisfactory fit (R^2=84.1%) and, overall, showed a positive effect of light intensity, $NaNO_3$ and $NaH_2PO_4.H_2O$, in contrast to $CuSO_4.5H_2O$.
- Overall, EPA and DHA production in *P. gyrans* was favored by low light intensity and presented a positive quadratic effect for $CuSO_4.5H_2O$. EPA also presented a positive quadratic effect for $NaNO_3$ and a positive and linear interaction between light intensity and $NaH_2PO_4.H_2O$. DHA showed to be dependent on a linear interaction with a negative coefficient between $NaNO_3$ and $NaH_2PO_4.H_2O$, as well as negatively correlated with the level of $NaH_2PO_4.H_2O$.
- The optimized conditions for improved *Xmax* in the RCCD were defined as 700 µmol.photons.m^{-2}.s^{-1} of light intensity, 1500 mg.L^{-1} $NaNO_3$, 6 µg.L^{-1} $CuSO_4.5H_2O$ and 40 mg.L^{-1} $NaH_2PO_4.H_2O$, promoting a 3.8-fold increase in biomass production of *P. gyrans* (2.26 g AFDW.L^{-1}). In addition, the biomass produced under these conditions increased its EPA content, but mainly its protein, PUFA, n-3 fatty acid and DHA content compared to the control conditions (Walne's medium).

- The multivariate approach was also successful to maximize the carotenoids production of *P. gyrans.* Amongst the seventeen variables, were identified the key parameters responsible for improving the accumulation of Fx (light intensity and $NaNO_3$) and TCar (light intensity, NaNO3, salinity, cobalt, and iron).
- According to the outcomes from the PB design, the optimum growth conditions defined for Fx accumulation led to a 1.5- to 2.4-fold increase compared to the control conditions. Regarding the TCar, the defined growth conditions nearly doubled the carotenoid content of *P. gyrans*.
- The implementation of strategies relying on the two-phase cultivation of *P. gyrans,* reducing the light intensity at the end of exponential phase, was successful allowing a 1.5- fold increase in Fx content.
- The nutritional indices based on FAs profile, and the carotenoid enriched biomass proved the nutritional value of *P. gyrans* for potential application in food and feed products.

5.2 GUIDELINES FOR FUTURE WORKS

Overall, this thesis has described and confirmed the strict correlation between growth conditions and their impact on microalgae growth, as well as their metabolic composition, highlighting the importance of mastering microalgae growth and their nutritional requirements as a crucial skill for cost-effective microalgae production. To complement the work here described some guidelines for future work can be suggested:

- Validation of the optimized growth conditions at large scale for high biomass production, high accumulation of n-3 fatty acids and carotenoids in P. gyrans.
- Life Cycle Assessment and Life Cycle Cost Analysis of the optimized formulations to understand if the strategies here developed present economic and environmental advantages against the traditional medium formulations and the commercially used n-3 FAs- and carotenoids-rich microalgae species.
- Re-assess the vitamin supplementation in order to define the minimum amount required without compromise the *P. gyrans* growth.
- Explore the two-stage growth strategy of *P. gyrans* by managing other growth parameters (i.e. nutrients or LED lights) to enhance the production of EPA, DHA and other carotenoids than Fx.
- According to the nutrient requirements defined in the optimized growth conditions, explore the utilization of agro-industrial by-products as an alternative growth medium.

- Evaluate the implementation of new technologies (e.g. moderate electric fields) for downstream processing of *P. gyrans* biomass, to facilitate the dissemination of FAs- and carotenoids-enriched extracts for nutraceutical and pharmaceutical applications.